Biomechanical evaluation of user fatigue during burring with the MAKO RIO surgical system

Matthew Banger

A thesis presented in fulfilment of the requirements for the degree of

EngD in Medical Devices

Biomedical Engineering

University of Strathclyde

Glasgow, UK

2018

DECLARATION OF AUTHENTICITY AND AUTHOR'S RIGHTS:

This thesis is the result of the author's original research. It has been composed by the author and has not been previously submitted for examination which has led to the award of a degree.

Signed:

Date:

ACKNOWLEDGEMENTS

My first acknowledgement goes to my supervisor Professor Philip Rowe. Thank you for allowing me free reign to explore this project and the wider Biomechanics field, while also curtailing me back into reality.

The MAKO Surgical team were always welcoming on our visits and ever an ear to listen to ideas.

The Glasgow Royal Infirmary team, especially the three consultants involved in the trial, Mark Blyth, Bryn Jones and Angus MacLean for allowing me into theatres and made themselves available for questioning.

Many hours were spent toiling in the Lab for which I would like to thank Abibat, Julie and Shailesh to lend a hand and push around a Robot.

Strathclyde has been my home from home for the past few years, and there are many people that I have met that have inspired and humbled me. Thank you all.

Finally, I would like to thanks my parents for supporting my idea to move to Scotland and look at robots.

JLB & EWB

ABSTRACT

The MAKO RIO (MAKO Surgical, Stryker, Mahwah, NJ, USA) is an assistive surgical robotic arm system developed to increase the accuracy of bone cuts in joint replacement surgery. A high-speed cutting burr is mounted on the arm and is manoeuvred by the surgeon. The robotic arm allows free movement of the burr through the calculated cutting volume but restricts movement, and hence cutting, outside of this volume.

Localised fatigue anecdotally reported during burring from high output users of the MAKO RIO system is an issue. An ergonomic assessment of the MAKO RIO was carried out to review possible causes of the complaint of discomfort and fatigue. A clinical trial was observed and assessed for typical use of the system. This assessment culminated in a time analysis review of video footage recorded, defining a typical workflow of the surgery and details of its constituent parts. The clinical trial didn't represent a high output use of the system, but a number of users presented discomfort associated with fatigue.

After observing fatigue in users of the system, the project explored the biomechanical reasons for potential causes of this fatigue. A testing protocol of optical tracking, EMG and a force transducer was developed to assess users performing repetitive burring stages of the surgery. The output from the assessment showed high levels of muscle activity, poor posture and large forces that ultimately led to fatiguing of muscles in the lower arm. Specifically, the most significant fatigue was seen in the intrinsic muscles of the hand, with the high grip forces being held for extended periods and a splayed hand over the handle of the robotic arm.

A new prototype handle was also available for assessment to investigate if this would resolve the issues with the current handle. While there were some improvements in some muscles, extension and grip muscles were still presenting fatigue. The manoeuvring of the burr is still shown to take an extended length of time and require large forces from muscles that eventually cannot be met. Within high output users, either this accumulation of demand on these muscles over the day or the increased probability of a patient with sclerotic bone on a surgical list would lead these users to experience fatigue when working with the MAKO RIO system.

Finally, some conceptual ideas for improvements to the system are suggested throughout the thesis. Fundamentally, however, the cutting method of a burr while enabling accurate cuts and ability to create unique shapes in the bone is not suitable for large volume resection of hard, sclerotic bone.

Contents Page

List of figures

List of Tables

Glossary

AKS – American Knee Score

ARV- Average Rectified Voltage

ATI – ATI Industrial Automation, Inc.

ATP – Adenosine Tri-Phosphate

AUC – Area under curve

AV – Average

Bi-UKA – Bilateral Uni-compartmental Knee Arthroplasty

BMI – Body Mass Index

CAD – Computer Aided Design

CAOS – Computer Aided Orthopaedic Surgery

CAS – Computer Aided Surgery

CI – Confidence Interval

CoV – Coefficient of Variance

CPD – Continual Professional Development

CROSS – Centre for Robotic Orthopaedic Surgery at Strathclyde

CT – Computer Tomography Imaging

CV – Conduction velocity

DAQ – Data Acquisition

DoF – Degrees of Freedom

EE – End effector

EMG – Electromyography

ET – Endurance time

FDA – Food and Drug Administration

FL – Florida

GRI – Glasgow Royal Infirmary

GUI – Graphical User Interface

HDU – High Dependence unity

ICR – Instantaneous Centre of rotation

ICU – Intensive Care Unit

IEMG – Integrated Electromyography

IMDF – Instantaneous Median Frequency

IT – Information Technology

JASA – Joint Amplitude and Spectral Analysis

KA – Knee Arthroplasty

KL – Kellgren and Lawrence

MAKO – Not an abbreviation

MCP – Metacarpophalangeal

MDF- Median Frequency

MET – Maximum Endurance time

MFPV - muscle fibre propagation velocity

MIE - MIE Medical Research Ltd

MIS – Minimally invasive surgery

MIT – Massachusetts Institute of Technology

MPF – Median Power spectrum frequency

MPS – MAKOplasty Specialist

MRI – Magnetic resonance Imaging

MU – Motor Unit

MUAP – Motor Unit Action Potential

MVC – Maximum Voluntary Contraction

MWU – Mann–Whitney *U* test

NDI – Northern Digital Inc. (Company)

NHS – National Health Service

OA – Osteoarthritis

OR – Operating Room

PC – Personal Computer

PDS – Product design specification

PKA – Partial knee Arthroplasty

PPE – Personal Protective Equipment

PSD – Power Spectrum Density

PSDF – power spectrum density function

PUMA – Programmable Universal Machine for Assembly

RIO – Robot Arm Interaction System

RMS – Room Mean Square

ROM – Range of Motion

SAE – Surgical action efficiency

SD – Standard Deviation

SNR – Signal to Noise Ration

ST – Surgical Time

STAMP – Suggested Time and Motion Procedures

TGS – Tactile Guidance System

THA – Total Hip Arthroplasty

TKA – Total Knee Arthroplasty

TKR – Total Knee Replacement

TPA – time per action

TPS – Toyota Production system

Tri-UKA – Tricompartmental Knee Arthroplasty

TT – Tourniquet Time

UK – United Kingdom

UKA – Unicompartmental Knee Arthroplasty

USA – United States of America

VOC – Voice of consumer

WMSD – Work related musculoskeletal disorders

WSD – Work related stress disorders

Chapter 1 Introduction

The MAKO RIO surgical robotic system is an assistive surgical device in the treatment of osteoarthritis of the knee. High turnover users of the system have anecdotally reported to the company (MAKO surgical) of lower arm fatigue when using the system extensively in a single day (MAKO user preference study summary, 2010). In response to this an ergonomic review of the robotic system was conducted in house. The system had been ergonomically redesigned from the companies first generation model (MAKO 2009 THA and Knee User Research Status Summary, 2010) and the company continually monitors the use and practicalities of the system.

The MAKO RIO surgical robotic system is a new disruptive technology for arthroplasty surgery. Characterised by a loss of joint cartilage, pain and loss of function, primarily in the knees and hips, osteoarthritis affects 9.6% of men and 18% of women aged >60 years. This number increases with age, which along with an expected increase in global life expectancy, projects the future number of people suffering from the condition to increase (Woolf and Pfleger, 2003).

Current standard treatment for end-stage osteoarthritis is a total knee replacement, but before this stage tissue sparing early intervention through robotic solutions are becoming available, although not currently offered in the UK. It is the aim of these systems and companies to assist surgical ability and consistency for this increasing demand on knee replacements, providing new approaches to OA treatment. If successful, these systems standardise knee outcomes for all skill levels of surgeons and offer a platform for new surgical approaches not otherwise available outside of specialist surgeons. This growing global burden has made financial investment in new technologies a viable market and has seen a number of new technologies developed for these surgical procedure (Navigation, robotic assistance, patient specific jigs and implants).

The RIO is FDA and CE marked for stereotactic CT image guided knee and hip replacement surgery. The system augments the resection of bone allowing greater positioning consistency of implants. Backers of the technology believe this positioning accuracy is associated with clinical benefits in postoperative knee function and implant survivorship, however others refute these claims. Most agree, however, that larger randomised clinical trials are required to definitively assess the technology (van der List et al., 2016). Trials, such as those conducted at the Glasgow Royal Infirmary, aim to assess the use of the system for unicompartmental knee arthroplasty (UKA) (Bell et al., 2016).

The adoption curve of orthopaedic technologies has been shown to be steadily increasing, but still, computer-assisted surgeries only contribute less than 2.5% of primary knee replacements (National Joint Registry for England and Wales 12th Annual Report 2015, 2015). To review the barriers to adoption of the technology MAKO, in collaboration with the University of Strathclyde, proposed the assessment of the early adoption of the system in an NHS based clinical trial. The key outputs for the evaluation of the system would be a time analysis comparison of the new technology versus the current practice. Along with these outputs, the robotic system's general usability was considered in a wider scoped ergonomic evaluation. Parts of this ergonomic evaluation are presented in this thesis for their specific contributions to the understanding of fatigue when using the robotic arm.

Anecdotally, operator fatigue has been recorded as a consequence of the use of the RIO system in high turnover orthopaedic units where a surgeon may undertake multiple RIO assisted procedures in a day (MAKO user preference study summary, August 23, 2010). To review this issue of fatigue in the surgeons, this project designed assessment tools to attain a better understanding this fatigue issue and present possible solutions to the problem. Many factors contribute to this, the most apparent of which is hand and forearm fatigue induced by the current hand grip and end effector combination. These issues were at the time of initiation of this study addressed through the ergonomic re-design work of Seth Banks (MAKO 2009 THA and Knee User Research Status Summary, 2010) along with a planned future release of a new handle setup for the RIO. Further confirmation of fatigue has come about through interviews and discussions with RIO users, highlighting a further issue of added resistance to burring from sclerotic bone resulting in acute localised fatigue.

While still at an early adoption stage, it is evident some ergonomic biomechanical issues related to the human operation of the RIO remain. The most notable of these include the effort required to move the robot arm around during the resection of bone. Force is needed to manipulate the cutting burr through the bone and also against the haptic boundaries created to guide the surgeon's resection. The biomechanical loading put on the human operator with different handedness, surgical approaches and joint operations makes isolation of causes of fatigue complex and subjective.

With a growing demand of knee replacements surgeries and following the wider acceptance of surgical robotics in orthopaedics, the number of systems and users of the MAKO RIO system is set to increase. Issues relating to fatigue would also increase with the growing number of surgeries. This work aims to continue this review at a site outside of the United States with an observational review of the use of the system during a clinical trial and a biomechanical assessment of possible reasons and impact of fatigue in users.

Chapter 2 Literature review

The project assesses the MAKO system in clinical use and a controlled environment and to reflect this the following literature review is divided into two themes. The first is the clinical review of orthopaedic robotics to contextualise the problem and development of the field. The second theme is the testing methodologies that could be applied to assess the issue of fatigue with the RIO. As fatigue in muscles is difficult to measure directly, many different methods were reviewed and developed in this project. These have been drawn from ergonomic and wider scientific literature, along with existing examples of use in the surgical field. Finally, the ergonomic principle of the limitations of the human body is explored in the upper limb sections to give quantified context to the results measured in the laboratory sections.

2.1 Orthopaedic and Robotic Surgery:

Orthopaedic robotics is a growing field attempting to address clinical difficulties with a growing healthcare burden of orthopaedic surgery. There has been a steady increase in the number of primary knee operations from 60k to 86k per annum in England and Wales between 2005 and 2013 (National Joint Registry for England and Wales 12th Annual Report 2015, 2015). Projection from the United States predicts a 673% increase in primary knees by 2030 from 2005 numbers (Kurtz et al., 2007). This growing demand has led to the development of some knee approaches including Patient-specific jigs, navigation and robotics. The MAKO RIO is the first in the second wave of robotic devices coming to market as an alternative knee replacement procedure. MAKO Surgical (Fort Lauderdale, Florida) targeted UKA procedures as a viable marketplace, suitable for this disruptive technology.

2.1.1 UKA specific procedures

Unicompartmental Knee Arthroplasty (UKA) is a surgical treatment option for end stage unicompartmental osteoarthritis (OA) of the knee. When compared to Total knee arthroplasty (TKA) or high tibial osteotomies, other surgical approaches, UKA is a less invasive approach The UKA procedure only replaces bone in one compartment of the knee, while retaining both cruciate ligaments. This tissue sparing approach helps maintain proprioceptive levels (Fuchs et al., 2002), as well as presenting good clinical outcomes and function (Banks et al., 2005; Confalonieri et al., 2008; Fuchs et al., 2004, 2002; Newman et al., 2009; Repicci, 2003). The UKA can be considered to be a reduced invasive, bone preserving, pre-TKA procedure (Repicci, 2003).

However due to the historical inconsistency of durability and survivorship (Mannava et al., 2012), difficulty in the accurate positioning of the implant through a minimally invasive approach (Whiteside, 2005) and stricter inclusion criteria (Kozinn and Scott, 1989) this procedure is carried out less often with 8% of all primary knees being unicondylar in England and Wales between 2005-13 [1]. Hence, when aided by technology this number has the potential to increase. As an example, the observed centre in this study conducted 20% of primary knees as UKAs. More widely England and Wales has seen an increase of UKAs from 5,700 to 7,000 between 2005 and 2013.

Realignment of the joint is one of the main goals of the knee replacement surgery. The progression of osteoarthritis leads to the surfaces of the bone to become worn resulting in a malalignment of the bones with one another. From x-rays and using soft tissue balancing as guidance, the surgeon decides on the resection depths, orientation and implant size.

This alignment procedure in conventional approaches has a number of difficulties relating to accuracy and clinical complications when using standard Instruments (Strohbusch, 2010), these include:

- Improper cutting block pin to bone alignment
- Vibration of the saw blade can cause deflection and skiving
- Intramedullary alignment guides (standard for femur) are invasive and can cause pulmonary emboli upon tourniquet release
- Extramedullary alignment relies on the palpation of bony landmarks underneath varying thicknesses of soft tissue
- Small incisions limiting access to the bone

This stage in itself is an area of debate with a question of whether a neutral alignment is best and how it is defined (Conditt et al., 2004; Griffin et al., 2000; Gulati et al., 2009; Luo, 2004; Middleton and Palmer, 2007; Sugama et al., 2005; Walker et al., 2010). There is an additional debate as to whether there is any significance to clinical outcomes based on the alignment, both for (Huang et al., 2012) and against (Chareancholvanich et al., 2013; Kim et al., 2012; Yim et al., 2013) for all new surgical methods (CAS – Computer aided surgery, PSCG – Patient Specific cutting guides). When compared with conventional approaches the alignment reported by these new techniques appears to be improved (Bäthis et al., 2004), if not the same. Potentially given the ability of robots to accurately control where a cut is made, there is now scope for refinement of alignment targets, but as to the clinical relevance of this improved accuracy remains unclear. This clinical relevance is largely the question being asked by a current clinical trial in Glasgow (Bell et al., 2016; Blyth et al.,

[1] Njrreports.org.uk. (2017). Welcome to NJR. [online] Available at: http://www.njrreports.org.uk/ [Accessed 1 Aug. 2017].

2013; A. Motesharei et al., 2014). Results from this trial showed reduced postoperative pain, higher implant accuracy in all dimensions and more excellent American Knee Society scores at three months (Blyth et al., 2013).

Through navigation, robotics and patient-specific cutting guides, this issue of accuracy is being addressed (Citak et al., 2012). However, this technology still hasn't attained the legacy of outcome and longevity studies current procedures offer. This lack of acceptance in the surgical community is highlighted in the National Joint Registry of England and Wales where *"only 2.5% of primary knee replacements had used image-guided surgery"* (National Joint Registry for England and Wales 12th Annual Report 2015, 2015).

2.1.2 Robotics in Surgery

Robotics systems in surgery are largely assistive technologies to increase the effectiveness of existing procedures through increasing the accuracy and repeatability of fine movements and manipulations of tools by a surgeon. Davies (2000) defined the main uses and purpose for robotics in this field. In his description, there is a lot of mention of repeatable and accuracy of positioning and orientation. These systems at the time were active and moved the cutting tool. Given this active state the robotic systems would be "tireless" and "tremor free" (Davies, 2000). At the time of Davies' writing, systems were being developed for both orthopaedic and endoscopic procedures. From the further description of 'without the aid of vision and without forgetting the path or the location' (Davies, 2000), almost infers the limitation, or complication, of a human user in the system. These systems were autonomous (active) for the most part and required minimal physical user input.

Robotic systems are largely complex systems that complete relatively simple tasks quickly and accurately, but outside of the routines are largely unable to adapt. Surgeons, on the other hand, have the ability to review complex routines and can adapt quickly. However, they are limited in unassisted accuracy and speed (DiGioia, 2004). A number of market and legal factors have led to a need for both. With advancements in computer autonomy this may not always be the case, but, for the time being, the interface between robotic systems and surgeon is of growing research interest with the increasing prevalence of the robotic systems themselves.

2.1.2.1 Types of robotic systems

Medical standards are continually being developed to define robotic and computer assistive technologies (IEC SC62A, ISO TC184/SC2 and IEC 60601[under revision]). The classification of robotic systems refers to the means of guided assistance to the surgeon. Different surgical work flows can utilise the different levels of guidance based on their benefits and draw backs.

A passive system is one that locks in place when the required position has been found manually through feedback. These are often used to guide tools or to hold a subject in place (i.e. a leg during an X-ray or for the duration of the surgery). These systems are often simpler in design and can be used in existing surgical workflows. An example of this is an articulating arm that is manually guided with a probe for the registration of an object. This was utilised in the Acrobot system for the registration of the joint (Cobb et al., 2006), with an encoded robotic arm used to track the location of a registration probe. Similarly, for the same system, two other arms in the robotic system tracked and held the limb in place during the surgical procedure.

An alternative approach is an active system. This is one that will drive a movement from a routine or through a predefined path. This was implemented early in robotic design to move the heavy systems, that would have been too cumbersome for user movements. These systems are large and often required minimal patient movement during the procedure. This kind of system requires a 'go' and 'stop' command from the surgeon that looks on during the automated trajectories. A typical example of this type of system is the Robodoc. This system and development is reviewed specifically below, highlighting benefits and disadvantages.

A further development is the semi-active system (Davies, 2000). This development is one of interest when considering user interfaces. The system has both the ability to actively resist and assist in a movement, and is often force controlled from a handpiece or console. This system type has the added benefit and synergy of both surgeon command and robotic control. It is this interaction that this project is exploring.

Imaging modality also varies between systems as clinicians try to minimise patient radiation. Pre or intra operative imaging technique with CT images enables 3D patient specific models at the cost of increased exposure to the patient. Otherwise the system utilises population bone shapes that are not specific to the patient. These classifications and examples of robotic systems are defined below in Table 2.1-1.

2.1.2.2 General Robotic CAOS procedures

Orthopaedics surgeries are routinely carried out throughout the world with both elective and trauma case. The following table is a historical review of the type of robotic systems used in arthroplasty surgery; further details can be found in Kazanzide's and Faust's reviews (Faust, 2007; Kazanzides et al., 2008).

Table 2.1-1 Robotic systems in the literature focusing on Hip and Knee Surgery presenting imaging modality of patients leg, guidance of robotic system, mounting of cutting equipment and means of tracking patient's leg.

Name	Surgeries	Image	Guidance	Mounting	Tracking
Robodoc	TKA, THA	CT	Active	Robotic arm	Encoders
CASPAR	TKA, THA	CT	Active	Robotic arm	Encoders
Acrobot	UKA, TKA, bespoke orthopaedic implants	CT	Active	Robotic Arm	NDI
MAKO RIO	UKA, Bi-KA, TKA, THA	CT	Semi-active, Haptic	Robotic arm	NDI
Sculptor RGA (2nd Generation Acrobot)	UKA	CT	Semi-active, Haptic	Robotic Arm	NDI
Navio PFS	UKA, Bi-KA	Imageless - probed	Semi-active	Handheld	NDI

NDI - Northern Digital Inc. (Ontario, Canada) products

The table above is in historical order spanning almost 30 years from the 1986 start of Robodoc. It shows the current second generation of robotic systems integrating the NDI tracking and a semi-active robotic arm and no longer relying on active guidance. As a company NDI Medical produces a recognised optical tracking system heavily used in navigation and as such has a legacy in the surgical environment. This approval made these tracking systems straight forward to implement in the medical robotics field and have been adopted by all companies. Similarly, the robotic components are also very similar giving rise to legal actions between the three main companies over IP infringements. At the time of writing the MAKO RIO and Navio PFS are the only surviving commercial products of this legal battle ("MAKO Surgical Sues Blue Belt Technologies," 2014), with continued cases between the two companies now owned by Stryker (Kalamazoo, Michigan) and Smith & Nephew (London, UK) respectively. While not prolific, the field is highly competitive.

The second generation of robots came about after the commercial failings and lack of uptake of the original systems. The weakness of one of these systems, the Robodoc, has been reviewed for THA (Faust, 2007). This reviewed showed significantly longer surgical times were recorded than those of a control patient group (Bargar et al., 1998), with an extension of 15-30 minutes after the initial learning curve. An additional risk from the registration bone pins for neurological damage and additional post-operative pain (Faust, 2007). High revision rates (due to dislocations) were reported

in one clinical trial leading to considerable morbidity (Honl et al., 2003), but these effects were not seen across other similar clinical trials (Faust, 2007). Further clinical complications resulted from poor surgical planning with failure to protect soft tissues, rupturing hip abductors and a change in bone finishes due to thermal necrosis. These issues were an issues with the forces not being measure by the system. Further this lead to robotic failure in as high as 18% of cases, with 70% of this due to force cut outs when cutting sclerotic bone. This failure rate dropped to 3.4% with force sensing improvements.

The Robodoc system was stopped being used in Europe and was widely considered to have ceased use, but a further review (Ritacco et al., 2016) shows the Robodoc is still in clinical trial use in Asia and branded as TSolution One by THINK Surgical Inc. Ritacco's chapter reviews the clinical accuracy reports showing better results than conventional surgery along with a review of the workflow after the rebranding of the device. A major improvement is the CT registration no longer requires pins locators as previously placed with an additional procedure pre-surgery. However, after the system registers the bone with the CT model the bones are not able to move, with bone motion monitoring arms tracking any movements. Re-registration is required when the bones are moved resulting in longer surgical times reported for both THA and TKA. The original extended surgery times resulted in significant increase in blood loss (Bargar et al., 1998). The active component of the system is monitored by the surgeon, with options to pause, stop and abort the use of the robot. Algorithms calculate these movements from a pre-operative plan. While some improvements have been made to the system, these don't amount to significant developments from the original system (Figure 2.1-1).

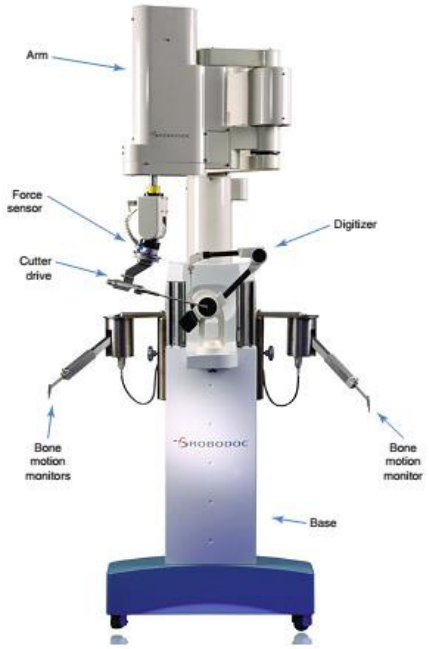

Figure 2.1-1 Current Robodoc model. THINK Surgical Inc. TSolution One. The all in one system actively moves the cutter to the bone held by the two bone monitors. The surface of the one is positioned through the digitizers.

Given the longevity of the field, it is surprising that there has been limited development of the systems beyond the Robodoc setup, especially when comparing the developments in the wider field of robotics and autonomous systems. The major improvements have been the addition of haptics and optical tracking of the limb, with all current systems run off a similar setup. Given the competitiveness of the field, there is large media exposure and prediction for the next generation of systems. Unfortunately, these are likely being restrained from publication to maintain intellectual rights over the design. This lack of open discussion could be limiting the development and integration of these systems into routine use.

Control of the cutter, such as through haptics, facilitates the surgical manipulation of the burr within the resection volume, allowing the system to work with changing density of bone. This also created a human interface, with ergonomics now having to be considered in the design process. While systems such as the Robodoc and Acrobot could be manually positioned the cutting was largely automated. The new generation of currently available systems all requires user manipulation of the cutting mechanism in the joint. While there are obvious legislative reasons for keeping the surgeon in control of the system, there are also other control reasons, such as the difficulty of an automated system to monitor and adjust for bone density, thermal management of the burr and soft tissue retraction. For a system to control these factors, a number of additional sensors would be needed to ensure that issues of thermal necrosis and high forces in the joints are dealt with. Alternatively, haptics has developed to a stage that the surgeon can engage with the benefits of the

accuracy of the robotics system, while also being able to control the complex conditions at the point of cutting. Hence, the introduction of the surgeon into the cutting process.

The additional optical tracking has allowed for real time tracking of the limb and subsequent clinical assessment of the soft tissues around the knee. There is natural varying laxity in the joint through a range of motion, generally tighter in extension due to the posterior capsule with increasing laxity through flexion to a maximum at approximately 30 degrees, to then decrease with further flexion (Bergfeld et al., 2001; Markolf et al., 1997). In previous systems, the limb was held in place throughout the procedure through bone fixators (Pearle et al., 2010; Plate et al., 2013). Now the joint can be moved and stressed to assess the soft tissue envelope without losing the registration of the bone. In conventional surgery, this stage is reliant on the 'feel' of the knee to the surgeon. 1mm incremented spacers in the conventional surgery instrument set allow for the assessment of the laxity at 20 and 90 degrees of flexion after the tibial plateau has been cut. This assessment allows the calculation of the femoral resection, or an additional tibial cut, to minimise the laxity difference at 20 and 90 degrees (Biomet., 2012). As in navigation, the robotic system can graphically represent the varus and valgus gaps through a range of motion in a pre-resected state. The positioning of the implants can be changed to compensate for the multiple data points, allowing the surgeon to restore the alignment and anatomically defined laxity of the joint in sub-millimetre increments (Pearle et al., 2009). This accounts for most of the intra-operative decision making in the theatre that is assessed for both these procedures in the time analysis chapter.

2.1.2.3 Typical stages of surgery

Procedurally robotic and manual UKA are very similar. The key differences (Table 2.1-2) are the additional pre-operative imaging and processing, and robotic calibration stages. While there is procedural documentation relating to both practices, there is no detailed review of these stages, with access to this information limited to those with clinical experience of the procedures. Social media has been a forum for showing these procedures as patient information in the form of webcasts and live video footage from surgery[2][3]. However, no detailed formal review of the procedures has been published in the field.

The currently published materials on the procedures are presented below. These workflows are reviewed in detail in the time analysis chapter, with a comparison of efficiency and analysis of the

[2] YouTube. (2017). MakoSurgicalCorp. [online] Available at: https://www.youtube.com/channel/UC_eDjlv1Um6OqIfMZH3D2iA [Accessed 1 Aug. 2017].

[3] Orlive.com. (2017). ORLive, Inc.: MAKOplasty® Robotic Arm Partial Knee Resurfacing. [online] Available at: http://www.orlive.com/makosurgical/videos/makoplasty-robotic-arm-partial-knee-resurfacing1 [Accessed 1 Aug. 2017].

different stages in each surgical approach. It should also be noted that the Oxford procedure has released a new approach and tooling system with the Oxford PKR microplasty. This was subsequent to the clinical trial and this study. Additionally, the Davies workflow is a description of the Acrobot's approach to UKA (Davies, 2000). This is a slightly different approach to the current robotic systems, but was a foundation to their development and used as a framework for assessing the two systems.

Table 2.1-2 Typical stages in UKA knee surgery for a typical robotic approach and manual Oxford approach.

Typical Robotic UKA stages (Davies, 2000)	Typical BioMET Oxford UKA procedure (Biomet., 2012)

• Pre-operatively:
  ○ Image patient
  ○ Edit images and create three-dimensional model of leg
  ○ Create three-dimensional model of prostheses
  ○ Superimpose prostheses over three-dimensional model of leg
  ○ Adjust and optimise location
  ○ Plan operative procedure
	• Pre-operatively:
	  ○ Preoperative Planning templating on X-Rays

• Intraoperatively:
  ○ Fix and locate patient on table
  ○ Fix and locate robot (on floor or on table)
  ○ Input three-dimensional model of cuts into robot controller
  ○ Datum robot to patient
  ○ Carry out robot motion sequence
  ○ (Monitor for unwanted patient motion)
  ○ Burr plan resection
  ○ Remove robot from vicinity
  ○ Trial implants and assessment of kinematic changes check quality of procedure
  ○ Cement Implants
	• Intraoperatively:
	  ○ Positioning the Limb
	  ○ Incision
	  ○ Excision of Osteophytes
	  ○ Tibial plateau resection
	  ○ The femoral Drill Holes
	  ○ Femoral saw cut
	  ○ First milling of the condyle
	  ○ Equalising the 90˚ and 20˚ Flexion Gaps
	  ○ Confirming equality of the 90˚ and 20˚ flexion and extension Gaps
	  ○ Preventing Impingement
	  ○ Final Preparation of the tibial Plateau
	  ○ Trial Reduction
	  ○ Cementing the Components

• If further cuts are necessary:
  ○ Re-clamp patient
  ○ Reposition and datum robot to patient
• Repeat robotic procedure	

2.1.3 MAKO TGS

Understanding the historical iterative development of the MAKO RIO gives an insight into the design procedure and objectives of the product. MAKO was founded in 2004 as an independent company, having been initially developed by Z-Kat Inc., Barret Technologies[4] and MIT. MAKO's Tactile Guidance System 1.0 was launched in November 2005, with first clinical use in 2006 for UKA under surgeon Martin Roche. Subsequent versions 1.2 and 1.3 were released in the first and third quarters of 2008. All early clinical trials were completed on this system (Figure 2.1-2).

Figure 2.1-2 MAKO Tactile Guidance System (TGS). This is the first commercial product from MAKO.

The system subsequently was redesigned for an additional degree of freedom at the end effector. Aesthetically the system was changed with a plastic single colour shell, along with additional ergonomic features such as a handle at the elbow. Farm Design completed the work along with additional ergonomic assessment by Black Hagen. MAKO Surgical relaunched this system as their first commercial robot, MAKO RIO.

2.1.4 MAKO RIO

The MAKO RIO (Robotic arm Interactive Orthopaedic system aka TGS 2.0) was launched in 2010 as the commercial successor of the tactile guidance system from MAKO Surgical, FL, USA. The system comprises a robotic arm, a guidance module with a tracking NDI camera and surgical monitor, and a control console for a technician to aid in visualisation and the workflow of the procedure (Figure 2.1-3).

[4] Barrett.com. (2017). Barrett Technology, LLC - Applications - Surgical. [online] Available at: http://www.barrett.com/applications-surgical-article1.htm [Accessed 1 Aug. 2017].

Figure 2.1-3 MAKO RIO System. The MAKO system is made up of three units; the robotic arm (left), guidance system (middle) and console (right).

The system allows for a pre/intra –operatively planned CT model of the patient's knee to guide a surgeon-driven haptic guided burring robotic arm for resection of the bone. The system tracks arrays attached to the bones and a robotic arm in real time to allow for intraoperative adjustments of the plan based on the kinematics of the knee from soft tissue passively corrected range of motion (Plate et al., 2013). The haptic guidance creates a three-dimensional virtual stencil for the surgeon to manipulate the 6mm ball burr through for more precise resection of complex shapes from the bone allowing advances in implants design (Conditt, 2009; Lonner et al., 2009).

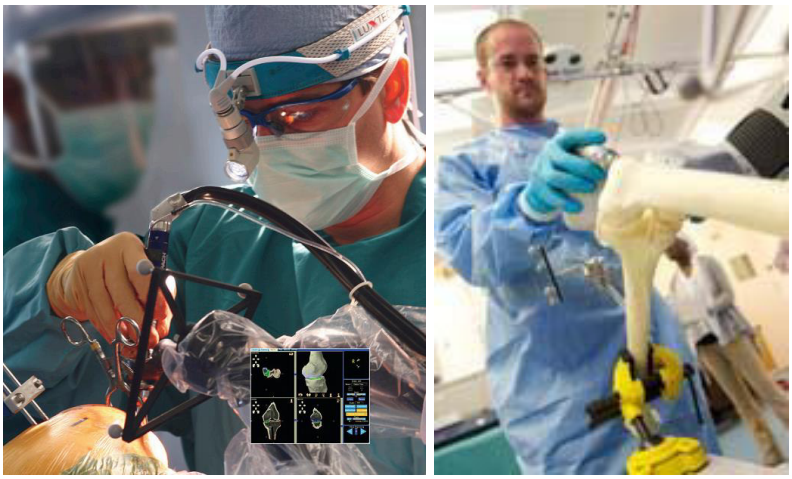

Figure 2.1-4 Image of the change in handle design. TGS (Left) was a 5-degreeof freedom robotic arm and held like a pencil. The MAKO RIO (Right) is a 6-degree of freedom robot and held with a spherical prehensile grip.

Currently, the platform supports UKA, PKA and THA with the scope of the platform to allow for TKA and other orthopaedic procedures.

Figure 2.1-5 MAKO RIO Handle (End effector) with scale from cm ruler. This handle/end effector mounts the burr and is manipulated by the surgeon freely moving within a set haptic volume but otherwise restricted to that volume by the robotic arm. The burr is activated through the depression of the trigger and is only position in the haptic volume, if this moves outside of this area the burr is stopped or cannot be activated.

Robotic arm

The robotic arm of the MAKO RIO (Figure 2.1-6) is a 6 degree of freedom robotic arm. Positional data of the joints is measured from optical encoders and forces measured from voltage changes across the motors giving position, orientation, force and torques on each joint.

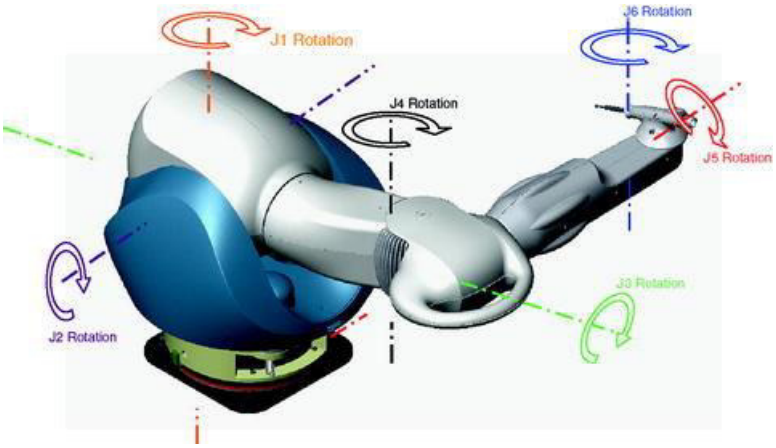

Figure 2.1-6 Exploded view of the MAKO RIO robotic arm. The 6 dof system is controlled by a cable driven system to create the haptic boundary (Hagag et al., 2010)

The cable driven system allow low friction passive movement of the robotic arm to minimise fatigue when using the system, while also enabling 'back drive' ability to stop this large robotic arm to within 1mm cutting accuracies (Hagag et al., 2011). This 'back drive' creates the haptic volume for the surgeon to manipulate the burr through.

Haptics

The stereotactic haptic boundary physically manifests the boundary edge of the planned cut from the virtual plan. The surgeon grasps the end effector (Figure 2.1-5) and moves the high speed ball

burr to the resection areas of the bone. The virtual burring plan is visualised on a screen showing the area that has and still require burring (Figure 2.1-7).

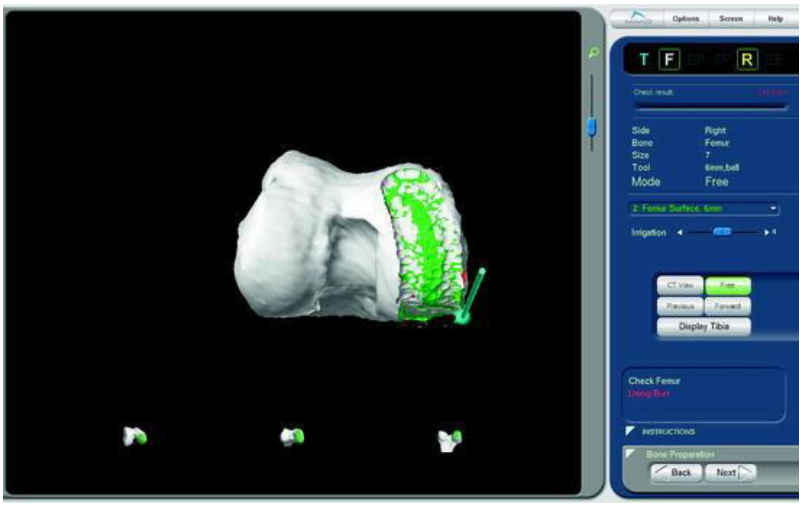

Figure 2.1-7 Femoral resection virtual burring environment example. Green is that volume to be resected, white is the bone to remain from the CT model of the femur. The burr position is shown in green/blue in real time. (Hagag et al., 2011)

The robotic system therefore gives tactile, visual and audible feedback to the surgeon during burring. Publically available manuals for the complete workflow of the robotic systems are available through the Stryker website (MAKO Surgical, 2009)[5].

2.1.4.1 Clinical Trials

Given the shortcomings of the others systems, clinical trials have been set up to assess the new generation of surgical systems. Given the established works of the Acrobot system in the field of orthopaedics, MAKO set out to show the application in the UKA market. Accuracy was established in a pilot study (Lonner et al., 2009) as being more accurate in rotational alignment for all three planes than the manual technique. This was then followed by Pearle et al. (2010) that reiterated the surgical accuracy improvements and established the first published time analysis of the first 10 cases. Soft tissue balancing protocol for the system was evaluated by Plate et al. (2013). These ideas were then further established at clinical conferences through presentations and poster dissemination (Branch et al., 2012; Jinnah, 2009; Mofidi et al., 2012; Strohbusch, 2010). Full details of publications can be found on the MAKO surgery website[6].

Finally, the largest clinical trial for the review of the MAKO UKA system (Bell et al., 2016; Blyth et al., 2013; A. Motesharei et al., 2014; Arman Motesharei et al., 2014) was conducted in Glasgow. The

[5] https://www.strykermeded.com/media/1698/mako-mck-planning-and-surgical-technique.pdf [Accessed 11 Jan. 2018]

[6] Makosurgical.com. (2017). Orthopaedics - Mako Robotic-Arm Assisted Surgery : Stryker. [online] Available at: http://www.makosurgical.com/physicians/clinical [Accessed 1 Aug. 2017].

outcomes of this trial compared with the Oxford UKA procedure and showed better pain score, functional outcomes, surgical outcomes and implant accuracies.

Despite these studies, the system is still only just coming to 10-year outcomes in the initial patients, and significant changes have already taken place in the system and its use. We must, therefore, continue to consider the MAKO RIO to be establishing itself, with early indications of improved outcomes.

2.1.4.2 User experiences

As of December 2012, 156 RIO systems were established with a total of 10,204 MAKOplasty procedures performed worldwide[7]. This formed a community of over 300 surgeons using the system. As of 2016, the number of surgeries completed is more than 50,000[8]. To contextualise this in 2006 the US performed an estimated 520,000 primary knees a year (Kurtz et al., 2007), with 86,000 being performed in England and Wales (National Joint Registry for England and Wales 12th Annual Report 2015, 2015) in 2013. Hence, this represents a small number of the total primary knee cases and a fraction of the orthopaedic surgical community.

As reviewed in 2010, Pearle (2010) states that while there are advantages to the robotic system over conventional and navigated techniques, there are a number of 'drawbacks' (Pearle et al., 2010). The high overall cost is a massive capital expenditure that limits the number of sites, and health care systems (NHS), that can afford these systems. Along with this capital cost is the additional maintenance cost for the life time of the system, placing more financial risk on investing in a system. The additional CT scanning cost, while leading to a patient specific model is more expense and increased patient exposure.

In a review of the workflow of the MAKO RIO Pearle also commented on the complex setup of the robotic system, especially the draping of the system (Pearle et al., 2010). Due to this complexity the MAKO system requires additional skilled personnel in the OR (MAKOplasty Specialist (MPS)) to provide assistance in the surgical procedure. Another drawback of the complex work flow are the longer surgical times than conventional UKA time, but this time was expected to decrease with familiarity, skill development and future technological developments.

[7] Sec.gov. (2017). [online] Available at: http://www.sec.gov/Archives/edgar/data/1411861/000089710113000266/mako130784_10k.htm [Accessed 1 Aug. 2017].

[8] Stryker.com. (2017). Orthopaedics - Mako Robotic-Arm Assisted Surgery : Stryker. [online] Available at: https://www.stryker.com/en-us/products/Orthopaedics/MakoRobotic-ArmAssistedSurgery/index.htm [Accessed 1 Aug. 2017].

This review holds that a number of problems highlighted under previous systems are still an issue. These issues were mentioned when using the old TGS system and the current RIO appears to have inherited these same issues. Given the general workflow and concerns of the length of surgical time, this project is aiming to review the workflow and learning curves of the users during the early stage of the clinical trial. Observed reasons for delays in early adopters of the technology can be reviewed and give further context to the issues raised by Pearle.

2.1.4.3 Issues with the systems

Adverse events are reported to the FDA and made public for review[9]. As part of this continual review, the company has only recalled for correction 0.15% of the cases over a three-year period. While a number of recalls have occurred over its existence, these rates of failure and conversion to manual procedures are minimal and often put down to user error. These are far lower than the 18% experienced in the Robodoc system that was mostly genuine technological faults. This highlights that these surgical delays with early adopters are not technical issues that will result in adverse clinical outcomes, but are more efficiency demands of the robotic systems to match the current manual procedures.

2.1.5 Conclusions

Porter (2010) describes the term 'value' in healthcare to be centred on the patient outcomes. Given that outcomes are relative to the cost, this encompasses efficiency. Health care systems are therefore driven to drive cost reduction without affecting care. As reviewed in Gomes (2012), the accuracy of the robotic systems are being fulfilled however the claim of reduced time has not been successfully met. While there has been a number of improvements in efficiency and workflow, setup times often result in lengthier surgical times when compared to conventional counter parts. This conflict between accuracy against health economics, with fewer procedures being able to be carried out has resulted in market drivers from patients having larger influence on the use of these systems under a US framework. The true value of the MAKO RIO system to a healthcare system outside of the US is still not realised.

From the literature, there are obvious issues with the time taken for the robotic surgery with additional stages required. Thus, the concept of time analysis of a surgical workflow is review in the following section.

[9] Anon, (2017). [online] Available at: http://fdazilla.com/maude/adverseevents/search?q=mako+surgical [Accessed 1 Aug. 2017].

2.2 Time Analysis

Currently, surgical workflows are described in medical textbooks, formalised by protocols and learnt by personnel in training courses and on the job experience. The growing pressure of cost efficiencies is pressuring healthcare systems to impose specialisation of experience, equipment and room requirements (Herfarth, 2003). One means of sharing and assessing these workflows is through time analysis.

Time analysis has a background in industrial efficiency (Scientific management or Taylorism (Taylor, 1911)) that looks to develop a means of assessing and indicating areas of improvement to the workflow of the procedures studied (Lopetegui et al., 2012). These principles are the measures used in the corporate structure of work; the adage 'time is money'. While this is true also of the healthcare financial structure, there is also a clinical benefit to efficient workflow with more surgeries completed within a surgical list and the reduced risk to patients under perioperative care.

Here clinical outcomes, efficiency, cost and time all require balancing along with logistical difficulties when measuring these for all cases. These outcomes make the time analysis of surgical procedures more complex to analyse and more challenging to justify changes to the workflows. However, many tools can be transferred from the industrial methodologies. Picking the right level of assessment is best defined by Buxton's Law stating that:

"It is always too early [for rigorous evaluation] until, unfortunately, it's suddenly too late." (Ramsay et al., 2000)

Given the cost and added infrastructure required to support regular time analysis in the health care system, there is an obvious reason for underutilization. There is difficulty applying these methods to more stringent ethics in the medical field, along with the availability of expertise. Ramsay (2000) argues that there is not enough uptake and robustness of any time analysis methodologies within the medical profession. However, with the added integration with IT that is starting to be observed throughout the healthcare system, including surgical equipment, the availability of time analysis data is increasing. It is only a matter of time before these metrics are used more regularly to access current standards and practice. Much of the assessment and development of this project is designed to fall within these boundaries of usable, typical practice, quantitative data and analysis.

2.2.1 Methodologies

There are a number of other names for time analysis: (Surgical action efficiency (SAE) (Dankelman et al., 2004; Meijer et al., 2000),Time Action Analysis (Minekus et al., 2003; Oldenrijk et al., 2008),Time motion studies (Bratt et al., 1999; Burke et al., 2000; Cao et al., 1996; Lopetegui et al., 2012)) and techniques (Time (Minekus et al., 2003), Movements (Cao et al., 1996)) that are based on similar methodologies. With assessment being proceeded at different technical levels for data captured (Hierarchical(*Task analysis*, 1971), Task) and analysis (Surgical process modelling (Neumuth et al., 2012), Boosted Segmentation (Padoy et al., 2007)). Ranging from a stopwatch to detailed assessment of the movements of robotic systems, these all assess the efficiency and learning curves of users. As to which is best, is a reflection of the research question. There was not a methodology in the literature that had this direct application of orthopaedic procedural comparison, such that a new assessment and presentation of data was developed, influenced by the different techniques.

For clarity, below is a table (Table 2.2-1) of definitions used in this thesis, with equivalent terminology on the right, along with a definition.

Table 2.2-1 Time Analysis terminology used in this thesis with definitions or similar use in the literature

Use in this thesis	Other Description from literature
(Action)	Action: a fundamental element of the semantic interpretation of the scene, for example, picking up tool
(Step)	Activity: is a collection of actions
(Stage)	Phases: meaningful collections of activities\steps with defined purpose
(Workflow)	Workflow: The complete collection of phases
(Time-action analysis)	Time-action analysis is a review of the number of times an action is repeated and the time that the action took.
(Time-motion analysis)	Time-motion analysis is a review of the motions over time that was conducted over a period; this is the automated version mostly.

A generic time analysis approach as defined by Groover (2007) for time analysis is:

1. *"Define and document the standard method.*
2. *Divide the task into work elements.*
3. *These first two steps are conducted prior to the actual timing. They familiarize the analyst with the task and allow the analyst to attempt to improve the work procedure before defining the standard time.*
4. *Time the work elements to obtain the observed time for the task.*
5. *Evaluate the worker's pace relative to standard performance (performance rating), to determine the normal time.*
6. *Note that steps 3 and 4 are accomplished simultaneously. During these steps, several different work cycles are timed, and each cycle performance is rated independently. Finally, the values collected at these steps are averaged to get the normalized time.*

7. *Apply an allowance to the normal time to compute the standard time. The allowance factors that are needed in the work are then added to compute the standard time for the task."*

At a basic level, time analysis can be quite a simple procedure to allow for easy implementation of observing workflow and standardising approaches. But even at this level, the tasks observed have to be well defined, as do start and stop points to allow for real-time annotation. In a linear process that has a highly predictable order, general tasks can be recorded with hand-written notes in table format. When more detailed tasks are defined, this recording process can utilise electronic capture aids for in-situ and post processing annotation. The level of complexity can describe every action of the interactions of the user. Robotic systems can quantify these for inter/intra-user comparison relatively easily given access to the motor and encoder recordings. The actual movement of the user requires additional equipment in video recording or for more detailed biomechanical studies, optical tracking.

2.2.2 Examples of the implementation of time analysis:

There is considerable variation in the detail provided in time analyses of surgical workflows. The least detailed is the amount of time that the operating room (OR) is in use (Cardoen et al., 2010; Weinbroum et al., 2003). The usefulness of the measurement is for site management, with a number of different types of surgeries often being recorded. This is in contrast to Jun et al. (2013) who broke tasks of Laparoscopic surgery into individual movements, or 'Therbligs' recorded by the robotic system. These movements can quantify the performance of the surgeon, by comparison with other experienced surgeons. For example, the more movements a surgeon takes to complete a suture would indicate weaker performance. Both extremes are asking different questions of the time analysis data but are still considered time analysis.

In the original industrial application of time analysis, the observer can review the actions by simply being on site and recording the time points manually. This is a cheap and easily implementable protocol but does require a high level of concentration of a dedicated observer. There is a suggestion that the error involved is dependent on the recording party, and self-reporting should be avoided if possible (Burke et al., 2000).

As an example of a simple approach, arterial tourniquets are widely used in orthopaedic anaesthesia to reduce blood loss and provide better operating conditions with a bloodless surgical site. Tourniquet-induced ischemia should not exceed 2 hours and hence this has perfect application in UKA surgeries. There are a number of clinical complications using tourniquets (Aziz, 2009; Kam, 2005), and minimising the length of ischemia to the lower limb will decrease the likelihood or

prevalence of these complications. Most modern tourniquets have a timer on them for clinical outcome measures. In the hospital under study, the tourniquet time was recorded for all surgeries as part of the clinical notes. Complications can come about with the resetting of the device. Recording of this information is left to clinical staff as part of the documentation checklist. Otherwise, it is a reliable indicator of surgical time but gives little detailed data for analysis.

Many new surgical applications have inbuilt clocks due to the presence of a computer. Through automation of this process, a number of variables can be recorded without any direct impact on the surgery during observation. However, this will limit the recording of actions and time to when the systems are being used. For example, during Laparoscopic surgery with the da Vinci system, all but the initial preparation and final completion are fulfilled with the robot and hence, can be recorded automatically. In orthopaedics, however, there are numerous actions that are performed with manual instruments and would otherwise not involve a time stamp in an automated system. Additionally, the software to manage time analysis would require validation and CE marking to be included as an inherent tool of the system. If this is not present from the beginning, it is difficult to add this to the proprietary software.

Given a clinical application the presence of observers are not always appropriate (Burke et al., 2000). Video recording in this environment is a very sensitive issue as well, giving rise to complications of ethical approval and legal issues. Automated action recognition from a video recording is highly complex. Gesture recognition is one of these methods monitoring movements of the surgeons and interactions with different pieces of equipment. The scope of Gesture recognition analysis is appropriate for this application as indicated by current research (Cavallo et al., 2013).

Once a specified means of collecting this data is decided upon, analysis and data mining can be performed to provide evidence and answers to given hypotheses and questions. However, caution should be taken when considering associated causes with patient outcomes. Typical postoperative factors are analgesia requirements, transfusion requirements, duration of stay in HDU/ICU, the length of stay in the hospital, morbidity, mortality and cumulative survival. While these are relatively easy to collect and commonly used, these are only indirectly related to patient outcomes (Hopper et al., 2007). Specifically related to arthroplasty are (Bjorgul et al., 2010): time to complete the task, the number of X-rays necessary, the rate of complication, radiological parameters, screw placement, the proportion of satisfactory results, etc. Along these lines, time analysis can only indirectly be related to patient outcomes, and instead has more procedural importance than clinical outcome relevance.

2.2.3 Existing data on the MAKO and similar surgeries.

A number of studies have been produced to review the learning curve of MAKO surgeries (Ballash, 2012; Coon, 2009; Jinnah, 2013; Pearle et al., 2010), along with its main competitor BlueBelt (Pittsburgh, USA). The main focus of these papers are the number of surgeries to achieve a steady state timing for the procedure and standardising efficiency i.e. typical/expected timings for a MAKOplasty procedure. Currently all the published work has been from self-reporting studies from early adopters of the technology. Additionally, this information is not from peer reviewed journals but instead largely from published presentations from conferences and as such should be considered best case scenarios. However, these publications give a general idea of the variability of reporting of time analysis.

The first available information relating to the learning and time analysis of robotic surgery was with the first generation of the system (Coon, 2008), improvements in the current system should be taken into consideration during comparison of this data. The paper presented the average tourniquet times, but there is a clear trend of decreasing tourniquet times to around 40 minutes at what can be considered proficient use of the system.

In a further review of time analysis of the MAKO systems by Jinnah (2009), 5 surgeons performing 244 UKAs with at least 30 surgeries each with the new technology. The surgical time was defined as the time from the insertion of the bone pins to the acceptance of the implant component trials, and was the average for the last 20 cases. Further to this the number of surgeries required to have 2 consecutive and 3 total surgeries completed within the 95% confidence interval of the steady state surgical time of that particular surgeon was also noted. The average surgical time for all surgeries across all surgeons was 59 ± 21min (range: 27min to 165min). The surgeon with the shortest steady state surgical time averaged 43 ± 8min, while the surgeon with the longest steady state surgical time averaged 76 ± 16min. The number of surgeries required to have 2 consecutive surgeries completed within the 95% confidence interval of the steady state surgical time was 7 (range: 4 to 12). The number required to have 3 surgeries completed within the 95% confidence interval of the steady state surgical time was 8 (range: 5 to 13).

The surgical times between half an hour and over 2 and half hours shows massive variability in the ability of the surgeon to complete the surgery. There is no indication of how these numbers were achieved both longest and shortest, whether major faults were observed or if the workflow was particularly slow. Along with this there is no clear definition of steady state and the tolerances that this definition entails. Also then to follow on from this with achieving steady state with 2 of 3 surgeries falling within 95% confidence interval, there is no clear indication as to the confidence

interval that is being established. The nature of the data, this is unlikely to be normally distributed and more likely negatively skewed given the nature of learning curve. Given the lack of information on these confidence intervals it is hard to interpret the number of surgeries to steady state.

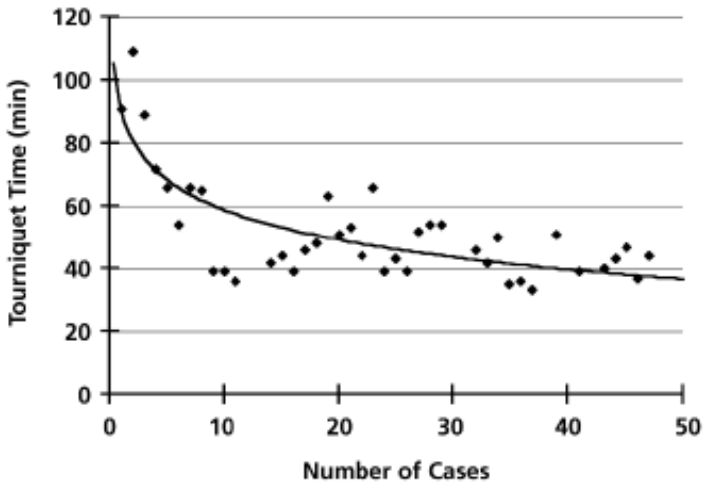

Figure 2.2-1 A typical MAKOplasty learning curve (Jinnah, 2009) showing a decreasing tourniquet time with the numbers of cases completed.

Above is a single sample of a surgeon's performance for the first 50 surgeries and most likely to be an ideal best scenario profile (Jinnah, 2009). Additionally, this is self-reporting which is known to have issues of accuracy. A tourniquet time of <35 minutes is remarkably quick given all the procedural approach required, however these low numbers were also reported in Coon, et al. (2008). Additionally, tourniquet can be released at different times depending on the procedure.

In an additional study presented by Ballash (2012), 892 patients received a UKA by 11 different surgeons with a robotically guided implantation system. Surgeons had performed at least 40 surgeries with the new technology at high volume usage sites. Further information from the presentation showed average surgical time for all surgeries across all surgeons: 56 ± 20 min (range: 22min to 180min); Surgeon with shortest steady state surgical time: 39 ± 9 min; Surgeon with longest steady state surgical time: 64 ± 16 min. No explanation can be derived from the presentation as to the disparities between the surgeons.

Similarly, when reviewing the number of cases performed by the surgeons Ballash (2012) suggests there could be decreasing average of the steady state time. From this data it could be suggest that both the frequency and total number of surgeries have an influence on the skin time metric. While Ballash (2012) showed some trend with increase cases leading to low steady states, two users achieve quicker steady states in fewer cases than the other users. In more detailed breakdown of the data, two surgeons, show a steady learning curve with similar case surgical time. The third surgeon seemed to slow extremely quickly for the initial first 20 cases, and then increase to

a higher surgical time, representing more caution in the workflow. Furthermore, the variance of the time is quite significant even after steady state is achieved, with a minimum to maximum range of 40-60 minutes.

Similarly, in the same presentation two surgeon's surgical times were compared (Ballash, 2012). The work flows were divided into a list of tasks (full details not available) and the large differences in the time indicated with green arrows. Surgeon A was presented as an experienced proficient surgeon. It was suggested that faster times could be expect for surgeon B as proficiency increases. This methodology would be adapted in the time analysis to allow similar comparisons between surgeons and between different surgical

In a supplementary article Coon (2009) reviews the early adoption of the MAKO system, with improvements from initial surgical times of 80-120 minutes to 40 minute in surgeries comparable to the self-reported UKA times mentioned previously. This article was a report from a sponsored consultant of MAKO Surgical.

In a paper reviewing the time taken for the MAKO TGS surgery Pearle (2010) measure different sections of the surgical procedure, reproduced in Table 2.2-2. Of note here is the first review of the time taken to burr during the case. These started at 42.8 minutes and showed a significant learning curve over the next 5 cases, dropping down to 27.3 minutes. This presents data that can be extracted from surgical workflow analysis for specific questions, such as how long does surgical burring stages take and how do these improve with increased number of cases.

Table 2.2-2 Length of time taken specific actions in the MAKO procedure for the first 10 cases with a TGS system. Taken from (Pearle et al., 2010)

Action	Average Time taken for first 10 cases (minutes)
Setup by MPS	41
Intraoperative registration	7.5 (6-13 minutes range)
Burring first 10 cases average Burring first 5 cases Burring next 5 cases	34.8 (18-50 min range) 42.8 minutes 27.3 minutes
Tourniquet time	87.4 (68-113 minutes range)
Operation time first 10 cases Operation time first 5 cases Operation time second 5 cases	132 minutes (118-152 min range) 140 minutes 120 minutes

Comments by Pearle *"consider[ed] it acceptable"* clinical stages to take these lengths of time for a system that was *"being developed and validated"*. The times for the actions above were also

anticipated to further decrease given the learning curve of the first 10 cases. Finally, while the time for the procedure is costly the "*precise bone burring is particularly important"* for future applications of the robotic system (Pearle et al., 2010).

2.2.4 Blue Belt Technologies, Navio times

Simons (Simons and Riches, 2014) presents all the stages measured on saw bones (Attach pins, registration, implant plan, cutting, post holes and total surgical time) apart from the cutting tool setup showed a significant learning curve. With the most significant average time change from the first to last were in the cutting time (41.25 to 22.85 minutes ($p < 0.001$)) and total surgical time (85.4 to 48.25 minutes ($p < 0.001$)) (Simons and Riches, 2014).

2.2.5 Conclusion

Time analysis can be a relatively straightforward means of measuring the proficiency of surgical workflow for different users and procedures. The more detailed analysis of the burring action to highlight possible factors contributing to the fatigue of the users, the most obvious being the length of time burring takes. There is no recognised standard time profile of use for either the MAKO or Oxford procedures, i.e. a proficient user should take X minutes to complete a MAKOplasty procedure. Video based recordings and detailed time analyses will allow for a temporal comparison of the workflows of the surgeons with additional qualitative review of the technique. The qualitative review can be used in examination of the ergonomics of the MAKO system, which is considered in the next section of this literature review.

2.3 Ergonomics

This thesis, as explained earlier, is focused on factors contributing to the increase in fatigue of a user operating the MAKO RIO and borrows methodologies from the wide discipline of ergonomics. Ergonomics is a holistic review of a system, how it works and how this integrates into larger systems and methods of practice. Biomechanics, on the other hand, is a specific field, and a subspecialty when applied in an ergonomic context. Partly, biomechanics reviews the physical limitations of a user/subject, reducing the effectiveness of performing a task. For this reason, a more focused biomechanical approach was taken. However, to contextualise this question other ergonomic reviews were also conducted. Below is a review of how human factors have been applied in the surgical field and how these have influenced the testing stages of this project.

2.3.1 Human Factors in surgery

With a growing array of surgical equipment being developed, robotics being included in this, there has also been an increasing adoption of human factors discipline in surgery, having originated in other fields. Ergonomic reviews of surgery have been focused on specialist fields, such as laparoscopy, with increasing amounts of equipment development to increase the dexterity and manipulability of tools at the surgical site and other associated ergonomic issues (Lawson et al., 2007).

As we have seen from the orthopaedic review, the accuracy of the cuts is an important consideration of the UKA procedure. The design of these robotic systems has understandably prioritised the accuracy of the milling process (Conditt, 2009) instead of a user centred or total design process. However, as has been shown by the user fatigue issue, there are recognised issues with the instruments and their usability to achieve this outcome. Outside of industrial evaluations of these systems, that occasionally become published (Ballash, 2012), there is minimal published information about this assessment of semi-active robotic practice, especially methods that could be implemented at a local scale. Transfer of knowledge is achieved on a local hospital/centre level through observed practice, at conferences through the presentation of practice or at training courses. Additionally, these knowledge transfer practices don't always consider surgical efficiencies, the usability of tooling and efficiency of communication to the same extent as other disciplines, most notably the aviation industry (O'Connor et al., 2012; Sexton et al., 2000). For these reasons, the project aims to review the clinical use of the MAKO RIO system.

With the increasing complexity and quantity of technological equipment being used in the theatre this information is becoming easier and more vital to attain; as the surgical theatre is likely to be an increasing analysed area. Imparting industrial engineering approaches has led to a new

term of achieving a 'lean healthcare' system (Herfarth, 2003). Methodologies such as those developed at Toyota (TPS) (Jimmerson et al., 2005; Weinstock, 2008) are being applied to healthcare.

Orthopaedic surgeons are required to apply forces ranging from maximal grip force to minimal delicate manipulation of tools through a large range of postures. With the range of patient diversity, there is a need for surgeons to move around and position themselves to gain line of sight with the object of interest. Postures can be further limited due to additional clothing, such as the protective headwear and double glove protection (Shih et al., 2001). These factors further complicate comparison and assumptions that can be drawn from other studies that are recorded in other manual jobs to assume working demand. Given the limited knowledge of the physical demands of using these surgical systems this project aims to measure and evaluate how these contribute to the fatigue in users. One novel assessment in this project is the effects the haptic resistance of the robot arm has on the user's movements of the cutting tool.

With Greek etymological roots, haptics is the perception of touch and interaction with objects. When interacting with a virtual environment, haptics is a physical feedback to compliment the visual and auditory senses. There is an increasing prevalence of haptic devices in many fields (Saddik, 2007), especially in medicine (Fager and von Wowern, 2004; Satava and Jones, 1998) and specifically surgery (Banks, 2009; Okamura, 2009). Within systems such as the Da Vinci the slave system fully relies on haptics for textual information about the environment. The bone has an actual resistance to the burr during cutting, it is in addition to this that a virtual haptic boundary of the resection volume is imposed by the robotic arm. In effect this is a superposition of both real world and virtual haptic perception. These resistances are undefined in terms of the force required by the user to manipulate the system. These forces will be defined in the testing lab along with the monitoring of the users.

Assessment and evaluation of the operator handle is a fundamental component in the human system interaction. Other literature approaches have evaluated these interaction points through biomechanical assessment tool including; Optical tracking (Boyer et al., 2013; Choi et al., 2010; De Magistris et al., 2013), EMG (Böhlemann et al., 1994; Mirka et al., 2002), force information (Boyer et al., 2013; De Magistris et al., 2013), modelling [force (Choi et al., 2010; De Magistris et al., 2013), endurance (Gnaneswaran, 2010; Gnaneswaran et al., 2013)] and subjective questionnaires (Hsia and Drury, 1986; Li and Yu, 2011; Mirka et al., 2002). These have been developed largely for industrial evaluation, however there is a growing interest in applying these evaluations to the healthcare field.

All of these methods are applied in the laboratory testing of the users moving the robotic arm in the haptic cutting boundaries to monitor use and signs of fatigue.

There have been no reported cases of localised fatigue resulting in clinical complication or a failure to complete a surgery, but fatigue of the operator is obviously unwelcome. In the context of ergonomics and work physiology, muscle fatigue is defined as any exercise-induced reduction in the maximal capacity to generate force or power (Lin et al., 2004; Vøllestad, 1997). This leads to a reduction in the surgeon's fine motor control and, hence, a reduced precision of the surgeon's hand movement (Slack et al., 2008).

Fatigue is a very subjective term and is defined here through localised muscle fatigue and its associated discomfort as an indicator. While there are clinical measures of fatigue (Chalder et al., 1993) these were not suitable or specific enough for the targeted research that was being carried out here and hence a recognised discomfort scale was used. In addition to this electromyography (EMG) was implemented to further indicate the muscle groups that were fatiguing and provide a validation for the biomechanical model. These methods are explored more in section 2.5 Fatigue of this chapter.

Kahol (2008) presented the effect of central fatigue affecting the cognitive abilities of surgeons, while this is not the type of fatigue that is being studied here this is an indication of the impact on surgery that fatigue can have and hence fatigue should always be limited as much as possible (Kahol et al., 2008).

Roberts (2007) reports that, outside of robotic surgery, orthopaedic surgeons tool use can exceed 26 minutes. These timings could increase with different procedures. Especially surgeries such as bi-compartmental, tri-compartmental and totals that involve different numbers and complexities of bone cuts. An understanding of typical trigger times for different knee arthroplasty would give an understanding of typical usage at the moment. This is one of the main reporting points of the time analysis. A key understanding of the use of the system can be achieved through a detailed time analysis of a system.

"Symptoms which were statistically more prevalent in orthopaedic surgeons were tingling of fingers while working, and numbness in fingers while working" (Roberts et al., 2007). Although there is no confirmed link to this condition in relation to vibrations of power tools, excessive vibration such as those seen when using heavy industrial equipment has been shown to have an increased likelihood of developing work-related musculoskeletal disorders (WMSD) (Bovenzi et al., 1991). In plant workers, disorders have an increased risk in highly repetitive actions (example: < 30 second

cycles, 50% of work time spent doing tasks) (Silverstein et al., 1986), and further compounded by higher forces (>4kg at the hand) and sex (females with a higher risk). Appreciation of the surgical workflow and actions are required to ensure that these systems are unlikely to result in WMSDs, as defined by forces and repetition.

Questionnaires and observations are the most common method of recognition in relation to usability, but a collection of this data is difficult for a larger population group about sensorineural symptoms (Kuorinka et al., 1987; Roberts et al., 2007). A similar result could be expected from a smaller MAKO RIO population group (Ballash, 2012), but any conclusions would be difficult to show as significant.

Roberts (2007) even calls for an in vivo risk assessment evaluation of orthopaedic power tools based on the recommendations of the European Directive 2002/44/EC in vivo testing of orthopaedic tools. This request further emphasises the limited assessment of these processes that are currently being carried out. With the increasing demand on the healthcare system, these issues are likely to become more prevalent.

2.3.2 Conclusion

There is a growing interest in the application of ergonomics assessment to surgery. This project attempts to develop a blueprint for such an evaluation, in particular, the relation to the robotic orthopaedic surgery using a burr and the biomechanical limitations relating to the fatigue of the hand and upper arm. Techniques for objectively detecting this physiological change in these muscles must also be reviewed to design the experimental setup of the project. The remaining sections of this literature review set out the proposed approach, starting with the anatomy and biomechanics of the upper limb.

2.4 The upper limb

To understand the ergonomic design issues, appreciation of both the abilities and limitations of the upper limb must be realised. The hand is the effector of the upper limb that interacts with the robotic arm through the handle, but it is through the structure of the rest of the limb that enables the hand.

The hand of the user holds and manipulates the handle of the robotic system. An important factor in this interface is the handle design. The handle function can largely be designed for the typical forces that will be applied to it. For the robotic system gripping and turning, along with pushing, pulling, pressing and lifting are the main forces of interest. How these forces are produced and affected by posture and handle design is reviewed in this section.

2.4.1 The hand

The hand is an integral component of a human's ability to engage with their surroundings through fine articulations of the hand for subtle manipulations and gestural expression. With sensitive ends, the hand can be a tactile sensory view of the world. To compliment this the hand, being the end effector of the arm, is also required to create and maintain large force transfer in prehension tasks such as carrying and body support (Nordin and H. Frankel, 2012). While the hand is versatile, these actions are difficult to enact at the same time.

An anatomical understanding of the structures of the hand is important for an appreciation of the function of the joints (Pheasant, 1996). The upper extremity is made of 37 joints with 11 degrees of freedom from the shoulder to a single fingertip. While all joints in the upper arm contribute to the positioning of the fingers, the wrists position has a large effect on the force generation of the digital muscles due to the interaction of both muscular and bone structures (Amis, 1990; Nordin and H. Frankel, 2012).

2.4.1.1 Boney Structures

The complex structure of the wrist allows for the range of motion and stability of the joint for the function of the fingers. The osseous structure of the hand is made of 28 bones, in the palm alone there are 19 bones with 14 joints. These form the semi-rigid framework to allow the flexibility and dexterity of the wrist, hand and fingers. The stable segment of the hand is formed by the distal row of carpal bones along with the second and third metacarpals. As the name suggests these form a relatively fixed structure with minimal movements between the bones. The remaining metacarpals and phalanges make up the dexterous mobile segment.

The soft tissues structures of the wrist cross the joint attaching the distal ends of the radius and ulnar to the carpal bones.

These passive structures maintain the stable segments and integrity of the joints through limiting the range of motion to varying degrees. Some joints, such as the wrist and phalangeal joints, are allowed to articulate, while the carpal joints are more secure with minimal motion between the bones. Defining rigid and non-rigid structure in the hand is important for accurate tracking, as described later in the thesis. Further detail of the anatomy and basic biomechanics of the wrist can be found in (Berger, 1996)

2.4.1.2 No force state of the hand

Figure 2.4-1 demonstrates the natural position of the hand to fall given no muscular activity. The soft tissues give rise to three recognised arches in the hand that allow within-the-hand congruency and manipulation. At this point the passive structures of the hand are maintaining its posture and as such should have reduced muscle activity, minimising fatigue (Choi et al., 2010) and enabling recovery. Similarly, any deviation away from this posture will require activity either from external forces, or the intrinsic and extrinsic muscles of the hand.

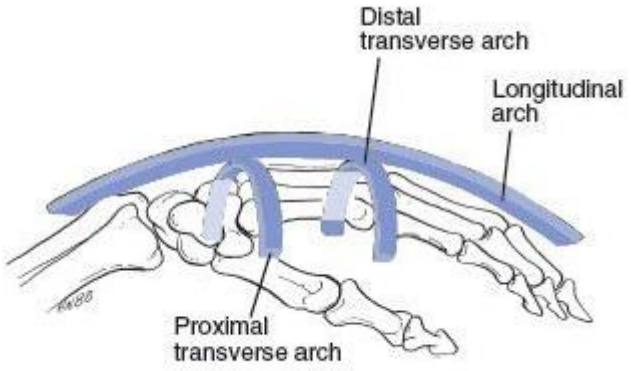

Figure 2.4-1 Passive posture of the wrist Image from (Nordin and H. Frankel, 2012) and (E.E.F. et al., 2005). The posture is the result of the soft and hard tissue resisting gravity passively and hence no energy is consumed.

The passive posture of the fingers and wrist has also been shown to change with the change in joint angles of the shoulder and elbow (Lee and Jung, 2014). This paper highlights the importance of the definition of a 'resting' position of the hand when considered in the design and also the inter-relationship of the structure of the whole arm.

2.4.1.3 Muscle

Functionally, the proximal segments of the upper extremity carry the large, high force generating muscles, while the distal ends carry the more dexterous muscle groups. Similarly, the muscles that

move the hand and fingers can be grouped into two groups (intrinsic and extrinsic). The 20 extrinsic muscles are mostly located near the elbow and act across multiple articulating joints articulating. These muscles create the large forces and gross movements required for heavier functional tasks. The other group of muscles are the intrinsic group, made up of 19 muscles. These, as the name suggests, are the muscles confined within the hand and control the fine movements of the hand. These muscles are much smaller and so cannot produce the same levels of force as the extrinsic muscle groups, but instead are responsible for the alignment of the digits for the extrinsic muscles. Hence, both are required for the controlled movements and control of prehensile and nonprehensile tasks of the hand. A table of muscles and action can be found in (Nordin and H. Frankel, 2012) for further details. By understanding the functional action of muscles these can be targeted by EMG electrode positioning to estimate the muscular demand.

Many of the muscle's actions are across multiple joints. When considering these in postural co-contractual combinations of activity there are many different possible combinations, yet due to some inherently shared control systems, the healthy populous as a whole perform fairly standardised movements and means of interacting with objects. These actions can be further refined for efficiency during repetition and the learning process. These more efficient states rely more on the passive structure of the hand (capsules, bursa and ligaments) for postural maintenance, along with minimised forces to reduce energy requirements.

As reviewed in (Everett and Kell, 2010), muscle function is affected by the anatomy of the muscle and its surrounding tissue structures. The fibre type makeup of muscle, physiological cross-section area, the angle of pull, length-tension relationship, the stable anatomical base of support and the sequence and pattern of muscle stimulation all affect force production. The most effective conditions for producing forces are reviewed in the following sections.

2.4.1.4 Movement in the upper extremity

2.4.1.4.1 Degrees of Freedom

Standard anatomical terms describe the position and movement of the forearm, wrist and hand. The wrist's circumduction movements can be captured in a conical shape with the tip at the wrist. The wrist's three planes describe the movements of the wrist, shown in Figure 2.4-2.

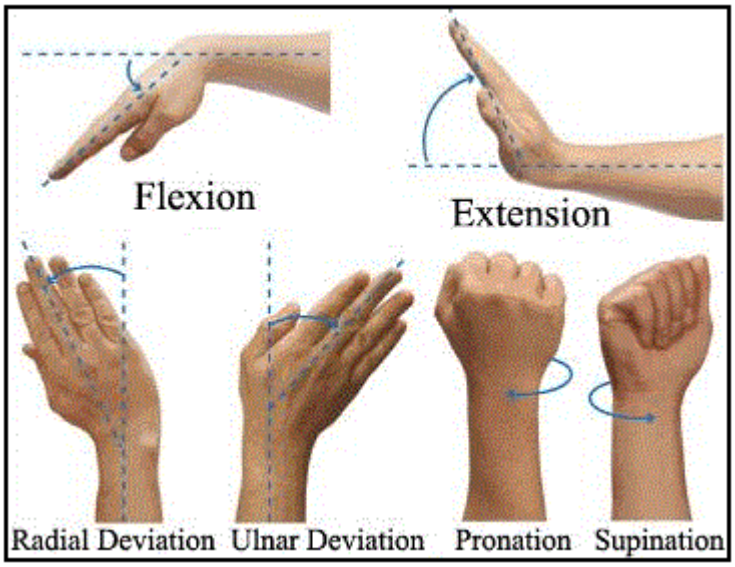

Figure 2.4-2 Degrees of freedom of the hand in all three planes and shown at the limits of the range of motion along with angle measures from neutral in blue.

A model by Youm et al. (1978) for the range of motion places the centre of rotation at the head of the capitate. The primary flexion-extension axis if defined between the radial and ulnar styloid processes, the pronation-supination axis is defined from the joint centre to the elbow centre, with an axis orthogonal to these defining the radial and ulnar deviation axis.

Pronation and supination by definition do not occur at the wrist, which has no inherent rotation in this axis. In this project, however, Pro/supination is defined as wrist movements as it is calculated from the wrist anatomy about the elbow. Please see Optitrack methodology for further details (6.2.3.1).

Ulnar deviation is also referred to as adduction of the wrist, while radial deviation alternative name is the abduction of the wrist. Deviations will be used as standard throughout this thesis.

2.4.1.4.2 Range of motion

The range of motion is a function of the articulating surfaces and tension surrounding soft tissues. Below is a revised list of the active ranges of motion for the upper extremity for a healthy population.

Table 2.4-1 Active range of motion of the upper extremity joints as defined in the literature

Shoulder	Abduction	165.7 ± 5.8 (Gunal et al., 1996)
	Adduction	48.8 + 6.0 (Gunal et al., 1996)
	Internal	95.5 ± 12.6 (Gunal et al., 1996)
	External	65.9 ± 9.4 (Gunal et al., 1996)
	Flexion	116.7 ±8.6 Horizontal (Gunal et al., 1996)
	Extension	27.7±11.0 6 Horizontal (Gunal et al., 1996)
Elbow	Flexion	140.0 ± 5.6(Gunal et al., 1996)
	Extension	182.8 ± 5.1(Gunal et al., 1996)
	Supination	86.5 ± 8.3(Gunal et al., 1996) 85-90 (Magee, 2008)
	Pronation	90.4 ± 12.0(Gunal et al., 1996) 85-90 (Magee, 2008)
Wrist	Flexion	55-75 (Nordin and H. Frankel, 2012) 80 to 90 (Magee, 2008)
	Extension	59.4 ± 6.2(Gunal et al., 1996) 70 to 90 (Magee, 2008)
	Radial Dev	17.6 ± 6.7(Gunal et al., 1996) 15 (Magee, 2008)
	Ulnar Deviation	35-40 (Nordin and H. Frankel, 2012) 30-45 (Magee, 2008)

As presented by Marshall et al. (1999), the range of motion of the wrist is a complex given the posture of the proximal joints. Highlighted are the inter-relations of rotation angles, in the neutral plane the wrist can deviate over 20 degrees, but this is significantly reduced with the wrist in flexion. This underlines the complexity of the movements of the wrist and also the consideration of the proportion of the range of motion used for given tasks. Ideally, actions should be optimised for the functional hand posture and avoid extremities of the range of motion.

Following this principal, there will be postures best suited for minimising energy consumption and also for mechanical advantages of muscles. One position is the functional position of the hand.

2.4.1.5 Functional position of the hand

The posture is between 20 and 35° wrist extension with ulnar deviation of 10 to 15° (Lannin et al., 2003; Pendleton, 2012). Soft tissues in this position are optimised, for example, the effects of the extensor muscles and tendons on finger flexion are limited, such that effective grips can be produced. Deviation from this position, such as extreme flexion of the wrist due to insufficiencies in the passive extensor structures reduces the ability of the fingers to flex. This position is maintained

for extended periods after hand surgery to reduce stiffness and contractures (Also known as Intrinsic plus) (Dobson et al., 2011; James, 1962).

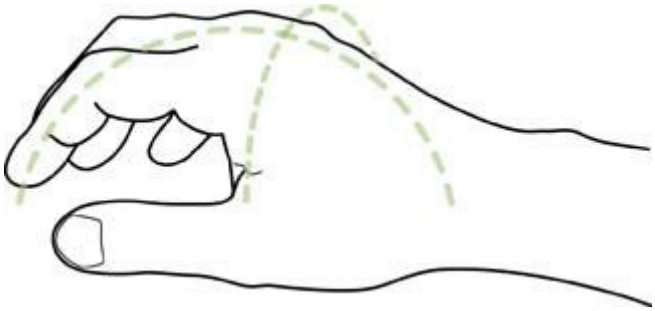

Figure 2.4-3 The functional position of the hand optimising/compromising for all soft tissues.

2.4.1.5.1 Functional range of motion

The functional range of motion is different from the absolute range of motion that is the physical limitations of movements. Instead, the functional range is the range of typical use during daily tasks. These are task dependent but over the battery of tasks evaluated 60 degrees of extension, 54 degrees of flexion, 40 degrees of ulnar deviation, and 17 degrees of radial deviation were required (Ryu et al., 1991). A majority of these tasks only required 70% of the maximal range of motion at the wrist. Hence this paper suggests a normal functional range of 40 degrees each of wrist flexion and extension, and 40 degrees of combined radial-ulnar deviation.

Similarly, Brumfield and Champoux (1984) tested the range of motion for daily living tasks, including personal care and picking up the phone, and found 10 degrees of flexion to 35 degrees of extension were required for optimal completion of these tasks. These daily tasks are more a test of dexterity over strength, but excessive force generation also needs to be avoided.

2.4.1.5.2 Effective range of motion:

Palmer performed 52 typical standardised tasks (Personal hygiene, Culinary, Activities of daily living and task performed by different professions) with an electrode goniometer pinned (Steinmann pins) to the bones of 10 healthy subjects. Of these tasks, 5 represented typical surgical tasks (use a scalpel, scissors, and a needle holder in a uniform manner). The average position of the hand was recorded for these actions was flexion and ulnar deviation, although there was a wide ROM variation. For all the tasks a functional range of motion at the wrist can be limited between 5° flexion to 30° extension, along with 10° radial deviation to 15° ulnar deviation (Palmer et al., 1985).

Magee (2008) further describes the normal wrist, highlighting ulnar drift of the fingers adversely affecting grip strength. Functional ranges of motion of the fingers for grip activities are given below:

Table 2.4-2 Functional finger ranges of motion

Joint	Functional Flexion
Metacarpophalangeal	60°
Proximal interphalangeal	60°
Distal interphalangeal	40°
Thumb Metacarpophalangeal	20°
Thumb Interphalangeal joints	20°

2.4.2 Types of grip

Prehension tasks are of fundamental importance to how a human interacts with its environment and objects. Some of the first definitions of grips were defined by Napier (1956) with the description of both power and precision grips, shown below.

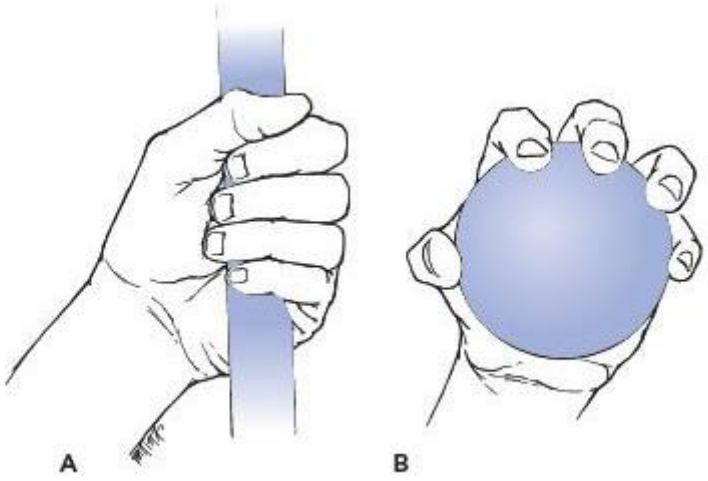

Figure 2.4-4 Taken from (Nordin and H. Frankel, 2012) A. Cylindrical Power grip. B. Spherical precision grip

2.4.2.1 Power Grip vs. Precision grip/handling

A power grip is the forceful grip of an object, usually seen in sports and manual working tasks with handles designed for this purpose. The grip is described by the fingers being bent at all joints with the thumb positioned to create counter pressure, approximately in the plane of the palm. While not always the case the wrist is usually ulnarly deviated to aid the tension action of the flexor muscles aligning the thumb and forearm axes. The fingers, and sometimes the thumb, are used to clamp the object to the palm (Pheasant, 1996).

The precision/handling grips are the alternative positions to those described above for fine, low force manipulation of objects. The fingers are semi-flexed, and the thumb is palmarly abducted and

opposed. The object is manipulated on the pads (tips or sides) of the finger and thumb (Pheasant, 1996).

Grips cannot always be so distinctly placed into either category. The example of a golfing grip shows the compromise of a grip force by placing the thumb along the shaft of the handle from the dorsum of the digits. This instead allows the hand to manipulate the position of the club with greater precision and also maintain a hold on the grip (Nordin and H. Frankel, 2012).

2.4.2.2 Other grips

Other grips such as hook grips are described in the literature as further intermediaries of grip descriptions. Additionally, when the main contact points only consider the digits of the hand, these can be described through tripod and pinch grips. While some pinches can still be considered 'power pinches' these are producing reduced forces. Key pinch (as to hold a key) averaged 22%, while pulp pinch (Thumb tip to fingertip) averaged 16% of maximum grip (Crosby and Wehbé, 1994). This shows that slight changes in the posture of the fingers in the grip can impact the strength being produced.

2.4.3 Grip Strength:

Hand strength, like other muscle groups, can vary by a factor of 1:3 in able bodies individuals (Pheasant, 1996). Grip strength is a measure of the force being produced at the point in the grip (i.e. fingertips, palms, etc.) to have the desired effect on the objects for the task. For example, a key pinch would be measured between the tip of the thumb and the side of the finger. An alternative example is a power grip would be measured between all the fingers and the palm/thumb. These form complex contact area shapes with hand held tools (El-Khoury et al., 2013; Pérez-González et al., 2013). Grip strengths are often measured for epidemiological studies with specialist/standardised equipment, such as a handheld myometer for power grip strength (Mathiowetz, 2002). This would mean that the forces involved in real world tasks have to be inferred or measured through indirect methods (i.e. EMG, modelling).

Grip strength has been shown to be related to anthropometric measures of BMI (a function of weight and height), age, gender, wrist/arm posture, the presence of gloves, handle size, tool weight, and vibration (Schlüssel et al., 2008). Assuming these can be measured indirectly, an understanding of the variability of grip strength give further context to the effort required for a task.

2.4.3.1 Wider population:

Epidemiological data is often used in design to ensure that the wider population can use a system. From having enough strength to perform tasks, to having a large enough hand to hold an object, all demographics will have an influence on the task.

2.4.3.1.1 Age

Within the wider population there is a distribution of strengths in healthy individuals showing a decrease in grip strength with age >40 in women and >50 in men. Additionally, BMI was associated with hand grip strength for all age groups, but only underweight males should a significant difference (Schlüssel et al., 2008). Similar trends are also shown in Peters et al. (2011).

2.4.3.1.2 Gender

Mean maximum grip for mean 41.77kg in men and 25.20kg in women (Hong Han et al., 2011). Or as an average for the populations 44.66kg (Gilbertson and Barber-Lomax, 1994). Peters et al. (2011) shows a decrease in grip strength for age > 50 years, in both male and female populations.

(Crosby and Wehbé, 1994) reported mean maximum grip strength of 137 lb (62.1 kg). However, this is shown to be much higher than would be expected from the other journal, and should be taken with caution. But this does highlight the variability in this measure within a population, with the 5th percentile showing approximately 80% of average grip strength (Peters et al., 2011).

2.4.3.2 Surgeons

A group of orthopaedic surgeon's grip strength was presented as 47.25 kg (Subramanian et al., 2011). Their strength was shown to be statistically higher than anaesthetic counterparts, but given the manual demands from orthopaedic surgery this is only just higher than the population average in Gilbertson (1994) (44.66kg) and is not higher than the population median in Peters et al (2011) (47.25kg = 104 Pounds). Assuming these are majoritively male, this is below the male average in Crosby et al. (1994) and higher than Hong Han (2011). This would suggest that surgeons are average, if not slightly higher, when compared to the wider population.

US surgical consultants are on average 50.9 years (or a range 41-55),or 47.5 years in an AAOS census ("Orthopaedic Surgeon Census - AAOS," 2004). This age is the point at which there is starting of a decline in grip strength, having risen to this point with age. There is not a large change in normal healthy individuals grip strength between 20 and 60. From this it can be assumed that age should not be a major factor in the physical abilities of surgeons.

More significant is the difference between male and female. While orthopaedic surgeons are in a majority male, the female profile should be used to define the minimal strength profile of the working population with a mean grip strength 60% of the male mean. A 95 percentile inclusion of the male profile would exclude a majority of the female grip strength profile from Peters et al (2011). Strength is by no means a prerequisite for orthopaedic surgery, or even successful clinical

outcomes. However, the design must be assessable to wider population demographics with strength being a major factor in muscle endurance and hence fatigue.

2.4.3.3 Grip Coordination

When considering the force required to maintain a grip there are observations that the force used is higher than is actually required. This is to allow for perturbations of the system that could knock the object out of the grip. A user should look to minimise these grips when possible, however this is very much a question of experience to appreciate potential perturbations. As will be shown in the following sections the force generation is highly variable with contact points, posture and contact material.

2.4.3.4 Presence of gloves

Gloves are a recognised personal protection equipment in many fields, but in surgery this has the added requirement of sterility for the surgical site. Tactility is important in the feedback mechanism of the interaction of the hand and an object. The presence of gloves are shown to decrease this tactility, decreasing maximal (Buhman et al., 2000) and increasing overall submaximal (Willms et al., 2009) grip force production in industrial gloves. While some gloves increase the friction between surface, latex gloves over multiple layers reduce the friction below that of bare skin on the hand. In lifting tasks (Shih et al., 2001), this was shown to increase the submaximal forces applied. In a static maximal fatigue studies gloves were shown to decrease the grip strength, but this had no effect on the endurance times of the muscles (Shih, 2007). This is another variable to be considered in defining the resulting fatigue in the users of the MAKO RIO system.

2.4.3.5 Grip generation

While a large amount of force is applied to the palm, the fingers are the active force generators between the hand and the object. When reviewing the grip force being produced by the individual fingers it is shown that the larger middle finger contributes the most (28.7%) to the grip due to mechanical advantage over the other fingers (Freivalds, 2004), with the smallest little finger contributing 20.2% when pulling meat hooks. In addition to this the contribution of the phalanges is different when considering the action of the fingers. In a gripping task the distal phalanges contribute more force than the proximal, however in pulling tasks this reverses with the proximal phalanges contributing more force.

Along with this, there are recommendations that the index finger force should not exceed 10N for sustained contraction, and if required to, multiple fingers should produce this force (Freivalds, 2004). The index finger is often used for the compression of buttons and triggers, with 10N measuring at about a third of the fingers strength.

A lateral pinch, seen in Figure 2.4-5, is reported as being significantly lower than the handgrip. From Kumar, this is reported at 7.5 kg for females and 12.5kg in males (Kumar, 2003). For the same group of grip strength was reported as 34kg in females and 64kg in males. 5 participants were used in each female and male groups, and as such present a small sample.

Figure 2.4-5 Lateral Pinch. This pinch has a significantly lower strength than those measured in power grips.

2.4.3.6 Grip Strength variation with joints changes

The wrist allows for flexible positioning of the fingers and hand for functional tasks, but also requires stability for large forces to act through the joint. The strong gripping muscles of the hand are positioned in the lower arm and act across the wrist, with the relative length from origins to insertions changing with joint angle. Muscles have a known force-length relationship (Hill, 1938). Hence, changes in wrist position will affect the grip strength.

The main understanding in handle design is that grip strength is greatest in a neutral position, with any deviation away from neutral resulting in a respective decrease in grip strength (Pheasant, 1996). Neutral here is not defined by the 0 angle method, but instead slight extension and 10-20 degrees ulnar deviation. This is due to the different lengths of the carpal bones in the palm. However, there are a number of different views in the literature.

Parvatikar et al. (2009) and Susta and O'Connell (2009) agree that there is a reduction in the grip force away from neutral. Kumar (2004) the strength was also taken at different positions of the elbow and shoulder, but the main observation is that wrist extension results in a drop in grip strength. Similarly, Hallbeck and McMillin (1993) showed that increasing the wrist joint flexion/extension angles >45°, decreases the percentage of maximal/neutral grip force, with flexion having more of an impact. Pryce (1980) showed an increase in grip strength with 15 degrees extension, while Bhardwaj et al. (2011) suggest that extension of the wrist through a cast maintains,

if not slightly increases, the grip strength compared to neutral. Finally, O'Driscoll et al (1992) presents the idea of deviation away from a self-selected position, with a 10-15 change away from this showing a decrease in grip strength. The self-selected position was 35 degrees of extension and 7 degrees of ulnar deviation. With only 15 degrees of extension and neutral deviation, the peak force dropped to 66-75% of maximum. These papers, however, show strength at a limited range of motion.

Along with the sagittal plane, full wrist pronation was shown to decrease grip strength in both men and women, with supination not having an effect (De Smet et al., 1998). Additional loss of grip strength was found in radial deviation (Lamoreaux and Hoffer, 1995; Terrell and Purswell, 1976). Over a dynamic range of motion however, only supination of the wrist above 70 degrees is shown to have an effect on grip strength (LaStayo et al., 1995). However, Hazelton et al. (1975) suggests that wrist position has no effect on the finger flexor action.

Along these similar lines the proximal joints of the upper limb also have an impact. While the ideal, repeatable, posture for grip testing is often referred to as being a neutral wrist and shoulder with a 90 degree flexed elbow, Kattell et al. (1996) observed a peak grip strength at a 135 degree flexed elbow. Further to this a decrement of 42% was seen at extremes of elbow flexion and ulnar deviation.

A model of change in grip strength was proposed below for these deviations from neutral.

$$\% \text{ Grip Strength} = 95.7 + 4.3\ PS + 3.8\ FE - 25.2\ FE^2 - 16.8\ RU^2$$

Here PS, FE and RU give the proportion of the range of motion from neutral (0) to maximal joint angle (1) for the wrist in pronation, flexion and radial deviation respectively (Freivalds, 2004) (Terrell and Purswell, 1970). This is one of the first attempts to model the three planes of the wrist with grip strength. However, as the literature suggests the angles cannot be considered independent from one another, such that more complex models are required to define these (Lee and Zhang, 2005). These models inspired the Anybody application of this project to explore the issues with using these models to calculate the forces indirectly/inversely for these design approaches.

The posture of not only the wrist is important to the generation of the grip strength, with the proximal joints of the arm also having an effect. These studies justify the measuring the joint angle all the way to the shoulder when considering the muscle actions of the arm. The literature review also highlights how ill-defined the abilities of the hand are currently defined.

2.4.4 Wrist Strength

While the grip strength is a means of maintaining a hold of the object for a task, the movements of the object and hand comes from the joints proximal to the hand. Along with grip strength, through a similar mechanism, wrist strength is also shown to change with posture (Delp et al., 1996; Morse et al., 2006). Morse et al. (2006) was a dynamic, isokinetic, test with wrist torque representing flexion/extension torques. Both however, show a peak flexion moment at 40 degrees of flexion in an otherwise neutral wrist.

Overall, the wrist has a higher strength in flexion (Delp et al., 1996; Morse et al., 2006). The remaining wrist torques can be ordered in terms of strength as radial deviation, ulnar deviation and wrist extension. As a ratio the extensors show 50% of the flexor torque, with ulnar deviation presenting 80% of the radial deviation torque (Magee, 2008). Ultimately the wrist is more effective lifting and bringing objects towards the head and body as this is the typical use of the hands for tasks such as eating; heavy objects closer to the body also reduces the moment arm allow for more efficient carrying.

La Delfa (2015) measured four torques (Extension, Flexion, Radial deviation and ulnar deviation) at the wrist in three different postures (neutral, 90° Pronation and 90° supination). These torques were normalised to the neutral forearm rotation to present relative change in the user. Further to this the test group was divided into male and female participants that showed different patterns. While supination was only shown to change grip strength at the extremities of movement, La Delfa (2015) shows that supination at 90° significantly decrease flexion, radial and ulnar deviation in male and similarly wrist deviation in females. However, more significant to this project, pronation of the wrist saw a significant decrease in ulnar deviation torque, and a significant increase in extension torques for the male group.

A neutral wrist allows for a compromise for all wrist movements, and is often designed for to reduce the strain of soft tissues. However, as will be shown, the orientation of the wrist is not always optimised and can lead to limitations in muscle actions.

2.4.5 Elbow Strength

Similarly, the function strength of the elbow is also represented in Guenzkofer et al. (2011). Wrist pronation/supination does not significantly change the moment at the elbow, with elbow flexion having a more significant effect with a maximum between 60 and 90° in extension. Again this is only presented at 5, 30° increments of elbow flexion.

The same paper expands this analysis, plotting both elbow and shoulder flexion against elbow torque (Flexion and Extension). The shoulder profile shows a more significant drop in elbow flexion moments with increased shoulder flexion. Both flexion and extension show maxima at a neutral shoulder posture, the extension torques were 79% of maximum elbow flexion.

2.4.6 Handle Design

Handle design has been a more obvious outcome of ergonomic assessment throughout the years. Given the historical use of tools in manual labour, the use of handles is wide and varied given the number of functions of use. However, the key determinant of the design of a handle is the definition of its purpose. Much of the historical literature is based on maximizing force and power transfer from the user to the object, but the MAKO RIO's design process has been developed to decrease the biological power of a worker with the increasing mechanization and automation of tooling.

Some key principals defined by Pheasant (1996), reviewing Greenberg and Chaffin (1973), and Freivalds (2004), for a good handle design should avoid static muscle loads, awkward wrist and finger postures, tissue compression and repetitive finger movements.

2.4.6.1.1 Handle size

Given the postural effects in the wrist force, the same could be said for finger posture. There is a lot of work determining the optimized grip diameter. According to Eastman Kodak (1983)(Chengular et al., 1983), the recommended diameter for power grip tools is 4 cm (1.5 in) with an acceptable range of 3 to 5 cm (1.25 to 2 in). 4cm is also shown to have the maximal number of cycles before fatigue (Ayoub and Presti, 1971). When reviewed for subjective comfort, force and EMG optimisation an optimal handle diameter is defined anthropometrically as 19.7% of the user's hand length (Kong and Lowe, 2005) when reviewed over 3-5cm diameters. Increasing the diameter of the handle shows a significant decrease in the maximal grip force produced. Consistent with these findings, (Hansen and Hallbeck, 1996) placed interdigital spacers between 0, 4 and 8 mm and showed a decrease in maximal grip strength with increased spacing. In a similar test Eksioglu (2004) the optimal grip relative to the anthropometric measure of the modified thumb crotch length (base of the thumb to the middle finger middle interphalangeal joint) found that the most comfortable, efficient and highest grip was achieved at 2cm smaller than the thumb crotch length for a gripping task.

While grip will be a major factor in this project, it should be noted that; force applied perpendicular to the surface are less affected by the size of the object, and alternatives to high grip forces are high precision tools that require smaller handle sizes of 8 to 16 mm (Pheasant, 1996).

2.4.6.1.2 Handle Shape

For vertical target surfaces pistol grips are recommended, while horizontal surfaces recommend in line handles (Armstrong et al., 1986). The angle of the handle needs to be reflective of the grasp angle to allow for the maintenance of a neutral wrist for strength and control reasons (Freivalds, 2004). Additionally, the shape of the handle needs to reflect the movements that are likely to be used with specific shapes giving preferential biomechanical advantages. For example, in lifting tasks different shaped handles attached to a tote box were assessed for maximum pull force and fatigue endurance. A downward facing tip of a triangle showed the statistically significant highest pulling force, but no difference was found in the fatigue time (Scheller, 1983).

2.4.6.1.3 Vibration

While referenced numerous times in papers, the literature often relates to large heavy industrial equipment (Bovenzi et al., 1991; McGeoch and Gilmour, 2000; Necking et al., 2002) and not the smaller power tools that surgeons use. The effects of vibrations are linked with the degeneration of the muscles, reduced joint function, neural degeneration and even the malalignment of the fibres in the muscles. Exposure to these levels of vibrations was measured in hours (2-4) for jobs such as rock crushing and forestry work. When using certain tools, the vibration led to an increase in the grip force being used for the same task. Additionally, increased frequency lead to further increase in grip force production (RADWIN et al., 1987). Vibration could be an examined issue in orthopaedics, but with current short trigger times these are not resulting in any reported issues.

2.4.6.1.4 Sustained forces

Pheasant (1996) presents in a book chapter guidelines for operational controls. Any force that needs to be continuously exerted for a period of time (undefined in the book) should not exceed 10 to 15% of the maximum strength. These levels are especially critical for regular occupations tasks or when the task is repetitive, with a risk of leading to musculoskeletal disorders. Further limitations from Pheasant states that for short periods of exertion the muscle should not exceed 30% of the maximum strength. Occasional or brief periods should not exceed 60%.

2.4.7 Summary

The wrist and hand are a complex system of tissues. Care needs to be taken to review the use of the upper limb in a holistic fashion when considering functional tasks and limitations in posture, movements and handle design. To try and address all these variable a number of methodologies are to be used to inform, as best as possible, any findings in relation to the user's exertion and indicators of fatigue.

2.5 Fatigue

2.5.1 Introduction

Fatigue and its detection are of fundamental importance to this project. Anecdotal evidence of fatigue in MAKO RIO users requires more definitive proof and understanding of its mechanisms. Up to this point in the review, the factors affecting muscle usage have been explored. On review, there are many different methodologies of detecting fatigue and there are many different kinds of classification of fatigue. These methods, along with an understanding and definition of fatigue for this project, will be presented in this section.

2.5.2 Muscle function

Muscles are the functional mechanical units of the body and whose activity accounts for much of the body's energy consumption. Limitation in supply or depletion of resources will result in what is defined as fatigue.

While the skeletal system forms a passive structure of bones and ligaments, it is the muscles that are the actuators of movements and provide maintenance of posture against gravity. These mechanical systems are controlled through a complex, plastic, neurological network of open loop reflexes. In combination fine motor skills can be made, learnt and made more efficient through observation, trial and repetition (Martini et al., 2011).

At a molecular level, the neurological release of acetylcholine (Ach) from the motor end plate results in the depolarisation of the sarcolemma. This wave of depolarisation from the influx of Na^{+} is transferred to the sarcoplasmic reticulum within the muscle fibre and Ca^{2+} is released from the membrane. The calcium ion binds with troponin that is blocking the active site on the myosin head and allows the cross bridging to occur with the tropomyosin. This allows the production of movement from the head movement through the expenditure of ATP.

A single twitch produces a given tension over a short period of time. It is the repeated stimulation of a fibre that results in a usable outcome. The twitch is made of three stages include the stimulation, the contraction, and the relaxation. A stimulation that occurs before the muscle has completely relaxed, resulting in the effect of Treppe in which the tension that is achieved is slightly higher than the previous one due to the increase cross bridging that is present in the muscle. As the stimulations get closer together, these contractions can summate in an incomplete tetanus contraction. Here there is still an element of relaxation and recovery of calcium levels. It is only once the rate of contraction increase over 50Hz that there is no real recovery and a steady tension. The

fibre will reach a maximum tension that is defined by the maximum number of cross-bridges, this state is known as complete tetanus.

While muscle fibres can create tension, it is the control of the entire muscle that is of interest from the physiological and biomechanics point of view. The maximum contraction that a muscle can produce is a summation of all the complete tetanus contractions of all the fibres. The fibres are controlled by individual motor neurones that control multiple fibres, collectively known as a motor unit. During a constant contraction, an asynchronous motor unit stimulation cycles the recruitment of fibres throughout the contraction. Recruitment of motor units is generally on a size basis (Henneman's Principal), with the slower, lower tension fibres initially recruited and then the faster more powerful units. This produces a force activation frequency profile. This principal is important for two reasons; physiologically the small fatigue resistance muscles are recruited first, minimising fatigue in the larger muscles groups. Secondly, this allows fine movements with the low force fibres recruited first that is overall more energy efficient with a smooth recruitment profile.

2.5.3 Physiology of fatigue

Colloquially fatigue is a weakness or pain or a decrement in performance, but these are not definitive enough for suitable quantitative testing (Merletti and Parker, 2004). One of the first recognised studies of specific muscle group fatigue from exertions that do not overtax the cardiovascular system was that of Don Chaffin (1973) that led to the recognition of localised muscle fatigue, or Chaffin's fatigue. His review recognised the effects localised fatigue have on the physiological change in the muscle and impacts on fine motor control, specifically in industrial applications.

Another definition of fatigue can be categorised through a number of different states (Martini et al., 2011):

1. Depletion of metabolic reserves within the muscle fibres
2. Damage to the sarcolemma and sarcoplasmic reticulum
3. Decline in pH within the muscle fibres and the muscle as a whole, decreasing calcium ion binding to troponin and altering enzyme activities
4. A sense of weariness and a reduction in the desire to continue the activity due to the effects of low blood pH and pain on the brain.

These can be placed into larger categories of central and peripheral fatigue. The last point can be considered to be a central fatigue state. However, of more interest here the first three points forming the peripheral fatigue category. These factors are occurring at a localised level to the muscle, with points 1 and 3 forming the acute conditions that directly results from the muscles actions. There are two commonly accepted mechanisms for fatigue as stated by Enoka et al (2011).

The first hypothesis is a question of energy availability to the muscles. As previously described the final energy source of muscle actions is through ATP. Depletion of this and other metabolites (glucose, oxygen and Phosphoryl-Creatine) in the biochemical chain will lead to an inability of the muscle to indefinitely contract.

The second hypothesis is concerned with the build-up of hydrogen ions from by-products such as Lactic acid and Ammonia. These ions affect the extracellular pH balance associated with sodium ion potential across the membrane, reducing excitation and action potential propagation. Additionally, the affinity of calcium to fibre binding sites is reduced, reducing the effectiveness of the contraction. Finally, glycolysis is inhibited affecting the energy supply leading to an exacerbation of hypothesis one.

These hypotheses can be empirically shown through the histological testing of fatigued tissues and the in-vitro introduction of ions. However, understanding of fatigue biochemistry is still limited and debated. Fundamental understanding of these mechanisms are required to appreciate alternative testing methodologies as biochemical, and histological testing is not practical for all applications.

2.5.4 Detection Methods

Fatigue can be seen to manifest itself in three further categories; subjective, objective and electrophysiological (Emam et al., 2001). These categories have come about from methodological differences.

Subjective assessment of fatigue can be observed in psychological parameters such as alertness, mental concentration and motivation. For field applications, these scales are designed for ease of application and reviewed to have correlations with the following alternative detection methods at higher loads (Dedering et al., 1999; Oberg et al., 1994). Subjectively questionnaires report through musculoskeletal disorders(Kuorinka et al., 1987), pain (Borg, 1998) and discomfort scores(Corlett and Bishop, 1976). Specifically, in surgeons, there is a reporting of discomfort as the main result of postural and ergonomic issues with tools and setup (Soueid et al., 2010). In Laparoscopy and endovascular procedures, there are complications with shoulder, back and neck regions reported in subjective questionnaires (Szeto et al., 2009). Similarly, when comparing general and orthopaedic surgery, there is a high prevalence of shoulder and lower back complaints in orthopaedists, with a higher number of complaints in junior surgeons when compared to senior (Mohammad Mirbod et al., 1995). Reported numbers of issues with upper extremities are small and limited to vibrations and tool time usage (Mohammad Mirbod et al., 1995). In comparison with other surgeries, numbness and vibration from tool usage are observably higher in orthopaedics than gynaecologists (Roberts et

al., 2007). The overriding theme in all the papers is a call for more ergonomic considerations in working practice, especially considering long term work related musculoskeletal stress disorders (Liang et al., 2012; Punnett and Wegman, 2004). In addition to the subjective nature of the results, the questioning continuously raises the discomfort issue with the participant, potentially exaggerating receptiveness to discomfort. Questionnaires are also not sensitive to determining a low-grade or unaware feeling of discomfort.

The most straightforward method of detecting the manifestation of Chaffin's fatigue is an objective assessment of performance under isometric ergometrically applied loading, Maximum voluntary contraction for instance (Chaffin, 1973). This required additional testing alongside the assessment task. This mechanical assessment indicates muscular fatigue from an inability to produce a required level of force. But as reviewed by Cifrek (2009), this is not a continuous reflection of the physiological change in the muscle, but should be considered a binary presentation of fatigue in a muscle group at a point of testing. Even if repetitively testing a task until it can no longer be completed, is still only a terminal definition of fatigue of which you cannot assume fatigue prior to termination (Merletti and Parker, 2004).

Finally, electrophysiological assessment of fatigue can, through sEMG, instead offer a non-invasive, in situ, real-time fatigue monitoring of particular muscles performing defined work with the correlation between biochemical and physiological changes in muscles during fatiguing (Cifrek et al., 2009). Historically, fatigue has been measured in the isometric, constant force condition, but there is a growing emphasis on using EMG for dynamic monitoring. However, there are questions about the suitability of dynamic testing of EMG signals (see section 2.7.3).

2.5.5 Conclusion

Muscle fatigue is a complex and subjective change in the physiology of the muscle that results in the change in the ability to control and function. At an extreme, the muscles lose all use resulting in a failure to complete a task. This is not the case here with only an increase in difficulty and/or discomfort being reported. Hence a more continuous and dynamic means of measuring fatigue is required before this terminal point. EMG of muscles in the arm was chosen to be the main indicator of fatigue in the setup, but other methodologies were required for testing in theatres where EMG was not practical. Before reviewing EMG itself, fatigue of the lower arm will be specifically discussed.

2.6 Lower arm fatigue

Given the specific issue with the lower arm and hand, a more specific review of the literature is formed here. There are a number of daily functional work tasks that require the active engagement of the hand and wrist. Fatigue in these cases can, to an extent, be overcome with good design and consideration of the biomechanics of the hand. Muscle fatigue occurs with prolonged or repetitive use of muscle groups, manifesting as weakness and discomfort. The mechanism of this fatigue can be assumed to be a multifactorial process involving the central nervous system, peripheral nervous system, muscle units and individual muscle fibres. With all these possible reasons and the complex anatomy the reporting of fatigue at the hand is difficult to locate and quantify.

2.6.1 Monitoring fatigue

Fatigue with the hand and arm can be monitored through subjective assessment (Borg CR10 (Borg, 1998), NASA-TLX (Hart and Staveland, 2005), Likert scale questionnaire), or physiological assessment (heart rate, oxygen consumption, EMG, consumed endurance (Hincapié-Ramos et al., 2014)). Fatigue is by definition a physiological, biochemical change, but measuring these involve invasive procedures, for example, blood samples, that are hard to justify for monitoring functional task such as those in this study. Many physiological measures have been shown to correlate with these biochemical changes so can be relied upon (Rietjens et al., 2005; Vøllestad, 1997). Less invasive options, while more convenient for testing, have a questionable sensitivity to subjective responses and often require higher sample numbers. A prime example of this analysis is angle based fatigue.

Angle based fatigue is the concept that fatigue can be assumed from finger movements when using handheld computer products (Choi et al., 2010). By tracking the movement of a user interacting with a device, the motion capture data gave a metric for the movement of that joint as a function of the no force state and maximal range of motion. The metric gives a higher value for more difficult movements, i.e. those at the extremity of the range of motion. Within a design process, this metric can be used to avoid these difficult movements. This type of review justifies the application of movement science in ergonomic reviews. While still not validated against recognised other review processes, this is a representation of useful qualitative information that can come from movement science.

Following on from this argument for movement science, the subtlety that can be measured over time and changes in movements can also be measured with these systems (Qin et al., 2014). With a highly repetitive task, there is an expectation for high kinematic variability associated with increasing fatigue. Joint angle variability was analysed through Tukey's paired comparison for 20-minute time

slots. This concept was not explored in this project but is another analysis tool that could be applied to the dataset.

2.6.2 MET – Maximum endurance time:

Along with indication of movement limitations, there are also indications for design practices related to the maximum expectation of use of static muscle contractions along with recovery times. In the case of gripping tasks, for sub-maximal contraction, a maximum endurance time (MET) indices indicate how long these can be maintained. As a review of 24 models Imbeau and Farbos (2006) presents the single compiled model for these expectations. Similarly, Law and Avin (2010) gives a meta-analysis of the endurance time (ET) of joints from a review of the literature. Figure 2.6-1 presents the endurance times as function of contraction intensity (Standardised intensity). Intensities were recorded as values between 0 (0% MVC) and 1 (100% MVC), where 1 represented maximum voluntary intensity. While these are subjective and variable within a populous, these produce indicators for design considerations, especially when considering a continual level of static activity.

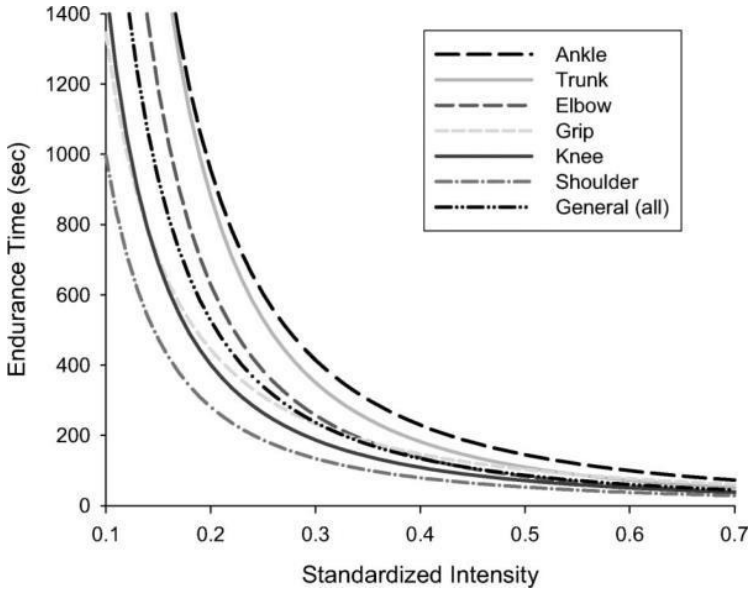

Figure 2.6-1 Maximum endurance time for standardised intensity for a number of different actions (Law and Avin, 2010). Decreasing the intensity of the activity leads to longer endurance times.

Finneran and O'Sullivan (2013) explores the earlier presented analysis of the angle of the joint with the endurance times of pinches and grips. A 50% ROM flexion of the wrist was shown to decrease the Pulp pinch, chuck pinch and power grip endurance. The most significant change was the power grip changing from 77 secs (SD 41.86) to 32 secs (SD 19.93).

2.6.3 Conclusion:

Specific to the task that is being studied here is the grip of the hand to the handle of the robot. Models of expected physical demand need to be measured and compared to population performances to review if the tasks are too demanding. It has already been shown that the angle of the wrist effects the ability to create grip force in the hand, the previous sections showed that this has a direct contribution to the fatigue in the hand as well. From considering the posture of the user, the activity of the muscles and the length of time that the muscles are engaged an understanding of the limitations of users can be applied to the study of fatigue, along with population based design parameters to ensure these issues are minimised. Central to this is EMG, which is described in detail the next section.

2.7 EMG

Electromyography (EMG) is an experimental technique for measuring and analysing the myoelectrical signal. When measured from the surface, these electrical signals are formed from the summation of the motor unit action potentials travelling through the loaded tendons and other tissues. Changes in this signal are a reflection of the physiological and biomechanical variations in the state of the muscle fibre membranes (Basmajian, 1985; Merletti and Parker, 2004).

EMG sits alone as a discipline, but also alongside other biomechanical assessment tools in the assessments of movements and fatigue (Konrad, 2005). EMG itself is not a direct index of fatigue; instead, fatigue is a variable in the EMG signal that requires extraction. Additionally, EMG is a function of multiple physical variables that need to be considered along with the signal. Differing co-activation of antagonistic muscles can produce a redundant range of summated forces and torques. However, the surface EMG signals will vary for the different recruitment patterns. Mechanically alone these muscles create an indeterminate system with a number of combinations to produce a single resultant, it is only through EMG that an indication of the muscle activity can be produced for these systems (Kumar et al., 2002).

2.7.1 Application of EMG

Ergonomic applications of EMG aim to measure the muscle activity and fatigue for problematic areas associated with daily functional tasks (Merletti and Parker, 2004) and work-related musculoskeletal disorders (WMSD) (Gazzoni, 2010; O'Sullivan and Gallwey, 2002; Perez and Buchholz, 2000; Taelman et al., 2006). Many of the studies are trying to reduce the rate of pathologies that can arise from various muscle activity, but also best practice for all work e.g. efficiency of repetitive actions on a production line can be improved.

2.7.1.1 Muscle activity

There are a number of studies that have used EMG to validate muscle activity ("Dimitrova and Dimitrov, 2003; Gil Coury et al., 1998; Hägg et al., 2000; Luttmann et al., 2000), but also warn of caution with the level of interpretation that can be taken from this data. At the simplest level of analysis muscle activity, above or below a threshold limit of the electrical activity can be considered an On/Off state in a muscle. This can be important for measuring the timing of muscles contraction to perform movements; this is extensively used in gait analysis (Berger et al., 1984; Hodges and Bui, 1996). Changes in the timing of the contraction are used as an indicator of pathology and also the changing condition of the muscle.

Taking the EMG signal over a more continuous range of submaximal contractions, an increase in activity could be considered an increase in voluntary muscle activation or effort required by a muscle. In an ideal system, more activation would result in more force, similar to a motor. However as reviewed by Enoka et al. (2011) the force/activity relationship cannot be considered linear or constant.

2.7.1.2 Torque and force estimations

A muscle's main function is to produce tensile forces that, when controlled, will result in the movement of the body. Knowing all the forces and sites of application, a mechanical system for this movement can be calculated. While mechanical properties of these tissues can be calculated from cadaveric samples and make up complex computational models, in situ force measures often require surgical exposure that is destructive to the surrounding tissues and are ethically hard to justify. Instead, the superposition of multiple model systems is used, but as a whole can never be empirically proven. Non-invasive EMG, along with external force measures can be applied to these model system as inputs to get an idea of the motor control strategies involved in completing tasks (Merletti and Parker, 2004). Force and torque measurements and calculations give an insight into the demand placed on all tissues, at the point of action, during daily and working lifetimes.

The active models, such as those in the Anybody modelling software, definition of EMG-torque and force estimation are a point of contention, requiring an sEMG input, as calculations of force or torque are only regressional assumptions. Additionally, due to variability these need to be calibrated for each subject and changed between isometric and dynamic (Gazzoni, 2010). Given the application of EMG to control prosthesis (Manal et al., 2002), as an example, this is an active arm of research (Doorenbosch and Harlaar, 2003; Erdemir et al., 2007; Lloyd and Besier, 2003; Shao et al., 2009), but the current complexity of these models often make the application of these approaches impractical. It is believed by this author that eventually these models will be applicable to fewer exceptional cases and used more routinely for design.

2.7.1.3 Fatigue

Localised muscle fatigue first defined by Chaffin (1973), is manifested as a function change during contraction states, with the inability of muscle to maintain a level of force and sometimes accompanied localised discomfort (Chaffin, 1973). However, this definition is thought to fall short with physiological events leading to fatigue being thought to start with the onset of activity (Bigland-Ritchie and Woods, 1984). To this regard, fatigue should be defined as any decrease in capacity to produce force.

This change in the condition of the muscle, for instant during fatigue, will be shown in the changes of electrical and inferred muscle activity from the EMG signal (Christensen, 1986; Dingwell et al., 2008). From examples in the literature, there are a number of means of analysing the electrical activity to infer muscle activity from the signal; these will be explored in the signal processing section.

2.7.2 Signal processing

The signal processing of an sEMG can give a number of indications of the type of work being done and neurological demands placed on the muscles. Two examples include a force ramp up experiment; a muscle can be seen to increase in voltage amplitude and frequency components with increasing force production (Moritani et al., 1986). Another example of concentric contractions with different joint speeds was shown to vary in mean power frequency (MPF) (Moritani and Muro, 1987).

To capture these characteristics the three main processing techniques that are implemented in this project are normalisation of the EMG signal, Power spectrum density functions and amplitude characteristics of the EMG. Many more detection, processing, and classification methods can be found in the literature (Raez et al., 2006).

2.7.2.1 EMG Normalisation

The first, amplitude normalisation, is a means of comparing muscle activity between subjects. Given the differences in sizes of motor units, their relative distance from the surface (and hence electrode), and the impedance variations this amplitude cannot be considered an absolute measure of activity. Instead, the signal must be considered a relative signal, requiring normalisation to a signal expressed during a standardised and reproducible condition, often the maximum voluntary contraction (Farina et al., 2010; Sousa and Tavares, 2012).

A common process for EMG signals is for normalisation from a static (isometric) maximal voluntary contraction (MVC) taken before testing (Konrad, 2005). Normalisation is important for the comparison of different users as to the neuromuscular effort being required to perform the task. Similarly, this also gives a means of comparison of tasks for demand as a percentage of maximum activity.

The main drawback with these systems, similar to the rest of EMG applications, is that we must assume the electrode is measuring the optimal signal (Konrad, 2005) and is not affected by changes in the muscle length due to dynamic movements, motor unit synchronisation increasing the electrical superposition within submaximal movements.

Alternative normalisation methods when MVC is not practical include; amplitude normalisation from the internal mean, Task-specific reference activity (consistent weight or joint torque), Submaximal (Dufour et al., 2013). However, taking these method changes the interpretation of the data.

2.7.2.2 Power spectrum density function

Power spectrum density function (PSDF) converts the EMG signal to the frequency domain through fast Fourier transform (FFT) for static testing and short-time Fourier transformation (STFT) or Choi-Williams distribution (Raez et al., 2006) for dynamic tests. STFT PSDF is one of the most recognised means of detecting fatigue (Phinyomark et al., 2012). Fast (phasic) type two muscle fibre's activity can be observed around 126-250 Hz, while Slow (tonic) type I muscle fibres are around 70-125 Hz. Fatigue is manifested as an increase in the lower frequencies of power density function with the de-recruitment of type II fibres for the same force production. Phinyomark et al. presents (2012) several possible reasons for the changes in the EMG signal, such as the modulation of recruitment firing rate, the grouping and slowing of CV, and synchronisation of the signal (Cj, 1983; Luca, 1979; Viitasalo and Komi, 1977). Others theorised deactivation of fibres specific to tasks to the body making the system more efficient and not always following the size principle of recruitment (Blake and Wakeling, 2014).

There are a number of studies reporting a decrease of the mean and median frequencies of this power spectrum (Al Zaman et al., 2007; Blackwell et al., 1999; Clancy et al., 2008; Doix et al., 2013; Farina et al., 2002; Luttmann et al., 2000; Marina et al., 2011; Moritani and Muro, 1987), and this is by no means an extensive list of the studies. However, there is still no standardized approach to this problem with a number of variables still resulting in inconclusive outcomes (Joint angle, % MVC force, filters, Skin thickness, inter-electrode distance, muscle fibre content, electrode location) (Phinyomark et al., 2012), despite standards being set for the reporting of EMG outcomes (Merletti and Di Torino, 1999). Hence, the area is still under development and growing in the number of possible applications.

Mean frequency is defined as the sum of the product of the EMG power spectrum and the frequency divided by the total sum of the power spectrum.

$$MNF = \sum_{j=1}^{M} f_j P_j \Big/ \sum_{j=1}^{M} P_j \,,$$

Here f_j is the frequency value of EMG power spectrum at the frequency bin j, P_j is the EMG power spectrum at the frequency bin j, and M is the length of frequency bin (Phinyomark et al., 2012).

While the median frequency splits the PSD into two equal regions with the same area, the median frequency is generally slightly higher than the mean, given the skewness of the PSD profile, and a higher variance. However, the estimation of the median frequency is seen to be less affected by noise and more sensitive to muscle fatigue (Stulen and De Luca, 1981). For this reason, the median frequency is going to be used in this study.

2.7.2.3 Amplitude testing & RMS

The inherent EMG signal is assumed and processed as a zero-mean random (Stochastic) signal whose standard deviation is proportional to the number of motor units firing (Clancy et al., 2002; Kamen and Gabriel, 2010). Signal demodulation removes the noisy neurological signals by a low pass cut off filter, so as to describe an assumed muscle response. These new profiles are processed for the area, slope and other characteristics that are more intuitive on inspection.

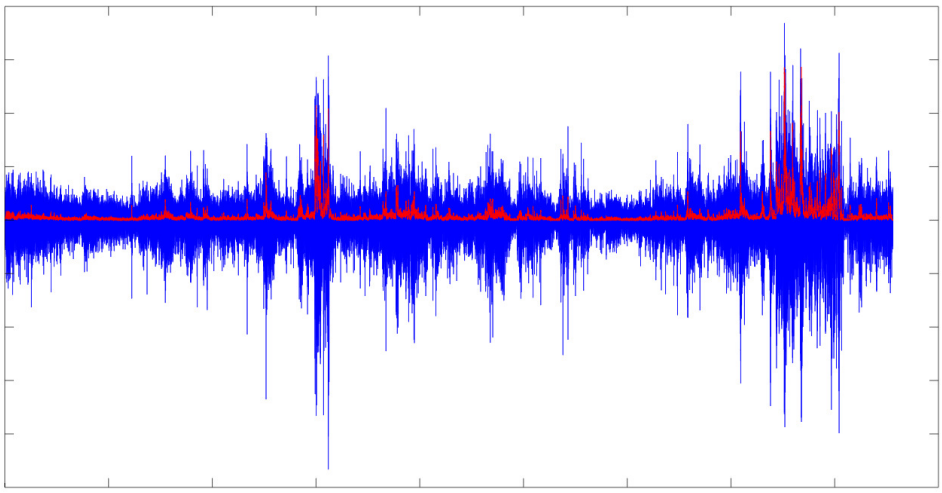

Figure 2.7-1 Typical raw EMG voltage (Blue) with processed RMS (Red). The processed signal is a more intuitive presentation of muscles activity.

Above a raw EMG signal (Blue) has been processed for its RMS amplitude (Red). The windowed samples are squared and averaged.

$$RMS(t) = \sqrt{\frac{1}{T}\sum_{t}^{T} EMG(t)^2}$$

T equals the window length and EMG(t) equals the data within the window. The squaring of the signal, rectifies it for similar interpretation as a full wave rectification, with a single polarity. For this reason, the RMS approach is not affected by the cancellation of positive and negative phases unlike the ARV (Basmajian, 1985; Kamen and Gabriel, 2010).

The amplitude of the signal is the summations of the neural drive of the muscle and is the function of the fibre recruitment, firing rate and conduction velocity. Along with MDF, amplitude measures and root mean square are reported to generally increase during sub-maximal contractions and have generally been shown to increase with fatigue due to decreased muscle fibre propagation velocity (MFPV), increased motor unit (MU) firing rate, increased MU recruitment and increased MU synchronization (Rogers and MacIsaac, 2013).

2.7.2.4 IEMG

Finally, Integrated EMG is an indicator of fatigue in submaximal isometrically contracted muscles. Due to fibre exhaustion the force contribution reduces and requires the recruitment of additional units to maintain the force. This is seen with the increase in the EMG activity of the same force production (Viitasalo and Komi, 1977).

2.7.2.5 Dynamic contraction fatigue

This is not to be confused with the real-time tracking of dynamic movements. Instead, this is the static assessment of fatigue that is a result of dynamic tasks. Many EMG assessments are based on static, short duration (5 min), high force assessments. Changes include increases in EMG amplitude and spectral compression (Basmajian, 1985; Lindstrom et al., 1977; Merletti et al., 1990; Merletti and Lo Conte, 1995; Moritani et al., 1986). However, there are problems when trying to apply these principals to force varying, low MVC (20-30%), dynamic contractions. At low forces unphysiologically high frequencies can be obtained (Clancy et al., 2005; Hof, 1991; Kamen and Gabriel, 2010). Frequency analysis is influenced by joint angles (Matthijsse et al., 1987) and force(MacIsaac et al., 2001). The main solution to these issues is to define short period of time (0.5-1sec) windows that can assume short sense stationary conditions(Kamen and Gabriel, 2010; MacIsaac et al., 2001). This process is explored in the Pseudostatic methodology section (0).

During a 24-hour motorcycle race, riders are known to become fatigue during the demands of acceleration and braking. However, when studied by Marina et al. (2011), only the MVC values and mean amplitude at 50% MVC showed a significant difference. With only an overall trend of decreasing median and mean frequencies were observed. This highlights the difficulty of using EMG indices for defining fatigue in dynamic situations. Similarly, as reported by Clancy et al. (2008) and Eksioglu (2006) for intermittent, long duration contractions, these frequency changes are not always consistently observed.

Practical approaches to reviewing EMG have been reviewed from (Merletti and Parker, 2004) with the application of fatigue indices over varying loading patterns. Fatigue indices are shown to

have poor sensitivity below 20% MVC, and with daily activities ranging from 0-30%. Testing protocols have been suggested to review such tasks.

The first is a submaximal test contraction of a known load during short breaks in the tasks. Similar to the motorcycle race, this requires breaks in the testing that can disturb workflow but allows for controlled static assessment of the muscles. Specialised equipment to control for submaximal contraction along with training is encouraged to ensure consistent results (Konrad, 2005).

The second is the continual spectral and activity monitoring of the EMG signal during activities, defined from Joint analysis of EMG spectral and amplitude (JASA). This process, however, requires a constant load to be applied during the task.

2.7.2.6 JASA

Joint analysis of EMG spectral and amplitude (JASA) allows the change in electrical activity to be either associated with force changes or fatigue with a continual spectral window assessment of the raw EMG. The follow graph is used to represent the time plot:

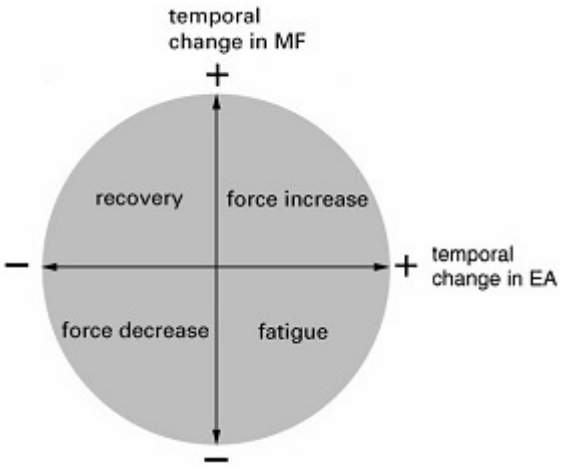

Figure 2.7-2 Schematic of the method of JASA. (Luttmann et al., 2000). Based on the tempral change in median frequency and electrical activity defines which quadrant the result is positioned and the associated description.

For a specific time window a value for the mean electrical activity and spectral analysis can be calculated. The relative change of these values between windows can be further calculated and plotted on Figure 2.7-2. For instance, given an increase in electrical activity (x axis) and a shift to lower frequencies (y axis) in the spectral analysis, fatigue (second quadrant) can be inferred. Similarly, if the electrical activity increases, along with an increase in the median frequency, then a force increase from that muscle can be inferred. Over the testing period, the centroid of the time plot can be calculated and the location of this centroid will define the overall state the muscle can be assumed to have be observed in.

JASA is was developed for the assessment of localised muscular fatigue during urological endoscopy procedures. In its assessment, fatigue was confirmed in 11 of the 14 operations in the right m. trapezius (Luttmann et al., 1996a, 1996b). With this information surgical practices can be changed or justification of additional technology to minimise fatigue in an attempt to reduce the level of risk to the patient.

JASA is a demonstration of the adaptation to the EMG methodologies to create a sensitive EMG fatigue output. These are the only observed uses of JASA, and as such, can be thought to have been an insensitive metric, especially with only one muscle showing any change or indication of fatigue. However, the theoretical setup of the system is in line with the literature on fatigue, so maybe highlights a limitation in the understanding of the EMG fatigue presentation in dynamic tasks. JASA also demonstrates one, of few, real world surgical application of EMG in the theatre.

2.7.3 EMG Limitations

EMG variables are based on a relationship with the complex physiological changes that are occurring in the underlying muscles. While a number of variables have been mentioned, the more recognised issues are presented here.

Due to the nature in which muscles articulate over one another and the conduction of the electrical signal through the layers of tissue, there is a high chance that a signal from an extraneous muscle is superposed. While there are means to neurologically isolate individual muscles, to stop this action, while clinically relevant, this is not a practical testing protocol and not reflective of normal use in these studies (Kumar et al., 2002). Instead, care needs to be taken to ensure that the SNR is reduced with proper electrode placement. Additionally, the surrounding tissues act as a natural filter of higher frequencies, with the effects increasing with depth. For this reason, superficial muscles should be preferred to deeper muscles (Kamen and Gabriel, 2010).

The temperature of the muscles needs to be monitored, as conduction velocities and excitability can be suppressed with decreasing temperatures. Cooling of the muscles can result in decreasing in the spectral frequency analysis that could erroneously be allocated to fatigue (Holewijn and Heus, 1992; Petrofsky and Lind, 1980). Similarly, the increase in temperature of the area and the expression of sweat has been shown to decrease the amplitude, but not spectral frequency, of the EMG (Abdoli-Eramaki et al., 2012).

Surface mounting of the electrodes lacks direct contact and tracking during movements of the muscle, unlike needle electrodes. As the muscle contracts, there are relative 3D movements with the

electrode, creating movement artefacts with the changing conduction characteristics. In cyclical movements, these can be overcome to an extent (Pancherz et al., 1986; Shin and D'Souza, 2010).

In dynamic muscle activity, the assumption of no de-recruitment for a static model no longer stands, as muscles are required to turn off. De-recruitment of fibres can occur at different rates (Blake and Wakeling, 2014) leading to more natural variation during more complex tasks with not only on, but also off timings. Given a repetitive task to complete, it has been shown that the SD of the EMG is higher than that on the isolated force and angle movements signals (Konrad, 2005). Finally, while movements and forces can be characterised as typical, the balancing of antagonistic and synergistic muscles can vary, even outside of the fatiguing conditions. This is the reason for taking a number of repeats or different users to create a typical example of use and also a variation of muscle activity.

While EMG has a number of limitations, it is still the most practical means of measuring the activity of muscles during a task. Large efforts have gone into developing EMG system further through wireless electrodes (Youn and Kim, 2009) with inbuilt accelerometers and IMUs to detect motion. These will further the field's accessibility to more applications.

2.7.4 Force production and EMG signal correlations

There are a number of schools of thoughts as to the relationship between force and EMG signals. While EMG-force relationships can be drawn for individual muscles (Alkner et al., 2000), these models and relationships can only be considered for those specific conditions of testing, generally isometric or slow movements. Air temperature has been shown to have a further effect on this sensitive relationship (Bell, 1993). Regression models for the same muscles at different postures are not consistent. These models are generally considered to be curvilinear/quadratic functions, albeit that some smaller muscles are linearly recruited.

These models, however, do suggest a relationship between the EMG and force so as to define a means of estimating functioning loading of the muscles. Errors have to be estimated for changes in the condition of the muscle. Additionally, for dynamic changes in the muscle output during fatigue, higher levels of activity can be a factor of more mechanical force or more innervation on a fatiguing muscle (Merletti et al., 1991).

2.7.5 Conclusion

EMG is a viable technique for detecting fatigue beyond questionnaires and strength change studies. The signal can be used to monitor assumed physiological changes in the muscle. As well as a number of other techniques to monitor the demand that is being required by a muscle in real time

to give further perspective on the observations of the user. The issues with these setups are the lack of well-defined dynamic tests, with much of the literature recognising isometric testing methodology. There are some dynamic tests that have been proposed as part of a new line of techniques to monitor real-time changes in the muscles without the need to break from the task of interest. From this review, there are a number of methodologies that will be explored in the assessment of fatigue during robotic surgery.

2.8 Motion Capture:

Motion capture is a process of recording the movements of an object or subject. As has already been stated, tracking movements is a fundamental part of time-motion analysis with a potential to indicate bad practice in terms of biomechanical efficiency. There are a number of means of assessing these in the field with video recordings and paper based data capture. However, given the availability of motion capture technology a number of industrial groups are looking to exploit it as a review process (Bandouch et al., 2008; Horejsi, 2013; Tian et al., 2007; Wu et al., 2012). This project explores motion capture as a review tool. Here stereophotogrammetry is applied with the Optitrack system (Corvallis, Oregon, USA). The Optitrack system has no means of calculating the biomechanical joint angles, and so the following reviews the literature of methodologies of taking tracked marker data and calculating biomechanical angles in a biomechanical model.

2.8.1 Optical tracking

There are a number of optical tracking systems that implement a number of different techniques extensively reviewed in the literature (Moeslund and Granum, 2001; Zhou and Hu, 2008). Passive marker optical tracking systems calculate the 3D position of a reflective marker attached to the subject of interest. The cameras emit Infrared light and filter the returning light of other wavelengths from the image to allow an isolation of highly reflective spherical marker material from a 2D image. Markers are separated from the background through thresholding of the light intensity to the camera. Once detected, the isolation of these markers from the background then describes position of a marker relative to the camera. Multiple cameras are required to triangulate the position in the capture volume, usually requiring at least 2 cameras, ideally 3, to be able to view the marker at any one time for 3D reconstruction.

Tracking over time relies on the ability of the system to identify the marker in the new frame. In human motion and ergonomics this is made difficult from:

- Merging markers coming close together
- Occlusion from the cameras
- Large numbers of markers
- Change in lighting conditions
- Highly articulating subject
- None rigid bodies

These issues demand the requirement of a specialised laboratory to minimise their effects.

2.8.2 Biomechanical principles in motion capture

Stereophotogrammetry in human movement analysis looks to describe the instantaneous position and orientation of the underlying skeletal system from markers placed on the skin. A 'body' is described as being rigid if all the points used to describe that body remain at a constant distance to any other point in that body, or that they are rigidly fixed to one another. This is a mathematical abstraction used to model near rigid bodies and a means of simplifying complex systems seen in nature. As points also remain in the same orientation to each other they can be simplified to be described from an origin and a local axis system. Making these axis systems orthonormal allows a number of mathematical behaviours to describe the position of that system in a global reference system and movements in relation to other local frames (Zatsiorsky, 1998a).

By placing multiple markers on a number of different sites on the subject, markers can be assumed to create rigid or semi-rigid structures. The underlying body part, for instance the humerus or Upper arm, can now be defined as a segment with an origin and reference frame. Defining multiple segments allows a description of relative translations and rotation between segments/ local reference frames and the global/reference origin (Cappozzo et al., 1997). The collection of all the segments and joints attaching the segments forms the biomechanical model. Reviewing multiple segments the posture and change in postures on the subject (Moeslund and Granum, 2001) can be calculated in the model output.

The relative position and orientation of a rigid body can be described through the matrix method of a rotational (3x3) and translational (3x1) with a perspective and magnification matrix (1x4) to form a transformation matrix (Zatsiorsky, 1998a).

A rotation matrix defines the rotation of a body relative to a centre of rotation of that body. Given the rotation matrix has 9 unknowns this can be defined by 3 markers defined in a Cartesian reference frame (x, y, z) over two time points. Two methods of producing these rotation matrices have been recognised. The first defines orthonormal unit vectors of the reference frame from marker positions, known as the unit vector matrix. The unit vector matrix defines the rotation matrix from the global reference frame to the local. Through dot product multiplication with another reference frame, time point, or unit vector matrix the relative rotation matrix can be calculated.

A second, more mathematically elegant approach, is defined in (Arun et al., 1987; Challis, 1995), via Kwon[10]. Here the least squared estimation of the transformation parameters is calculated, with the use of single value decomposition. This second method has the benefit of attempting to account

[10] Kwon3d.com. (2017). Computation of the Rotation Matrix. [online] Available at: http://www.kwon3d.com/theory/jkinem/rotmat.html [Accessed 1 Aug. 2017].

for noise in the marker coordinates. Additionally, any number of markers (>2) can define a rigid cluster in this method. Practically it is not viable to have a large number of markers in a cluster, but a significant increase in accuracy with this methodology is seen with an increase from 3 to 4 markers (Challis, 1995). These markers need to be non-collinear to define the rotation parameters. However, the rotation matrix has no anatomical reference frames and so is instead more useful for defining an anatomical point and joint centres as will be seen later.

Currently, the rigid body is defined by a technical reference frame for the first method of rotation matrix definition. Local reference frames require to be orientated relative to anatomical planes, defined by anatomical markers, to have clinical relevance. These markers define both the joint centre and anatomical reference frame relative to the technical frame. This becomes the local coordinate frame of the segment, by defining a transformation matrix from the technical to the anatomical reference frame. Through dot product multiplication of these anatomically relevant segment reference frames,the joint angles can be calculated (Robertson, 2004).

The rotation matrix can then be decomposed into three rotations around 3 orthogonal axes to define any rotation through either Euler/Cardan angles theory, with the translations either being described in the local or global systems. This system is sensitive to the order of rotations about these axes, especially for large rotation (>1 rad). In total 12 different arrangements of rotations can be taken, and given the nature of these rotations the first will be around an axis in the origin system, the third an axis in the destination system and a second defined orthogonal to the other two (Woltring, 1991). Clinically these rotations are described through rotations about the three anatomical planes of the body (Cole et al., 1993). Given a 'correct' sequence of rotation, biomechanically recommended axes and rotation order are defined in (Wu et al., 2005), the decomposition of the rotation matrix resolve for rotations relative to anatomical axes.

For knee kinematics a joint coordinate systems is described for clarification of a specific Euler angle approach, nullifying the problem with rotation order(Grood and Suntay, 1983). This system uses the axial unit vector from two different segments and define an orthogonal floating axis to create a non-orthogonal reference frame that can be resolved through simple trigonometry.

A special singularity is observed in Gimbal lock where the first and last rotations cannot be individually determined but only defined in sum or difference, effectively losing one degree of freedom. This is observed in Codman paradox (Novotny et al., 2001; Pearl et al., 1992) and requires reference frame consideration or correction when rotations approach 90 or 180 degrees. Fortunately, this is not expected in the current testing, but is an issue with large shoulder rotations.

Centre of rotations

In order to create an anatomical reference frame to describe rotation movements, a centre of rotation has to be defined for all segments. As defined in (Zatsiorsky, 1998a), nominal joints or geometrically ideal joints are assumed to have:

- Pure rotation
- Orthogonal axes of rotation that align to anatomical planes
- Single joint centres

These have no real true application in biomechanics and serve as a simplified assumption of a joint for monitoring gross movement patterns. True joints should be assumed to:

- have joint motion that does not occur about a fixed axis of rotation
- this rotation axis is oblique to one or more anatomic planes
- joint motion involve translation
- the axes of rotation and translation may be different
- the axes are not orthogonal to one another.

Defining the position of the axes of rotation is important for determining the actions of muscles and tendons that are acting across the joints. Even relatively small inaccuracies in the positioning of these joints can lead to larger inaccuracies in calculating moment arms. Within Optical tracking there are two recognised different approach to this, predictive regression models for anthropometric dimensions and functional methods. Within this study the functional methods were developed for the shoulder joint from methods developed and validated for the hip joint.

All of these functional methodologies run under the assumption of planar movements for a nominal joint. This is the assumption that a three-dimensional movement can be described on a plane from at least two points on that segment, as they will produce the same arc. In a biomechanical sense, the assumption that the rotation axis remains relative to this plane will lead to inaccuracies. Taking this axis at instances of time can overcome this assumption and build a trajectory of instantaneous centres of rotation (ICR) that can be built into a centrode. The different methodologies are reviewed below.

Instant rotation in joints, *(Panjabi, 1982 Soudan 1979, Zatsiorsky 1984)*

Due to the complex geometry of articulating surfaces in joints defined by curvature and congruency, there is a movement of the axes of rotation in relations to the geometrical shape of the joint. The more consistent the curvature and higher the congruence the closer the axis is to the geometrical centre of the bones shape. This means that the ICR is not necessarily fixed to any part of the bony material.

Built on the principal that the two perpendicular lines taken from two velocity vectors, at different times during a movement, will intersect at the centre of rotation. Assuming that two consecutive marker positions describe a velocity vector, the principal can be applied to positional data recording in motion capture systems. Data needs to be carefully chosen as an input to this method as it is highly susceptible to measurement errors, leading to ill-defined tangents, and small angles lead to perpendicular distance reaching infinity.

Finite and instantaneous centrodes *(Reuleaux method) (Woltring 1985, Woltring 1990)*

Instantaneous centres of rotation are relative to specific instances of motion and are currently limited to planar motions within the algorithm used. The functional centre of an arc in 2D can be defined by Reuleaux's method as discussed in Zatsiorsky (1998b) that calculates axes of rotation through a finite period. This assumes that a three-dimensional movement can be described on a plane from at least two points on that body if controlled to produce arcs with the same centre. In a biomechanical sense, the assumption that the rotation axis remains relative to this plane has limitations and will lead to inaccuracies. Taking this axis as at finite steps of time can overcome this assumption and build a trajectory of ICR that can be built into a centrode. The Reuleaux method was altered to allow 3D data to be manipulated, but could only define planar arcs well. This method was validated, rotating a marker set around a fixed rotation point and the subsequent radial distances measured both physically and with the optical tracking system. Given that this is a reliable method this has applications in the monitoring of both the RIO, calculating joint centres, and pivoting joints, like the elbow and fingers. The accuracy of the measurements is imperative when estimating the highly sensitive axes of rotation. Normally in biomechanics, multiple sets of the same movements cannot be reproduced, but using the robotic system this limitation can be overcome.

Halvorsen et al. (1999) *(Halvorsen et al., 1999)* [11]

The Halvorsen et al. (1999) method takes finite elements of the movement data to produce the tangential lines, similar to Panjabi. Here the hip joint centre is defined by two frames. Points in these frames are assumed to sit on a sphere, given a static centre of rotation, and from which a line perpendicular to the line connecting the two points and at the mid-point will always pass through the hip joint centre. The main difficulty comes in deciding the frames to compare for a static joint centre, and how to compute this for a functional test.

[11] Kwon3d.com. (2017). Joint Center. [online] Available at: http://www.kwon3d.com/theory/jkinem/jcent.html#hal [Accessed 1 Aug. 2017].

Gamage & Lasenby 2002 (Gamage and Lasenby, 2002)

Gamage and Lasenby (2002) followed on from Halvorsen (1999) with a least square method for finding the centre of rotation and axis of rotation, with better performance than Halvorsen (1999). The system looks to minimise the cost function of the joint centre to the average marker position on a joint. The advantage of this method is that it can handle multiple markers at once. The basic assumption is that the spheres formed by the markers have a common centre (hip joint).

Following on from the centre of rotation calculations described in Gamage and Lasenby (2002), the concept is extended in the 2002 paper and here as well (Hiniduma Udugama Gamage and Lasenby, 2001) to also define the centre of rotation of a hinge joint that is ill-defined as it can mathematically, take any point along the axis of rotation. So both an axis and a point on that axis need to be defined to describe the hinge joint of the upper arm and RIO joints. The axis is an assumed fixed minimum of the distance from all marker trajectories around the same axis.

Halvorsen Compensation 2003

Halvorsen (2003) added a further bias compensation to the Gamage and Lasenby method. Unless they are evenly distributed around the centre of rotation any measurement error will lead to a bias/error, effectively showing sensitivity to measured noise. To overcome this, an iterative approach to compensating for this error is presented in the paper.

Functional centres in the shoulder.

These functional centres were largely applied to the hip joint centre due to the high prevalence of gait analysis. In the shoulder these systems have been tested (Lempereur et al., 2010) and have shown that Gamage and Lasenby gave the least error in a comparison with an MRI position. Considering this and while a further compensation of Gamage and Lasenby have been proposed by Halvorsen with better results, due to added complexity, the initial 2002 methods were used in this project.

2.8.3 History in Medical/life sciences:

While motion capture is more ubiquitously recognised for entertainment applications, motion capture originated in the life sciences and medical field. The ability to track the movements of a subject with minimal physical interference is a great tool for exploitation. James.R. Gage at Gillette Children's hospital was a pioneer in the exposure of the technology to the medical applications, specifically gait analysis in cerebral palsy for multi operative intervention. Gait is often used clinically as it is a good reflection of the ability of the user, given its complexity and use of multiple systems in the body. Additionally, and probably more importantly, gait is a well defined cycle of stages. Mathematically these stages can be averaged and reviewed and compared with 'normal' profiles to

review deviations. Away from these cyclic movements, motion analysis has to rely on further analysis tools for comparing movement, which in terms of ergonomic use of systems is difficult. In this project, a number of different analysis tools are used to describe the movements of users.

2.8.3.1 Surgical application

Robotic surgical systems have brought optical tracking systems into the theatre to allow real time kinematic tracking of patients. This is especially prevalent in orthopaedics given the complex movements of joints in the human body and the ability to track surgical tools in blind minimally invasive surgical openings. With applications such as the MAKO RIO and other systems, there is still a lot of innervation yet to reach the markets and surgical theatres (Cleary et al., 2005; Wolf et al., 2005).

2.8.3.2 Upper arm protocols

The arm needs a high degree of freedom to allow the positioning of the wrist and hand, the functional component of the arm. This leads to difficulty in marker models tracking of the upper arm for all purposes, with many being extensions to lower limb models (Rau et al., 2000). Due to the complex functional nature and high dependence of the joint in daily living, there have been a number of methodologies and reviews (Anglin and Wyss, 2000)(Buckley et al., 1996) on the subject. These range from the methodology of detecting pathology and driving biomechanical models, to comparisons of daily movements. The level of detail and accuracy is reflective of the complexity of the recording methodologies.

Shoulder

The shoulder, the most dynamic joint in the body, is a complex system of bones, muscles and ligaments. Due to this complexity, there are a number of different approaches to define its motion that can be taken with ranging levels of detail (Anglin and Wyss, 2000).

The shoulder can be seen as a movement of the Humerus relative to the thorax in the Thoracohumeral joint. This is a simplified model of the shoulder and does take into account the glenoid movements relative to the thorax (Baker, 2013). Alternatively, the shoulder can be described in movement details through the tracking of the scapula and clavicle to describe both glenohumeral and scapulothoracic movements (van der Helm, 1997). However, large assumptions have to be made with optical tracking systems due to the large skin and subdermal tissue movements and require bone pins or additional imaging to calculate the accurate position and orientation of the skeletal structures.

The centre of rotation of the shoulder is either described through functional testing or through anthropometric regression models for the subjects size and marker position (Williams et al., 2006). The functional method requires an additional calibration stage, but whose accuracy is less reliant on correct marker position. The anthropometric regression model only requires a static pose but require measurement of body segments or additional markers to define subject anthropometrics.

Elbow and Wrist

The elbow is a much simpler joint with both flexion/extension and pronation/supination being described from the hinge joint. As described in (Murgia et al., 2004; Schmidt et al., 1999) a refined marker based system for the description of both elbow and wrist movements, one with triad marker clusters and the other with individual markers. For small movements, the individual markers were observed to be accurate enough for descriptions of daily living.

Similarly, the wrist can be defined as having both flexion/extension and radial/ulnar deviation as degrees of freedom. Given no subsequent joint, the wrist is defined from the position of the hand relative to the wrist joint centre. This requires all degrees of freedom to be described either relative to the wrist or at the hand itself (Schmidt et al., 1999).

Upper extremity models

The description of other segments of the upper extremity create more contextual information about the movement of an activity (Hingtgen et al., 2006; Lobo Prat, 2011; Mackey et al., 2005; Rab et al., 2002; Rau et al., 2000; Slavens and Harris, 2008; Williams et al., 2006). The head, neck, shoulder girdle and pelvis can be added with similar individual markers.

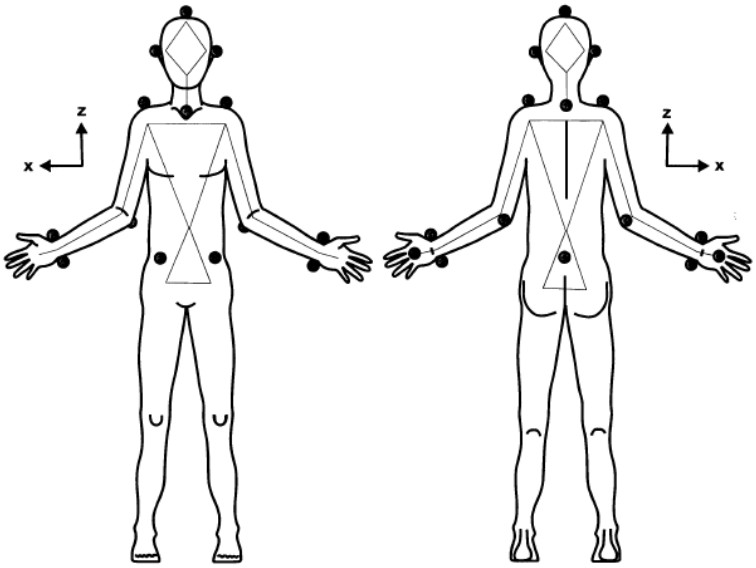

Figure 2.8-1 Reduced motion tracking markers positions for the upper body. Taken from (Rab et al., 2002)

Highly simplified models by Rab et al. (2002) have been validated for upper extremity kinematics. These simplified models present a straightforward testing protocol, but require a number of corrections to account for errors in constraints. An example of this in the above model is a hyperextension of the elbow resulting in the elbow centre flipping to the other side of the elbow marker to maintain a flexion angle. These, therefore, lead to more complicated conditioning and coding to handle these factors.

On review, two models were developed; one for the user using individual anatomical markers, and the second for the MAKO RIO robotic arm using rigid body cluster methods. These are fully defined in the Biomechanics chapter methodology (6.2.3.1).

2.8.4 Optical tracking capture systems:

For recognition of the equipment chosen for this project, a review of the systems available was produced. In the department, the main system used is VICON (Oxford Metrics, Oxford, UK), however, this project was an opportunity to assess a relatively new Optitrack system against an existing system.

VICON

VICON has been used for a number of years of use in medical and life science, allowing its default status as a reference standard. It is often used to compare different motion tracking methods and technologies. The VICON system available in this testing has a higher specification in resolution and frame rate than the Optitrack system (Table 2.8-1).

Optitrack

Optitrack are a new introduction to the field of motion capture. Originally developed for cheaper end entertainment applications, a number of groups (reviewed below) have recognised the system as a more open access, due to pricing, assessment tool for medical and life science applications.

Specification

Within the bioengineering department at Strathclyde, we have been lucky enough to have access to a number of different optical tracking manufacturers and models. Below is a table of the systems available and a comparison of specifications.

Table 2.8-1 All systems currently out and all those currently available in the department.

	VICON[12]					Optitrack[13]	
	T series		Bonita		612	V100:R2 (now Flex 3)	Flex 13
	T160	T40S	B10	B3			
Resolution	16	4	1	0.3	1	0.3	1.3
Max Frame rate at highest resolution	120	515	250	240	120	100	120
Price per camera	£250,000 whole system 12 mixed Camera (Carse et al., 2013)			€5000-7500[14]	£150,000 8 camera (Carse et al., 2013)	$599	$999
Year	2010		2014		1993	2011	2013

Between 1993 and 2014 VICON have developed a number of systems with a range of resolutions and frame rates. The VICON 612 was the standard model in 1993 with a resolution of 1 megapixel. The new Bonita system use the same, or lower, resolution, as do Optitrack, but the cost is dramatically lower. At the top end of the specification list expensive systems are still available, but these have a much higher resolution and frame rate.

Performance of the camera system is an interaction of hardware (lenses, camera sensor resolution) and software (Calibration algorithms and reconstructions algorithms). Hardware deals with the focusing of the image and its detection. Better lenses reduce image distortion and allow larger depths of field, and hence capture volumes, to be in focus. Higher resolutions allow for more detailed data for the detection of markers, increasing the distances a marker can be from a lens and the distance between markers. Improvements to computing hardware have allowed more processing power to be available the software calculations. These calculations have been developed to account for factors such as lens distortions and collocating markers from multiple cameras (e.g. direct linear transformations). Software is often proprietary so much of the development is often not made available, with a black box approach to the data production of the 3D reconstructions from the 2D images captured by the camera.

While there is some comparison literature referenced in the next section, there is little research into the full effect that these specifications have on different uses. While there is still a lot of

[12] Anon, (2017). [online] Available at: http://www.vicon.com/System/Bonita [Accessed 1 Aug. 2017].

[13] OptiTrack. (2017). Compare Cameras. [online] Available at: https://www.naturalpoint.com/optitrack/hardware/compare/ [Accessed 1 Aug. 2017].

[14] Anon, (2017). [online] Available at: http://www.roboticsschool.ethz.ch/airobots/programme/presentations/AIROBOTS_Summerschool_ACXControlFramework_ETH.pdf [Accessed 1 May 2016].

uncertainty as the best means of the calculating of kinematic parameters, the best specification of the camera system is also the most expensive leading to a cost-benefit balance. Typically, a VICON system will cost more for the same hardware specifications, but has a much more recognised and verified software and calculation background.

In animation, there is a call for the increase of the use of cheaper systems for certain applications with small capture volumes and frame rates, and even open source software (Gomide et al., 2011). Keeping appraised on these developments in research and clinical environments could allow this technology to be exploited in more decentralised ways. This is why this work has looked to exploit the cheaper end of the optical tracking environment.

In a comparison with a high end VICON to low end natural point comparison (Carse et al., 2013; Thewlis et al., 2013, 2011) the Optitrack system was seen to have an maximum absolute error of 1.08 mm (0.84%) (Thewlis et al., 2013) and sequential comparative absolute disparity of 1-3mm (Carse et al., 2013). Other multi-system comparisons by Richards (1999) reported dynamics RMS errors of less than 2mm and static RMS errors of less than 1mm. So given more contemporary errors in low-end systems achieving those of systems pre 1999, there is validity in using these systems here for human movement calculations.

The accuracy of all available systems is increasing with the improving technology of not just the camera resolution, but also the algorithms for detecting and subsequent tracking of movement markers. Richards (1999) published results at the time for all system with a specialised motorised platform to measure both static and dynamics (linear and rotational) motions. This is effectively set a standard for validation of systems needing both single measurement accuracy of markers and relative orientation of these markers with one another. At the time dynamic outputs were considered to be good for sub cm marker accuracy with 1 degree angular accuracy. These are now seen as a minimum standard for motion tracking.

2.8.5 Data manipulation and software

There are a number of existing software packages that were available for processing and visualisation of motion capture data MoCap Toolbox (Burger and Toiviainen, 2013), Visual3D[15] or MotionBuilder[16] , and applications that are primarily used for recording data (such as Qualisys Track

[15] C-motion.com. (2017). C-Motion - Biomechanics Products. [online] Available at: http://www.c-motion.com/products/visual3d/ [Accessed 1 Aug. 2017].

[16] Autodesk.com. (2017). 3D Character Animation Software | MotionBuilder| Autodesk. [online] Available at: http://www.autodesk.com/motionbuilder [Accessed 1 Aug. 2017].

Manager[17] or Vicon Nexus[18]). Optitrack Motive enables the capture of 3D coordinate positional data of markers, but at the time of development could only pass the data onto third-party software packages. These packages largely handle the data in the same way as the means in which this project handles the data, however in the pursuit of full control and understanding of the data a MatLab protocol was developed. This allowed open ended manipulation of the data and analysis given the ability to develop the codes along with access to a number of other toolboxes.

2.8.6 Conclusions

One of the additional challenges of this project was to monitor the movement of the user with an alternative capture system to the VICON system. Given the minimal movements of the user this refined system, in the Optitrack system, is viable for this application. With reduced publication interest in the upper arm, when compared to the lower leg, the complexity of the situation becomes apparent. Here the system will run a bespoke algorithm to functionally calibrate the user and robotic arm with a minimal marker set attached to review the movements of both user and robotic arm. This algorithm has been inspired from and applies the calculations that have been reviewed above.

[17] Qualisys.com. (2017). QTM 2.2 is released! | Qualisys. [online] Available at: http://www.qualisys.com/products/software/qtm/ [Accessed 1 Aug. 2017].

[18] VICON. (2017). Nexus Motion Capture Software. [online] Available at: http://www.vicon.com/products/nexus.html [Accessed 1 Aug. 2017]. (VICON, 2017)

2.9 Literature conclusion

While the field of orthopaedic robotics has been research active since the 1980's, the new systems being released show a new invigoration of the field both in research and clinical terms. The number of systems being used in the U.S. is increasing and with the $1.6 billion purchase of MAKO surgical, this shows signs that the market is expected to continue to grow. Within this growing discipline, the increasing information that can be generated by these systems allows scope for greater analysis of use for a means to improve and develop further generations of the systems.

Increasing the efficiency of these systems has both clinical and economic benefits with decreased surgical times and more completed cases in a surgical session. Previously systems have not demonstrated these benefits and were very much a limitation to balance against the increase in accuracy. With analysis and development, the typical surgical times can be reviewed along with what should be considered achievable.

Time analysis has been shown to be a relatively straightforward means of capturing efficiency and the state of learning in the medical, and other fields. Through detailed time analysis, a typical time profile of use could be constructed and assessed for effects of errors on surgical times as well as typical models of use of systems and surgical approaches.

Further, with proposed increased use of these systems, what would be the effect of ergonomic limitations to these systems? Anecdotal reporting of muscle discomfort has already been noted. Current monitoring of surgical ergonomics is limited with reduced exposure of issues due to the sensitive environment that the tasks are being completed in. Ethics can be approved for video recording for research applications, but for more rigorous routine application of these tasks often the resources are not available. If these systems of monitoring could be automated, while not monitoring any sensitive patient information, this kind of analysis could become routine.

Time analysis and biomechanical assessments address two assessable issues with the robotic system that have been identified from the literature and current knowledge. Both these issues require the application of promising novel research methodologies to create a deeper understanding of the limitations of the system. This understanding will aid in the progression of the efficiency, usability and overall design of the current and future robotic systems.

Chapter 3 Research objective and approach

3.1 Research objectives

The overall purpose of this project was to review user fatigue during burring with the MAKO RIO surgical system. A biomechanical approach was proposed to study this, but a number of key objectives were required before an experimental setup could be defined.

Localised fatigue was anecdotally reported during burring from high output users of the MAKO RIO system is an issue (MAKO user preference study summary, August 23, 2010). Given the lack of evidence the first aim was to determine if users are becoming fatigued when using the robotic arm in the clinical application of the system. An observational review of the was conducted with an aim to highlight any indications of fatigue during burring. Notes on possible ergonomic issues with the robotic system were taken, along with unstructured interviews with the surgeons. Finally, a discomfort questionnaire was used for a single surgeon performing three sequential robotic assisted surgeries. This would indicate if fatigue was a compounded issue as a result of high output use of the system.

To add a further qualitative element to this review, detailed time analysis was conducted for the work flow of the MAKOplasty, Oxford unicompartmental and Zimmer NexGen total knee arthroplasty. This work was completed to review surgical efficiency, an extraneous question to this fatigue study, but broke down the timings of bone resection for these three procedures. Localised muscles fatigue, biomechanically, is effected by both duration and intensity of contraction. Through understanding the typical clinical timings of tool use in the robotic assisted surgery and other equivalent manual procedures for a comparison could be performed.

To determine the intensity of contraction as a variable of localised muscles fatigue a biomechanical testing simulation of the surgery was conducted. This aimed to determine the location (muscle groups) and nature of the fatigue in a mock surgical environment. The biomechanical stimulation allowed the use of more sensitive systems (Motion capture, EMG and force transducer) that could not be practically used in surgery. From this data a kinematic, kinetic and electrophysiological assessment of user manipulating the robot could be conducted along with objective measurements of fatigue.

One of the keys factors in ergonomics of tooling is the handle design. Having gone through an ergonomic redesign for the MAKO RIO, a new pistol grip design was developed for the attachment of different tools for different surgical procedures, namely total knee and total hip arthroplasties. The biomechanical assessment was repeated for this new handle design to determine if a handle design was a factor and possible resolution of the development of localised muscle fatigue when burring.

Through an appreciation of observations, time analysis and biomechanical assessment of users manipulating the robotic arm mechanisms for fatigue are proposed. Following validation of these mechanisms, future design considerations can address these issues to minimise the impact on users.

3.2 Thesis structure

To address these different issues, structurally the thesis is split into two experimental sections and a final review section

Section 1 – Clinical Observation (Chapter 4 page 78 & Chapter 5 page 87)

An observational study of the MAKOplasty surgery was carried out in the Glasgow Royal Infirmary during a randomised clinical trial comparing two different implants (MAKO Restoris UKA vs. Biomet Oxford UKA) and insertion techniques (robotic vs. manual/conventional). The surgery was analysed for time and workflow to find a quantified profile of use for the MAKOplasty surgery. Additionally, questionnaire feedback from the surgeons using the system and unstructured interviews of all staff during the procedure was utilised for feedback. This provided an initial understanding of the current typical use of the MAKO RIO system along with the recording of issues with the system.

Section 2 – Biomechanical Testing (Chapter 6 page 93 & 6.4 page 136)

The CROSS (Centre for Robotic Orthopaedic Surgery at Strathclyde) lab at the University of Strathclyde acts as a facility to enable mock surgery to be performed with robotic systems. With biomechanical testing equipment users were assessed for movement, force application to the RIO, muscle activity and localised fatigue. From this, a review of the factors contributing to the fatigue in the user was attained. As part of this analysis, a bespoke testing setup was developed along with proposed new analysis techniques for fatigue measurement, inspired by the literature.

Additionally, a comparative study of the existing handle and a newly developed prototype handle design was carried out. This formed a means of comparing factors that may result in fatigue in the two handles, and to review the feasibility of eliminating or reducing the impact of these issues through the handle design. This would further enhance the ergonomic user friendliness of the RIO system.

Section 3– Overview and discussion (Chapter 8 Page 190)

The final section is a review of the project with a discussion of the results and final understanding taken from the project.

Chapter 4 Observational review of the MAKOplasty procedure

An observational review of the MAKO RIO system was conducted with an aim to highlight signs of fatigue in the users (surgeons) and any other possible ergonomic issues. This was conducted through on-site observations and the analysis of video footage taken in conjunction with an ongoing clinical trial of the robotic arm with access to a team of three research orthopaedic surgeons at the Glasgow Royal Infirmary. The clinical trial was an assessment of surgical accuracy and functional outcomes with a comparison of the Oxford UKA vs. the MAKO Restoris implant procedure (Bell et al., 2016; Blyth et al., 2013; Arman Motesharei et al., 2014).

Operator fatigue had been recognised as a consequence of use of the RIO system in high turnover orthopaedic units where a surgeon may undertake multiple robotic assisted procedures in a day (MAKO user preference study summary, August 23, 2010). The proposed site was not a high turnover site for this specific procedure (1 per day) and as such was not anticipated to have any observed fatigue. If any fatigue was to be recorded this was captured through unstructured interviews with the surgeons or from observed signs of fatigue (stretching, resting).

4.1 Observation aims

The aim of the observation was to answer the following questions:

- Are any observable signs of fatigue shown from the users (surgeons) with low output of the system?
- What are the ergonomic issues with the MAKO RIO system?

4.2 Observation methods

Three surgeons were observed for 37 surgeries, of which 21 were MAKOs (Surgeon 1 11, Surgeon 3 6, and Surgeon 2 4). The MAKOplastys that were observed were within the first 20 MAKOplastys that were performed by the surgeons. While familiar with UKA, the surgeons were considered new to the MAKOplasty procedure. Observations were conducted by an onsite observer (author) and by video recording of the surgeries that were reviewed later.

Additionally, on a single day three surgeries were performed by the same surgeon. Due to this special opportunity of a higher case load, after each of the surgeries a questionnaire was completed to review the reporting of fatigue through discomfort and a usability assessment having just

completed the surgery. Discomfort was reported by body part (area) and on a scale of 1 to 7 (No discomfort to distracting discomfort - Figure 4.2-1). This questionnaire can be found in the (Appendix 4). This discomfort questionnaire was designed to review the potential compounding effects of 3 surgeries as a physical demand on a single surgeon.

Figure 4.2-1 Discomfort questionnaire scoring table

Area (to be filled out)	No discomfort		Mild discomfort			Distracting discomfort		Duration (approx. In minutes)
	1	2	3	4	5	6	7	

4.3 Ergonomic observation of usage of the MAKO RIO system

4.3.1 Posture Observations:

The general observed postures of the surgeons were standing between the patient's legs on the medial side of the operated leg, facing towards the robotics systems screen positions towards the head of the patient (Figure 4.3-1). The stance was a braced leg position during resection and manipulation of the patient's leg to allow for balance during the forceful movements and also permit a line of sight into the joint through the incision. The upper body was required to bend over to manipulate the leg holder and to look into the knee joint. This would then often relax into a more upright position with the feet closer together for the rest of the surgery. The neck was in a flexed and neutral rotation when looking at the knee, and more extended and slightly rotated when viewing the screen. The dominant hand was placed on the robotic arm with the non-dominant hand either assisting in the movement of the arm and burr or used to retract soft tissue. The user's dominant arm was flexed at the shoulder, flexed at the elbow, with a pronated wrist but otherwise near neutral. Further details of more refined movements were restricted from observation due to PPE clothing.

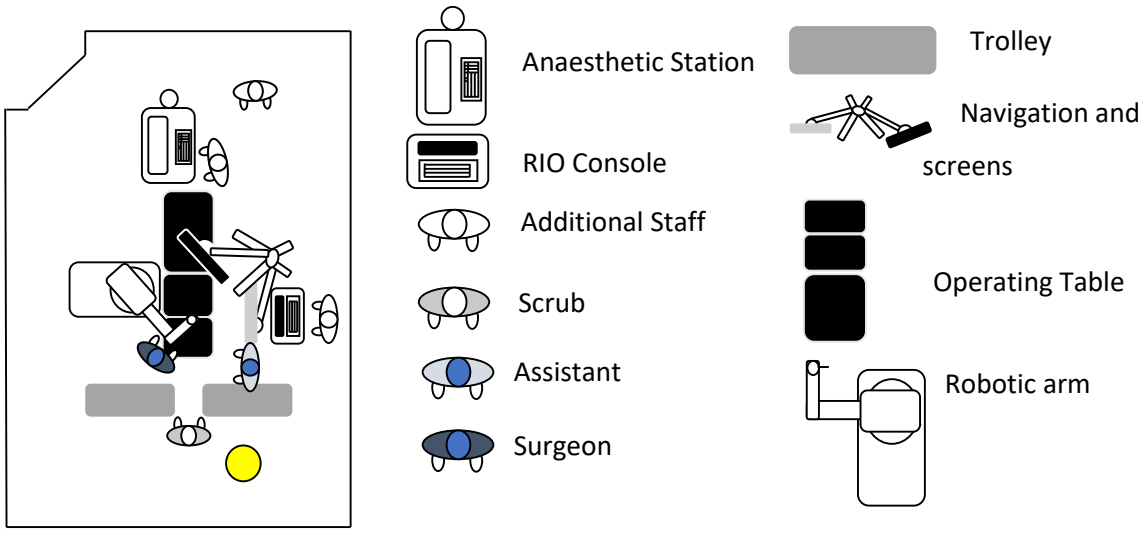

Figure 4.3-1 An examples of top down theatre layout.

The main elements affecting posture were the leg holder (Figure 4.3-2), the height of the supporting bed, position and size of the robot. The leg holder held the leg in place and allowed the foot to slide on a base plate to flex and extend the leg. This base plate meant the surgeon could not be square to the leg and would have to be on the lateral side of the knee. The knee holder in the Oxford procedure only supports the knee on the posterior side of the thigh to allow the surgeon to be much closer and square to the knee. This is important in the Oxford procedure given the need for alignment cuts relative to anatomical points, such as the pelvis and hip centre. The MAKO system setup is instead a compromise of Oxford and the TKA setup where the bed remains in place to support the limb. The positioning of the robotic arm on one side and the tracking system on the other mean that the surgeon could no longer stand next to the knee.

Figure 4.3-2 De Mayo Knee Positioner[19]. The leg position allows the surgeon to approach from the lateral or, as was seen when used with a split table, the medial side.

Often the bed height was the same as the Oxford procedure system but was shown to vary when measured with a laser measuring system during surgery. Given the setup of the RIO arm, with joint 1 being high off the ground, resulted in the surgeon's hand height being higher than with a relaxed shoulder (Figure 4.3-3). The height of the knee is a compromise of the distance between the surgical site and the surgeon's eyes with the optimal height for biomechanical advantages of the upper extremities.

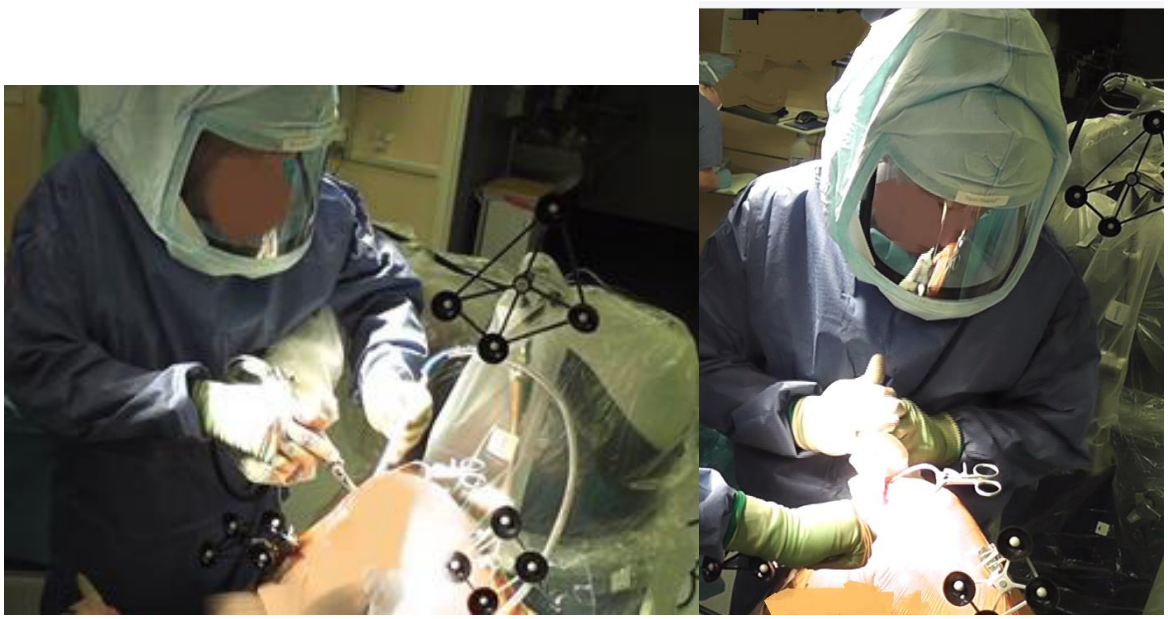

Figure 4.3-3 Images of relative position of the surgeon relative to the knee with the RIO (Left) and without the RIO (Right)

[19] Innovativemedical.com. (2017). De Mayo Knee Positioner®, Knee Holders, - IMP Medical Products. [online] Available at: http://www.innovativemedical.com/products/demayo_knee.html [Accessed 1 Aug. 2017].

The position of the robotic arm proved an obstruction to the positioning of the surgeon related to the knee. If too distal relative to the hip the robotic system would force the surgeon further away from the surgical site and would be limited functionally for the range of motion of the joint. The recommendation for setup is for joint one to align with the hip of the patient, this reduces the effects on the surgeon. But even with more optimal positioning, the surgeon is still further away from the surgical site than with other procedures. Additionally, the size of the system and the optical arrays in the patient often means the surgeon will not have assistance during resection. By moving the robotic arm distally this can allow more room for an assistant to be positioned by the hip for retraction and suction, but they are not able to view the surgical site themselves and require guidance that reduces workflow efficiencies.

4.3.2 Line of sight

The line of sight of the surgeon with the cutting surface is an important one, especially for new users of the system. All cuts were verified for depth after a small section of bone was resected with a probe and navigation system, this would verify that the real world and virtual were lining up with no bumped arrays or other faults. After this point, the more familiar the user was with the system, they would then rely on the virtual model as a guide for the rest of the surgery. In order to gain line of sight to the cutting point, the user would have to look over the robotic arm and burr that it is often impractical.

Another factor of the line of sight is also the distance from the surgeon to the surgical site. Often the incision is minimised for recovery reasons, but this limits the window into the knee. To see the posterior parts of the knee, the surgeon will have to get as close as possible to looked into the knee and will even have to rely on touch alone to assess for osteophytes, meniscal remnants and bone cement removal. Use of the RIO moves the surgeon away from the surgical site and will restrict the ability to observe the cutting point. Again given experience and confidence with the system, the surgery can be completed without the need to optimise the ability to view the knee given the use of the surgical model. Within these setups, the leg can be positioned to allow for a more neutral biomechanical setup with a lower bed height and knee.

4.3.3 Grip types in MAKO surgery

The handle of the MAKO RIO is the main interface point for the surgeon with the robotic arm. From observations of grips as part of the clinical trial, and also through online videos of other MAKO users a number of different grip type are adopted these are reviewed below.

Single hand

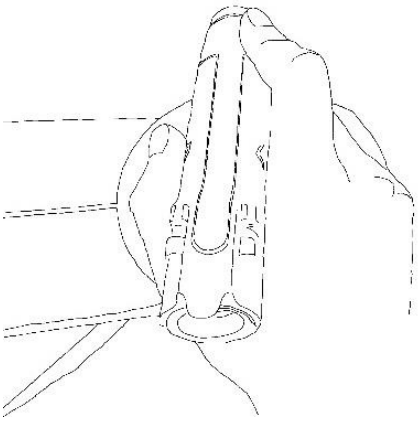

Figure 4.3-4 is the single hand grip type. Given the difficulty of access for an assist to retract the surrounding soft tissue, often the surgeon would be required to both retract and burr at the same time. Only a single hand it required to operate the handle, with the trigger being held by the index finger or a combination of the index finger and additional fingers.

Figure 4.3-4 Single hand grip

Double handed

When retraction and suction could be achieved from either assistance from staff or through retraction tools, the surgeon was able to hold the burr with both hands. This had three variations, one over the robotic arm (Figure 4.3-5), one under the robotic arm (Figure 4.3-6) and the last holding the elbow handle (Figure 4.3-7).

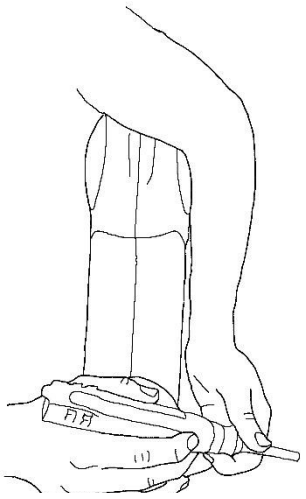

Figure 4.3-5 Double handed over arm grip

Figure 4.3-6 Double handed under arm grip

With both the over and under method the surgeon had the added control and assistance as the secondary hand can contribute to the control and fine movements, with the first hand controlling more gross movements. This was generally used for the initial tibial cut to ensure the burr tip was in the right area, however in the posterior sections of the resection; only a single hand could be used as often the HD attachment of the burr would be inside the knee with no room for the additional hand.

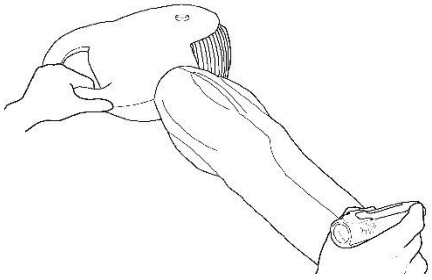

Figure 4.3-7 Double handed elbow handle grip

Placing the hand on the attachment has user safety concerns with the second hand being placed close to the cutting edge, but also the burr shaft that is rotating at 80,000 rpm.

Holding the elbow was only seen during the initial positioning of the robotic before resection. The handle helps with the manipulation of the first 3 joints, and especially joint 2, in the RIO for the gross positioning of the burr tip. Once in place there is little functional use of these joints

Old Handle Design

The first generation of the system from MAKO, the TGS (image here taken from the old promotional material), had a degree of freedom less and also a more exposed burr to allow for a hybrid grip between a precision and power grip (Figure 4.3-8). No observation has been directly made, but promotion video available online give an example of the use of the system. This system was ultimately upgraded to the current RIO system and branded as a more ergonomic system, inferring issues with this system. However, there is no great change in the posture of the hand as the barrel of the burr forms the main point of contact. The main difference is an added degree of freedom in what became joint 6 of the RIO.

Figure 4.3-8 TGS grip, a hybrid grip between a precision and power grip of the cutting burr

When reviewing all of these grips there is a deviation away from the classical grip definitions in the literature. The previous handle design did not allow for the contact of all of the fingers with the burr. When considering the small and ring finger contribute up to around 45% of the grip strength, this is a large amount of force to lose when trying to maintain a high enough friction force to manipulate the system. With the addition of the dome a larger surface area was available for the contact of additional fingers, however, still the little finger of the surgeon is not in contact with the end effector.

The general shape of the handpiece is not immediately apparent how to hold. The burr is mounted on a dome at an angle to allow a neutral flexion-extension angle at the wrist for the bone cut. However when this comes to the tibial cut, the wrist is required to be more flexed. The burr is engaged through a large trigger mounting a magnet that engages the burr motor. With the positioning of the Index and sometimes middle finger on the trigger and barrel of the burr these loose contact with the handle, reduce the surface area to the distal phalanges. Given the unpredictable movements with both linear and rotational movements, the design of the handle tries

to compromise for all of these conditions. The movements will be reviewed in greater detail in the biomechanics chapter of this thesis.

4.3.4 3 cases questionnaire

Table 4.3-1 Surgeons discomfort reported from 3 consecutive cases

Case	Area (to be filled out)	Score
1	R Lower arm	1
2	R Lower arm	4
3	R Lower arm	2

Table 4.3-1 presents the self-reporting discomfort scale the only area reported by the surgeon was the lower right (dominant) arm. The first case reported No discomfort (1), however, given that this was a self-reporting form the area of concern where the dominant forearm indicated an awareness of this area as a potential issue. The second surgery proved more problematic with a score of 4 reporting mild discomfort during milling, reviewing the timing of the procedure this was associated with a significant increase in the femoral resection time and a 3 minute (more than double) increase in trigger time. Finally, the third surgery reported a discomfort decrease of 2 with the shorter femoral resection time. Given that the third femoral resection time is shorter than the first, a slight increase in discomfort between the first and third could be an indicator of carrying fatigue from the previous surgery. However, this could similarly be a factor of the time in theatre leading to an overall fatigue being expressed in the lower arm.

4.4 Observation Conclusions

A number of observations of the difficulty of use related to posture have been highlighted. Generally, the surgeon is attempting to have a line of sight of both the burr tip and the screen. A number of different ways of achieving this are reviewed in the results, but the overall posture of the surgeon was difficult to determine given the protective clothing. These postures are reviewed in more details through optical tracking in the biomechanical testing of users chapter (Chapter 6).

Even the early stage in the adoption of this system, these observations can only be considered a review of new users to the system. As part of the learning curve process and regular use of the system, optimal use and positioning of the equipment can be refined. Consideration on how to allow access for the surgical assistance during resection could have implications on the workflow of the whole system, with the ability to have parallel workflows. A simple task as an example is the movement of the leg on the leg holder, which could be completed by the surgical assistant, allowing continual resection of the bone without the need to stop and move the joint. This has been

observed in the TKA and UKA workflows but is not being completed in the MAKO, with the need for the camera system to see the tracking arrays and the leg held in a stable position.

Finally, the most significant observation was the three examples of user discomfort/fatigue in a low volume situation. This significantly changes the question of fatigue from 5 cases in a day. Taking this forward, the construction of biomechanical testing can now be a question of how long can a user burr with the system until fatigue is induced for a single case, ignoring the recovery and other demands on the user between resections.

Chapter 5 Investigation of the MAKOplasty procedure through time analysis

5.1 Introduction

Following on from the observational study of the MAKOplasty procedures a further numerical analysis was conducted on the video footage in the form of time analysis. Through modelling the workflow of clinical use of the robotic arm the length of time taken to perform specific actions. This work was conducted to the review the efficiency of the MAKOplasty procedure in comparison to a manually equivalent surgical procedure (Banger et al., 2013). This detailed workflow allowed for an extraction of the burring times of the MAKO systems.

From its origin in industrial manufacturing and Taylorism, the tool sets out to improve the efficiency of a process. Within a medical framework, while there are economic benefits to this efficiency, there are also clinical advantages in the reduced risk of complications with shorter surgical times. In the literature (Faust, 2007), and across the clinical community, there have been historical concerns with the additional time taken when using robotic systems. Reporting has largely been through total surgery time or tourniquet times. While these have clinical relevance and enables comparison with other surgeries, these do not define the workflow of the surgery or indicate where delays occur.

In addition to efficiency measurement, time analysis of video recording also allows post session review of complex and quick moving actions over the whole procedure. This review can facilitate reliable classification of errors, timings and causation of usability limitations. The design of the testing is such that the filming should give a large quantity of in situ data with the new user group. From the observations in Chapter 4, single cases were shown to lead to fatigue. Time analysis for these cases can assess if different actions (such as burring) took longer for these cases. Hence, this analysis will allow a comparison of the MAKOplasty procedures that have been observed to lead to fatigue and those that don't.

There are no reported issues of fatigue or WSD (Work related Stress Disorder) relating to the Oxford procedure. Any difference between the two procedures would highlight areas of interest

relating to the other project question of fatigue related discomfort. Understanding the fatigue problem requires an understanding of the physical demands, of which a large element of this is the timings and repetition of actions in typical and unusual use. These demands can be defined from a good understanding of the typical workflow of the procedure.

5.2 Time analysis methodology

5.2.1 Camera Positioning

Time analysis of video footage is a simple outcome measure of surgical practice. The added detail that can be produced, as compared to tourniquet time captures, allows the further description of issues and episodes, and also allows for the identification of idiosyncratic behaviours of users for review and comparison.

Two video cameras (2 Panasonic SD60 Full HD Camcorder with SD Card Recording, X35 Intelligent Zoom, X25 Optical Zoom, Wide Angle Lens, iA + Face Recognition - Black) were mounted at a high level. One above the surgeons screen of the MAKO RIO system (equivalent position in the Oxford surgeries) gave a view of the surgeon's front on postural information, hand positioning on the robot, approximate position of the surgeon with the operated knee, facial recordings of the surgeon for timings of the surgeon looking at the screen.

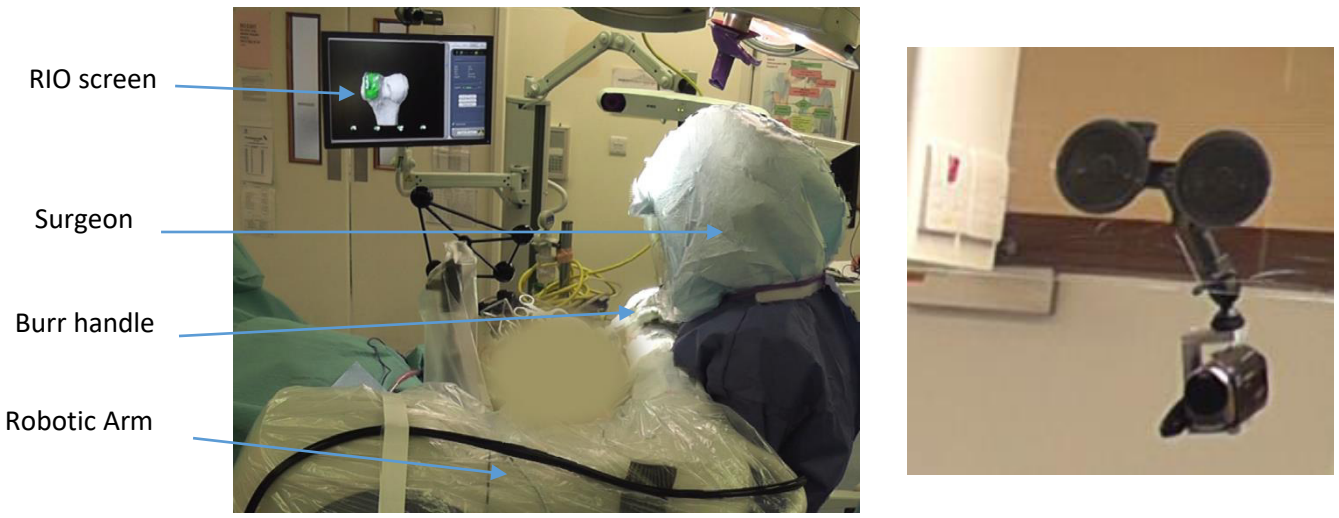

Figure 5.2-1 (Left) Example of video footage taken from GRI observational study. Presented is a shot of a surgeon performing surgery with the MAKO RIO looking at the CAD model of the patients knee on the screen of the RIO system. From this view the actions and movements of the surgeon could be monitored. (Right) Cameras were mounted on the laminar flow hoods through suction mounts to be out of the way of theatre staff.

A wider view was captured by the second camera, shown above (Figure 5.2-1). Initially, this was placed in the corner of the room on a tripod to give a view of the theatre from the opposite perspective, but during surgery a number of objects were put in the way, blocking the view. Hence the camera was moved and mounted on the laminar flow Perspex on the opposite side of the

theatre to the surgeon to give an orthogonal view of the surgeon and the surrounding theatre (Figure 5.2-2). This camera allowed assessment of staff movement in the rest of the theatre, along with more postural information of the surgeon with the side on view.

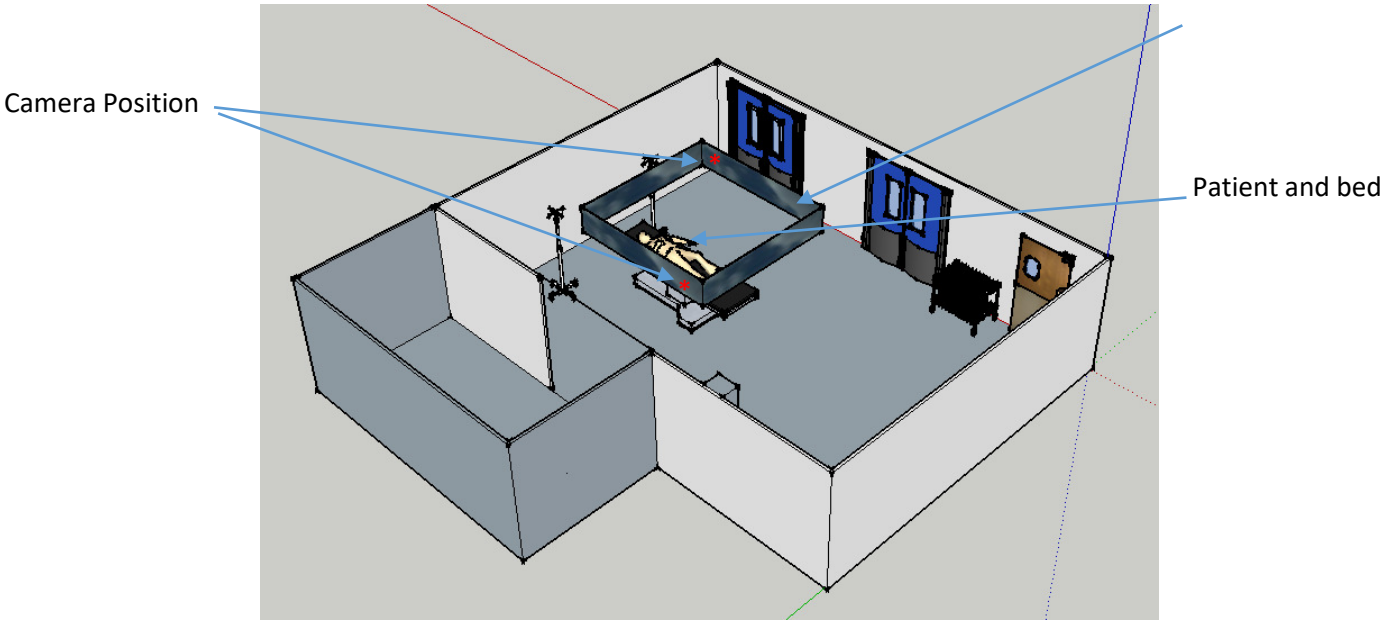

Figure 5.2-2 A 3D model of theatre with camera positions denoted. The main capture area was within the laminar flow of the theatre but there were large areas of the theatre that wasn't monitored.

* Denoting position of the camera on the laminar hood.

Ethical approval was granted under an amendment to the clinical trial with permission taken from individual patients pre-operatively. Verbal permissions were taken from theatre staff at each recording and details of the reason of recordings were given to all involved.

5.2.2 Video footage segmentation

The procedural stages are the large divisions of the surgeries from the definitions developed in this project. These stages give a more general overview of the procedures. Each individual stage is described from a series of actions. These actions are defined with a start and stop description that will allow the times of the actions to be taken, along with time between actions (Please see results for further information of actions in these stages, along with start and stop definitions in Appendix 1). The stages of interest were the tibial and femoral resection stages, but specifically the resection times of each of these stages.

Resection timings

All individual actions during both resections that were recorded such that the resection times could be analysed in detail for both procedures. Trigger times (how long a trigger was held down for)

would be calculated for both procedures. These trigger times could also be divided into the type of resection (surface or other) to define how long the different parts of the resection took. The surface cuts are defined as those resecting the bone for the positioning of the implant on the femoral and tibial condyle. The other cuts are additional cuts required, which in the case of the partial knee replacements are the peg holes. These required different tooling for the manual procedure and was hence was separated.

5.2.3 Analysis of procedures

The times taken for the actions described in Surface cuts, other cuts and total cuts were summed and treated as a single value. The mean values of these sections for both tibial and femoral cuts were calculated. After failing normality with the Shapiro-Wilk test, the MAKO and Oxford trigger times were compared with a Mann Whitney U test.

5.3 Time analysis results

5.3.1 Surgeon Experience

The Oxford procedure is a manual/mechanical UKA procedure that is seen as a standard procedure in the studied hospital and across the UK. The team involved 3 orthopaedic surgical consultants; all were experienced (100+ surgeries) in the Oxford Unicompartmental knee arthroplasty.

Following training with MAKO and an initial pre-trial period allowed the surgeons to become familiarised with the system. Subsequently, the surgeons were observed for 37 surgeries, of which 21 were MAKOs (Surgeon 1 11, Surgeon 36, and Surgeon 2 4) and 11 were Oxford procedures (Surgeon 1 5, Surgeon 3 6). The MAKOplastys that were observed were within the first 20 MAKOplastys that were performed by the surgeons. While familiar with the UKA, the surgeons were considered new to the MAKOplasty procedure.

Resections

Table 5.3-1 Mean and standard deviation of trigger times for the MAKO, Oxford and a single TKA measured case. Trigger time is the time spent supressing the trigger of the power tool or MAKO burr. Recorded for the surface (primary resection), other cuts (secondary resection such as peg holes), and cumulating to a total time.

Mean [SD]		Other cuts (mm:ss)	Surface (mm:ss)	Total (mm:ss)
MAKO	tibial	00:11 [00:09]	03:52 [01:32]	04:03 [01:33]
	femoral	00:23 [00:06]	03:25 [01:47]	03:46 [01:44]
Oxford	tibial	00:08 [00:02]	01:05 [00:15]	01:13 [00:15]
	femoral	00:40 [00:05]	01:03 [00:30]	01:43 [00:32]
TKA[20]	tibial	00:06	00:26	00:32
	femoral	00:36	02:14	02:50

Table 5.3-2 Max trigger times (mean of all the maximal time of a single suppression of a trigger) and the single longest time a trigger was suppressed for a tibial or femoral cut

Mean [SD]		Max (mm:ss)	Single largest continual trigger time (mm:ss)
MAKO	tibial	01:27 [01:00]	04:00
	femoral	01:11 [00:29]	02:09
Oxford	tibial	00:30 [00:10]	00:52
	femoral	00:31 [00:11]	00:55
TKA[21]	tibial	00:21	00:21
	femoral	00:37	00:37

Table 5.3-3 Statistical Mann Whitney U comparison of trigger times comparing MAKO with Oxford for tibial and femoral cuts from Table 5.3-1 and Table 5.3-2.

MAKO vs. Oxford	Other cuts	Surface	Total	Max
Tib	0.406	<0.01 *	<0.01 *	0.02 *
Fem	<0.01 *	<0.01 *	<0.01 *	<0.01 *

* Statistically significant results (P<0.05)

The MAKO procedure has extended times for use of the tool (burr vs blade) both as an average of the whole procedure (Table 5.3-1) and maximal single observed values (Table 5.3-2). Statistically, the difference between the MAKO and Oxford procedure are significantly different, bar the other cuts tibial trigger (Table 5.3-3).

Table 5.3-4 Time spent burring surface for reported cases with sclerotic bone. Sclerotic bone was determined by the surgeon at the time of surgery through examination of the bone.

Sclerotic Bone		Max (mm:ss)
MAKO	tibial	07:57
	femoral	09:55

[20] TKA was a single case, so Max and single largest continual trigger time are the same.
[21] TKA was a single case, so Max and single largest continual trigger time are the same.

Table 5.3-4 shows the extended burring times during the MAKO surgery as a result of sclerotic bone. These sclerotic burring times are outliers in the normal pattern of resection times. The average femoral resection burring times was shown to be larger than the tibial burring times.

5.4 Trigger time Discussion

The trigger time has been noted to be the most probable cause of fatigue in the users. As highlighted here, this is due to the significant increase in trigger time between the MAKO and Oxford procedure, somewhere in the region of 2-3 times the length. From the observations, experience and shown later in the Biomechanical testing section the amount of force required is only a fraction of the MVC, but it is the length of time that is required to manipulate the system that results in the fatigue. The fact that these are much longer than both the Oxford procedure and Zimmer TKA, it is fair to assume that a knee surgeon is not normally exposed to this type of demand and might not have the conditioning or appreciated techniques to avoid this occurring.

2 out of 21 cases showed significant increases in the trigger time as a result of sclerotic bone, reviewed from the video and by the surgeon. Given the inconsistency of this increased demand, the high throughput US systems, that anecdotally reported the fatigue, would have an increased likelihood of being presented with these more difficult cases leading to longer cutting times. This makes their experience hard to determine if the fatigue was down to single cases, as was observed in this project's observations, or a cumulative effect of multiple surgeries. While multiple surgeries were only observed once, it was a single surgery that resulted in the largest discomfort. The effect of continued use of the MAKO RIO is observed in the Biomechanical testing of users chapter (Chapter 6).

5.5 Time analysis conclusions

Trigger times for the MAKO procedure are significantly long that those of manual surgical procedures (UKA, TKA). Bones with sclerotic lead to a 3 to 3.5 increase in burring times. When presented with sclerotic bone, or longer burring times this is thought to have an increased demand on the surgeon both holding and manipulating the robotic arm in the haptic environment. The effects of this extended burring times is review in chapters 6.

Chapter 6 Biomechanical Testing of MAKO RIO users

6.1 Introduction

This chapter aims to investigate the anecdotal reporting of fatigue when using the RIO system in the USA. From the observations of surgery, time analysis and the surgeon's questionnaire responses in the previous chapter, it has been established that there is an intermittent issue with the manipulation of the robotic arm in theatre. Fatigue and discomfort appear to be associated with longer burring periods required with denser bone. The main biomechanical causes of this fatigue are not yet understood. The personal protective clothing and video camera positioning obscured the movements of the surgeons from the video footage of surgery. This led to a difficulty to biomechanically review potential causes of fatigue. Hence there was a requirement for further, more sensitive, biomechanical assessment techniques of the kinematics and kinetic factors contributing to localised fatigue while burring in a simulation of surgery. This is the focus of this chapter.

Muscle fatigue is a complex and subjective change in the physiology of the muscle that results in the change in the ability to control and function. At an extreme, the muscles lose all use resulting in a failure to complete a task. This is not the case here with only an increase in difficulty and/or discomfort being reported.

Fatigue was observed after the two consecutive cases at the beginning of the day during the clinical trial observations (Chapter 4). This would suggest that this fatigue is not just a factor of high use over a single day, but can be observed in two or even individual cases with extended cutting times. In order to create conditions comparable to an extended cutting experience, exaggerated conditions condensed multiple bone burrings into a single testing period for mock users. Exaggerated testing was controlled to recreate longer cut times, however, these were repeated sequentially with three surface resections for tibial and femoral pairs being completed in quick succession. No material was cut during burring for practical reasons, such that the resistive forces to motion of the burr were only those produced by the robot. These three resections combined were designed to mimic a single extended resection such as those seen during extensive sclerotic bone resections for time. This formed a mock surgery test.

During this testing the users were markered and EMG electrodes placed to monitor the movements and posture of the user and electrical activity of targeted muscles respectively. As outline in section 2.5.4 there are a number of methodologies that attempt to standardise a means of detecting and measuring fatigue. Given that no single definitive evaluation for fatigue has currently been recognised, this project explored a number of assessment tools available. These included optical tracking of user's movements, forces being applied during burring measured through transducers positioned in the robot and an EMG system to monitor the physiological changes in the muscles over the course of testing. These assessments were reviewed alongside discomfort questionnaires that had previously been used in the clinical testing of the system with the surgeons. From this biomechanical assessment a number of research questions can be proposed:

1. Are kinematics and postures of the user biomechanically suitable for the use of the robotic arm?

As reviewed in section 2.4, the posture of the hand, wrist and elbow have a varying degree of influence on the grip strength and joint torque at the wrist. Through measuring the posture of the users issues with the posture can be view for possible impact on the ergonomic use of the RIO.

2. Can fatigue be confirmed in users expressed as discomfort

Fatigue can be seen to manifest itself in three further categories; Subjective, Objective and Electrophysiological (Emam et al., 2001). A seven-point discomfort questionnaire allow for the subjective reporting of when and where fatigue occurred during burring. This aims to detail more specifically the presentation of fatigue than was described in the anecdotal reporting currently available.

3. Can fatigue be confirmed electrophysiologically (EMG)?

It is known that fatiguing muscles are altered electrophysiologically, some of the changes in these processes can be captured from surface EMGs and allow a determination of electrophysiologically defined fatigue. However, these measurements are dynamic and not dichotomous in defining fatigue, such that a range of signal processing tests are applied to the EMG signals.

By isolating muscles for either prehensile or wrist articulating allows an allocation of the muscle action to the resulting muscles fatigue. However, most muscles are multi-articular such that a number of different muscles were monitored in the hand and forearm.

4. How much force is required to manipulate the system?

Along with the dynamic movements, are the forces being applied to the robotic arm during these movements. To this end a force transducer was placed in the handle of the robotic end effector to measure the forces required to manipulate the robot.

5. How much force is introduced with the use of haptics for controlling the robotic system?

The introduction of the haptic boundaries forms virtual barriers that the user can push up against. Before the limit of this boundary is met, an increase resistance to movement in the direction of the boundary wall is reduce velocities near the wall but also increases the forces required to manipulate near the boundary edge. Explored here is the question of how much additional force does the user apply when interacting with these boundaries when compared to free movements of the system.

6. What are the differences in kinematics between the tibial and femoral cuts?

The two bony cuts are difference both shape and orientation in the knee joint. In order to understand some of the influences of the previous questions, differences between the femoral and tibial cuts allow for an isolation of results and possible contribute significantly more to possible mechanisms of fatigue.

6.2 Biomechanical Testing Methodology

6.2.1 Experimental design

The experimental design is split into three stages: Pre Testing (6.2.2), Mock surgery (6.2.3) and post testing (6.2.4). Pretesting defines the testing protocol before the mock surgery that was mostly subject EMG setup and strength testing. Mock Surgery defines the main testing sections, detailing motion analysis, force transducer measurements and mock surgery testing work flow. Finally post testing details the repeated pre testing strength tests and questionnaires.

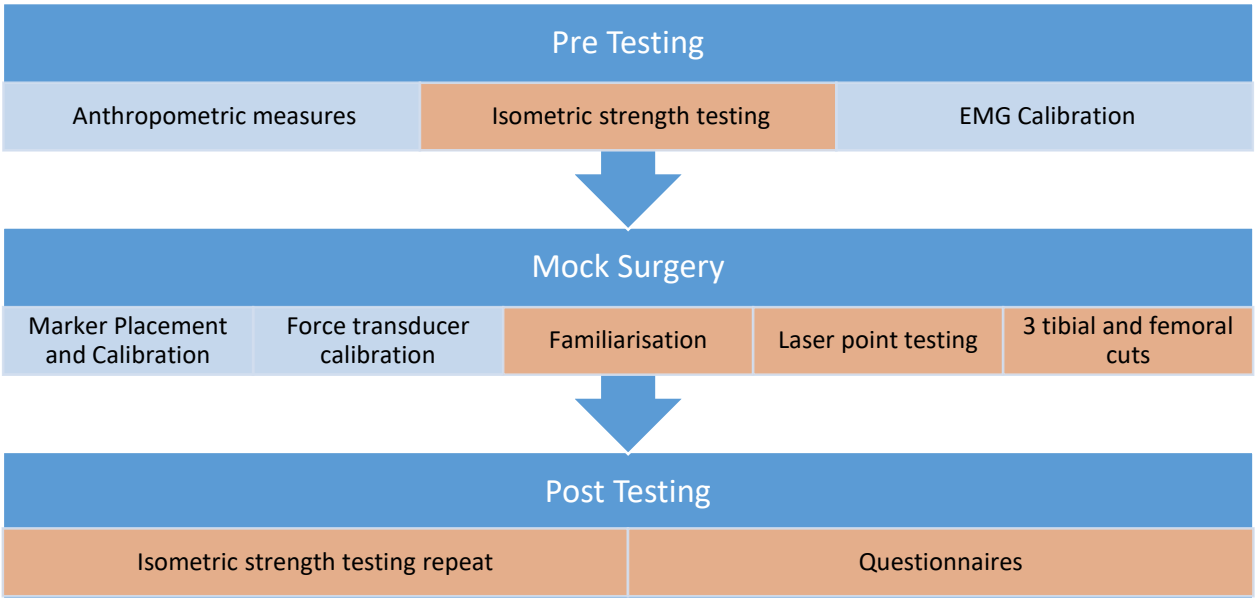

Figure 6.2-1 Overview of the workflow of the testing. Further detail on processing and justification found in the detail in the following sections: setup (Blue), testing with results (Orange)

The testing protocol was reviewed and accepted under departmental ethical review and a sample of users was invited from the departmental population. The biomechanical testing used a group of lay users (n=25). Lay here was defined as those not requiring previous clinical experience, however some users had some clinical (medical doctors) and surgical (1 trained MPS). Consent forms were completed prior to testing and after an explanation of the testing to be carried out. Any pre-existing neurological or musculoskeletal conditions that would limit the user to be active for up to 2 hours excluded the users from testing.

6.2.2 Pre-testing Methodology

Anthropometric measurements, previous experience, participant demographic information and health screening was carried out as part of a pre-testing questionnaire (Appendix 4).

Also as part of the pre-testing, the strength of the user's grip, wrist extension, wrist deviation, wrist flexion and elbow flexion was measured. EMG electrodes were placed over 4 muscles, and a

maximal voluntary contraction was performed. This allowed the calibration for the EMG along with a measure of strength before the mock surgery testing.

6.2.2.1 EMG

EMG analysis gives an insight into the activity and changes in the physiology of the muscle related to its recruitment patterns.

Positioning of electrodes

The EMG system used was an 8 channel DataLink (Biometrics Ltd, Newport, UK). It was sampled at 1000Hz and synchronised with the Optitrack system. During the longer burring phases, the EMG software continuously recorded for the length of the testing. An analogue sync output from Optitrack system marked the recording periods of the motion capture. The EMG signal file was then cropped, and sections saved in MatLab with filenames matching those from Optitrack recorded (further details can be found in the Appendix 3). All processing was completed offline.

Four bipolar electrodes were positioned on the active arm of the participant. This was the maximum number of electrodes supported by the Datalink system. The muscles selected for monitoring were those required for gripping and movement of the wrist and elbow. Due to the nature of surface EMG, the most superficial muscles that cause wrist flexion, deviation and supination, along with thumb adduction for grip fatigue in the hand, were chosen. Table 6.2-1 shows the muscles selected, along with the multiple actions of all the muscles.

Table 6.2-1 EMG channel, targeted muscle and action description

Channel	Movement required	Muscle chosen	All actions of muscle
1	Wrist flexor	Flexor carpi radialis	Wrist flexion and abduction
2	Wrist extensor	Extensor digitorum	Extension of hand, wrist and fingers
3	Thumb adduction	First dorsal interosseous	flexes, radially deviates (abducts) and pronates the index MCP joint and radially adducts the thumb basal joint
4	Elbow flexion	Bicep brachii	Flexes elbow, flexes and abducts shoulder and supinates radioulnar joint in the forearm
4 Alternative	Radial deviation	Extensor carpi radialis longus muscle	Extensor at the wrist joint abducts the hand at the wrist

The bicep electrode was only used for the first 13 users before it was deemed to show little activity and no fatigue. The Extensor carpi radialis longus muscle was chosen to replace the bicep electrode in the remaining 17 user tests, as this is responsible for radial deviation (wrist abduction). This is marked at channel 4 alternative in Table 6.2-1.

The EMG site was prepped with a dermatological scrub and electrodes fixed with Biometrics proprietary fixation tape. Additional micropore tape was used to ensure maintenance of fixation and secure the cables. The orientation of the electrodes matched the assumed longitudinal direction of the muscle.

Figure 6.2-2 (Left) Electrode attachment through stickie strips and micropore tape. (Right) Example of cable management

Calibration

The normalisation of the EMG signal requires individual calibration during a maximal isometric force. The subject was asked to apply maximum effort in the exercises below, which was deemed to be their MVC. The force production was recorded through a Dynamometer or myometer as a measure of strength. The setup was standardised to allow repeatable procedures. Anthropometric measurements were used to convert these recorded strengths into moments where suitable. Subjects were not trained, but instead, verbally motivated to 'try as hard as they can'. Three sequential repeats were completed for each exercise, with a ramp up to MVC over 2-3 seconds and then held for 2-5 seconds. A 20-30 second break was taken between repeats to minimise fatigue. A 50ms sliding window average of the absolute signal was taken to be the peak EMG for normalisation purposes. All subsequent recordings were then normalised to this maximum value.

6.2.2.2 Isometric Strength Testing

Grip strength Test

Force generation is compromised in a fatigued muscle by definition, so a straightforward metric of fatigue is to measure the maximal force production in the muscles. Additionally, given the task relating to the strength of the user, a Jamar grip strength comparison could be drawn between the test subjects and a wider orthopaedic surgeon profile of strength.

With an unsupported 90 degree flexed elbow, a maximum grip was applied to the Jamar hydraulic hand dynamometer (Patterson Medical, Warrenville, IL). The dynamometer has five adjustable grip positions. The grip distance, position 1 on the dynamometer, was maintained for all the users. The maximum force for this test was recorded along with EMG to give MVC values.

Figure 6.2-3 Example of Dynamometer use for grip strength test. User was sat with the arm at 90 degrees of flexion at the elbow and a neutral shoulder.

Wrist Extension Test

With the forearm resting on a table and with a pronated wrist, the user's hand was placed through a myometer (Digital Analyser - Myometer, MIE Medical Research Ltd, Leeds, UK) strap, fed through a hole in the table (Figure 6.2-4). The participant was seated upright with an extended arm to minimise the activity of the biceps. A further strap was used to maintain forearm position, but this was not substantial enough to stop bicep flexion, so additionally the participant was encouraged only to extend from the wrist. The myometer strap was positioned slightly proximal to the knuckles. The maximum force for this test was recorded with EMG from the digital readout of the digital myometer.

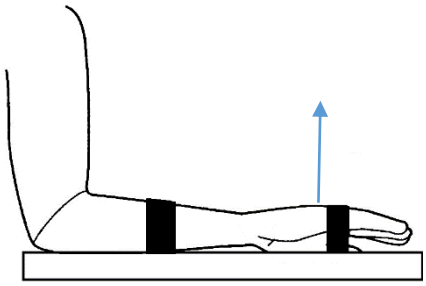

Figure 6.2-4 Wrist Extension. Hand strapped in placed with myometer strap and additional forearm strap, blue line indicated the direction of force production

Wrist Flexion Test

Similarly, the wrist was supinated and placed in the same setup (Figure 6.2-5). The bicep would activate, but again the user was asked to maintain only wrist flexion. Again, the force and EMG were recorded.

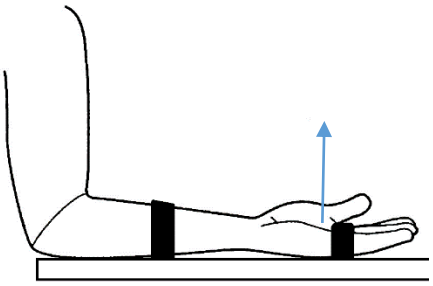

Figure 6.2-5 Wrist Flexion. Hand strapped in placed with myometer strap and additional forearm strap, blue line indicated the direction of force production

Radial deviation Test

The wrist was placed in a neutral position such that the thumb pointed vertically upwards, and the strapping lay over the knuckles of the user (Figure 6.2-6). The user was then encouraged to deviate the wrist for MVC radially.

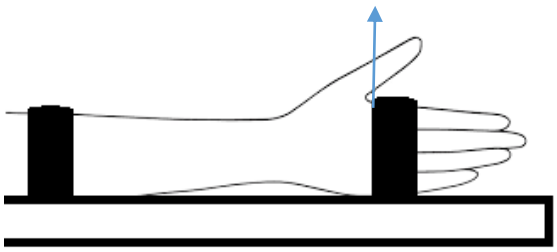

Figure 6.2-6 Radial Deviation. Hand strapped in placed with myometer strap and additional forearm strap, blue line indicated the direction of force production

Elbow Flexion

With the wrist in a supine position, this time without the strapping on the forearm, the user was asked to pull up on the strap as hard as possible for the active the bicep to MVC (Figure 6.2-7).

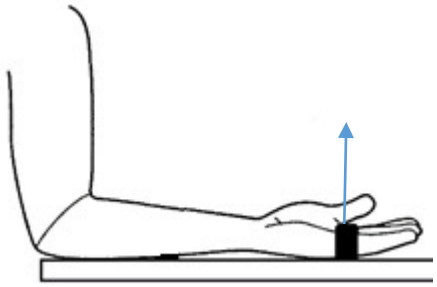

Figure 6.2-7 Elbow Flexion. Hand strapped in placed with myometer strap, blue line indicated the direction of force production

6.2.2.3 Pre testing Data analysis

Data analysis isolated to the pretesting results was limited to a comparison of the users profiles with an averaged orthopaedic surgeons' profile (Subramanian et al., 2011) and the strength of orthopaedic and a wider population model (Schlüssel et al., 2008). The user group data was shown to be normally distributed and statistically compared with student t-tests with the reported data.

6.2.3 Mock surgery Methodology

The mock surgery sections consisted of a familiarisation (section 6.2.3.3) and 3 resections of the tibia and femur (section 6.2.3.5). The electrodes from the pretesting remained in place, while optical tracking markers were placed on the user (section 6.2.3.1) and the static and functional poses were captured by the motion capture system. A forces transducer in the MAKO RIO monitored the amount of force being applied through the headpiece (section 6.2.3.2).

6.2.3.1 Motion capture methodology

Body movement data can be calculated from optical tracking of markers placed on the user. The Optitrack system is a relatively inexpensive product for kinematic analysis. It was designed for the animation industry. However, no existing interface for calculating biomechanical outputs existed hence an algorithm was developed to calculate the joint angles of the upper extremity. The wrist angles, as indicated in the literature, have a large effect on force production at the hand. The sensitivity of the optical tracking systems allows them to monitor the postures of the arm over time. The robotic arm's movements were also recorded through markers placed on the RIO arm.

6.2.3.1.1 Optitrack system

The Optitrack setup was an array of 12 x 0.3 MP resolution cameras ran at 100 FPS and streamed through Natural point's Motive 1.0 software platform. The motion capture software tracked markers

placed on the arm, trunk and pelvis. The developed algorithm, run offline in MatLab, gave the user's wrist, forearm and shoulder angles. Additional markers were used to calculated the joint angles of the robotic arm.

Given the importance of tracking the medial elbow marker, there were a number of times when this would become occluded for longer periods of time. For this reason, an algorithm was developed to assume when the medial elbow marker became occluded, a vector normal to the plane defined by the wrist, elbow and shoulder joint centres was used estimate the position of the marker.

6.2.3.1.1.1 Marker Placement

A simple marker set was chosen to monitor the subject's movements illustrated below in Figure 6.2-8. The need for markers to be position around the EMG electrode meant, especially for smaller subjects, that rigid clusters proved too inflexible for fixations sites. Furthermore, the Optitrack system and PC could only handle a limited number of markers for a limited time. Therefore, following the RIO and surgical bone markers were too many for the system to process. Hence single marker in pragmatic location were used. For further justification of marker placement see the appendix (Appendix 3).

6.2.3.1.1.2 Calibration

The subject was positioned in the centre of the capture area for maximum accuracy and taken through the calibration process verbally. A static pose of the subject with both hands down by the sides followed by a transition to straight arms abducted at the shoulder (T-pose) was taken to define anthropometric measurements and the natural alignment of the subject.

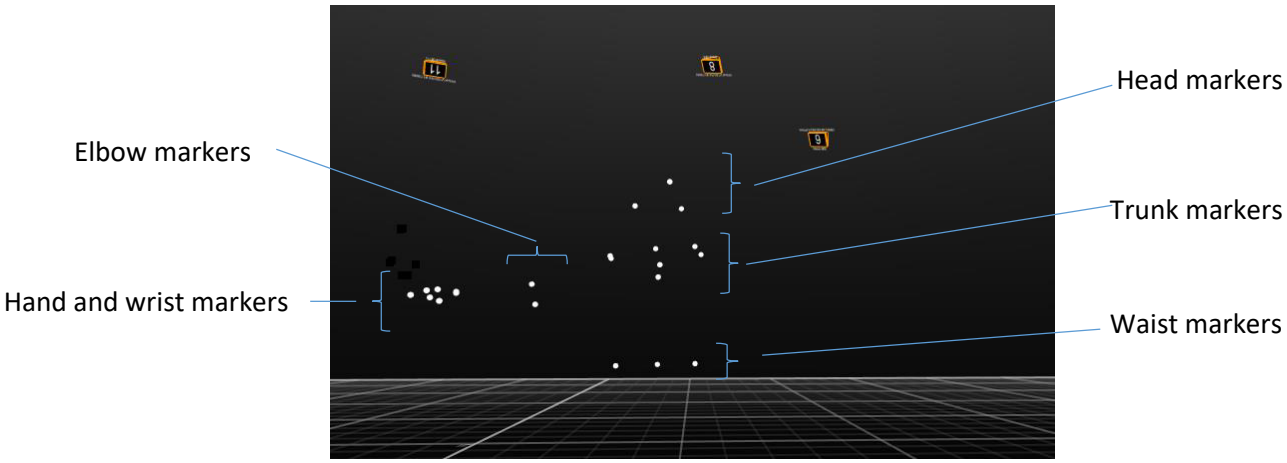

Figure 6.2-8 Static calibration capture of user in a T pose capture taken from a screenshot of the Motive software

For the functional calibration, the subject was asked to manipulate individual joints of the arm for approximately 20 seconds. The joints included were the wrist, elbow and shoulder. Joint centre were calculated using the Gamage and Lasenby methodology (Gamage and Lasenby, 2002). These

functional joints centres are used to measure the length of the segments for anthropometric measurements of the user.

6.2.3.1.2 RIO Marker

6.2.3.1.2.1 Placement

The robotic arm was also markered and tracked to report on different manipulations of the system. Marker clusters were positioned on the three main segments to measure the angles of 5 out of the 6 joints of the robotic arm. Additionally, a marker cluster was positioned on the handle/End effector of the system to track its movements.

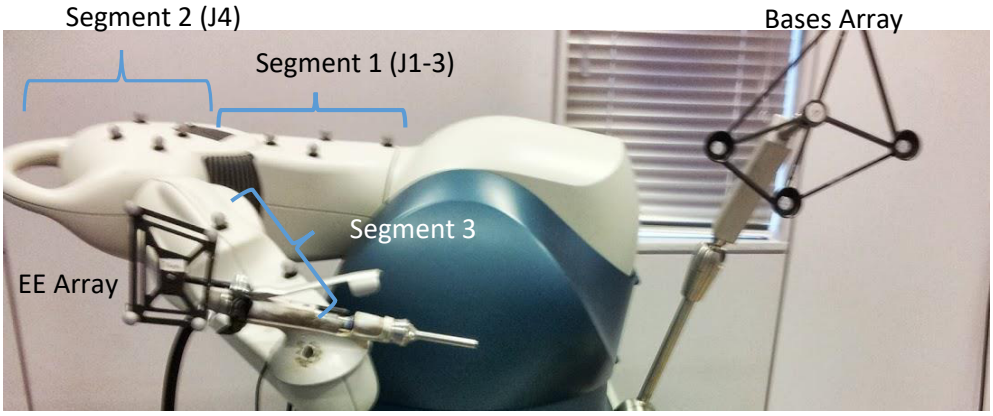

Figure 6.2-9 RIO tracking Markers positons. Markers were positioned in clusters to describe the articulations of all 6 joints of the robotic arm. The Base array was used by the robotic system to define the location of the robotic system.

6.2.3.1.2.2 Calibration

The calibration of the robotic arm marker set was performed before each testing session took place. Markers on the RIO arm largely remained in place for the main segments only having to be moved for two left-handed users. The end effector array was recalibrated for every subject as there was a high chance of the setup being moved during end effector removal. This frequently occurred as the end effector is removed for the calibration of the robotic arm software required before every test. To calibrate the marker set, individual joints of the robotic arm were manually moved to define joint centres functionally using the same methodology as the user joint centre (Gamage and Lasenby, 2002).

6.2.3.2 Force transducer methodology

A force transducer (Nano 25, ATI) was mounted in the end effector housing to measure the force transfer from the user to the system. A suitable gap between the end effector and the Rio arm end plate was used to allow the transfer of force only through the transducer. Deflection of the force transducer was minimal under the expected forces. The force information was captured into MatLab through a National Instruments DAQ board as raw voltages and converted to forces using a pre-recorded calibration matrix.

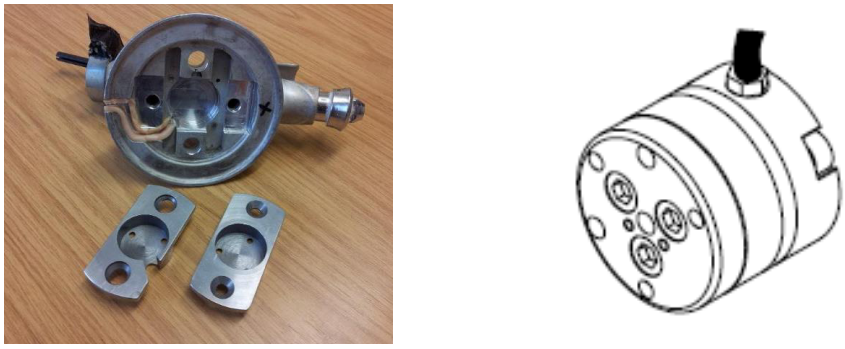

Figure 6.2-10 Bottom side of the EE showing cavity create and mountings (Left). Diagram of Nano 25 (Right)

Figure 6.2-11 RIO handle with force transducer location. This measured the force being applied to the handle in all 6 dof. The user was limited to using one hand to ensure that all force was applied through this transducer.

To ensure that all the force was applied through the force transducer the user was restricted to holding the robotic arm by the end effector. Single arm use is seen in the observations, but normally the other hand can be used to manipulate the robot. The elbow of the robotic arm acts as a handle for a second hand, but this is only used for gross realignment of the robotic arm and was not needed during burring. This is normal practice for the user, but other grips have been identified (See 4.3.3 Grip types in MAKO surgery).

The force transducer was synchronised through a timing cable from the optical tracking system and calibrated (warmed up and zeroed) prior to use. All forces were transformed from the transducers reference system to the handle end effect reference system for more intuitive interpretation of the results.

6.2.3.3 Familiarisation with the RIO robotic arm

The test subjects were invited to explore the use of the system in a free play session to familiarise themselves with the system. This also allowed for free manipulation of the system to be recorded ensuring that all the joints in the robotic system were capturing data.

6.2.3.4 Laser pointer testing

A laser pointer was placed on the end effector of the robot. The participant was invited to trace twice a 17 point pattern using a laser pointer and RIO arm on an A4 sheet stuck to the wall (Figure 6.2-12). This was a standardised movement test that would allow a comparison of the use of the system from all users as many of the movements in surgical burring are non-standardised. The scaling of the image was chosen to reflect the typical range of motion that would be expected from the system.

Figure 6.2-12 Tibial shape with numbered points for laser target task (left) Laser Pen attached to end effector (Right)

The laser testing was added to allow a structured familiarisation to the system and a standardised movement test for all the users. A laser point was placed on the end effector of the robotic arm and the users were asked to follow a numbered patterned of points around a tibial baseplate outline placed on the wall. The movements of the robotic arm are smooth and requires minimal force outside of haptics. This gave a profile of usage (force and movements) for the manipulation of the system without any cutting or haptic resistance and hence, give an idea of the additional force required the haptics introduced.

6.2.3.5 Tibial and femoral resections

The participants were then taken through three consecutive burring tests of the MAKOplasty surgery, resecting the virtual bone of the femoral and tibial Condyle for a left medial UKA procedure. The two bones were fixed and placed in a realistic orientation to those that would be expected in surgery. The user then virtually cut the tibia and femur using the visual feedback (Figure 6.2-14). For safety, and practical reasons, no burr was used with only the haptic boundary created by the robot provided a physical resistance. As the Sawbone was not cut it did not offer resistances to the tests.

This, therefore, reflected the effort of moving the arm within the haptic volume, but not the extra effort of cutting the bone. As the Sawbone was not cut, the two distal ends of the sawbones were removed to allow the remaining burr mounting to pass through the virtually cut volume as seen in Figure 6.2-13. This method therefore reviews the theory that fatigue is the result of manipulating the robotic arm in haptics for extensive cutting times.

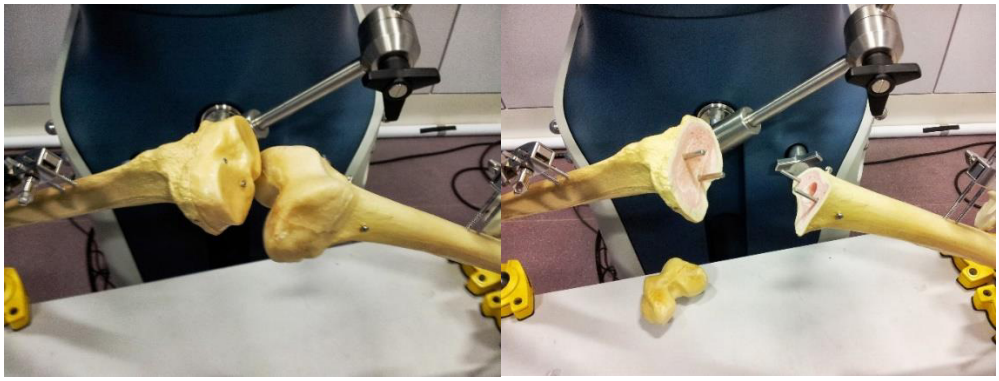

Figure 6.2-13 Saw Bone with and without resection volume. The ends of the sawbones were removed to allow the burr to be passed through the resection volume without the need for cutting of any material.

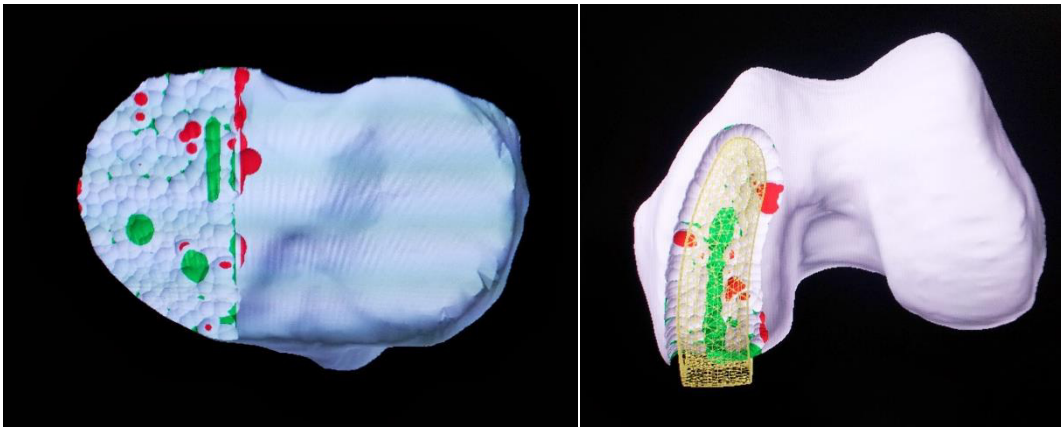

Figure 6.2-14 Example of acceptable resection in the MAKO user interface. The models are created from the scan of the bone. Where the planned implant over laps the bone the model becomes green, once the virtual burr passed through the volume the bone is assume cut and the model disappears. Red points should resections large than 0.5mm deep. The remain green points are secondary cuts that were not part of this testing.

The subjects were given 7 minutes to complete a single bone resection, or until a suitable amount of resection had occurred according to the visual display. Seven minutes reflected the resection time that the surgeons had been observed taking in the theatre (Banger et al., 2013). While this was longer than the mean, it fell within a single standard deviation above the mean (Resection time +1SD = tibia 8:30 min, femoral 7:41 min).

Breaks were inherently built into the testing through the necessity to reset the resected virtual model, reposition the saw bone and perform the robotic system's calibration checks. These pauses amounted to <1 minute between bones and <2 minutes between repeats.

Saw bone cutting

A single user Sawbone cutting test was added to review the effect of resistance to the movement of the burr and the change in forces required to manipulate the system with a saw bone present. This was a potential limitation of the design, and its possible impact on testing required reviewing.

The Sawbone material was made of a polyurethane expanding foam in the mould of the bone shape to allow for registration in the RIO system. The finished material did not have the same resistance to cutting bone, having a lower density and hardness, but did produce a harder shell on the outside where the resin would set hard against the polypropylene sheet, surrounding the porous foam structure internally. These materials are often used as they allow for the crafting of shapes while maintaining structural coherence.

6.2.3.6 Questionnaire responses

The questionnaire allowed for subjective responses for discomfort with the reporting of body parts and scoring of these parts. The users were to score only the areas that they felt required reporting. A body map with area descriptions was given to standardise reporting areas. A 7 point scoring system for the discomfort was used. This started at 1 with no discomfort and finished at 7 for distracting discomfort. The scoring is shown below in Figure 6.2-15, the rest of the questionnaire can be found in the appendix (Appendix 4).

Area (to be filled out)	No discomfort		Mild discomfort			Distracting discomfort		Duration (approx. In minutes)
	1	2	3	4	5	6	7	

Figure 6.2-15 Discomfort questionnaire scoring table. The area was defined from a map of the body and the duration was defined the time of peak discomfort, or when the discomfort was most noticeable.

In addition to area and level of discomfort, the time of onset of discomfort and duration was also recorded in the questionnaire. The user's description was qualitative, 'beginning of second femoral burring'. These descriptions were changed to a numerical system to allow averaging. The numbering was from 1 to 4. The whole number representing the test (1, 2 or 3) and decimals reference the bone (tibia <0.5, Femur>0.5). For example, the end of the second tibial cut would be given 2.5.

6.2.3.7 Data Analysis

6.2.3.7.1 EMG processing during mock surgery burring testing

While the pre-post testing showed indicators of fatigue, the mock surgeries are longer and less constrained in the activities of the user and so require an altered approach to processing. The tracking of the physiology of the muscle over time can be achieved by analysing EMG signals, but the dynamic nature of the test adds additional analysis difficulties. Due to this a number of methods

were used to interpret the signals, along with a proposed new method based on theory in the literature.

Frequency analysis of dynamic testing

Given the dynamic nature of the testing being performed this application was extended to calculated instantaneous median frequency. This applied to the periodogram functionality to a moving, overlapping window over the time course of the testing. The signal was processed with the Welch periodogram technique, with a 30% overlap, 256 sample (0.256 second) window (an integer power of base two allows the FFT to run faster). This window length was chosen to give a higher sample rate for comparison with the movement data, without compromising the frequency resolution. The literature recommends between 0.5-1 second windows for dynamics trials (MacIsaac et al., 2001), but a minimum EMG window is defined between 250-500ms for stable estimates in static conditions (Kamen and Gabriel, 2010). Given the slow movements that were predicted, a shorter window was chosen leading to a Pseudo-static IMDF calculation described below.

The average gradients of the median frequencies for the same bone cuts were calculated through linear regression. Here a negative gradient shows a decrease in the frequency component during testing showing a change in recruitment and an indicator of fatigue in the muscle.

Pseudostatic fatigue metric

Novel to the biomechanical testing setup, to the best of my knowledge, was the further sampling of the instantaneous frequency information with the joint angle data from the Kinematic model. While the short sample windows can assume pseudo-static condition, the further relation of joint angle with the frequency analysis is resolved in this process. The concept of Pseudostatic testing assumes that under reasonably similar submaximal forces over the testing periods, the EMG signal could be sampled when the joints are in the same position. This would in effect give Pseudostatic conditions to test the muscles frequency components over the duration of a test.

As the muscle moved beneath the electrode the frequency component of the signal can change as the different parts of the muscle. For more sensitive metrics, the joint angle can be used to isolate these movements from the EMG signal and measure the muscle in the same pose. This work is regularly used to measure fatigue in cycling that have well defined cyclical movements (Dingwell et al., 2008). Given the repetitive movements seen in the use of the robotic arm, a similar methodology was used in this experimentation.

Given time synchronization between the EMG recordings and the kinematic model, the time course of the kinematic model first decimated to the same sample frequency as the EMG

windowing. This sampled data was split into bins of 1 degree joints angles for wrist flexion, radial deviation and elbow supination. These joint angles all describe the movement and positioning of the wrist. Joint angle bins contributing less than 1% of the over testing period were ignored to negate noise from the joint angle calculations. All bins were assessed for linear regression of the associated change in instantaneous frequency over time. A negative gradient would be an indicator of fatigue. All electrodes were assessed relative to the joint angle of the primary action of the muscle, for instance, the pseudostatic calculation for a wrist flexion angle range from 0.5-1.499 would sample the median frequency for all muscles while within this range. A simplified experiment with bicep curls was conducted to validate findings and can be found in appendix 2.

The gradient of the median frequency (vs time) for each sampled section was calculated with linear regression. Sampling the signal can lead to high gradients for samples close together, so instead of the gradient, a change in frequency is calculated. The change in frequency is a multiplication of the gradient by the length of time between the first and last point within the angle bin. All bins for the same electrode were then averaged. The pseudostatic fatigue are calculated from 1-degree joint angle bin, average median frequency change for each cutting test, along with a mean change for all three cuts for the same bone.

All the muscles are for the primary joint motion of that muscle. The First dorsal interosseous is an intrinsic muscle in the hand and should only be dependent on the first finger and thumb movements, or otherwise independent of all of the joint movements used as comparators here. The change in frequency was consistently high for the other joints but showed the highest difference when isolated for the wrist joint angles. Hence the wrist flexion comparator was chosen to present the first dorsal interosseous.

RMS

The RMS is being interpreted here as the innervation of the muscles, or the neurological demand of the muscles. This electrical activity is the summation of muscle activity from isometric and dynamic contractions. Appreciating the activity of a muscle can identify how users are trying to achieve the task. Further understanding will come with the combination of the postural information. The mean and peak RMS value can be reviewed against population models of abilities, such as endurance models, to see if users should be considered able to complete the task without complications, such as fatigue. As before, the RMS is taken from the normalised data such that the values are a fraction of the EMG signal recorded during the MVC task. The mean and peak RMS value for the tibial and femoral tests for all users was calculated and the two bone resections were compared using statistical analysis.

Length of Tests from grip

The RMS of the first dorsal interosseous muscle is directly linked to the grip activity of the hand. To attain how long the grip was held (comparable to the trigger time) a 5% threshold was applied to the RMS of the first dorsal interosseous muscles, defining and on and off states for the grip. The total length of this grip was summated and average for all users.

IEMG

The integration of the EMG signal is a summation of all the activity over the testing time. The integration was calculated from the normalised RMS signal. While an IEMG is normally given in units of mVs, given this is the RMS normalised signal the output is effectively time in seconds (or %s). Specifically, this was calculated with a Trapezoidal numerical integration in MatLab and the resulting cumulative value calculated for the whole trial.

The tables and graphs below compare the average total IEMG value for tests, grouping the tibial cuts, femoral cuts and average bone cuts. Within the methodology, users would first complete a tibial cut and then a femoral cut, and then cycled through three times with Tib1 denoting the first tibial cut.

6.2.3.7.2 Motion analysis Data analysis

User range of motion

While the electrical activity of the muscles gave an idea of the physiological state of the muscle, the joints kinematics give movement and postural information which can further highlight possible causes of the fatigue in the muscle to be explained. As an example, postural deviations away from neutral, especially at the wrist, will have a detrimental effect on force production of articulating muscles possibly resulting in higher demand from the muscle. The deviated position of the wrist is, therefore, a contributing factor to fatigue. It is important to evaluate joint position to understand the causes of fatigue.

Given the length of tests (7 minutes each), a number of repeats (3 repeats for 2 bones) and the number of subjects (n=25) a pragmatic approach has been used to review the ROM data. The kinematic information was divided into histogram range of motion graphs. These histograms show the number of frames a joint angle was seen in that 1-degree bin range for all the users.

Further kinematic calculations were performed on a 95% distribution of the individual participant's data; this ignored the top and bottom 2.5% to negate outliers or errors affecting the range of motion. The range was calculated for individual participants and then averaged for all users. The minimum and maximum for these ranges were also calculated individually, defining the

extremities of the range of motion, and averaged for all users. A mean angle was calculated for the three tibial trials and also averaged for all trials. This mean angle describes the average posture for the procedure.

Difference in ROM between tibial and femoral components

The change in the average angles and range of motion is an indicator of differences in the use of the burr for the two cuts, and the different muscles used. We have seen there to be some difference in the EMG of wrist articulating muscles between the cuts; these should be highlighted in the movements of the joint. Calculated is the difference in postural approach for the two bone resections. These differences are the tibia variable minus the femoral i.e. the change in position from the tibial to the femoral cut.

Cumulative joint angular displacement

The cumulative movement of the user's joints is a measure of the amount a joint movement was used. While postures represent the 'static' positions, this is a measure of the dynamic nature of the joint. Calculated are the cumulative angular displacement for the wrist, elbow, and shoulder joints.

The cumulative movements of these joints were defined from the area under the angular velocity profile graph. This method negates the effect of the initial offset of the joint and summation of negative joint angles. Units of the cumulative displacement is radians.

Femoral and tibial cuts were compared through a two tailed t-test. A difference between cuts would highlight significant movement differences between cuts. Similar or continual use of a movement over both tests would be at risk of fatigue muscles when measure along with a high magnitude of displacement.

RIO Kinematics:

While the kinematics of the users have shown patterns of use, the use of the RIO can also be reviewed for the contribution of the joints to the movements of the burr.

Tibial and femoral cutting path

It is instructive to look at the passage of the burring being produced to understand why these joint ranges of motion are necessary. The burr tip was calculated from the location of the end effector cluster with known translations and rotations to define this point. To graphically represent the cutting path, the position of the tip of the burr over time was plotted in 3D.

Burr tip movement:

Given the ability to tracking the tip of the burr during the testing, the cumulative distance travelled for all the users could be averaged and reviewed. It should be pointed out that these

distances were only calculated from the recorded periods of the movements, so the distances will be a slight underestimate of the total distance. The burr tip's position was calculated from the movement of the cluster attached to the end effector of the RIO handle.

RIO ROM and Posture

The range of motion for both tibial and femoral cuts were averaged over all participants and presented for the individual joints of the RIO. Once again the joints more proximal (lower numbers - Figure 6.2-16) contribute to the gross movement of the burr with the finer movements coming from the distal joints (higher numbers - Figure 6.2-17). Joint 1 is the largest joint at the origins of the system, numbering through to joint 6 which is the handle or end effector of the robotic arm.

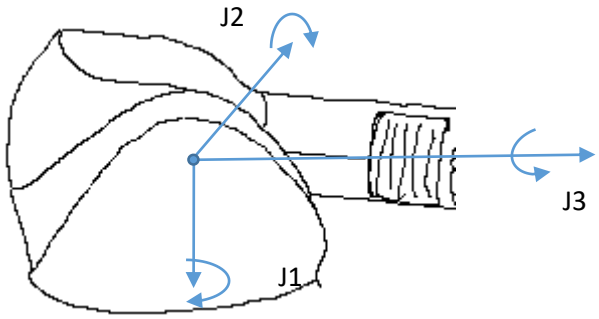

Figure 6.2-16 RIO Joint origin, axis and rotations definitions. Joints 1 to three have the same origin

The range of motion of the joints is an indicator of how much of their range is used on average, and this can be reviewed in the comparison between the two resections.

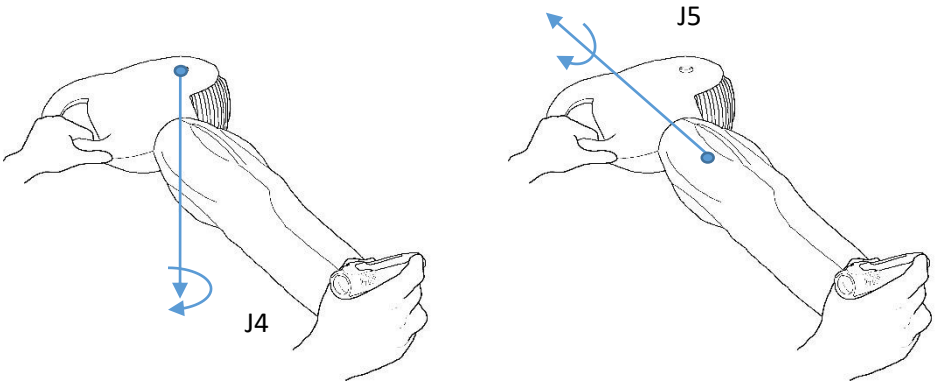

Figure 6.2-17 RIO Joint 4 (left)and 5 (right) rotation axes definitions

The average 'posture' of the system that this range of motion articulate about is of interest as well as this will affect the orientation of the hand.

Similar to the joints of the user, the RIO joint angles velocity profiles were calculated for each joint and then the area under this curve found. This represents the contribution of the joint, through a change in angle, to the movement of the burr. All the segments/links of the RIO have different lengths, so the angle change is not normalised for the difference distances moved at the burr tip. For

example, a movement at joint 1 will have a bigger linear displacement of the burr tip than joint 6 for the same angular displacement.

6.2.3.7.3 Force Transducer Data Analysis

Mean force

The average forces for the manipulation of the system gives a sense of the direction of the force being applied by the hand. In surgery these forces are overcoming the resistances from the robotic arm's stereotactic boundary and inertia, and also the cutting tool through the bone. No saw bone was cut during this testing, such that all the measured forces are the resistance caused by the robotic system. Through isolating these forces, the effects of fatigue can be attributed to the design of the robotic arm (haptics and ergonomic design). The resistance of the system is under software control and hence subject to refinement in the design of the system.

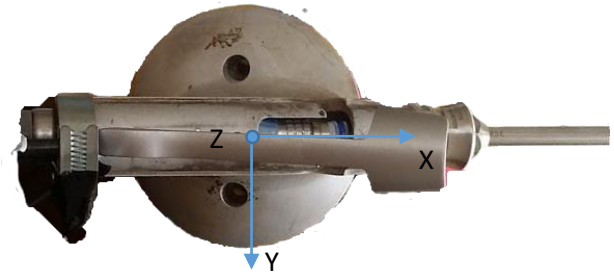

Figure 6.2-18 RIO EE with reference frame of transducer. Relative to the burr X (forward), Y (Right), Z (Up).

A 6 degree of freedom force transducer mounted in the End effector of the robotic arm measured the forces being applied by the user. The positive orientation of the force transducer was such that the Fx was in the direction of the burr, Fy was facing Right (or away from the RIO base) and Fz was upwards. The saw bone was a left leg with a medial UKA planned, putting the tibial spine in the positive Fy direction.

The forces and moments applied through the force transducer were calculated as the average (mean) and average absolute value (absolute). The absolute value of the forces was taken to show the magnitude of the force; how much was the handle pulled or pushed. The average direction can be assumed from the average force. The femoral and tibial resections were then compared with a Mann Whitney U test after it was deemed to not be normally distributed.

Max Force

Extremes of use was calculated from the average maximum force across participants and the maximum observed forces observed in a single participant. Again a Mann Whitney U was implemented to monitor changes between the cut average forces. These are important as, while not

sustained at this level, these forces are being demanded from the muscles without any break and will contribute to fatigue.

6.2.3.7.4 Questionnaire

The median discomfort scores and time of discomfort were calculated for responses from all users and the associated inter quartile range presented.

6.2.3.7.5 Statistical analysis

Student's T-test was used to compare continuous variables with a normal distribution of data. Mann-Whitney Test was used to compare continuous variables whose distribution was not normally distributed. Normality was review with the Shapiro-Wilk test. These analyses were performed in Microsoft excel (ver 2007, Microsoft, Washington, USA) and MatLab (MathWorks, MA, USA).

6.2.4 Post Testing Methodology

Repeated EMG work

The same pretesting routine (section 6.2.2) was repeated to assess post testing isometric strength of the participants.

Questionnaire

Discomfort scores reported by the user were recorded through a standard discomfort questionnaire (Appendix 4). This was carried out by the participants with the investigator present to answer questions from the user and to fill out the form if the participant had difficulty after testing. The questionnaire was self-reported and included the whole body as required.

6.2.4.1 Pre-Post Data Analysis

Strength Testing

The comparison of pre-post strength was calculated from the difference in the mean results of the three repetitions. These were statically compared with a paired, two-tailed t-test after normality was verified.

Pre-testing vs. Post Testing EMG

Testing the state of the EMG of the muscles at maximum voluntary contraction is a means of determining if fatigue has occurred. This is often repeated throughout testing, but this was not practical here and can induce further fatigue. Instead, it was completed before and after 3 mock surgical cuts.

Pre/Post Isometric RMS

The RMS of the EMG is a measure of the activity and innervation to the muscle. During the MVC assessment, the muscles can be assumed to be at maximum activity and represents the maximal value pretesting. If fatigued the muscles should not be able to reach the same level of electrical activity. Hence, the overall EMG activity of a fatigued muscle will be lower than in its pre-fatigued state for the MVC test. The magnitude of this decrease can be used as a metric of fatigue.

Pre/Post Isometric IEMG

The average integrated electromyography signal (IEMG) for the muscles under isometric MVC testing was calculated with a Trapezoidal numerical integration in MatLab.

Pre-Post median frequency change

Finally, the frequency of the EMG signal was calculated for the isometric MVC. Change in frequency is normally tested below MVC to allow for a change in recruitment of motor units, change in fibre activity and a resulting change in frequency.

6.2.5 Lab layout

6.2.5.1 Testing area

A 3m x 3m scaffolding mount for the Optitrack motion system was free standing and purpose built for the experiment. The accuracy of the Optitrack system was shown to be most accurate (±0.214 mm dynamic testing) at the centre of the capture volume, as all cameras were aimed at this point. This centre was used as the location of the cutting site of the robotic system (i.e. the knee centre).

The MAKO RIO system was setup to the manufacturer's recommendation (MAKO Surgical, 2009), with the exception of the visualisation screen which was moved outside of the capture area to reduce marker occlusion. The MAKO workstation and a table with 2 desktops running the Optitrack, EMG and force transducer software were positioning at the edge of the testing area to allow for line of sight of the participant by the researcher. Pin boards were used to block any incidental noise for the optical system and allow for the positioning of the laser target. Setup is shown in Figure 6.2-19.

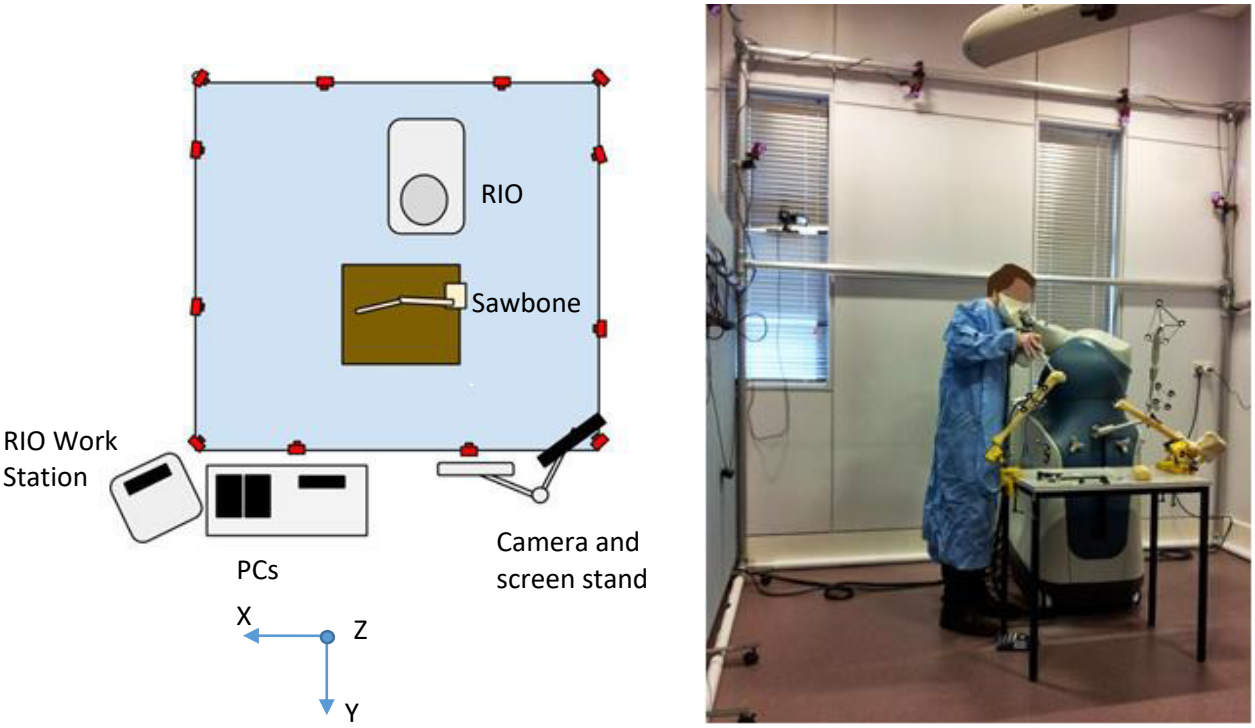

Figure 6.2-19 Example of right-handed setup. (Left) layout of the components with the blue area representing the capture volume. (Right) photo of a using burring in the capture volume.

6.3 Biomechanical Testing results

6.3.1 User (Test Subjects) Profiles

In total 30 participants were recruited. Of these 25 completed the whole testing protocol and were include in this analysis.

Table 6.3-1 Details of testing population along with literature values for orthopaedic surgeons

N=25	**Dominant Gender**	**Age**	**Height**	**Weight**	**Dominant Hand**	**Number of surgeries in total**
Mean or mode	Male	28.9	1.78 m	73.2 kg	Right	Nil (0.125)
Range	Male= 20 Female=5	23-45	1.6-1.93m	55-114kg	Left = 2 Right=25 Ambidextrous=1	(3 users with KA experience)
Surgeon Population Mean or mode	Male [1]	50.9[2] 41-55[3]	1.78m[4]	77.47kg[4]	Right [5]	

[1](Heest and Agel, 2012)
[2](“Orthopaedic Surgeon Census - AAOS,” 2004)
[3](“2011 Surgical Workforce Census Report — Royal College of Surgeons,” 2011)
[4](Knudsen et al., 2014)
[5](Lui et al., 2012; Schott and Puttick, 1995)

6.3.1.1 Cohort average profile

This testing group details presented in Table 6.3-1 was a predominantly young, right-handed male group. When compared to the wider surgeon population, from limited literature of orthopaedic surgeon demographics, this group is reflective of the gender, handiness and height, but otherwise younger, lighter and less experienced in surgery.

6.3.2 Population Strength

Table 6.3-2 Grip strength testing taking pre and post burring testing to indicate fatigue. Additional measure of wider orthopaedic grip strengths from Subramanian (2011).

N=25	Jamar Peak Grip Strength [N] with (SD)	
	Pre-Testing	Post Testing
Population Mean Maximum grip	Male: 418.9 (100.5) Female: 251.1 (54.7) Average: 382.6 (115.0)	Male: 372.8 (108.9) Female: 218.8 (65.7) Average: 340.9 (117.7)
Range Maximum grip strength	Male: 235.4-647.46 Female: 176.6-353.2	Male: 215.8-627.8 Female: 107.9-294.3
Surgeon Population Average	Male 463.5 (68.2) (Subramanian et al., 2011)	-

The recorded pre-testing grip strengths (Table 6.3-2) are comparable with the Brazilian-based whole population which used the same Dynamometer (Male Right Handed Age 25-29 449.3N (112.9), Female Right-handed 266.8 (93.7)) (Schlüssel et al., 2008). This shows that the recruited group are reflective of the wider population at that age (Male P value equals 0.1935, Female P value equals 0.7088). For the male recruited participants there was a significant difference from a male surgeon sample tested by (Subramanian et al., 2011) (two-tailed P value = 0.0485). Hence there is a case to say that the group is reflective of the wider population but weaker than male orthopaedic surgeons.

6.3.3 Post Testing isometric testing

Table 6.3-3 shows the calculated change in average strength testing between pre and post-surgery testing.

Table 6.3-3 Change in strength measures and statistical test between pre and post burring tests

Test	Mean Strength Change (SD)	T-Test (Paired, two tail)
Grip Test (N)	-4.26 (4.71)	<0.01
Wrist Extension (N)	0.53 (2.95)	0.167
Wrist Flexion (N)	0.66 (4.08)	0.191
Elbow Flexion (N)	-0.114 (0.281)	0.281
Radial Deviation (N)	0.069 (1.57)	0.406

* Statistically significant results (P<0.05)

For the entire testing group, the grip tests showed a significant reduction of >4N between pre and post burring. The other tests showed no significant change in maximal force produced.

6.3.3.1 EMG

6.3.3.1.1 Pre/Post Isometric RMS

Table 6.3-4 Max value of RMS EMG signal taken for both pre and post burring strength tests, with statistical analysis

	Strength Test	Pre-Testing (Normalised RMS Max)	Post Testing (Normalised RMS Max)	T-Test
First dorsal interosseous	Grip	0.906	0.739	<0.001 *
Extensor digitorum	Wrist Extension	0.856	0.812	0.314
Flexor carpi radialis	Wrist Flexion	0.804	0.811	0.858
Extensor carpi radialis longus muscle	Wrist Abduction	0.514	0.467	0.398
	Wrist Extension	0.673	0.604	0.353
Bicep	Elbow Flexion	0.837	0.809	0.639

* Statistically significant results (p<0.05)

As seen in the strength tests (Table 6.3-4), the maximum RMS average signal for the testing showed a significant decrease in the first dorsal interosseous for the grip test. While decreases were seen in the Extensor digitorum and Biceps muscles, these were not significant. The flexor carpi radialis showed a slight increase between pre and post cutting, but again this was not statistically significant.

Reviewing the extensor digitorum for the grip strength test (Table 6.3-5) showed a significant change in the maximum levels of innovation. Gripping is a secondary and antagonistic action of the muscle and should be interpreted as an indirect measure decrease in the action of the finger flexors.

Table 6.3-5 Extensor digitorum max value RMS EMG change for grip strength test pre and post burring to review the secondary antagonistic action of the muscle.

	Strength Test	Pre-Testing (Normalised RMS Max)	Post Testing (Normalised RMS Max)	T-Test
Extensor digitorum	Grip	0.569	0.497	<0.001 *

* Statistically significant results (p<0.05)

6.3.3.1.2 Pre/Post Isometric IEMG

Table 6.3-6 Integrated EMG signal measured during pre and post burring strength tests with statistical comparison

	Strength Test	Pre-Testing Mean IEMG (V.s)	Post Testing Mean IEMG (V.s)	T-Test
First dorsal interosseous	Grip	2729.14	2109.64	<0.001 *
Extensor digitorum	Wrist Extension	3207.79	2742.12	0.009 *
Flexor Carpi Radialis	Wrist Flexion	2842.72	2633.57	0.216
Extensor carpi radialis longus muscle	Wrist adduction	2006.87	1695.88	0.290
Bicep	Elbow Flexion	2594.95	2598.18	0.99

* Statistically significant results (p<0.05)

The data in Table 6.3-6 shows a significant reduction of the integrated EMG from pre to post isometric testing in the first dorsal interosseous and the extensor digitorum and hence a decreased level of cumulative activity. While decreases in the wrist flexion and wrist adduction task, these were not significant.

6.3.3.1.3 Pre-Post median frequency change

Table 6.3-7 Median EMG frequency changes during pre and post maximal strength testing

	Strength Test	Pre-Testing Median Frequency (Hz)	Post Testing Median Frequency (Hz)	T-Test
First dorsal interosseous	Grip	117.5	132	<0.001 *
Extensor digitorum	Wrist Extension	107.3	109.6	0.3
Flexor Carpi Radialis	Wrist Flexion	82.8	87.9	0.07
Extensor carpi radialis longus muscle	Wrist adduction	83.4	83.6	0.9
Bicep	Elbow Flexion	72.6	76.8	0.1

* Statistically significant results (p<0.05)

Measuring the frequency component at maximal voluntary contraction showed that there was an increase in the median frequency during contraction for all the muscles (Table 6.3-7). Statistically significant increases were seen in the first dorsal interosseous and flexor carpi radialis.

6.3.4 Mock Surgery

6.3.4.1 Questionnaire responses

Table 6.3-8 Average discomfort questionnaire responses taken at the end of testing

Area	Median Score (IQR)	Numbers reported	Median Time of occurrence (IQR)
Average Discomfort	4 (3-5)	85	2.5 (2-2.5)
Hand (And fingers)	5 (4-6)	30	2.5 (2-2.5)
* Hand only	5 (4-6)	21	2.5 (2-2.5)
* Fingers	6 (5-7)	9	2.5 (2-2.5)
* *Thumb	6 (5-7)	4	2 (2-2.5)
Lower Arm (not elbow)	4 (4-4)	11	2.5 (2-2.5)
Wrist	5 (5-5)	12	2.5 (2-2.5)
Upper arm	4 (4-4)	7	3 (2-3)
Shoulder	3 (3-3)	16	3 (2-3)

* Subgroup of hand

** Subgroup of fingers

The most frequently reported area was the hand/fingers (Table 6.3-8). This was reported in all of the tests. The average score of 5 puts this on the top end of mild discomfort and entering into distracting discomfort. The thumb and fingers had the highest discomfort scores, but these were only reported in 4 and 9 cases respectively. The fingers highlighted were the fingers associated with the trigger mechanism. The areas of the lower arm showed lower discomfort numbers. These results further support that there is an issue with fatigue in the distal upper extremity.

The Upper arm and shoulder were mentioned 7 and 16 times respectively, but with only mild discomfort being reported. These muscles groups act as gross positioners of the wrist and hand.

6.3.4.2 EMG Mock Surgery Burring Testing

6.3.4.2.1.1 Gradient change of instantaneous median frequency (IMDF)

Table 6.3-9 Dynamic Spectral frequency change with time. The gradients of the median frequencies vs time were defined for both the tibial and femoral cuts. The gradients were averaged for all repeated bones cuts and for all user.

Gradient of median frequency (Hz/s)	tibial Cut mean	tibial Cut SD	femoral Cut mean	femoral Cut SD
Flexor Carpi Radialis	-0.0045	0.0062	-0.0038	0.0077
Extensor digitorum	-0.0029	0.0049	-0.0016	0.00677
First dorsal interosseous	-0.008	0.0129	-0.0075	0.01907
Bicep	0.0008	0.0101	-0.002	0.0063
Extensor carpi radialis longus muscle	-0.0003	0.0054	-0.0013	0.00877

Nine out of 10 gradients showed a negative mean value, the exception being the Bicep during tibial resection (Table 6.3-9). Negative trend lines over time for similar levels of activity are an indicator of change muscle fibre activation associate with fatigue. This would suggest that all muscles as an average trend are showing fatigue, with first dorsal interosseous showing the largest changes.

6.3.4.2.2 Pseudostatic fatigue metric

Table 6.3-10 Pseudostatic median Frequency change (Hz) for primary movement of muscle. A negative results indicates a decrease in median frequency with time as an indicator of fatigue. Greater magnitudes to be associated with great physiological changes as a result of fatigue.

Specific isolation angle	Tibial Mean	Tibial SD	Femoral Mean	Femoral SD
Flexor carpi radialis	-5.66	3.69	-4.17	0.19
Extensor digitorum	-4.85	0.85	-3.59	2.14
First dorsal interosseous	-10.16	2.79	-5.85	8.95
Bicep	0.86	2.91	-0.59	1.15
Extensor carpi radialis longus muscle	-0.24	0.72	-0.40	0.48

In the Pseudostatic metric, a negative value represents a decrease in the median frequency, while a positive value represents an increase in the median frequency over a single bone cut. The smallest magnitudes of changes are the Bicep and Extensor carpi radialis longus muscle with minimal change in the frequency (Table 6.3-10). The wrist extensor and flexors are then showing larger decreases in the frequency and finally the first dorsal interosseous shows the largest signs of fatigue, especially in the tibial resection.

6.3.4.2.3 EMG RMS

Table 6.3-11 EMG RMS mean, peak and t test for tibial and femoral cuts. EMG RMS is a measure of the MVC normalised activity of the muscle during testing.

		Tibial (%)	Femoral (%)	t-test
Flexor carpi radialis	Mean	3.3	3.4	0.642
	Peak	18.2	19.9	0.266
Extensor digitorum	Mean	14.8	18.7	<0.001 *
	Peak	65.6	68.8	0.185
First dorsal interosseous	Mean	11.3	12.2	0.159
	Peak	64.4	64.2	0.954
Bicep	Mean	6.5	6.7	0.747
	Peak	37.6	28.6	0.059
Extensor carpi radialis longus muscle	Mean	7.4	11.5	0.011 *
	Peak	39.3	47.7	0.136

The mean values for the two extensor muscles were shown to be statistically higher in the femoral cut than the tibia cut showing a higher level of activity for this cut (Table 6.3-11). Otherwise there were no significant difference between the root mean squared EMG signal for the remaining muscles.

6.3.4.2.4 Length of Tests from grip

Table 6.3-12 Length of time spent gripping the end effector during tibial and femoral burring, as calculated from EMG RMS through thresholding.

	Average time [sec] (Standard Deviation [sec])
tibial 1	284 (106)
tibial 2	250 (102)
tibial 3	230 (99)
femoral 1	267 (89)
femoral 2	241 (103)
femoral 3	213 (87)

The tibial and femoral resection times were similar and both showed decreasing times, demonstrating learning curves over all users (Table 6.3-12). The average active cutting period for all bone resection was 4 minutes and 7 seconds.

6.3.4.2.5 IEMG

Table 6.3-13 Comparison of the tibial and femoral mean IEMG. The IEMG is a measure of the cumulative activity of the muscle from the EMG RMS signal.

	Tibial mean (V.s)	Femoral mean (V.s)	T-test
Flexor carpi radialis	11301.37	9543.492	0.002*
Extensor digitorum	52584.43	55974.93	0.086
First dorsal interosseous	37627.85	36211.83	0.4178
Bicep	20255.21	16884.58	0.0749
Extensor carpi radialis longus muscle	27327.79	37093.47	<0.001 *

* Statistically significant result ($p<0.05$)

The cumulative activity of the muscles all showed a decreasing trend with the number of repeated resections for both the femoral and tibia resections. The flexor carpi radialis was significantly larger for the tibial resection (Table 6.3-13). The Extensor carpi radialis was significantly larger for the femoral resection. The largest magnitude of activity was shown in the extensor digitorum.

6.3.4.3 User range of motion - Overall Average of range of motion

6.3.4.3.1 Tibial cut

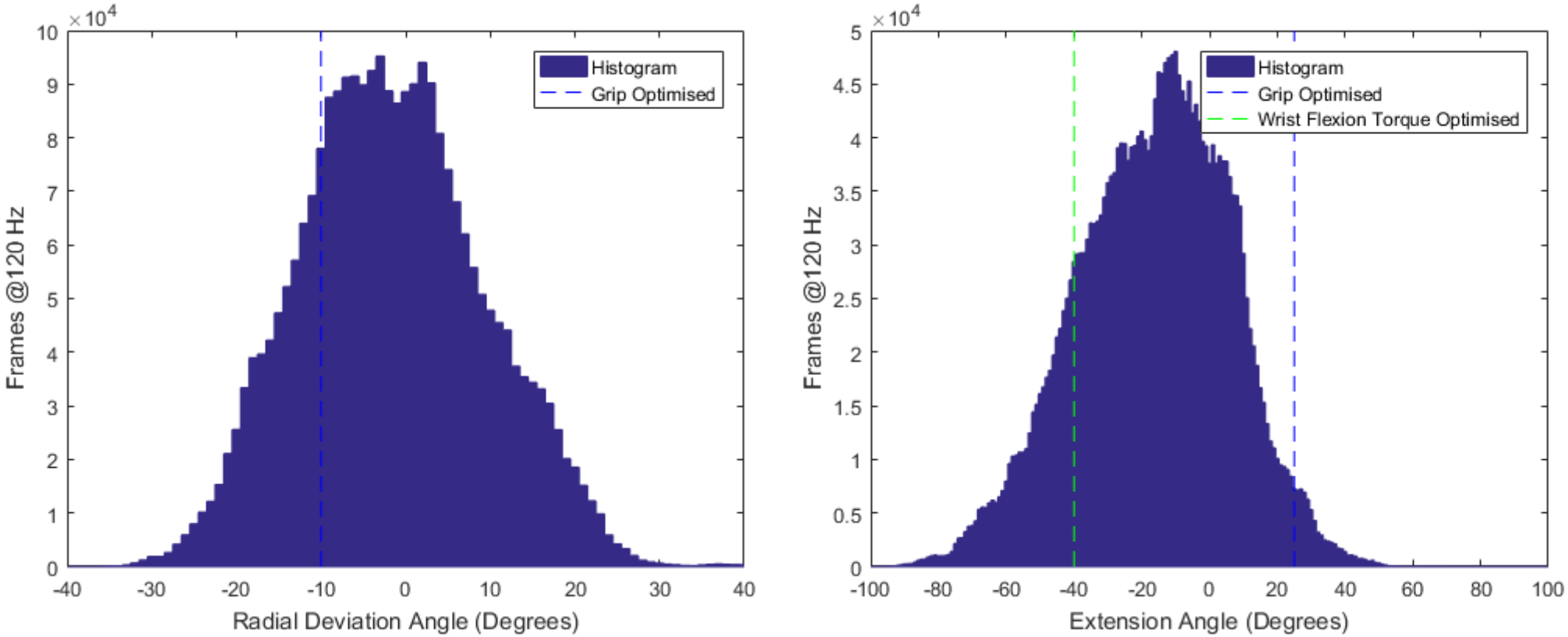

Figure 6.3-1 Tibial ROM Histograms of the wrist for the number of frame at a given joint angle. The graphs have been limited to the anatomical extremes of the range of motion for the joint. Additional vertical lines denoting the wrist angle for optimised wrist flexion torque and grip strength have been added.

The wrist ranges of motion in Figure 6.3-1 centred around neutral (-1.79 degrees (Table 6.3-14)) for radial deviation and 10 degrees flexion with both having limited usages at the extremities of the ranges of motions of the joint.

Table 6.3-14 Tibial ROM summary for the major movements of the arm. The range of motion and postures of the arm are a review of the biomechanical advantages/disadvantages of the muscles. Postures at the extremes of the range of motion of a joint should be avoided.

Tibial (degrees)	Range of Motion Av		Min Joint Angle Av		Max Joint Angle Av		Mean Angle for all trials	
	Mean	SD	Mean	SD	Mean	SD	Mean	SD
Wrist Radial Deviation	22.047	6.885	-11.661	3.266	10.387	5.999	-1.792	3.372
Wrist Extension	45.557	10.268	-36.889	8.806	8.668	8.328	-15.226	6.813
Elbow Supination	55.022	31.689	-34.031	8.247	20.991	28.635	-12.531	10.291
Elbow Extension	46.369	21.765	-103.213	6.590	-56.844	21.120	-83.105	6.333
Shoulder Flexion	51.751	22.660	12.711	13.303	64.462	15.409	38.234	6.693
Shoulder Abduction	55.082	26.116	15.306	19.683	70.388	10.889	43.114	7.399

A limited period of time was spent near the extremities of the range of motion and the range of motion was not extensive for the tibial resection (Table 6.3-14).

6.3.4.4.1 Femoral cut

The following are histogram plots of the relative joint angle for a single resection stage i.e. femoral cut 1, for all of the subjects, split into 1-degree bins.

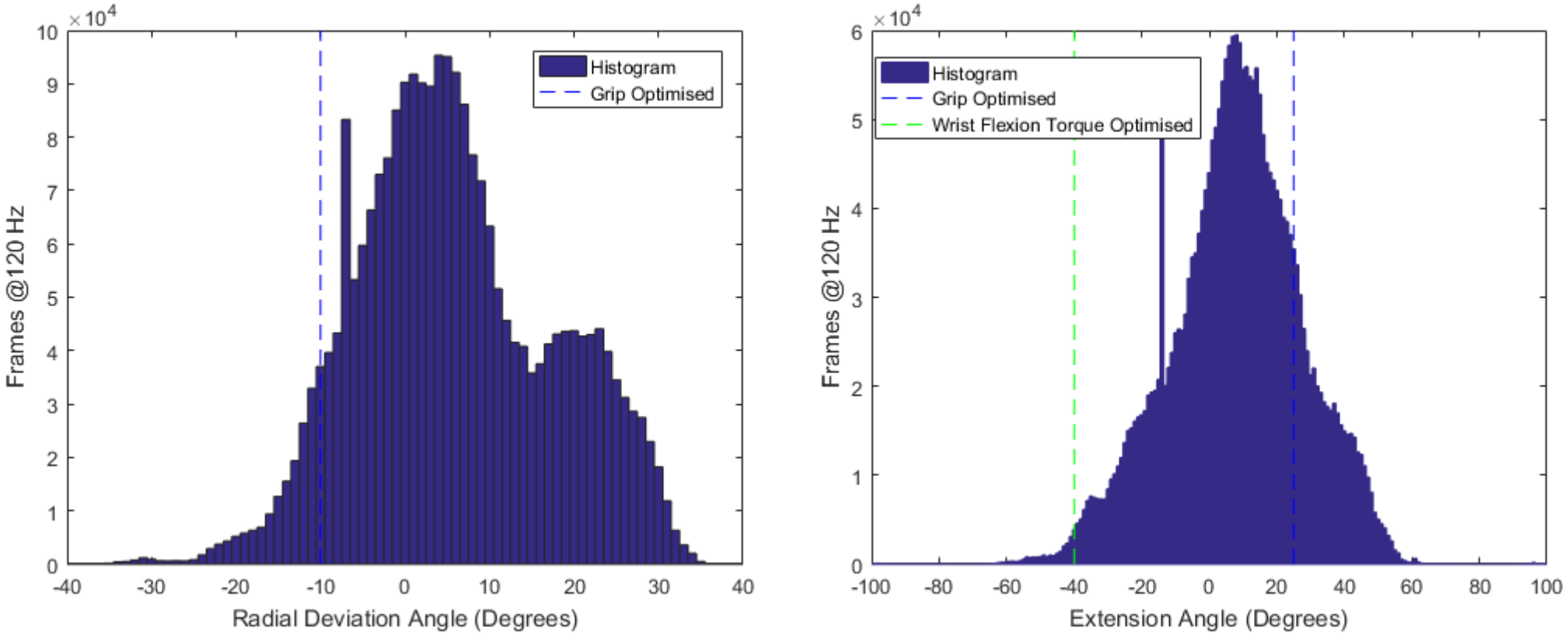

Figure 6.3-2 Femoral ROM Histograms of the wrist for the number of frame at a given joint angle. The graphs have been limited to the anatomical extremes of the range of motion for the joint. Additional vertical lines denoting the wrist angle for optimised wrist flexion torque and grip strength have been added.

The wrist ranges of motion in Figure 6.3-2 is centred around neutral (4.65 degrees (Table 6.3-15)) for radial deviation and 10 degrees extension with both showing limited usages at the extremities of the ranges of motions of the joint.

Table 6.3-15 Femoral ROM summary for the major movements of the arm. The range of motion and postures of the arm are a review of the biomechanical advantages/disadvantages of the muscles. Postures at the extremes of the range of motion of a joint should be avoided.

Femoral (degrees)	Range of Motion Av		Min Joint Angle Av		Max Joint Angle Av		Mean Angle for all trials	
	Mean	SD	Mean	SD	Mean	SD	Mean	SD
Wrist Radial Deviation	20.105	3.868	-5.420	3.209	14.685	3.195	4.650	2.324
Wrist Extension	40.385	8.987	-12.984	4.404	27.401	7.058	7.028	4.196
Elbow Supination	35.165	19.410	-31.441	7.995	3.725	15.612	-16.583	5.678
Elbow Extension	36.021	16.641	-94.105	5.683	-58.083	16.235	-78.219	5.290
Shoulder Flexion	37.162	17.892	8.206	10.068	45.367	12.078	27.291	5.146
Shoulder Abduction	36.490	19.639	7.207	16.701	43.697	7.662	27.363	4.360

A limited period of time was spent near the extremities of the range of motion and the range of motion was not extensive for the femoral resection.

6.3.4.5 Difference in ROM between tibial and femoral components

Table 6.3-16 Range of motion comparison between tibial and femoral cuts with statistical difference. A positive difference values calculated shows a larger value for the tibial resection.

Tibial - Femoral (degrees)	Range of Motion Av		Mean Angle for all trials	
	Difference	T-Test	Difference	T-Test
Wrist Radial Deviation	1.943	0.035	-6.442	0.000
Wrist Extension	5.172	0.001	-22.255	0.000
Elbow Supination	19.857	0.000	4.052	0.003
Elbow Extension	10.347	0.001	-4.886	0.000
Shoulder Flexion	14.590	0.000	10.943	0.000
Shoulder Abduction	18.592	0.000	15.751	0.000

The range of motion and average postures for all the user was significantly different between the femoral and tibial resections (Table 6.3-16). The largest difference for the wrist posture for the femoral resection was the amount of extension. With the wrist also showing more radial deviation and pronation. The tibia resection used more wrist supination range of motion, along with more range of motion of the elbow and shoulder.

6.3.4.6 Cumulative joint angular displacement

Table 6.3-17 Cumulative total joint angle movement at the wrist for tibial and femoral cuts, with statistical comparison.

Wrist Angles		Tibial cut (rad)	Femoral cut (rad)	2 tail t-test
Radial Dev	Cumulative angular displacement	1778	1691	0.427
Extension	Cumulative angular displacement	3163	3057	0.640

For the wrist, there was a low significance for the difference in movement of the joint representing a weak decrease in the femoral movements when compared to the tibial (Table 6.3-17). Of note here is that there are almost twice the angular movements in the extension of the wrist than the radial deviation for both cuts.

Table 6.3-18 Cumulative total joint angle movement at the elbow for tibial and femoral cuts, with statistical comparison

Elbow		Tibial cut (rad)	Femoral cut (rad)	2 tail t-test
Supination	Cumulative angular displacement	2694	2139	0.0840
Flexion	Cumulative angular displacement	2447	1754	0.0075*

* Statistically significant difference ($p<0.05$)

The movements at the elbow both change between cuts, with supination and flexion showing near significant and statistically significant less movement for the femoral cut respectively (Table 6.3-18).

Table 6.3-19 Cumulative total joint angle movement at the shoulder for tibial and femoral cuts, with statistical comparison

Shoulder		Tibial cut (rad)	Femoral cut (rad)	2 tail t-test
Flexion	Cumulative angular displacement	2540	1509	0.0035*
Abduction	Cumulative angular displacement	2465	1519	0.0006*

* Statistically significant difference ($p<0.05$)

Finally, the shoulder shows statistically significant more cumulative movement for the tibial resection than the femoral (Table 6.3-19).

6.3.4.7 RIO Kinematics:

Tibial cutting path

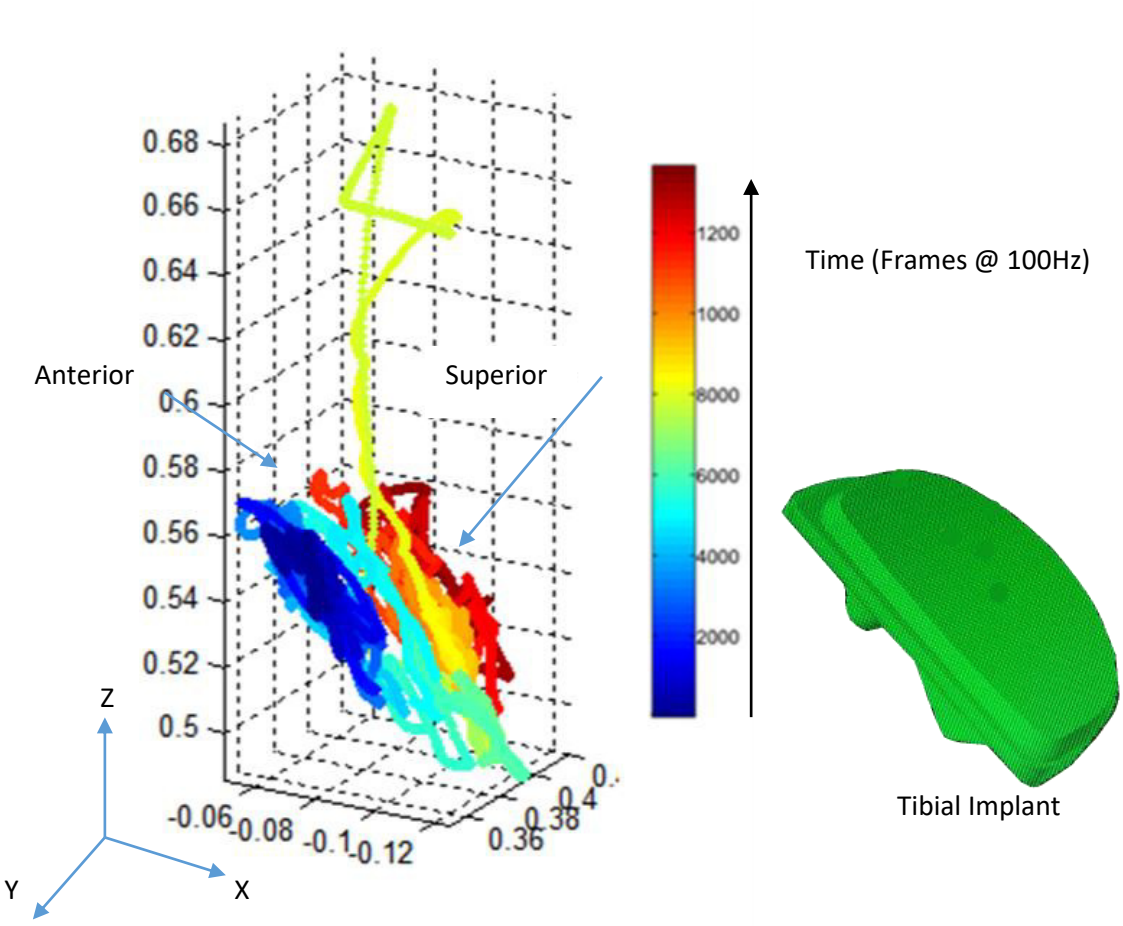

Figure 6.3-3 Temporal resection order (Left) with a top-down view of the tibial implant design (Right). Cooler colours (blue) represent the beginning of the resection with warmer colours (red) presenting the latter stage of the resection.

The approach shows the colder blue points on the anterior face of the tibia. The burr then moves medially and laterally while also progressing posteriorly (Figure 6.3-3). The flat planar nature of the tibial resection can be seen, with more anterior posterior movements of the burr being used.

Femoral cutting path

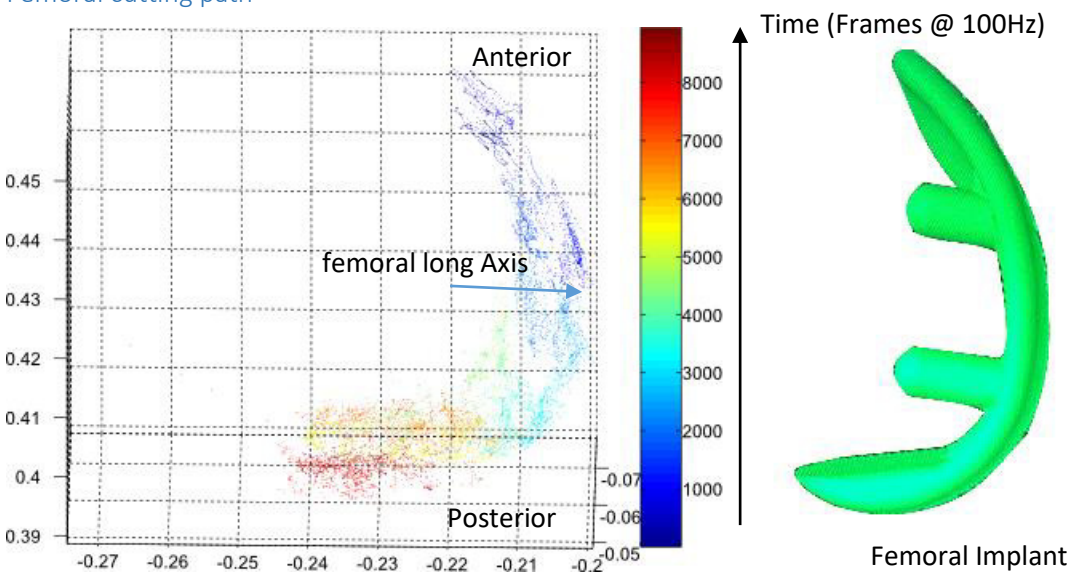

Figure 6.3-4 Femoral resection order (Left) With femoral component in the same orientation (Right). Cooler colours (blue) represent the beginning of the resection with warmer colours (red) presenting the latter stage of the resection.

Figure 6.3-4 is a 3D plot of the position of the burr and its path with a colour map describing the progression of the burr over time. It is clear to see that the lower frame count numbers represent the beginning of the burring (in blue) are located at the anterior section of the femoral resection, with a gradual progression to the back of the implant (the warmer reds and yellows). The curved profile of the femoral implant can be made out from the silhouette from the burr path.

Burr tip movement:

Table 6.3-20 Cumulative distance moved of burr tip

	Cumulative Distance (mean) (m)	SD (m)	Cumulative Distance Min (Max) (m)
tibial	9.883	4.949	3.019 (27.170)
femoral	8.361	3.451	2.968 (19.027)

The average for the tibial and femoral resection shows that the tibial resection covered more distance, this is similar to the time analysis trigger time assessment that showed an increased time of usage for the tibial resection over the femoral (Table 6.3-20). Through a t-test this was shown to be a significant difference (p=0.0305).

RIO ROM and Posture

Table 6.3-21 RIO range of motion for tibial and femoral resection

Joint	Range Tib (Degrees)	Range Fem (Degrees)	t-test (2 tail)
1	33.7	33.1	0.92
2	20.6	22.9	0.68
3	17.5	16.6	0.88
4	22.1	18.6	0.17
5	81.6	71.2	0.12
6	41.5	36.9	0.089

* Statistically significant result (p<0.05)

During the tibial cut more of the RIOs range of motion was used, however, no significant differences were seen between the ranges of motion of the RIO (Table 6.3-21).

Table 6.3-22 Average RIO Joint Angle. This describes the average posture of the RIO between the two bone burring.

Joint	Average Angle Tib (Degrees)	Average Angle Fem (Degrees)	t-test (2 tail)
1	-6.33	-11.97	0.1931
2	-7.86	-16.80	0.0027 *
3	-5.65	-8.57	0.2037
4	-21.81	-21.69	0.8730
5	32.66	17.64	<0.001 *
6	-33.14	-22.47	<0.001 *

* Statistically significant result (p<0.05)

All but joint 4 showed a difference in average position of the RIO joints, with 2, 5 and 6 showing a significant difference (Table 6.3-22).

Table 6.3-23 Cumulative joint angle movements of the RIO during burring.

Joint	Cumulative angular displacement Tib (Degrees)	Cumulative angular displacement Fem (Degrees)	t-test (2 tail)
1	373.62	298.66	0.156
2	330.98	271.68	0.032 *
3	269.81	148.30	0.181
4	409.33	273.00	<0.001 *
5	2026.37	1689.80	0.002 *
6	956.39	837.13	0.01 *

* Statistically significant result (p<0.05)

When reviewing the amount of movement each joint achieved in comparison to the other resection through an accumulation of angles moved by joint 2, 4, 5 and 6 were shown

to have moved significantly more in the tibial resection than the femoral, with joints 5 then 6 performing the most angular movements (Table 6.3-23).

6.3.4.8 Force Transducer

Mean force

Table 6.3-24 Mean and absolute force for tibial and femoral resection. Absolute force is a measure of the magnitude of the force used, with the mean used to describe the average direction.

	Mean tibial (N)	Absolute tibial (N)	Mean femoral (N)	Absolute femoral (N)	Mean Mann Whitney U	Absolute Mann Whitney U
Fx	5.82	7.03	3.56	5.66	0.004 *	0.023 *
Fy	-6.53	8.56	-6.87	8.39	0.959	0.749
Fz	-3.89	6.10	3.31	5.59	0.000 *	0.101
Mx	-1.01	1.06	-0.33	0.57	0.000 *	0.000 *
My	-0.13	0.24	-0.15	0.26	0.529	0.703
Mz	-0.12	0.44	0.04	0.43	0.000 *	0.992

* Statistically significant result ($p<0.05$)

Table 6.3-24 presents the tibial absolute forces and moments as significantly larger for Fx and Mx. The mean forces for the tibial resection were significantly more positive in Fx and more negative in Fz, Mx and Mz.

Max Force

Table 6.3-25 Average Maximum and absolute forces for the tibial and femoral resections. Absolute force is a measure of the magnitude of the force used, with the mean used to describe the average direction.

	Tibial (N)	tibial (absolute) (N)	Femoral (N)	femoral absolute (N)	Mann Whitney U	Mann Whitney U absolute
Fx	27.78	29.99	24.12	26.09	0.04	0.022
Fy	-25.01	34.16	-22.00	38.33	0.829	0.205
Fz	-10.25	31.03	27.14	32.87	0.001	0.327
Mx	-3.99	3.99	-1.92	2.91	<0.001	<0.001
My	-1.10	1.37	-1.37	1.37	0.298	0.585
Mz	-1.12	2.62	0.60	2.48	0.008	0.317

* Statistically significant result ($p<0.05$)

The average maximal forces (Table 6.3-25) showed significant positive increases in tibial Fx and significant negative increases in Fz, Mx and Mz. Also significant was the increase absolute Fx and Mx used for the tibial cut.

Table 6.3-26 Highest recorded forces and torques during tibial and femoral cutting.

Max	Tib (N)	Fem (N)
Fx	45.503	41.172
Fy	52.645	72.995
Fz	54.510	54.050
Mx	-2.624	-4.672
My	1.699	-2.361
Mz	3.273	3.411

(The average maximal forces (Table 6.3-25) showed significant positive increases in tibial Fx and significant negative increases in Fz, Mx and Mz. Also significant was the increase absolute Fx and Mx used for the tibial cut.

Table 6.3-26) shows the largest individual forces, with the femoral resection showing significant increased forces in Fy, Mx and My.

Saw bone cutting

Table 6.3-27 Forces measured by the end effector transducer during the burring of a single tibia and femur Sawbone. Absolute force is a measure of the magnitude of the force used, with the mean used to describe the average direction.

	tibial Mean (N)	tibial Mean Absolute (N)	tibial Max (N)	femoral Mean (N)	femoral Mean absolute (N)	femoral Max (N)
Fx	3.787	5.593	33.776	4.154	5.494	31.113
Fy	-1.104	5.943	46.636	-2.385	5.209	-31.033
Fz	-7.951	8.374	-62.160	-1.844	3.311	41.912
Mx	-0.408	0.428	-2.020	0.033	0.164	1.075
My	0.278	0.345	1.913	-0.023	0.145	1.006
Mz	-0.184	0.436	-2.589	0.203	0.382	2.327

Differences were seen in Table 6.3-27, for the tibial Fy and Fz, and femoral Fy, Fz, Mx and Mz means between the saw bone group and the larger group. The changes all show a decrease in the force being applied for the Sawbone group. Additionally, the average values were lower in the other forces as well.

Laser Testing

Table 6.3-28 Laser cutting ROM, Maximum range of motion and mean angle

Degrees	J1	J2	J3	J4	J5	J6
ROM (Degrees)	5.82	3.76	2.97	4.20	20.61	4.21
Max ROM (Degrees)	34.93	30.98	30.10	19.19	54.81	7.89
Mean Angle (Degrees)	-11.15	-8.57	4.28	-8.49	71.27	-46.04

Table 6.3-28 presents the a similar over position of the RIO, with increased rotation at joint 5 and 6 when compared to the values in Table 6.3-22. Similarly the range of motion at joints 5 and 6 are decreased in comparison when burring in Table 6.3-21.

Table 6.3-29 Forces and moments measure from the transducer in the end effector handle during the laser testing. Absolute force is a measure of the magnitude of the force used, with the mean used to describe the average direction.

	Fx	Fy	Fz	Mx	My	Mz
Mean (N,Nm)	1.731	0.255	-4.551	-0.007	0.093	0.057
Abs Mean (N,Nm)	3.036	2.690	4.573	0.067	0.112	0.296
Mean Max (N,Nm)	4.842	-0.165	-9.094	-0.039	0.208	0.377
Max (N,Nm)	17.154	8.567	-6.276	0.253	0.401	0.953

Table 6.3-29 presents smaller forces for all forces when compared to burring (Table 6.3-24).

6.4 Biomechanical testing discussion

Determining the nature of the fatigue from the descriptions offered by high volume users proved difficult, given the lack of detail. When discussed with the current local users, they reported no concerns of fatigue when using the system, even when fatigue was observed in single cases with large volumes of sclerotic bone and longer trigger times (Chapter 5). With no access to interview the wider MAKO user community, an objective testing methodology was developed. This testing is unique and valuable in its own right as a bespoke approach to a muscle fatigue issue, but the main purpose of the testing is to isolate factors that are contributing to user fatigue in MAKO RIO users.

6.4.1 Pre Testing

This testing group was a predominantly young, right-handed male group. When compared to the wider surgeon population, from limited literature of orthopaedic surgeon demographics, this group is reflective of the gender, handiness and height, but otherwise younger, lighter and less experienced in surgery.

6.4.2 Pre-Post Strength testing

6.4.2.1 Force measurements

The only test that showed a difference in strength was the grip strength, and this was a significant decrease. This functional inability to grip in the post testing would indicate that the only issue with this system are in the grip forces required.

6.4.2.2 RMS Pre-Post

The decrease in all of the peak RMS values for the strength testing shows that there was some decrease in the activity in these muscles, but the only result that was measured to be a significant change, was the first dorsal interosseous muscle associated with gripping. This seconds the results of the strength measurements differences, here confirming that the muscle could not reach the same pretesting levels of activity.

A secondary result extracted from the grip strength testing was also the significant change in the extensor digitorum's ability to innovate. Additional analysis of the EMG data shows that the extensor digitorum shows a statistically significant (Table 6.3-5) decrease in the Max RMS mean for all 25 users for the grip strength test. The primary action of the muscles was shown to not decrease, and as such the muscles was assumed not to be

fatigue. However, given the antagonistic function of this muscle as a finger extensor, less demand may be required from it due to the finger flexor muscles weakening as a result of fatigue. The finger flexors were considered too deep for consistent measurement, and the intrinsic hand muscles were chosen instead.

6.4.2.3 IEMG pre-post

Once again the first dorsal interosseous metric of activity was shown to be decreased when comparing post to pre testing results. Further confirming the issue with grip strength required.

Also repeating a significant decrease was the extensor digitorum, however, for the primary action of wrist extension. These variables have been calculated from the same RMS signals as the maximum RMS calculations and indicate that the Extensor digitorum was not maintaining the same activity output over time in the MVC strength test. This suggests that while the muscle was able to produce a similar maximum activity level pre and post testing, the muscle was now not able to maintain this contraction as long, due to a reduced effort. While a significant result, this is not seen as being particularly meaningful.

Timings for the tests were standardised, but the length of the activity was subjective and is likely a measure of motivation. All lower arm muscles showed a decreased between pre and post testing, but not all significant, representing a lower exertion for these tests.

6.4.2.4 Pre-Post median frequency change

The first dorsal interosseous showed a significant increase in the mean post testing median frequency. There is little to no literature of fatigue frequencies analysis at 100% MVC, as testing is recommended to take place at sub maximal forces to allow for changing recruitment patterns, at maximal effort all fibres would be recruited. However, interpretation of this result would suggest a change in the frequency of the muscle's EMG during the testing, such that the higher frequency fibres (creating larger forces) are dominant during this maximum voluntary contraction. The sustained sub-maximal contractions during burring would result in fatigue in the middle frequency elements, under an assumption of Henneman's size principle for recruitment. The consistent reporting of fatigue in the first dorsal interosseous muscle would suggest some correlation with the other, more recognised, measures of EMG signals. This result is hard to ignore given the

significance of the results, but the surrounding theory and understanding is lacking to holding this in any regard in isolation.

6.4.3 Mock Surgery

6.4.3.1 Questionnaire responses

The questionnaire was a measure of the subjective reporting of discomfort for both locations on the body and approximate occurrence during burring. The overall average occurrence of discomfort onset was within the second femoral cut (2.5), with all the reporting times averages being reported before the final repeated test (<3). Another way of representing this is after the burring of 3 bones ($(2.5-1)*2$). The recorded time for an average single bone cut from the mock surgery was calculated as 4:07 minutes. Therefore the reported time to onset of fatigue was 12 and a half minutes of burring [$4{:}\,07 * (2.5-1)*2 = 12{:}\,21\ (mm{:}\,ss)$]. The longest observed cut for a single bone clinically in the previous chapter was 14:49 (Section 0), easily within the timeframe of the observed onset of fatigue in these users in this mock surgery. This shows that this mock surgery is replicating the longer clinical cases with similar discomfort being reported by the mock users as the surgeons.

The highest report, both in frequency and magnitude was the hand and fingers. This would agree with the measurements of electrophysiology in the first dorsal interosseous. So this further confirmed that fatigue is relating to the grip. However, the prehensile forces are created in both the forearm and the hand. While some levels of discomfort were reported in the wrist and forearm, the discomfort in the hand would suggest a further localisation of issues relating to the posture of the hand and fingers during the burring process.

6.4.3.2 Median Frequency gradient of EMG Mock Surgery Burring Testing

It has been suggested to this point that fatigue is likely to be located to the hand and secondarily to the forearm from the subjective responses to the questionnaires, and strength measurements changes. Review of the EMG signals during the testing should highlight further evidence of fatigue.

The gradient of the median frequency shows the trend of the spectral analysis of the EMG relative to time. A negative change of IMDF over cycles, as shown (Bonato et al., 2003,

2001) is indicative of a measure of fatigue. The highest change in frequency over the time course is seen in the first dorsal interosseous muscle for both the femoral and tibial cuts. This would suggest that this muscle is showing a greater rate of fatigue during the testing relative to the other muscles. Given that we know from previous indicators of fatigue that muscle showed pre to post testing fatigue, it is reasonable to state that this data shows a fatigue process during burring. The flexor carpi radialis also shows changes in the median frequency over the time course, with the tibial resection showing more signs of fatigue.

The standard deviation of the groups' gradients would suggest that these trends are not exclusively negative for all users. The literature has used this method across multiple users to show general trends, and it is by no means definitive for a single user (Viitasalo and Komi, 1977). Given that the largest gradients were shown by the muscles known to fatigue (FDI), this would suggest that the other muscles can be assumed to fatigue, but not to the same extent. This effectively puts a quantity on the measure of fatigue and can be used as a comparator between muscles, but the nature of this change is not fully understood.

These observations rely on the assumption that there is continual submaximal force being applied by the muscles. Given the multiple actions of the muscles to either create the gripping force or stabilise the wrist joint, this is a reasonable assumption for the lower arm muscles. The additional fluctuations will come from the additional movements of the wrist, but given the repetitive nature of the movements these can be assumed to average the length of a testing procedure to provide a consistent level of activity. To improve the sensitivity of these calculations as a fatigue metric, a pseudostatic fatigue metric was applied and is discussed below.

6.4.3.3 Pseudostatic fatigue metric

This metric is a proposed measure of fatigue during unstandardized functional activity through the sampling of the EMG signal relating to postures of the joints, relating to the articulation of the measured muscle. This is the first known application of this technique, so while some skepticism should be applied to the results, this new metric can otherwise be compared to the other metrics of fatigue for corroboration. It is difficult to assume that median frequency changes can be compared linearly between difference muscles as different muscles have different fibre type make up, will recruit differently and hence fatigue differently (Farina et al., 2010), hence muscle metrics should

only be compared with themselves. However, the largest negative results again are represented by the first dorsal interosseous muscles. This corroborates with the other recordings to suggest a relation between the level of fatigue, and the magnitude of this metric. Further analysis of this work and more controlled experiments would be required to interpret the magnitude of the fatigue metric in isolation.

Larger frequency changes were shown during the tibial burring than the femoral burring for the first dorsal interosseous, and these tibial changes were much larger than any of the other reported mean frequency changes. This suggests that the tibial cuts were more fatiguing for the intrinsic gripping muscle.

Otherwise, the flexor carpi radialis and extensor digitorum did show signs of fatigue, but not to the same extent as the first dorsal interosseous. These changes could account for the mild discomfort reported in the forearm, but were not significant to change the functional ability of these muscles. No changes were seen in the bicep or extensor carpi radialis longus muscle.

6.4.3.4 Length of Tests from grip

While a 7-minute window of testing was allowed, not all of this time was used, and some users only required a fraction of the time due to better proficiency. In Table 6.3-12 a definite learning curing over the testing process can be seen from the average of all users. The cycle of testing started with the tibial cut, and then moved onto the femoral cut, for the cycle to repeat 3 times. Progressing through these cycles the time is shown to decrease in time. This is seen as a decrease in time both between repetitions of cuts and the different bones.

Overall the average cutting time was 4:07 (m:ss), which is similar to the average trigger times reported from the time analysis (Tib 4:03, Fem 3:46). This highlights that the setup was reflective of the surgical procedure for recreating the length of time the system was used.

6.4.3.5 RMS

The mean RMS is a measure of the continual activity of the muscle; the peak RMS is a measure of the maximum activity recorded. Given the normalisation of the EMG signal for all muscles it was assumed to be appropriate the compare the results between muscles.

Assuming the first dorsal interosseous is only a reflection of the grip demand over the mock surgery period (247 seconds), the endurance models (Finneran and O'Sullivan, 2013) show a 20-25% level of force production before the onset of fatigue can be expected. The average values are below this suggesting that significant fatigue shouldn't occur in a majority of users, but this isn't reflective of the functional inability of the user at this stage. It could therefore be assumed that the cumulative effects of fatigue over a number of repeats leads to a fatigue. At these grip intensities fatigue could be estimated to onset at approximate 1200 seconds is sustained, or if divided by the average length of burring this would occur during the second femoral resection (<5 bone cuts) which was the median reported occurrence of hand/finger fatigue.

Also of interest are the highest peak values shown in the extensor digitorum and first interosseous muscle. The peaks values are well above this criteria average activity, but were only maintained for short periods of time. What can be assumed from this is the fatigue in the hand is not likely to be the result of just a sustained contraction, but more the demand of both a sustained contraction with instants of high demand.

As an intrinsic muscle in the hand, the first dorsal interossei can be certain to be contributing to the grip of the end effectors. However, the contribution of the extension from the extensor digitorum is difficult to determine, given its multiple attachment points, this could be contributing to the extension of the wrist or finger extension (anatagonistic to finger flexors). What is of value is the higher likely hood that these muscles will suffer fatigue before the other muscles, however from the pseudostatic fatigue metric, and strength tests indicates that the first interosseous is effected much more than the extensor digitorum.

6.4.3.6 IEMG

The averages for both the tibial and femoral IEMG show a downward trend for all users from resection 1 to 3. Given the novice experience of the users, a simple explanation for this could be the users showing a learning curve through using less energy to complete the tasks. An alternative explanation is the decreased length of time of testing for the repeated cuts; this is more likely a factor to decrease the overall exertion for shorter cutting periods. As the user becomes more familiar with the feel and manipulation of the system, there is less overall exertion applied to the system. The extent of a learning curve's impact on

fatigue is difficult to state, but a more experienced surgeon would be considered to exert less effort for the same conditions.

The extensor digitorum muscles saw higher activity in the femoral resection over the tibial. This was also seen in the extensor carpi radialis longus muscles, but not of the same magnitude. The Extensor digitorum communis is a complex muscle both extending the wrist and fingers. During the gripping of the handle, this muscle works in an antagonistic action to the finger flexors to create stable finger joints for the grip. However, both of these muscles extend the wrist and suggests a significant increase in extension during the femoral cuts. The wrist flexor shows higher activity in the tibial resection over the femoral. This would be a reasonable assumption given the opposite action to the wrist extensors that were more active during the femoral cutting. While the extensors were more active than the flexor throughout the testing, neither showed functional fatigue in the strength test, but both showed electrophysiological fatigue from the pseudostatic metric.

The Bicep muscles showed the lowest relative amount of muscle activity during this testing. Given that this is a gross movement and high strength muscle, its minimal activity shows the fine nature of the movements that the user is engaging at the distal joint articulations. On reflection, the Bicep's main activity is to support the weight of the arm, as such few high force flexion movements of the elbow are required.

6.4.3.7 User range of motion

The wrist radial deviation angle during tibia cutting is approximately neutral, at 1.7 degrees ulnar deviation. A typical range of motion at the wrist is around 50 degrees (Magee, 2008; Nordin and H. Frankel, 2012), 44% of this is used during the observed testing. This is a relatively large range of motion from this finer controlled wrist movement. While a majority of the time is spent in and around neutral, there are periods where larger rotations are evident from the histograms. The extremity of radial deviation was seen in the maximum joint angle average. Typical maximum radial deviation is given as 17.6 ± 6.7 degrees (Gunal et al., 1996). It is known that the functions of the hand (grip strength and joint torques) are compromised at the extremities of the range of motion and should be avoided. However, these results would suggest that users are using these limits for short periods of time.

The average flexion angle at the wrist is 15.2 degrees for all the tibial cuts. A slightly flexed (20-40 degree, green dashed line in Figure 6.3-1) wrist is ideal for maximising both flexion and extension moments. Outside of this range the ability to generate flexion moments drops by around 60% (Delp et al., 1996). Additionally, grip strength is shown to decrease away from the functional hand position (O'Driscoll et al., 1992), but this is between 20 and 35° wrist extension ("Functional position of the hand | definition of functional position of the hand by Medical dictionary," 2009; Lannin et al., 2003; Pendleton, 2012) (blue dashed line in Figure 6.3-1). This would suggest that this position is optimised for wrist torque at the sacrifice of grip strength optimisation. The total range of motion in the flexion/extension wrist is approximately 125 degrees in the sagittal plane, here 36% of that is used. This is again a small proportion of the range of motion.

The forearm is on average pronated by 12 degrees. At this angle, there is not a robust model to define the effect that this will have on sub-maximal contractions. From a review of the range of motion, the extremities of motion are not seen. (La Delfa et al., 2015) showed that the extremities (±90°) of supination and pronation had a significant impact on the wrist joint torques. In slight pronation, there is no assumed significant compromise to the function of the hand.

The elbow average posture was 83 degrees of flexion; this is ideal for torque production at the elbow, which have been shown to be optimal elbow torques (Guenzkofer et al., 2011). The range of motion used was 33% of the range of motion of the joint, this reflects a much smaller use of the joint and would suggest an optimisation for this joint for all users.

The shoulder has an average abduction of 43 degrees. This posture is a result of the height of the knee and approach of the burr onto the knee. The variation of the height of the users reflects the right skewed distribution of the average posture for abduction, with shorter users requiring higher abduction angles to raise their hands to the height of the saw bone.

Shoulder flexion similarly had an average angle of 38 degrees. The shoulder, like the elbow, is a gross positioner of the hand. Flexion of the shoulder will increase the hand's height and distance from the body. Along with shoulder abduction and elbow flexion, these postures are all relative to the height of the knee, height of the users and distance from the knee. These postures are a function of the setup relative to the user.

Overall the average postures show an acceptable range of movements for the gross positioners, in the shoulder and elbow, as well as the finer movements at the wrist. Positioning at the extremes of the range of motion are generally avoided and centred around neutral. The wrist posture is compromised for grip strength to the flexion of the wrist, possibly resulting in additional muscle activity to produce the same force.

For the femoral kinematics, the wrist is slightly radially deviated. This overall movement to radial deviation will weaken the grip force leading to higher demands on the muscles to produce the grip require to hold the robot handle. Additionally, 40% of the range of motion was being used. The range of motion can be seen in the number of frames captured in or over the normal range of motion of the joint in the radial deviation of the wrist. This shows that an unsuitably large amount of time is spent at this extremity.

Wrist extension averaged to 7 degrees. This posture is a compromise between grip and wrist torque, but otherwise ergonomically a reasonable posture. 24 percentage of the range of motion of the joint is used for the femoral resection.

The supination of the wrist is at an ergonomically acceptable 17 degrees pronation. At this posture, there is no compromise to the function of the hand and wrist. The average range of motion shows only 20% of the total range is used. This indicates that little motion and movement of the robotic handle came from the pronation of the wrist.

The Elbow is again at an average position to allow the best function of the hand at 78 degrees of flexion. The range of motion used represents 20% of the total range of motion of the joint. This is an acceptable range for this type of task.

The shoulder shows a posture similar to other reaching tasks, with a 27 degrees flexion and 27 degrees abducted shoulder. The percentage of the total range of motion was 20% of flexion and 20% abduction. These propose minimal issues for this task.

Other than high values of radial deviation for the femoral burring, there is little concern from the posture of the users or the range of motion. For both burring postures, the wrist is away from the ideal functional posture of the hand. It is difficult to determine the true effects of this on the presentation of fatigue, especially in prehensile muscles used for extended periods of time. Whether slight postural change could lead to improve fatigue resistance is explored in the next chapter with a new handle design functionally changing these posture during the same task.

6.4.3.8 Difference in ROM between tibial and femoral components

The tibial and femoral component resections are significantly different patterns of movements and postures for all joints.

The decreased wrist extension for the tibial cut, or alternatively the increase flexion of the wrist for the tibial component given an average 22° of flexion. The wrist is also more radially deviated and supinated in the femoral resection. Generally, these movements, radial deviation and extension, will raise the burr tip as the femoral surface was set up higher than the tibial surface.

Another change between the two cuts is seen in shoulder flexion and abduction. The tibial cut is shown to have more flexion and abduction to allow for the tibial slope and to allow reaching over of the burr into the knee joint. These findings occur with the added wrist flexion seen in the tibia cut. In other words, that the whole arm is used in the positioning of the burr.

A larger amount of the range of motion is used during the tibial cut for all the joints. The largest differences were seen at the shoulder and elbow supination, but all differences were significant. This shows that the tibial cut is more dynamic and requires a wider range of dexterity to manipulate the robotic arm through the haptic volume.

These differing postural and dynamic differences will require differing muscle requirements. For example, the increased flexion is seen as a significant increase in the IEMG of the flexor carpi radialis during the tibial resection, or the reverse with the IEMG of the Extensor carpi radialis longus showing a significant increase during the femoral resection. The combined review of all the results are given in section 6.4.4.

6.4.3.9 Cumulative joint angular displacement

The cumulative joint angular displacement is a measure of how much a joint was used in the testing. The extension of the wrist was the largest overall cumulative angular displacement. Higher displacements occur through highly repetitive movements over a wider range of motion. Ideally movements of the hand and end effector of the robot should come from the proximal joints of the arm, when force is required and the movements from the wrist when fine small movements are required. From the peak RMS EMG values of the wrist extensors we know that there must have been some demand on these muscles are

some points to result in such high values. Ultimately large wrist movements are not ideal for force based work and should be avoided, which is not the design of this system.

The gross movements of the burr that was seen comes from the elbow and shoulder. The elbow and shoulder movements showed a significantly increased contribution in tibial resection than the femoral. Given the plane of resection of the tibia, movement of the elbow and shoulder will result in linear movement of the burr backwards and forwards, the femoral components, however, are highly curved and hence different cutting motions are used. This is reviewed further in the cutting paths in the following section.

The lowest displacement was the ulnar and radial deviation. The wrist position relative to the end effector changes dependent of the pronation of the wrist. The movement of the burr in either the vertical or horizontal directions (Figure 6.4-1) was mostly manipulated through extension of the wrist and altering the pronation of the wrist. This otherwise isolated the ulnar deviation movements. This would account for the decreased RMS activity in the Extensor carpi radialis longus muscle.

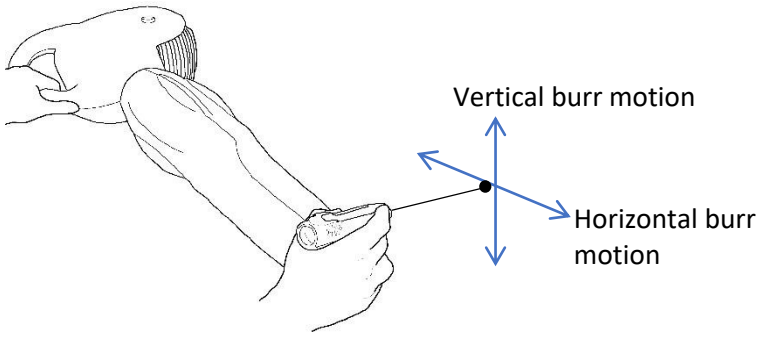

Figure 6.4-1 Illustration of vertical and horizontal burr motions as a result of wrist motion

Wrist flexion extension was shown to have the highest average periodicity at 1 Hz. While other joints also contribute to repetitive movements, the most consistently repeated movements, for both bones, was the wrist flexion extension.

6.4.3.10 RIO Kinematics:

Tibial cutting path

The tibial cut is the first of the two cuts and access to the bony anatomy is initially limited to the anterior surface of the tibial condyle. The approach shows the colder blue points on the anterior face of the tibia. The burr then moves medially and laterally while

also progressing posteriorly. While the surgeon is actually free to move around in the haptic volume, the resection is progressed in sections shown in the grouping of similar colours.

Once most of the superior volume has been removed, the surgeon is then left with the thin volume at the bottom of the tibial plateau that overlaps with the haptic boundary. In order to remove these last remaining pieces of the volume, the surgeon must push the burr tip towards the boundary in order for the material to be removed. This is a safety feature that allows for more control of the movement of the burr by the robotic arm close to the boundary of the volume.

In areas away from this haptic border, lower haptic forces led to a greater dominance of the inertia of the arm. In these regions the burr was seen to kick when it meets hard bone. These kicks are acceptable in the larger volume, but at the boundary edge, these can cause unnecessary bone resection and a danger of soft tissue laceration. Hence the increase in haptic force which the surgeon must overcome. The accuracy of the system therefore is assumed by the resistance to movement at the boundaries. However, this also leads to a greater force required to manipulate the robotic arm. The effectiveness of this boundary can be seen in the definition of the shape created by tracking the burr position. Other than the small deviation of the burr from the volume during a break in burring, the volume is well defined and reflects the shape of the tibial implant shown next to the plot.

Femoral cutting path

The femoral cut is the second cut so as to allow for greater access for the posterior resection of the femoral surface. The surgical incision allows for a large exposure to the distal segment of the femur and resection starts at the anterior tip, or close to it. This can be seen in the colour map with the gradual progress from anterior to posterior.

The general impression of the direction of burr tip path for the tibial cut was anterior to posterior while the femoral pattern is less obvious relative to the anatomy. This is thought to result in the larger elbow and shoulder movements for the tibial cut as previously mentioned.

The later, posterior, burring requires the awkward position of the wrist that was shown in the range of motion data. As Figure 6.3-4 shows, the red markings on the femoral condyle represent this posterior resection volume. The burr has to come under the bone and pull back and upward to create the cut (Figure 6.4-2). This is often performed with a

considerable extension of the wrist as shown in the range of motion and leading to large EMG in the wrist extensors.

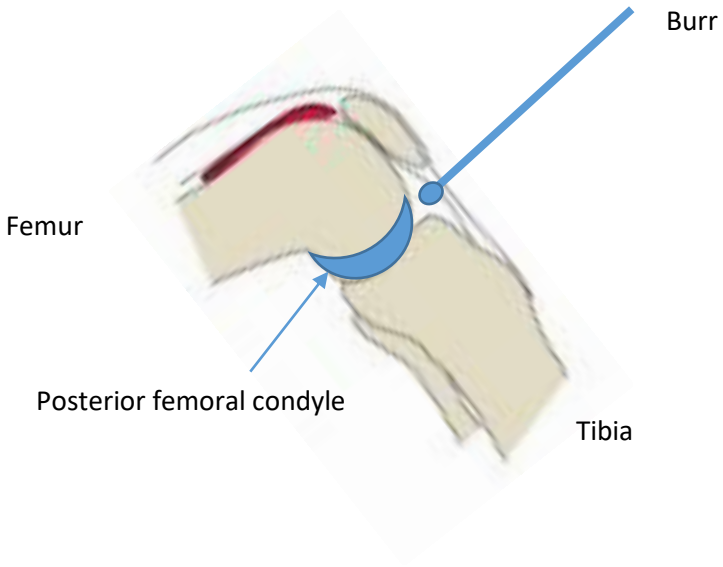

Figure 6.4-2 Burr approach for posterior femoral cutting. To get to the posterior femoral condyle the burr is required to tilt upwards.

Burr tip movement:

The resection volumes, are different with the tibial component being a larger surface area, and was positioned deeper into the bone resulting in a larger planned resection volume. These factors change slightly component sizes but as a general assumption, the tibial component can be considered to have a larger volume to resect shown by the significant increase in the cumulative burr tip distances. All mock surgeries used the same planned model, and hence the volume of bone to remove during the testing was consistent.

The minimum values were associated with a user familiar with the use of the system which required a short amount of time for resection. At the other side of the scale, the maximum distance was a user that required approximately 9 times the path length to achieve the same volume resection. Reviewing the discomfort scores both reported discomfort in the hand, with the experienced user scoring higher in discomfort, and also showing a larger decrease in grip strength post testing. This suggests that with experience the cut is made in a more efficiency manner, but still with discomfort.

RIO ROM and Posture

A repeated pattern in the range of motion and cumulative joints angles was the increased usage of joints 5 and 6. Joint 5 is the equivalent movement to the supination of the wrist, with joint 6 having the equivalence of wrist flexion. Approximately, Joint 5 moves the burr tip in the vertical direction and joint 6 in the horizontal. Given that joint 5's movements are approximately double joints 6's, this would suggest that a majority of the movements of the burr for both cuts is in the vertical motion.

These motion could be a result of the single hand use only manipulating the system with no force input directly being applied to the proximal joints. However, this single hand use was consistent with the observation of the use of the system in the clinical setting. Given the larger moment arms and more effective force transfer for larger muscles groups in the user, use of these other joints (1-4) could alleviate work done by the finer muscle controlled distal muscle groups with the other arm.

Joint 4 is the elbow joint of the robotic arm, and although fractionally higher in the tibial this is not significantly different. The higher movements are likely due to the higher anterior-posterior movement of the burr in the tibial resection in comparison to the femoral. Given the length of the link after joint 4, these small angle changes are amplified at the burr tip.

Joints 4, 5 and 6 presented a significant difference between movements of the two cuts. Given the volume differences and freedom of movement in this volume, the tibial showed a significantly larger accumulation of angles movements.

Figure 6.4-3 Average RIO arm orientation (tibial Left, femoral Right) relative to the saw bones

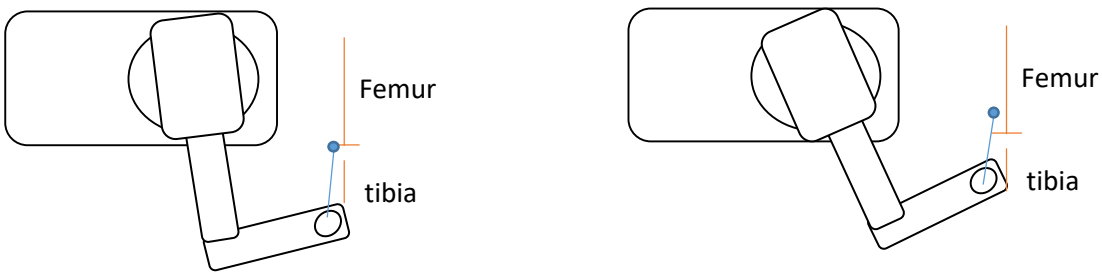

As we can see from the diagrams (Figure 6.4-3) there are subtle differences in the setup of the RIO for the different joints when viewed from above. To give the extra reach in the femoral resection the first joint 1 has rotated slightly moving the burr towards the head of

the patient. This is then followed with a rotation of joint 6 as well to correct for the change in orientation of the burr, however, this is much higher given the relatively smaller distance from the center of rotation (moment arm). Joint two is equivalent to shoulder abduction, and in the tibia cut shows an increase in inclination, raising the elbow to allow an approach from above the tibia. The last difference is joint 5 with a greater positive position in the tibial, positioning the burr lower and pointing downwards as the vertical position of the tibial is lower than the femur. These confirm the same approaches as those in the user kinematics.

6.4.3.11 Force Transducer

Mean force

For both tibial and femoral resections, due to the angle of approach from the medial side the Fx and Fy forces are not aligned with the anatomy of the bone as can be seen in Figure 6.4-3. During burring the Fx linear forces are on average away from the user. The mean Fy forces being applied takes the burr to the left and slightly away from the user. This resolves the average force vector forward and to left in Figure 6.4-4.

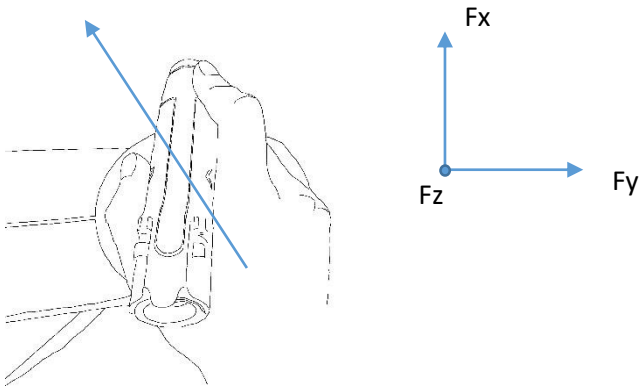

Figure 6.4-4 Example of a right handed user with the average linear force vector measured from the force transducer, along with force transducer axis system.

Given the task to resect as much of the planned section as possible, the only resistance to movement in this task was the tibial slope, posterior and lateral boundaries and the spinal wall. The Fx and Fy forces are produced by the muscles in the upper arm or even a transfer of body weight. The palm is far more efficient at transferring these forces than the fingers, in the opposite pulling direction. This is ideal when considering the bone for resection will be in front of the burr.

Reviewing the tibial forces, the mean Fz is understandably downwards on average, with the position of the tibia below the arm and cutting burr. However, the magnitude is larger than the average indicating some periods of positive Fz. This is thought to be due to the tilt of the end effector, when tilted forward, with the burr pointing down, the forward push will result in a positive rather than negative force.

The tibial moment My indicates on average a force tilting the end effector forwards Figure 6.4-5. Given the contact of the hand was limited to only one hand on the end effector, the only transfer of force would be through this hand with a limited moment arm. The direction of the moment My is created by the fingers at the front of the end effector, not only requiring apply force to create these moments, but also gripping to maintain contact with the handle. As a movement, this describes the tilting of joint 5 into the surface of the joint, resisted by the haptic boundary of the tibia plateau. We have seen that joint 5 was the most extensively used, and would indicate a high level of demand from the hand and fingers. Muscles such as the extensor digitorum that showed high levels of activity and some fatigue, and muscles similar to the first dorsal interosseous that were shown to significantly fatigue.

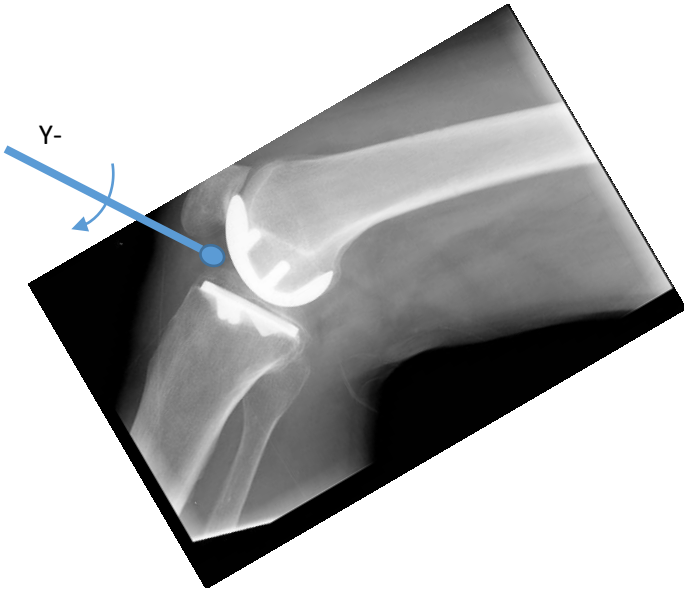

Figure 6.4-5 MAKO X-ray with burr and negative Y Moment to represent the direction of the burr relative to the bone.

The Mx moment is thought to be created by the Fy vectors from the palm, but also between the index finger and the thumb, given the arrangement in the Figure 6.4-4 above. Effectively the thumb is gripping below the height of the index finger causing a rotation in

the negative Mx direction. As the grip gets tighter between these muscles, this rotation increases. Given the magnitude of the absolute average this direction is almost exclusively in this negative direction.

The final moment, Mz, is the rotation of the end effector around the axis of joint 6. It is assumed that the linear forces will have a minimal effect on this moment as they pass through this axis, instead these are mostly created from the wrist extension movements. The negative average is thought to be a result of the spinal wall, with the burr having to be turned into this to apply enough force and resect the bone.

From the Figure 6.4-6 of the MAKO x-ray the anterior and distal section of the femoral implant are perpendicular to the burrs approach. The haptic volume is now shallow ahead of the burr, and narrower. Along with a different 'posture' of the robot, this also leads to a change in the forces required to manoeuvre the burr with Fx, for the femoral component has a statistically significant reduced mean and absolute force in comparison with the tibial component.

Due to the shape of the femoral implant, along with the orientation of the burr, there are few parts of surface that allow for a large negative Fz to be applied. If applied, the burr has a tendency to fall off the curve of the implant at the anterior and distal sections. This is fundamentally different when bone is present as this reduces this effect, but this point will be re-raised in the Saw bone testing example. The only surface that can account for the Fz positive direction, is the previously mentioned posterior lip. This results in the significant difference to the tibial mean, but the magnitude of the force required is low in the femoral cut.

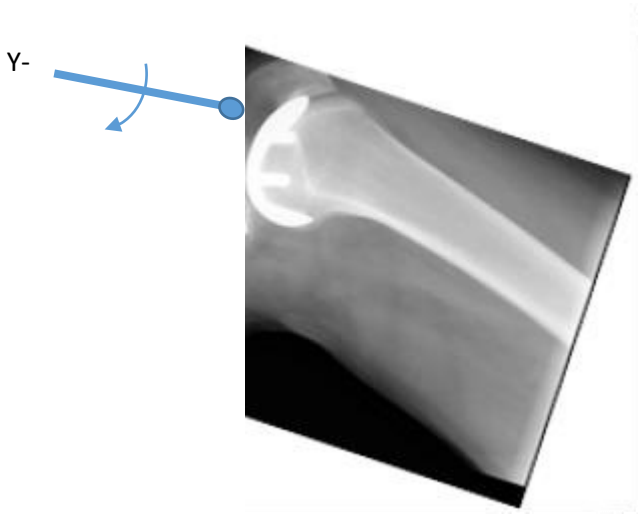

Figure 6.4-6 Diagram of a typical femoral burr approach. A negative My was required during the burring of the anterior and distal sections of the femur, with a positive My required for the smaller posterior section of the femoral resection.

While there is a difference in Fz, My is still shown to be in a negative direction in the femoral cuts, as it was in the tibial cut. Joint 5 was shown to change posture, but as shown in Figure 6.4-6 the burr still requires this moment to manoeuvre the burr to the haptic boundary.

The femoral component has two boundary edges (medial and lateral) relatively close together. When compared to the tibia, this leads to more interaction with both walls, while as previously mentioned the tibial has more freedom of movement is this plane. This leads to a slightly more balanced mean Mz with a smaller average, but overall the cuts have the same average magnitude.

Finally, Mx shows a rotation anticlockwise relative to the burr axis. Firstly, this is significantly smaller than the tibial forces. The palm does not produce the same forward and downward force as before, but the pinch of the index finger and thumb is still being produced.

Max Force

The maximal forces being observed in the force transducer, while short in duration, are high for a refined movement. Linear maximum forces ranged from 30 to 40 N after averaging over the sample groups, with individuals reaching 79N in the Fy direction. These instances of force can be made equivalent to carrying a weight of approximately 5kg. Similarly, the torques being produces were extremely high at points.

It is unlikely that these forces were being generated alone by the wrist and fingers, and are more likely being produced by the larger muscles in the proximal arm, but these muscles still need to stabilise the distal joints to allow the transfer of these forces. Weaker postures would lead to the heightened risk of fatigue of these muscles, and further justifies the need of the additional work to consider posture alignment with the line of action of force being applied.

Isolating Mz as a movement and torque can be assumed to be transferred through the rotation of the end effector by the hand. The posture of the hand and fingers, when holding the end effector can be likened to holding a jar, which from the literature states that a typical opening torque of a 72mm vacuum sealed lid is approximately 3Nm (Janson, 2007), while the maximum diameter of the EE is 100mm, the point of contact on the dome is likely to be smaller, and more equivalent to the size of a jar. For both tibial and femoral resection these forces were equivalent in magnitude, some even exceeding 3.4Nm.

Saw bone cutting

A single saw bone repeat of the measurements above, was used to highlight any possible difference in the forces that would results from the additional cutting of a material. Counterintuitively, the forces used by the larger sample group without the saw bone were larger than this single user, with the additional resistance of the Sawbone.

The tibial resection shows a higher tendency for forces in the negative Fz direction, or the long axis of the tibial. This would suggest that this single user was cutting down the long axis of the tibial bone.

On the femoral resection, as mentioned before, the added resistance of the saw bone material is shown in the change of the mean Fz from positive to negative. The material allows a surface to resist against as the burr moves anterior to posterior.

Peak forces and moments were not different, with only Fz showing an increase in force. This would indicate the all the other forces are peaking due to contact with the boundary edge, as this was the only constant resistant point in both tests.

Arguably, the Sawbone material allows for average lower force movements through the resection volume as the burr cuts the material. Saw bone cutting required larger amounts

of time to resection these volumes, and as the material is much softer than the resistance of the boundary wall, the average forces decreased for the single burring user. Burring is required all the way to the boundary edge, and as such, the boundary will always be present as a resistive force to the manipulation of the burr. Similar peak forces would suggest that the larger forces result from the interaction with the boundary wall. The lack of boundary walls is explored in the next section for free manipulation of the robot.

When presented with sclerotic bone, this resistance to movement will be higher than the sawbone material. Without measurements of these forces, it will remain unknown how hard the user has to force the robotic system to burr sclerotic bone, but will arguably lie between the force presented with the saw present, and those measured with only the haptic boundary. In this project, sclerotic bone is thought to lead to increased burring times, and arguably larger forces that are contributing to the fatigue of the user. The setup for the larger group of user hence, at worst, represents the higher force use of the system, but not outside of what would be expected from force used.

Laser Testing

Finally, when reviewing the forces in the laser testing there was no haptic boundary for the user to apply any force onto as a resistance to motion, so instead this is a measure of the inertial and motor resistance (loses/lag in the control system) to manipulate the system. Additionally, no significant forward and backward movements were required from the user to direct the laser. The rotation about Mz, to move between points using joint 6, measured 0.953 Nm maximum torque, which is a third of the peak forces during burring testing. This peak can only be a result of quicker movements between points and the inertial properties of the joint. Here the absolute mean also describes this movements, showing that nearly 70 percent of the resistance to movement in joint 6 comes from the resistance in the system. Given that there is a lot of lateral sweeping of the burr, it appears that the robot is causing most of this resistance. Joint 6 is the most resistant joint, most of which is to increase the effectiveness of the haptics. The resistance of sclerotic bone is likely to increase these force even more for the continual resection of the bone.

Fz mean is a sizable force with a similar absolute magnitude, indicating that the direction is in the negative direction. This mean force is equivalent to 460 grams, which is approximately the weight of an average male hand (70kg * 0.65% = 455 grams). The robotic

arm will hold its position in space, but this would also suggest that the robot can partially support the weight of a hand, especially for slow or static movements and postures.

Posturally (Mean Angle), the laser cutting was similar to the tibial cutting. This suggests some validity of this setup reflecting the same postures during burring, but ultimately there were some differences. Joint 5 required an upward rotation to allow for the laser pointer to target the points on the wall, as the burr normal is pitched downwards when joint 5 is in the neutral 0 position. This can be seen below in the video frame from testing (Figure 6.4-7).

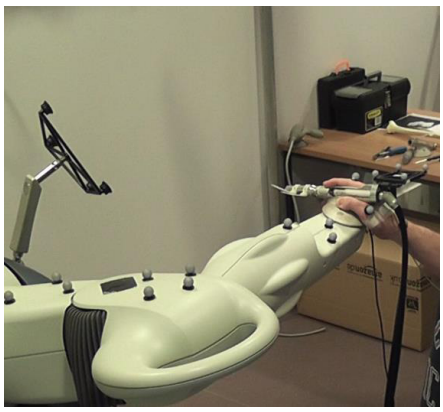

Figure 6.4-7 Laser testing showing Joint 5 angle. Due to the position of the tibial target of the wall the angle of joint five was slightly higher than the posture during manipulation of the robotic arm in the haptic volume.

Similarly, the range of motion is much smaller, given the greater restriction through the target. Typical ROM from joint 6 in this task for the user using this to move the system was 4.2 degrees, while in the mock surgery testing this averages 41.5 for the tibia. This represents a limitation in this test, when comparing to the no haptic movements of the mock surgery.

Both the forces and moments are complex, as these are a summation of the linear forces acting relative to the force transducer, and the pure moments applied by the user relative to the forces transducer. If the point of force application on the end effector could be defined the pure moments could be isolated, but this is not possible with the force transducer alone, along with other complexities. This means that the forces were described relative to the force transducer, with limited interpretation as to how the forces were produced, or even the muscles that produced these forces. Proposed further work to develop more detailed models of the user interface are described in the section 8.5.1.

6.4.4 Review of fatigue when using the MAKO RIO

From the responses to the discomfort questionnaire, the hand and the lower arm, were the two areas mentioned most frequently. The highest discomfort scores were reported in the hand. The intrinsic muscles of the hand are separate from the rest of the arm, and so forms the first site of fatigue. The second is the fatigue of the lower arm (Forearm) with muscle groups generating both gripping forces and wrist movements. In order to explain these results, there is thought to be the two mechanisms for discomfort when using the MAKO RIO system.

6.4.4.1 Mechanism 1 – holding the robotic arm

The first proposed mechanism of fatigue has slowly been developed during the discussion of the individual outcome results. The first interosseous muscle was chosen as an intrinsic muscle in the hand, and this muscle showed the highest measures of fatigue for both the tibial and femoral cuts. From the observation of clinical use of the robotic system, surgeons were seen in single cases having to rest and stretch out the hand and wrist. While this could also be linked to the discomfort in the lower arm from fatigue of the extrinsic muscles of the hand, this was thought to be an issue with the intrinsic muscles of the hand having to grip the handle.

The current handle is the second generation development from the original TGS. The original end effector was a simple mounting of the burr for handling with a pen type grip. Within its redesign, the TGS was ergonomically reviewed for typical uses, which led to the current end effector and joint configuration (increase to 6 dof) of the MAKO RIO. The end effector handle's hemispherical shape with burr mounting was developed to allow for the movement of the thumb to a stronger position and increasing the interaction of the 4th and 5th fingers with the surface. The design has been focused on the ability to push the robotic arm with the palm and thumb, as shown in the force transducer work (Figure 6.4-4). However, as was seen from the kinematic data and force transducer this is not the only movement that is performed by the system. Movement of the robotic arm other than being pushed with the palm, equivalent to a sawing action, requires a secure grip of the handle.

At least one finger is required to depress the trigger on the top of the end effector, this leads to a splaying of the finger across two levels (Burr barrel and dome) opening the fist, which increases the difficulty to hold onto the end effector (Figure 6.4-8). This deviates the fingers away from a recognised power grip. Finger span is known to have a direct impact on

grip force production (Eksioglu, 2004; Hansen and Hallbeck, 1996), with increased spans reducing efficiency and maximal strength.

Additionally, the finger abductors/adductors are required to stop the fingers from sliding down or up during gripping. The first interosseous muscle stops this sliding of the first finger by supporting the metacarpals during this prehensile task, and is one of many intrinsic muscles. The level of activity of the muscle was observed in the RMS of the EMG, for both tibial and femoral cuts. They were significantly larger than all of the other muscles activities, bar the extensor digitorum. Ultimately this led to the highest pseudostatic changes in the spectrum of the EMG, and the most prominent change in the EMG RMS signal indicating fatigue.

Given this splaying of the fingers, a number of other muscles are also likely to experience fatigue, hence the generic reporting of fatigue in the hand. Deviation away from neutral at the fingers, therefore, changed the loading forces and muscle lengths. The extensor digitorum showed a larger level of activity than the first dorsal interosseous for both bone cuts. While extending the hand and wrist, the action on the fingers could be an indicator of the level of activity required to maintain this less than ideal finger position.

Due to the longer lengths of time burring and large force transfers through the fingers, these muscles are shown to fatigue. This fatigue was bad enough during experimental testing, that four users had to stop using the system, due to the discomfort in the hand or fingers. Another user couldn't hold a pen and write on the questionnaire due to numbness and pain after the testing.

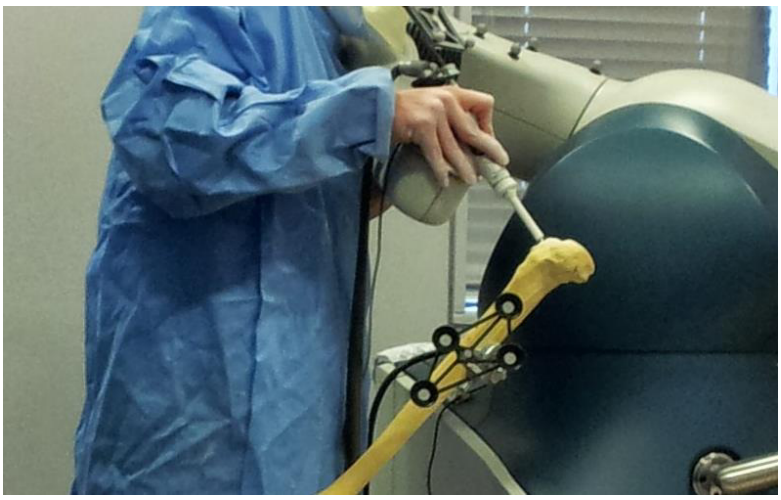

Figure 6.4-8 Side on view of a grip of the end effector. Note the splayed fingers and flexed index finger. This is a mixture of both a prehensile power and precision grip. The tips of the fingers are used to move the end effector which is highly dexterous, but reduces grip force.

This grasping mechanism, also suffers from cumulative effects from both tibial and femoral cuts. There were no statistical differences for the first dorsal interosseous muscle for all of the EMG based metrics of activity. This would suggest that this fatigue mechanism has no time for recover during burring, and would further reason for the presentation of discomfort during extended burring period such as those measure when burring sclerotic bone.

Ultimately this mechanism is an unergonomic splaying of the hand across the domed end effector of the robotic arm for extended periods of time.

6.4.4.2 Mechanism 2 – moving the robotic arm

The second mechanism is thought to come from the manipulation and movement of the wrist. While discomfort in the lower arm could be a result of extrinsic hand muscles, fatiguing under the demand from gripping, there is also a large amount of manipulation from the hand, especially flexion and extension. This mechanism, however, is not reported as being as significantly as the first mechanism, due to reduced indications of fatigue during testing. EMG activity levels and pseudostatic metrics all indicate a lower level of fatigue, in comparison with the muscles with finger actions, but the large repetitive range of motion in the flexion extension along with the large, near maximal torques, measured in the force transducer would indicate a sizable amount of work being performed by these muscles as well. While the extensor digitorum could not be isolated from actions on the fingers and wrist, the flexor carpi radialis was shown to have a higher pseudostatic change in frequency

during all three tests, and for both bones than the extensor digitorum. However, these change did not result in a change of functional ability of these muscle to produce the same near maximal forces after testing as were measured before testing.

As already discussed in this section, the burr handle is designed for efficiency, pushing the burr into the surfaces of the bones. The shape of the bones and depth of the volume, however, means that the user has to manoeuvre the burr in a number of different directions. For instance, the tibial plateau is a flat cut, ideal for the burr to be pushed through the volume. This increased movement in the tibial cuts also saw an increased, but not significant, pseudostatic frequency change for the wrist articulating muscles.

The forces required in manipulation of the robotic system is a culmination of the inertial effects of the robotic arm's joint and the resistance to motion at the haptic boundary. Large prehensile loads are optimised for a static neutral wrist (Pheasant, 1996). The coordination of wrist movements is made more difficult with the presence of the prehensile loads. Typically prehensile force and wrist movements are avoided for ergonomic reasons, and work related stress disorders (McGorry et al., 2014). Ideally motions should be minimised at the wrist, when used alongside large prehension demands, or alternatively grip forces should be minimized for finer control of wrist movements. The manipulation of the robotic arm required both of these in its current setup.

While this mechanism was not as significant as the first, it was still important to develop, in order to determine the nature of the elevated discomfort scores in the lower arm. These scores can be assumed to be both from grip force generation and wrist articulation.

6.4.5 Review of Methodology

A critical review of the methodologies used in this chapter caveats the findings. The caveats were recognised as the subjects used in the testing, issues with the setup and the EMG protocol. Understanding the limitations in the work, allows for a more informed progression of future work on this project.

6.4.5.1 Subjects:

Given the lack of experienced surgeons available, a cohort of users were invited for testing from the departmental population. Due to the physical nature of the issue at hand, the group were compared for grip strength against reported orthopaedic surgeons grip strength, taken from a journal article. Comparing the two groups there is a significant

weakness in the strength of the users, in comparison to surgeons. From the literature, the surgeon group have the same average or weaker, when compared to reports for the population averages for males, and given the user group in this testing were a mix of male and females of different statures, this would account for a difference seen here. Arguably the surgical population, albeit predominantly male in orthopaedics, is not exclusively male, neither is there an exclusion on physical stature. Only a smaller group of male users could be considered representative of the orthopaedic male strength. A sample group with a lower strength, would therefore be considered to require a higher percentage of their strength to manipulate the RIO. As a result of this, care was taken when concluding for this testing group. While not representing a 'typical orthopaedic surgeon' the group is representative of larger population variations.

While surgeons would have a greater understanding of the surgical workflow, the resection stage in the procedure was deemed not to require a high level of clinical experience to manipulate the robotic arm, and achieve resection of the planned volume. The burring stage has a computer interface to guide the user, and finding a sample group of equivalent size with experience with this robotic system was not practical. Instead the use of lay operators was pragmatic, but otherwise limits any conclusions to fatigue in inexperienced users of the robotic arm. It would be recommended that further extensive testing of the mechanisms proposed, still has value in being explored in lay users, for manipulation of the robotic arm without any prior clinical understanding required, as this is a physical demand issue and not a clinical experience issue. To definitively understand this issue in surgeons, surgeons would have to be used, but for a refined testing model given the issues with access and cost of using surgeons.

6.4.5.2 Setup

Ideally this type of testing should be tested in situ when exploring the fatigue state of surgeons. However, in more controlled conditions specific variables can be assessed. While fatigue can be induced through exertional clinical tasks outside of burring, this is not a direct result of the robotic arms design and use. Instead reviewed in isolation in this project was the effects of continual burring, highlighting fatigue as a results of burring alone.

Along with this a bone/cutting resistance was not used for this same reason, as to reduce the variability of this resistance. Within the surgery observation, higher density bone was seen to effect both time and fatigue levels. Instead within this testing the users

were asked to manipulate the system through the virtual boundaries alone, with only the robotic and haptic boundaries as resistance. Any observation and evaluations therefore are a reflection of the fatigue induced by the use and design of the robot (haptics and ergonomic design), variables that could be altered. Further consideration has to be taken as to the superposition of additional resistance to movement, when comparing this to the true situation and application. These additional resistances would further exacerbate demand to the muscles of the lower arm, along with possible changes in the ROM used along with the forces measured. Only the observation comparisons of the clinical and testing process, could suggest that there were not differences, but this is merely anecdotal and require more definitive work.

The presence of gloves are shown to decrease this tactility, decreasing maximal (Buhman et al., 2000) and increasing overall submaximal (Willms et al., 2009) grip force production in industrial gloves. While some gloves increase the friction between surface, latex gloves over multiple layers reduce the friction below that of bare skin on the hand. This was another consideration in the design of this setup, during surgery surgeons would often wear two pairs of latex gloves for sterilisation and PPE. Given no PPE requirement to wear these, and unfamiliarity working in and with gloves, it was seen as an additional complication to the setup for the user. Instead the users were asked to use the system bare handed. The EE has a polished metal finish, with smooth curves and finish. When considering the sterility of surgical devices, the ability to maintain cleanliness seems to have taken a preference over a rougher surface more ideal for gripping. Generally, as the hand gets warm, additional moisture would reduce the friction between the hand and handle, however through the glove this could arguable be the same case after the expiration of the moisture absorbing powder. An additional benefit in not wearing the gloves, was the allowance of the placing of markers to the skin to measurement the fine movements of the hand without additional movement artefacts.

Along with the addition of gloves, the vibration of the motor in the robotic arm is another factor not explored in this setup. When using certain tools the vibration led to an increase in the grip force being used for the same task (RADWIN et al., 1987). Assumptions about the impact of this additional vibrations would be speculative, but is unlikely to have a reduced impact on muscles demand or any resulting fatigue.

From the explanation of the kinematics of the system, it is obvious that the setup has a large effect on the position of the wrist and arm relative to the saw bone. The saw bone was placed on a table through a clamping system and moved to match both the tibial and femoral components at the knee, at a height considered comfortable for the users. While there was no comment or any obvious sign of discomfort as a result of this, the resulting angle of the tibial slope was angled at approximately 45 degrees to vertical. On reviewing the footage of usage of the system, this is not an uncommon approach angle, but given both the ability to change the height of the knee through the bed height, and the angle with height through flexion and extension of the knee, the clinical users of the system, had far more flexibility in the positioning of the knee. Below is a typical example of the position of the knee for tibial resection. Higher flexion allows for a more upright position of the tibia, while too much flexion can lead to compression of the joint through soft tissue tensioning.

Figure 6.4-9 Typical posture and positioning during a tibial resection. The surgeon is upright, lateral to the knee and looking over the robotic arm in the knee.

When comparing the above posture with the Sawbone example at the beginning of the chapter, the general postures are different. This is compounded with the height of the Sawbone user being shorter than the clinical user, and the positioning of the saw bone being more vertical, than other tests, along with the clinical user positioning the patient lower for MAKO cases, and the poor positioning of the MAKO arm base not being at the hip.

Ignoring the gross posture, at the wrist the Sawbone user is arguably more neutral in flexion with a slight ulnar deviation, while the clinical user is extended and ulnar deviated.

However, when not ignoring these factors, the alignment of the clinical user allows for the use of the larger proximal muscle groups to move the system. This highlights the issue of the movement, that are not created by these large muscle groups i.e. the grip, lateral and vertical movements in the resection volume.

A key element of the posture of the user was the issue of line of sight. Often a user will position themselves relative to the knee and robotic arm, so that the burr tip can be seen for manipulation, this was definitely the case in the observed surgeries. In order for this to be achieved, the end effector will have to be move towards the mid-line of the user, requiring the joints of the user's arm to compensate for this by moving from a neutral position in towards the midline (Figure 6.4-10). This requires changes in the pronation, extension and adduction of the wrist. If not at the midline the robotic arm, blocks the line of sight of the surgeon.

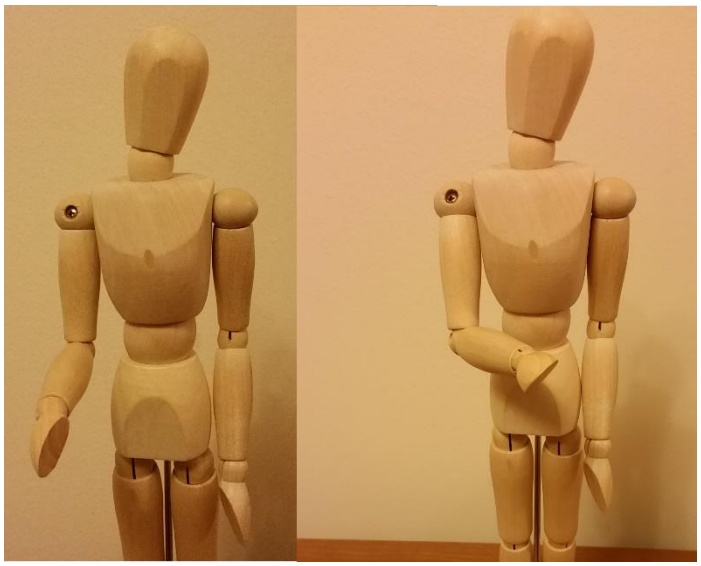

Figure 6.4-10 Movement of the hand to the body midline and resulting change of postures through pronation and flexion of the wrist.

Another setup issue is the position of the knee. The setup of the patient's knee in theatre has an impact on the kinematics of the user. However, in this experiment, the knee bone positions were the same for all users, so this effect was not included in the experiment. In reality, a knee in more flexion will lead to the tibial slope changing alignment relative to the surgical table. Levelling out of the tibial slope, will lead to a reduction in the flexion of the wrist. This manipulation of the knee can also change the muscle groups used to manipulate in the haptic boundary, for instance by using an extension of the elbow as opposed to the flexion of the wrist. However, these raised other issues, such as an

increased distance to the line of sight of the joint. There is unlikely to be a single optimum body position for burring for all patients, but an awareness of the issues being observed (Fatigue, line of sight, etc.) by the surgeon would allow setup of variation to be implemented.

This setup, shown below in Figure 6.4-11, also allows for good femoral posterior access. Other setups, have the base plate sloping down distally. This extends the hip allowing the femur to be parallel with the floor, while also leveling the tibial slope without the need for high flexion of the knee. The draw back here is the posterior femur is further around, requiring a more posterior, inferior approach, leading to extension of the elbow wrist in this case.

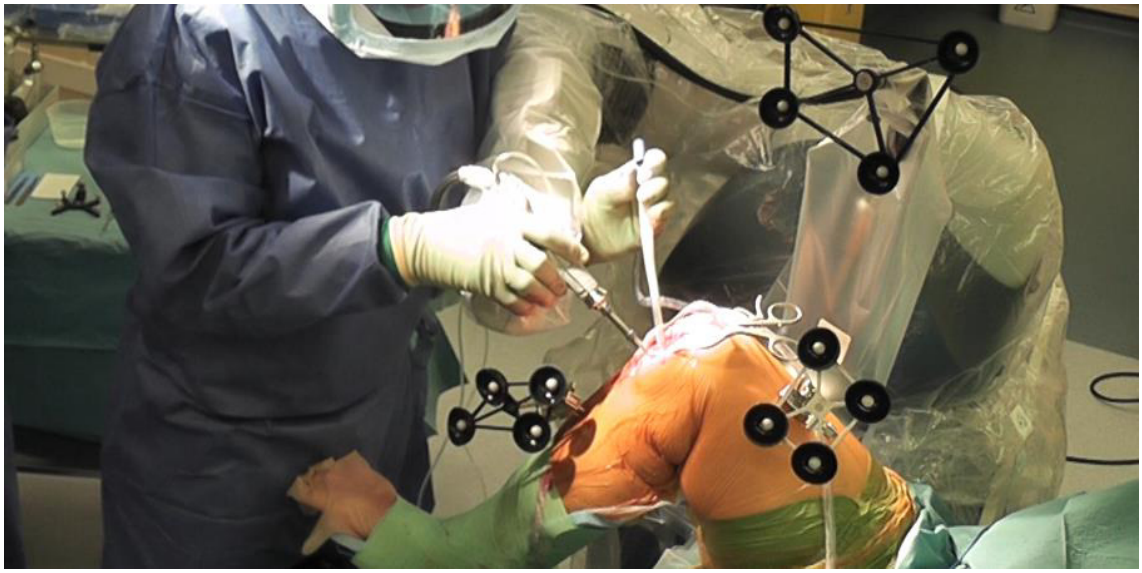

Figure 6.4-11 Example of tibial burring. Surgeon is using the system one handed.

These conditions are complicated through the repetitive movements within a large range of motion. At the extremities of the range of motion, albeit only for a short time, lead to weak postures for the application of forces through the wrist and hand. The movements are coming from all joints, from the wrist to the shoulder. All these variables can change for different patient leg lengths and setups. Often for single cases these will have minimal effect, but when sclerotic bone is presented positioning of the patient will minimize biomechanical disadvantages, and could reduce the risk of fatigue. Additionally, multiple surgeries will compound these fatigue factors.

While a review of the handle design has shown good application of ergonomic principals, the demand on the user is too high for the length of time required for burring.

Time could be decreased with the use of more destructive tools, but this could change the finish on the cut, and possibly induce unwanted secondary damage to the bone, by factors such as thermal necrosis (Larsen and Ryd, 1989; Lee et al., 2011). While some improvements can be made to technique through extensive teaching, such as under cutting of the bone being resected in the tibia, this is unlikely to have a dramatic impact on the gripping of the system, or increase the ability of the surgeon to undertake the cut more effectively. Realistically the user should be encouraged to use the effective cutting surface of the burr, and will have to accept that the surgery will take longer for harder bone.

6.4.5.3 EMG

6.4.5.3.1 Electrode review

Given the complexity of the proposed analysis, a limited number of electrodes were used to review the users. There have been numerous studies looking into high definition EMG reviews of muscle activity in the forearm to give a detailed picture of innervation pattern for given tasks, however, this was deemed to be superfluous for this early review of this process. It is noted as potential future work to review the detailed EMG signals of the forearm for controlled tasks, along with the manipulation of the MAKO RIO system to fatigue. Instead, a more refined approach was adopted, as it could not be determined pretesting which muscles would fatigue in the user.

Given the initial remarks of lower arm fatigue, the wrist movements were highlighted as the most likely muscle groups to reflect the comments. Given the relative ease of definition in the optical tracking joint angle calculations and muscle location, the wrist flexion and extension were targeted. Additionally, from observations of clinical use, these movements are extensively used in both of the bone resections. This was further backed up in the biomechanical testing with wrist extension showing the largest average ROM.

The grip strength endurance had been noted as a potential risk to fatigue, however these muscles are deep in the forearm and required very accurate positioning of electrodes. Given the small physical window, between tendons and other muscle groups, to record these signals for the dynamic nature of the testing, meant that these signals were too complicated for this testing. While the dynamic nature of the testing was also an issue with other muscle groups, the muscles chosen were due to their size, and superficial position in the forearm. This led to easier location from palpation, and high likelihood of tracking the same muscles through a range of motion.

The First Dorsal interosseous muscle is primarily a finger abductor, but also has a stabilising role during gripping. While other muscles (finger flexors) are the main agonist muscles for the gripping action, there are additional muscles that are innervated to stabilise the finger posture during the action of gripping. This can be seen with the level of activity in the muscle during the maximal voluntary contraction during the grip testing. Most of the agonist muscles for prehension tasks are outside of the hand itself, but from the observations in surgery, there was a pain resulting in the fatigue of muscles in the hand. Adduction and flexors of the thumb are positioned in the palm of the hand, but these could not be monitored with surface EMG without effecting the contact of the hand with the system. This left very few options to monitor possible fatigue in the hand, and so the interosseous muscle was chosen as a superficial muscle involved in the stability of the first and second fingers, as well as a pinching of the thumb to the handle of the robotic arm. An additional advantage to these muscles was the static nature of the muscle belly to the electrode. While contracted, the muscle would deform, but the handle maintained separation of the first and second finger, such to minimise this deformation and maintain relative position to the electrode.

The extensor digitorum communis was a highly active muscle as well. Given the multiple attachment points through ligaments, the system was quite hard to determine the isolation of the extensor movements. While the Extensor carpi radialis longus was added for additional information on the extensor, this too, also had abductor actions at the wrist, and showed a low activity during the MVC testing. Given the multiple action of all of the muscle, a true isolation of the action of the muscles was always going to be difficult.

Outside of the grip strength issue, the movement of the wrist and the forces generated at this point was a secondary hypothesised risk of fatigue. The complication in this review was the variability in which the users held the system. A grip was always required to control the system, while the manipulation of the burr inside the haptic environment could vary in cutting path and technique in the redundant positions of the knee. Linear movements away, and towards the body are made from the larger muscles around the elbow or the flexion extension of the wrist, while more medial lateral relative to the knee can be achieved at the shoulder or the wrist deviation. While the bicep was reviewed for a number of the users, it became obvious that the main muscles at risk of fatigue was going to be in

the forearm, with wrist related movements and contractions, hence the movement of the electrode.

While the electrodes could have been positioned in a number of different places, it was deemed that this approach review the wrist movements, and an intrinsic muscle that were predicted to experience discomfort.

6.4.5.3.2 Analysis

As reviewed in the literature, EMG is a complex superposition of muscle activity that can describe the level of effort being demanded for different tasks. Within these signals is also an ability to infer different fatigue states in these muscles. However, these descriptions are based on idealised testing conditions that are not always entirely practical for biomechanical and ergonomic testing. While there is research looking to allow real time testing of EMG signals for the time course of an assessment, this was deemed to beyond the scope and focus of the current project, as a general over view of the fatigue and use of the MAKO RIO system.

Reviewing the literature, optimal testing of EMG spectral analysis should ideally be completed under submaximal MVC, which is a limitation in this testing protocol. Instead spectral analysis was complete on MVC conditions, as these were completed for a review of the change of MVC forces. Additionally, the literature also states that there is inconsistency in spectral analysis for intermittent, long duration contractions. Albeit the signals were still reviewed for spectral changes with limited observations of fatigue. This is not surprising given the lack of control of the required testing conditions.

The most significant finding was the dramatic change in the first dorsal interosseous muscle, for all the EMG results. A number of tests were conducted with varying results for the other muscles, but consistently the first dorsal interosseous showed discomfort and fatigue. While many of the following results of the chapter review the posture of the arm and wrist of the user, this muscle is isolated from these movements. Instead this fatigue is a result of the posture of the hand, fingers and shape of the end effector. This pinching between the first finger and thumb must be high, to result in the fatigue of this muscle.

After this the wrist flexor and extensors were also seen to show indicators of fatigue, but not as significant as the first dorsal interosseous result. Both showed the high activity levels over the tests for both cuts and changes in the pseudostatic fatigue metric to indicate

fatigue, but were not shown to be functionally compromised. These muscles are composed of different fibre types and show higher resistance to fatigue for high levels of activity. These muscles maybe liable to fatigue with further extensive exposure to the observed forces along with the additional complications of central fatigue. However, these would be the result of additional demands on the surgeon outwith of the effects of burring with the robotic arm. This could result in higher levels of discomfort in the forearm that were not obviously observed in this testing, but could be included in the anecdotal comments on fatigue from US clinical users report lower arm fatigue.

Ultimately the mock surgery setup showed significant changes in muscles, both functionally and electrophysiological, to highlight issues with the continued manipulation of the robotic arm in its haptic environment.

6.5 Biomechanical testing conclusions:

In review of the aims and research questions at the start of the chapter:

1. Are kinematics and postures of the user biomechanically suitable for the use of the robotic arm?

Posturally, optimisation of the postures could be refined for grip strength and wrist torques, but largely the arm was positioned suitably for the manipulation of the robotic arm. The hands posture was not ideal for continued prehensile purposes. Ideally a static power grip should be adopted for this current application, but this will be at the sacrifice of precision coordination of movements.

Kinematically, the fatigue issue is not as significant, as the postural issues with the hand, and the effects of this may have become overshadowed. But there is still the risk to lower arm fatigue, as a result of continued articulation during the manipulation of the system in the haptic environment, for extended burring periods.

2. Can fatigue be confirmed in users expressed as discomfort

Fatigue expressed as discomfort was reported by all user. These were localised to the hand and lower arm. This confirms the anecdotal reporting of fatigue when using the system, but for the specific conditions of extended burring periods.

3. Can fatigue be confirmed electrophysiologically (EMG)?

The continual monitoring of the electrical signals of the lower arm showed significant fatigue in the intrinsic muscles of the hand, and to a less extent in the muscles articulating the wrist.

4. How much force is required to manipulate the system?

Peaks forces required to manipulate the system, especially around the haptic boundary are an issues with the system. This is a safety feature of the device, and required for the system to be viable. How much force is introduced with the use of haptics for controlling the robotic system?

5. What are the differences in kinematics between the tibial and femoral cuts?

The tibial burring showed a more dynamic, and more forceful resection, when the robotic arm was manipulated in only its haptic boundary. In addition, the kinematic data from the user, showed a different average posture due to the shape and position of the resection volume. While the fatigue metrics for the tibia showed a slight increase for the tibial cuts, these were not significant such that one of the bones could be isolated as contributing more to fatigue that the other.

The mock surgical testing has shown evidence of localised muscle fatigue during repetitive use of the MAKO RIO system. For this group and test setup the main issue was with the intrinsic muscles of the hand associated with grip of the end effector. While these muscles are largely isolated from the posture of the rest of the arm, the Flexor carpi radialis and extensor digitorum showed fatigue in the spectral analysis of the muscles that was associated with the range of motion and forces required to manipulate the robotic system at points during the resection.

Both novice users in this study and experienced users anecdotally have reported fatigue. This would suggest that the cause of the fatigue is not isolated to lack of experience of the system. The physicality of the group was shown to be indifferent to that of the population, but weaker than male orthopaedic surgeons. Strength however was also not shown to stop fatigue, and was shown is some cases to result in more fatigue when trying to move the system. So finally the most compounding factor to the presentation of fatigue is the time using the system under these conditions. While there were physiological changes observed during the first cut, the majority of the discomfort was presented in the second resections and beyond.

The MAKO RIO is a robotic system designed to assist in the accurate resection of bone. Given some of the high demands required to manipulate the system in the refined spaces of the knee, further consideration should be taken to allow a reduced force required to manipulate the system. This process from the results would suggest a twofold approach. The first is a handle design that will allow for continued grip and manipulation of the system. A new handle design is reviewed in the next chapter, and compared with this current handle design. The second suggestion posed as part of this project, was the ability of the system to aid in these movements. Adding a power assist would reduce the feedback of the system, and will increase the force through the bone, a failing of the original robotic systems.

A final aid and understanding would be dissemination of better practice of use could be designed, and taught to minimise the disadvantages the users have when using the system. While a best practice isn't suggested here, a method for reviewing changes in use has been developed. Repeated controlled practice can be monitored for both kinematic, kinetic and physiology changes in the user's performance.

Chapter 7 A Biomechanical assessment of a prototype handle

7.1 Introduction

To allow for additional tooling attachment to the MAKO RIO a new handle was developed by the company. The main design proposal for the new handle was for TKA surgical platform to be available with the robotic arm.

The handle is significantly different to the current in its pistol grip design. A prototype of the handle was made available for a small group of users (3) were asked to repeat the testing with the new handle in order to compare the fatigue metrics and kinematics of the users for both of the handle designs.

7.1.1 Review of the Handle

Figure 7.1-1 Images of the finalised handle grip (left) and current end effector (right). The pistol grip results in a power grip, which the current burr is held in a spherical prehensile grip (right).

Images of the handle in the CROSS lab are shown below Figure 7.1-2. The first difference is the position of the handle on the robot, being on the underside of the arm this requires joint 5 to be rotated through 180 degrees Figure 7.1-3. The kinematics on the users are reviewed below, but the handle is obviously lower as a result. The downsides of this position are the issues with the line of sight of the burr tip, reduced access to the surgical

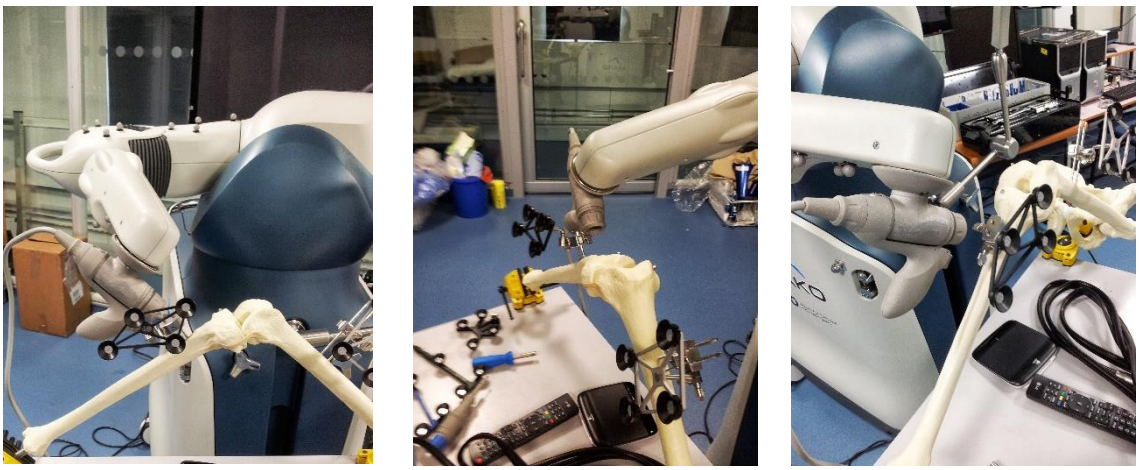

Figure 7.1-2 Photos of the new handle attached to the RIO. (Left) side on view showing the new approach angle. (Middle) View proximally relative to the patient. (Right) Typical view from a position slightly to the side of the surgeon's perspective.

site as the handle can be seen hitting the tibial base array. This latter point is an issue that can be resolved through angling the bone pins out of the way, but may require further soft tissue resection away from the midline of the tibia to allow access and bi-cortical attachment if the bone pins.

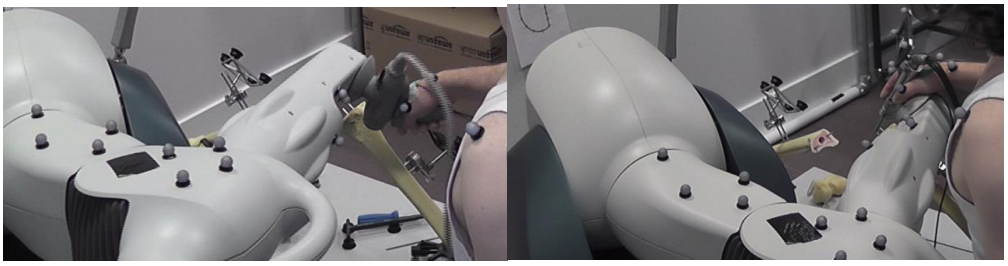

Figure 7.1-3 New prototype (Left) and current handle tibia cut (Right) in use during testing. The new prototype is positioned below and largely blocks the line of sight with the incision. The current handle is attached above and allows a view of the handle.

This new handle is designed to mimic a power drill, and the resulting alignment allows for large forces to be transferred through the handle towards the bone surface. Movements parallel to the surface of the bone are still not optimised in the new design. The pistol grip has been angled to allow for a natural power grip to form around the handle. In a pistol, the barrel is aligned with the top of the trigger finger to allow for accurate

aiming, similarly this grip aligns the barrel of the burr with the hand. This is thought to aid in the orientation of the graphical user interface with the obscured view inside the knee joint.

An additional degree of freedom has been added at the handle with the ability to re-orientate the grip around the long axis of the burr. This doesn't change the position of the burr tip, but instead allows for customisation of the position of the handle. Testing was standardised at a perpendicular angle for consistency between users. Customisation of this would lead to different kinematics.

7.2 Objective

The main objective of this chapter is to review the changes that the new prototype has on the outcomes of the fatigue testing when compared with the current handle. With the insight from the previous handle, the issues seen can also be reviewed to see if these can be rectified with this new design. Namely the issues of grip and manipulation of the robotic arm in the haptic volume leading to fatigue over extended resections time.

7.3 Methodology

A small group were chosen from the more competent and confident users of the robotic system, when using the current handle. These were all males, and on the stronger side of the large sample group to reflect the orthopaedic surgeon profile in the literature.

The assessment of the prototype handle followed the same testing protocol described in the previous chapter (Section 6.2). The electrode positioning took the latter approach, with the use of the extensor carpi radialis longus instead of the bicep.

The only major change to this testing was the lack of the use of the force transducer in the new handle. Given that the prototype was manufactured by 3D printing the integrity of the material would not allow for the modifications to allow for the mounting of the force transducer.

7.3.1 Data Analysis

Data analysis was otherwise the same as section 6.2.3.7, but limited to a comparison of averaged values given the reduced sample number working with the new handle (n=3), and hence some alternative statistical analysis compared results, or only a basic comparison of

data is performed. Given that three repeats for each user most tests were completed for n=9, with normality review with the Shaprio-Wilk normality test. T-test were used for normally distributed data, and Mann-Whitney U for non-normally distributed.

For this group the results from the current handle were extracted for comparison with the prototype testing. This ensured that the variations were a comparison of the same users.

7.4 Results

7.4.1 Pre Testing

7.4.1.1 Population Anthropometrics

Table 7.4-1 Mean maximal grip strength measure for the current and new handle for both pre and post burring

N=3	Jamar Peak Grip Strength [N] with (SD)			
	Current Pre Testing	Current Post Testing	Prototype Pre Testing	Prototype Post Testing
Population Mean Maximum grip	477.5 (129.5)	444.7 (137.9)	418.6 (134.4)	412.0 (118.5)

Table 7.4-1 presents the total grip strength in the small sample group and showed no significant difference with the surgical group (current handle p=0.97, prototype handle p=0.90, two tail t-test). The comparison of the prototype handle users with the 36 orthopaedic surgeons reported in Subramarian et al. (2011) showed no different between the groups, with the two-tailed P value equalled 0.3148.

7.4.2 Pre and Post Testing

7.4.2.1 Isometric testing

Table 7.4-2 Change between the pre and post strength tests flanking 3 cuts of the two bones with the new handle design

Test	Mean Strength change (SD)	Average % Change	T-Test
Grip Test (N)	-9.778 (8.13)	-15.77%	0.110
Wrist Extension (N)	-1.633 (1.03)	-8.25%	0.011
Wrist Flexion (N)	-1.144 (0.41)	-8.12%	0.004
Radial Deviation (N)	-1.656 (2.65)	-10.54%	0.066

There is no observed grip strength change between the pre and post Jamar grip strength testing rig, as had been seen with the previous handle (Table 7.4-2). All users were able to

reproduce an average grip within 5% of the initial testing. Wrist extension decreased, while this number appeared larger than the other changes, only a single user had a 50% drop in force, while the others were only changing by less than 2%. The increase in wrist flexion strength is a relatively small increase, but this was not a large change.

Table 7.4-3 Sample of user groups current hand change in strength tests. For a comparison for this small group for both of the handles the changes have been extracted for both tests. The strength changes of this sample from the current handle and a comparison of the changes are shown below.

Test	Current Handle Change (SD)	Average % Change	Current Handle Pre-Post T-Test
Grip Test (N)	-3.889 (1.77)	-6.74%	0.362
Wrist Extension (N)	-3.233 (4.67)	-16.33%	0.057
Wrist Flexion (N)	0.889 (0.31)	6.30%	0.025
Radial Deviation (N)	0.156 (1.32)	0.76%	0.398

Reviewing this group for the current handle design, all showed a decrease in the ability to grip, flex and radially deviate the wrist (Table 7.4-3). This wrist flexor change is unique to the users in the smaller group showing a higher level of weakness. The larger group showed a significant change in the grip strength of the same magnitude as this smaller group.

7.4.2.2 Questionnaire responses

Table 7.4-4 Discomfort Scores for users. The discomfort scores for the questionnaires were a self-reporting questionnaire for area and discomfort from a scale of 1 (no discomfort) to 7 (distracting discomfort). Similarly, the data for these users have been extracted for comparison between the current and new handle design.

Area	Current Median Score	Numbers reported	Prototype Median Score	Numbers reported
Hand(including finger and thumbs)	5	2	5	5
Lower Arm	5	1	4	1
Shoulder	3	3	4	2
Upper Arm	-	-	3	2
Wrist	4	2	5	1

The prototype saw a higher incident of self-reporting of pain over a larger section of body areas, but there were no increases in the scale of discomfort reported (Table 7.4-4). The indication of low levels of discomfort in the upper arm were only report for the new prototype handle.

7.4.3 Mock Surgery

7.4.3.1 Prototype EMG Pseudostatic Fatigue metric

Table 7.4-5 Pseudostatic median frequency change of the new handle during mock surgery averaged for tibial and femoral cuts.

	Tibial Mean	Tibial SD	Femoral Mean	Femoral SD
Flexor Carpi Radialis	-3.033	3.365	-5.203	2.344
Extensor digitorum	-3.470	1.357	-7.817	3.260
First dorsal interosseous	-22.200	1.338	-14.257	1.501
Extensor carpi radialis longus muscle	-7.433	1.951	-9.500	1.537

Table 7.4-5 presents all muscles groups and showed a decreasing median frequency change, with by far the largest changes being measured in the first dorsal interosseous muscle. Decreasing pseudostatic median frequencies are an indicator of muscle fatigue.

7.4.3.2 Prototype EMG RMS

Table 7.4-6 RMS New Prototype results. Results averaged for the same bone cut trials, along with the average peak RMS signal to represent the highest levels of activity.

		tibial	femoral	t test
Flexor Carpi Radialis	Mean	0.1%	0.2%	0.350
	Peak	3.1%	3.4%	0.812
Extensor digitorum	Mean	2.2%	1.8%	0.691
	Peak	29.6%	18.6%	0.404
First dorsal interosseous	Mean	3.4%	2.9%	0.741
	Peak	78.0%	43.0%	0.182
Extensor carpi radialis longus muscle	Mean	2.7%	2.5%	0.861
	Peak	44.0%	28.4%	0.284

There were no significant differences between the tibial and femoral cuts (Table 7.4-6). RMS peaks showed much larger values that the average values, especially in the first dorsal interosseous.

7.4.3.3 Prototype IEMG

Table 7.4-7 IEMG for new prototype handle averaged for tibial and femoral cut

	Flexor Carpi Radialis	Extensor digitorum	First dorsal interosseous	Extensor carpi radialis longus
tibial	414.59	6671.29	9781.48	9015.62
femoral	537.56	5063.12	7366.93	7254.96

The tibial resection shows higher levels of activity in all but the wrist flexors, with the first dorsal interosseous and extensor carpi radialis longus muscles showing the highest levels of activity over the testing (Table 7.4-7).

7.4.3.4 User range of motion

Tibial Average of range of motion

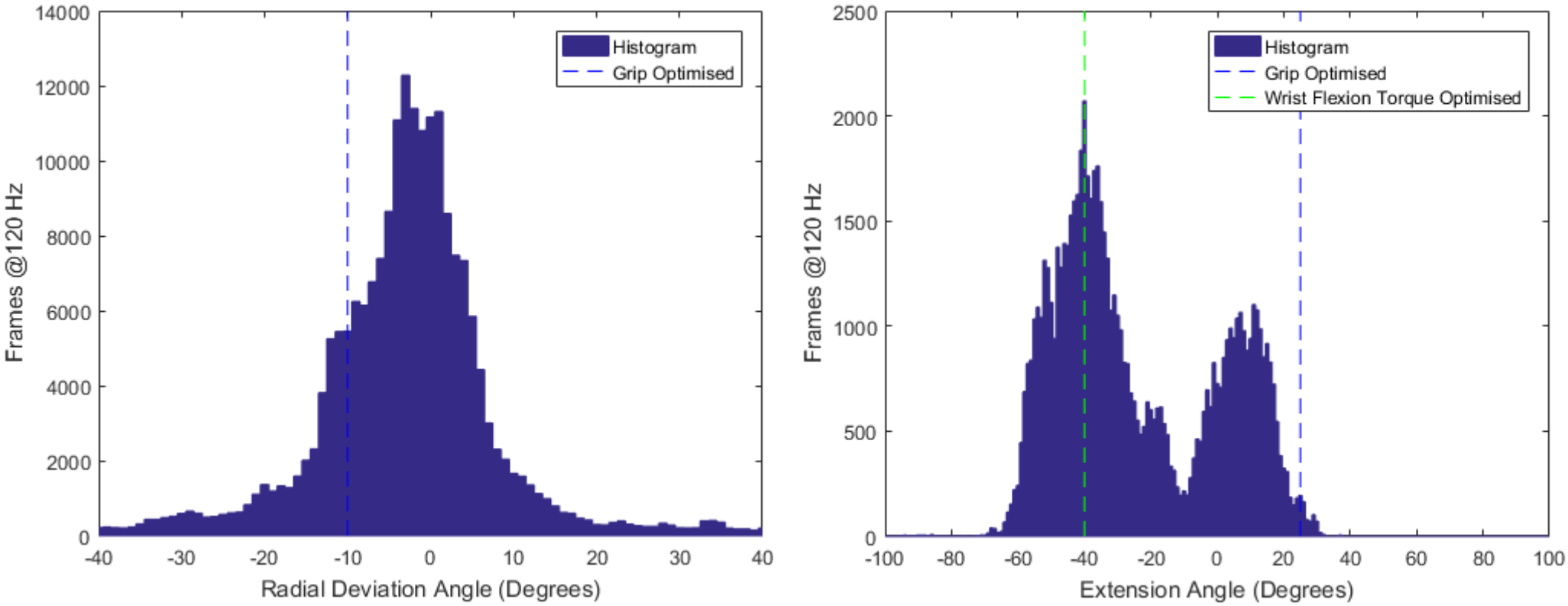

Figure 7.4-1 Tibial Range of Motion Histograms of the wrist for the number of frame at a given joint angle. Below and the proceeding pages is a number of graphs showing a histograms of the range of motion. These are used to describe the time spent in different postural positions, showing the number of frame that each 1-degree bin was recorded.

Femoral Average of range of motion

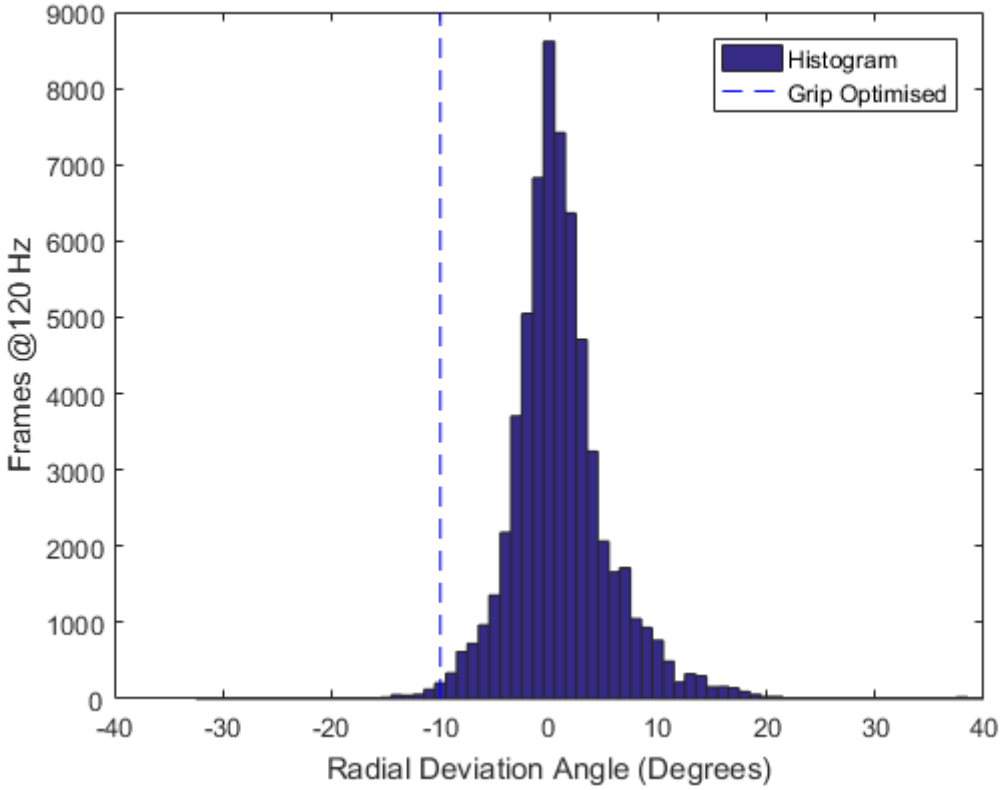

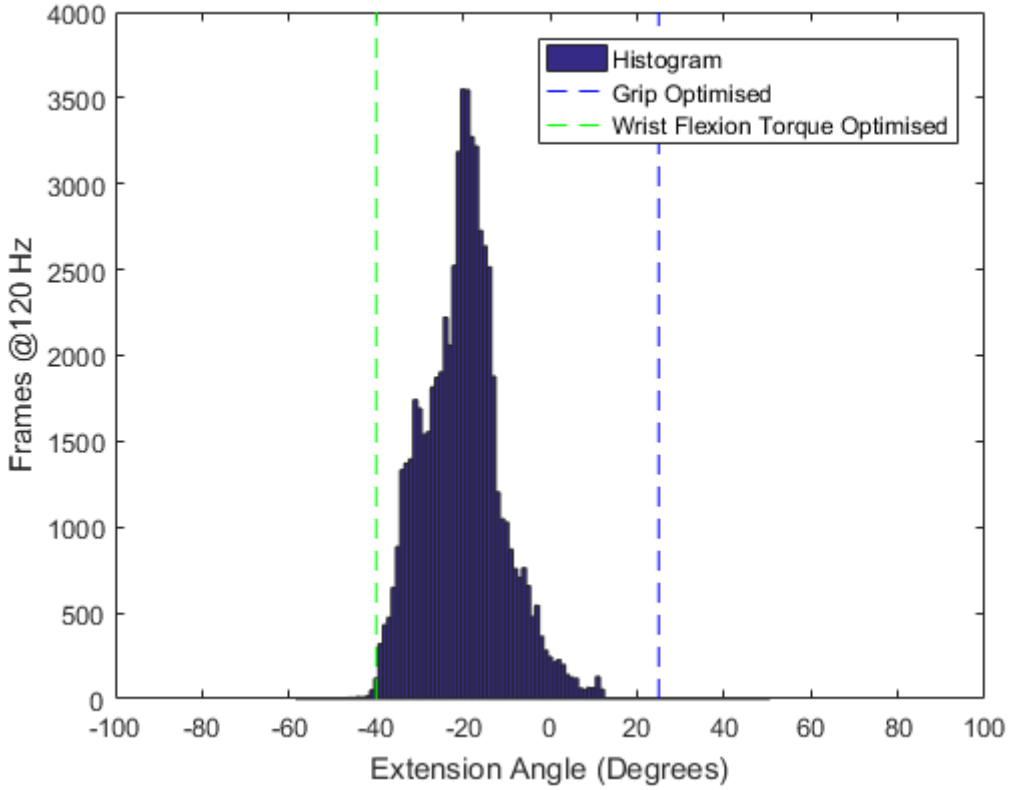

Figure 7.4-2 Femoral Range of Motion Histograms of the wrist for the number of frame at a given joint angle. Below and the proceeding pages is a number of graphs showing a histograms of the range of motion. These are used to describe the time spent in different postural positions, showing the number of frame that each 1-degree bin was recorded.

.

From Figure 7.4-1 and Figure 7.4-2 both femoral and tibial resections for radial deviation show a near neutral peak in the distribution, with both shaped as normally distributions. Wrist extension however show a bimodal distribution for the tibial resection and a skewed distribution for the femoral resection, neither presented means at neutral.

Table 7.4-8 Average range of motion for all users and the average joint angle for the (averaged posture) three tibial cuts along with the average of these for all the tibial cuts.

Tibial (degrees)	Range of Motion Av		Mean Angle for all trials	
	Mean	SD	Mean	SD
Wrist Radial Deviation	21.495	3.493	-2.533	0.942
Wrist Extension	43.610	8.346	-23.455	3.378
Elbow Supination	81.245	9.426	23.547	5.783
Elbow Extension	55.586	7.800	-59.304	4.570
Shoulder Flexion	64.696	20.843	40.556	3.802
Shoulder Abduction	63.997	14.762	43.437	5.837

Posturally for the tibial resection, the wrist is neutral in radial deviation, but otherwise flexed and supinated (Table 7.4-8). The wrist is positioned through the 60-degree flexion of the elbow together with a 40 degrees flexion and 43 degree abduction of the shoulder.

Table 7.4-9 Average range of motion for all users, the average minimum and maximum values of those range of motion, and the average joint able for the (averaged posture) three femoral cuts along with the average of these for all the femoral cuts.

Femoral (degrees)	Range of Motion Av		Mean Angle for all trials	
	Mean	SD	Mean	SD
Wrist Radial Deviation	19.698	3.425	1.599	1.252
Wrist Extension	35.879	5.231	-14.285	3.246
Elbow Supination	64.262	5.154	14.11	1.103
Elbow Extension	37.450	4.834	-43.493	2.006
Shoulder Flexion	48.766	3.175	31.425	1.002
Shoulder Abduction	36.381	2.324	28.107	1.577

For the femoral resection, the wrist is again in a neutral radial deviation, slightly flexed and supinated (Table 7.4-9).

Table 7.4-10 Differences in the average, range of motion and minimal and maximum joint angles between the tibial and femoral cuts.

Tibial -Femoral (degrees)	Range of Motion Av		Mean Angle for all trials	
	Difference	T-Test	Difference	T-Test
Wrist Radial Deviation	1.797	0.350	-4.132	0.000
Wrist Extension	7.731	0.060	-9.169	0.000
Elbow Supination	16.983	0.001	9.036	0.002
Elbow Extension	18.137	0.000	-15.811	0.000
Shoulder Flexion	15.930	0.069	9.132	0.000
Shoulder Abduction	27.615	0.000	15.331	0.000

The range of motion can be seen to be larger for all the joints in the tibial cuts than the femoral cuts (Table 7.4-10). This shows that the movements were more dynamic in the tibia and more refined in the femoral.

The change in posture between the two cuts is restricted at the radial deviation from the shape and orientation of the handle. However, wrist extension in the tibial is shown to be higher than for the femur by 8 degrees. Finally, the wrist is shown to be prone in the femoral cutting and slightly supine in the femoral cutting.

In the upper arm the tibial cut is observed to be more flexed at the shoulder and elbow, along with further abduction of the shoulder. This upper arm orientation is required to approach to the tibia from above.

Table 7.4-11 Difference in handle movements for tibial and femoral cuts between the current and prototype handle (New - Current)

Tibial Old - New (degrees)	Range of Motion Av		Mean Angle for all trials	
	Difference	T-Test	Difference	T-Test
Wrist Radial Deviation	-1.536	0.461	7.570	0.000
Wrist Extension	0.600	0.896	14.225	0.000
Elbow Supination	-17.766	0.198	20.345	0.000
Elbow Extension	-8.434	0.453	-36.303	0.000
Shoulder Flexion	-24.338	0.015	-44.996	0.000
Shoulder Abduction	3.526	0.800	1.488	0.602
Femoral Old - New (degrees)	Range of Motion Av		Mean Angle for all trials	
	Difference	T-Test	Difference	T-Test
Wrist Radial Deviation	0.795	0.727	11.490	0.000
Wrist Extension	6.837	0.116	11.509	0.000
Elbow Supination	-11.141	0.453	31.903	0.000
Elbow Extension	10.468	0.346	-45.473	0.000
Shoulder Flexion	4.187	0.694	-40.718	0.000
Shoulder Abduction	13.380	0.278	-2.776	0.309

Posturally the new handle is significantly different for all lower arm joint angle apparent from the shoulder abduction. Otherwise the range of motion used was only shown to significantly increase in shoulder flexion for the tibial cut.

7.5 Discussion

7.5.1 Pre Testing

7.5.1.1 Population Anthropometrics

The user groups for the prototype testing was shown to have no significant different between the orthopaedic surgeon profile. This would indicate that physically the small group of users are reflective of an orthopaedic surgeon profile, but many factors contribute to how a user interacts with the robotic arm. What can be determined is that given fatigue is still presented in this test group, hence the physical strength of the user is unlikely to be different in a surgical population and otherwise limitations in strength can be dismissed as a cause of fatigue with both stronger and weaker users presenting fatigue.

7.5.2 Pre Post Testing

7.5.2.1 Isometric testing

For isometric strength testing the significant changes from pre to post testing were seen in the flexion and extension measurements. This was an observation that was not measured in the larger group during the strength testing, but when reviewing the strength change in this smaller group of users there was a significant change in strength for the current handle as well. This is unique to this small user group and would be classified under the second mechanism of fatigue as defined in section 6.4.4.2.

While not significantly different, the grip strength changes are also worth noting. Firstly the strength change in this group did not match those presented in for the fatigue mechanism of the intrinsic muscles of the hand (6.4.4.1). However, the change in the grip strength for the current handle was nearly 7% change in the strength, for the new handle in the same users this increases to 16%. The sample numbers of the change in strength were two low for statistical comparison between the two handles, but this would suggest some observable change in the functionality of the prehensile muscles.

The magnitude of the wrist flexion percentage change was lower than the changes in the radial deviation. This strength test shows a significant decrease in strength for $\alpha=0.1$. To this extent the result should be considered as an important change both for the pre post testing of the prototype handle, but also when considering the change in the current handle that showed no difference.

Ultimately the test numbers are small, but describe a detrimental change from the current handle to prototype with increased functional loses from pre to post strength testing comparisons.

7.5.2.2 Questionnaire responses

Similar results between current and prototype handles for the average discomfort scores were reported, but the number of self-reported scores in the prototype testing were higher, with all users self-reporting the hand. The hand included the index and thumb as a specific subarea of the hand, hence the reporting numbers are higher than the sample number. While there was no significant observed change in the grip strength, the discomfort in the hand are more likely the intrinsic muscles of the hand, such as the first interosseous muscle.

Within this group there was minimal reported discomfort in the lower arm. The single user was the same in the current and prototype report mild discomfort for both tests, with a slight decrease in the discomfort from 5 to 4.

Again while there were no reports from this group for the upper arm during the current handle testing, there was discomfort reported in the upper arm by 2 users for the new prototype, scoring a 2 and a 4. This increase in reporting is not higher than the small sample being reported in the larger group, but could be an indicator of higher upper arm usage with the new handle design. Along with this there is a decrease in numbers reporting discomfort in the shoulder, however when reported the discomfort increases. This is a further indication of additional upper arm and shoulder usage. The user that reported discomfort in the current handle was only reporting a 2 on the discomfort scale, while a user reported a 5 for the shoulder during the prototype.

Finally, the wrist discomfort reporting changed for the users, with the two reporting discomfort with the current handle, and then no reported an issues with the prototype handle, but the other user then reported discomfort for the new handle. These are relatively high levels of discomfort and could show a disparity of usage between this user and for the two handles.

Of note the highest discomfort scores were reported in the hand and fingers for this group during both testing sessions. Between the handles the new protocol reported an increase in average discomfort reporting from 4 in the current handle to 5 in the prototype. Additionally, the highest discomfort score was reported in the prototype with a 7. All these results indicate a potential change in the areas of discomfort with potentially a slight increase in discomfort for this small group.

7.5.3 Mock Surgery

7.5.3.1 Prototype EMG Pseudostatic Fatigue metric

The first dorsal interosseous muscles showed the largest decreases in frequency for both bones, with a higher propensity to fatigue in the tibial resections. As was seen in the current handle, the prototype handle requires a tight grip during manipulation. Previously this was thought to be a function of handle design, but this significantly different shape shows the same, if not an increase fatiguing of the intrinsic muscles of the hand. This would suggest that the grip strength required is still an issue with this new handle design.

The Extensor carpi radialis longus muscle shows the second highest level of changes in frequency. In the current handle this was shown to have little or no change in frequency. This could possibly indicate increased wrist extension or abduction (radial deviation) demand. Given the increased

functional loses during the radial deviation strength tests, this would suggest an increase abductor requirement and possible resulting fatigue measurements.

Finally, the Flexor Carpi Radialis and extensor digitorum both showed decreasing frequency results. While the magnitude of these changes require further validation for interpretation in isolation, these changes in the prototype handle are of similar magnitude as the current handle for the larger group and appear to show the same level of fatigue in these muscles.

7.5.3.2 Prototype EMG RMS

Overall, the mean RMS for the new prototype only requires small fractions of the MVC when compared than the larger group. This is presumed to be due to the higher levels of strength in these users, requiring less of full strength of the muscles to manipulate the system.

The periods of higher activity, especially relating to the tibial first dorsal interosseous had an average peak of 78% MVC, are exceptionally high for all three users. High peak RMS measurements were also made in the extensor carpi radialis longus muscle and the extensor digitorum. These peak values will have lasting effects on the muscles when considering fatigue. These forces cannot be maintained for long periods of time, and result in an exponential shortening of overall endurance times of the muscles.

Even with the reduced average strength requirements these users still presented with fatigue and discomfort. Given the exceptionally high peak values, this would indicate that the impact of high demand on top of continual low level demand is still leading to fatigue in both the intrinsic and extrinsic muscles of the hand and wrist.

7.5.3.3 Prototype IEMG

The overall magnitudes of these results are smaller than the larger groups measurements for the current handle possibly due to the smaller percentages of muscles activity measured and shorter cutting times. However, a similar pattern of activity was seen with the first dorsal interosseous and extensor carpi radialis presenting the same magnitudes for the same boney cuts. The extensor digitorum is now smaller than these two measurements for the prototype test group than those measure for the current handle in the larger group.

The flexor carpi radialis showed the smallest cumulative activity. This would suggest that this muscle had the least demand for both cumulative mean, and from the RMS, the peak values of demand were also the smallest.

The difference in the bone cuts presented the tibia resection to have an increased level of cumulative activity. This is a slight change from the current handle that showed a mixed level of activity differences between the bone cuts.

7.5.3.4 Kinematics of Prototype Handle

The handle was now below the robotic arm, whereas in the current design this was on top. These two changes were seen in the significant postural average angles for the wrist and elbow joints. The wrist became less radially deviated with a neutral wrist for the prototype, but otherwise the wrist moved from extension to flexion and pronation to supination for the new prototype handle. The neutral wrist is advantageous for the grip force generation, but otherwise the prototype handle is not leading to a more biomechanically advantageous posture, just different.

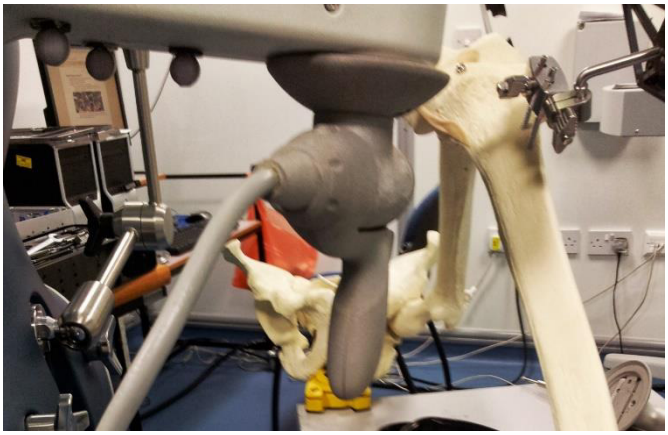

Figure 7.5-1 View from behind the prototype handle. Due to the position of the tibial array the handle required an approach from the medial direction resulting in a flexed wrist.

From the histogram assessment the wrist radial deviation showed a tendency to be marginally in ulnar deviation for the tibial resection and neutral for the femoral resections. Along with this the range of motion for this movement was also more dynamics in the tibial resection than the femoral, corroborating with the IEMG output. From reviewing the temporal plots of the users, the rhythmical cutting action is more apparent in the wrist extension movements leading to the assumption that the ulnar deviation is positional, while the wrist extension is resulting in the burrs cutting movements.

Given this observation that most of the cutting movements at the wrist are coming from the flexion extension of the wrist, the overall posture of the wrist is shown to be in flexion with some consistency over the repeated cuts. The main reason for this consistency is the positioning of the user relative to the burr. The users were aligning themselves with the burr away from the midline of the body to allow line of sight to the burr tips to reduce parallax, underneath the robotic arm (Figure 7.1-3). The hand relative to the knee is slightly lower in the prototype handle, along with the grip

handle angle this results in the wrist being ulnar deviated and flexed to match the tibial slope. While torques strengths are higher in flexion, the grip strength is reduced.

When describing the supination of the forearm the postural information shows a slight variation from supinated/neutral in the tibial resection to pronation in the femoral resection. Similar to the ulnar deviation mentioned before, this is the difference in the angle of the burr's approach. The Femur is positioned higher than the tibial and as such the burr needs to point upwards. This is mostly achieved in these users through the shoulder and elbow but at the wrist the user is trying to manipulate and aim the burr. Given the flexed position, adduction of the wrist results in supination as well, similarly abduction results in a slight pronation. This would suggest that this movement is a by-product of the other wrist movements. This is further reflected in the range of motion of the wrist in tibial and femoral resections, with the tibial resection showing much larger range of motion. This range of motion increase is reflected in the extensor carpi radialis and extensor digitorum having larger activities in the tibial than the femoral resections. While the torque is maximal at this point, the extensors are below half the strength of the flexors and as such will have to use a larger amount of their strength to perform the same movements. Additionally, the left medial UKA procedure will require more extensor action for a right handed user.

The extension of the elbow is about 10 degrees higher in the femoral resection. This is due to the added distance that the femur is away from the user when compared to the tibial. This added reach is enabled by straighten the elbow. When reviewing the temporal plots both cuts move through small amounts (<9 degrees) of flexion at the elbow.

Similarly, in the shoulder the amount of movement being contributed to cleaning is about 10 degrees, with the shoulder being more flexed and abducted in the tibial resection. This is slightly different to elbow postural in that a flexed shoulder would move the hand further from the body, however it is thought that to achieve the angles for the burr to follow the tibial plateau angle the shoulders are moved to raise the hand for the burr to be angled downwards at the wrist.

7.5.4 Comparison with current handle

When reviewing the prototype handle for the same testing procedure the results would suggest that the prototype handle is not resolving the issues of muscle fatigue. Grip fatigue was shown to potentially have increased in discomfort, functional loses and electrophysiological changes. Added to this, the changes in posture and articulation result in a changing of muscles required for manipulation of the system rather than a resolution of the fatigue. Hence, overall this would indicate that the new prototype is only bringing the benefit of the additional cutting tools. This also suggests

that this is a fundamental issue with the system that fatigue will result from extended or repetitive cuts.

The assumptions that stronger users would results in reduced fatigue appears to be unfounded as this stronger group while on average using a reduce amount of their strength still present fatigue in the lower extremities for both handles. This further reduces the impact of using user that do not meet the typical surgical strength profile and also realises that mechanism one is not strength dependent.

From observations of footage of the users, there is still a desire to move the burr throughout the tibial resection volume in a random fashion with both side to side and forward and backward motions, even with a pistol grip. Fundamentally the wrist is not particularly well designed to produce large add-and abduction or flexion extension moments, with no real mechanical leverage, instead these are more adapt for positioning of the wrist for finer movements. An ideal use for the pistol grip would be a sawing motion, pushing the burr through the volume, but this is not employed by users and hence fatigue is resulting from the use of the robotic arm in its haptic boundary.

Chapter 8 Project Summary

8.1 Project findings

An observational and biomechanical approach was taken to investigate anecdotal reporting of fatigue in high turnover MAKO RIO users. Due to the lack of any further substantial evidence or understanding of the fatigue reported, an initial observation of clinical use of the robotic system was undertaken. During this observation, surgeons showed signs of discomfort during single operations, which were severe enough during 2 of the cases for the surgeon to stop burring in order to recover from the fatigue.

To investigate possible reasons for this discomfort, specific action efficiencies could be extracted from a time analysis study that was conducted to review the surgical efficiency of the new robotic system. It was shown that when compared to the rest of the procedures that when present sclerotic bone resulted in extended (3-3.5 times) burring times. These findings changed the focus of the fatigue from excessive use of the system over a day, to the extended use of the robotic system in a single case.

To review this theory a biomechanical mock surgery was setup to assess for indications of fatigue during use of the robotic system for extended times equivalent to the burring times shown in the sclerotic surgical cases. From a questionnaire, reporting on the effects of fatigue, two sites in the arm were consistently highlighted after extended burring periods. These reported areas formed two theoretical mechanisms for fatigue.

The first mechanism was the fatiguing of the intrinsic muscles of the hand as a result of extended spherical prehensile gripping. The handle design is ideal for translations of the burr in the resection volume, but due to the freedom of movement of the robotic arm, this was also accompanied by rotational movements, that the hand has not sufficient mechanical advantage and could not deal with this movement. This resulted in excessive activity from the intrinsic muscles that eventually resulted in the fatigue on these muscles as confirmed through discomfort questionnaires, functional inability at a post testing grip strength test and electrophysiological changes in EMG associated with fatigue were noted.

The second mechanism defined the fatiguing of muscles extrinsic to the hand. This secondary mechanism was a result of the manipulation of the robotic arm against inertial and haptic boundary forces created by the robotic arm. This mechanism was less significant than the first mechanism, but

in the discomfort questionnaires, functional inability at post testing strength tests and electrophysiological changes in EMG associated with fatigue all indicated a fatiguing action. This mechanism is thought to arise from the demand of both gripping of the end effector of the robotic arm and its manipulation. The extrinsic muscles in the forearm are optimised for prehensile tasks in a static posture or refined movements of the wrist and fingers. Typically prehensile force and wrist movements are avoided for ergonomic reasons and for avoidance of work related stress disorders (McGorry et al., 2014).

For high turnover users, both mechanisms described are likely to induce fatigue. The first mechanism is thought to be more likely to presenting during cases with sclerotic bone, while the second more likely to present as a result of extended use of the system through a day.

8.2 Impact of findings

Fatigue should not be considered inevitable when using the system, and from the observational study is only rarely presented. Examples of fatigue and the results from this testing are an indicator of fatigue during longer than average burring periods. These longer periods resulted due to the inefficient burring of sclerotic bones.

The clinical impact of this fatigue is speculative as no problematical clinical outcomes of surgery, other than the increased surgical time, were recorded. From the literature (Peskun et al., 2012), THA replacements performed later in the day were significantly longer and had an increase chance of intraoperative fracture. However, this same study speculatively associates these outcomes with fatigue, that was not directly measured, and did not show differences in a range of other clinical outcomes or in TKA procedures. Arguably this form of fatigue, similar to those reported by Sturm (2011), are central fatigue and not an indication of localised fatigue.

While a number of other papers have reviewed localised fatigue and the impact on skill in laparoscopy (Hubert et al., 2013; Kowalewski, 2012) and endoscopy (Chandra et al., 2014; Luttmann et al., 1996b), limited work has been conducted in orthopaedics. The extreme cases are those simulated in this project, it is hard to imagine that a surgeon's skill and coordination would not be impacted, however whether this would lead to clinically significant changes to surgical outcome, would require assessment rather than speculation. This would require a sensitive localised fatigue metric that could be used in theatre and correlated with surgical outcome. Given the range of surgical and patient variables to consider, this study would require large sample sizes and a significant cost associated with this process.

Only after the development of a sensitive measure of localised fatigue during dynamic movements, could definitive wider spread recommendations of 'awkward' positions during surgery, handle design, number of surgeries per list be given. The recommendations would have far reaching implications, more than just surgical impact, but would also enable the ergonomic review of any physical demand during a task. This project further emphasises the need for a practical way of measuring localised fatigue during dynamic physical tasks.

8.3 Project contributions

While the project set out to ergonomically review the MAKO RIO surgical platform, a number of developments were required to attain this assessment. The project was initiated with time analysis of the use of the system in a clinical environment. The time analysis within this project produced a profile of use of the MAKO RIO at the Glasgow Royal Infirmary. While feeding into the later sections of the thesis, this has also shown the impact that new technology can have on the clinical work environment (published external to this thesis (Banger et al., 2013)). Through comparison with the Oxford UKA it was shown that the new MAKO procedure would most likely take more time for the added benefit of clinical outcomes relating to the increased accuracy.

The MAKO technology would normally be reviewed through typical industrial processes internal to the company, however, the approach presented here was novel, with the tools and systems requiring development before being implemented. The Optitrack system and associated biomechanical model are unique for this application through the bespoke code in MatLab. The code controls the synchronisation of the EMG and force transducer with the Optitrack system, along with the automation of all assessment in this biomechanical testing section. This model and system has been validated either against recognised existing technology or reviewed against the literature. From the output of this technology, further analysis tools were developed based on similar approaches developed in the literature. From these tools the activity and state of fatigue could be quantified for targeted muscle groups thought to be at risk of fatigue when using the robotic arm. These states of fatigue have no absolute metric and as such were compared with each other to show relative activity and sign of physiological changes in the muscles. Questionnaires corroborated the relative findings with a large number of reports of discomfort in the hand and fingers that matched with the measurements from the first dorsal interosseous muscle. This highlighted issues with the extended length of time and demand on these muscles to manipulate the system. This in itself is a novel application of this testing technology to review the MAKO RIO.

There is an argument that the testing was not an optimised setup and the users were new to the system, where, given time, they could become more proficient at managing the use of the system.

However, the examples shown are still within the recommendation for use, and this is leading to fatigue in the user over longer periods of cutting. As to the level of fatigue that is likely to be seen with these systems, it is difficult to predict. From the time analysis variation in the bone density and cutting times has been shown to result in discomfort to the surgeon. By performing this exaggerated testing, the emphasis is on trying to recognise the potential problems that might arise given poor postural and usage techniques. This therefore justifies using the type of testing that was applied, such that the testing wasn't considered typical use, but took every precaution to control for recognised variables.

8.4 Proposed Improvements to the system

Given the continued improvements and redesign of this system, a number of possible improvements to this robotic arm is suggested. This is divided in changes to the robotic system and changes to user improvements.

8.4.1 User Improvements

Biomechanically the user is at a disadvantage when trying to manipulate the system with any movements other than pushing or pulling the burr into the bone. To this extent two possible changes are, that the surgeon is encouraged to only move in a forward cutting plane analogous to planning wood. This would discourage the rotational movements and work to the current handles and add advantage in utilising the stronger proximal muscle of the arm. The second is the surgeon needs to consider applying forces to other points on the robot with the other hand or with the body. This will aid the movement of the system. The draw back to the changes will be the reduced control of movement of the system as the finer controlled movements of the wrist and fingers are not being exploited. The surgeon also fully relies on the haptic boundary to control these forces. To this extent deployment of this technique can be encouraged only when sclerotic bone is present to defuse the risk and concern.

Additionally, the burr orientation needs to be considered, with the burr cutting more efficiently along its axis. This idea was explored with the new handle design. While still observing similar levels of fatigue in users, the application of force in the anterior-posterior plane of the knee would be much more efficient for the muscles in the lower arm. It is thought that the freedom of movement in the boundary is resulting in awkward postures and additional haptic could result in better fatigue resistance. Although this has not been tested as part of this project.

8.4.2 Robotic system improvements

For the same reason, a semi-automated burring mode could be implemented. This could be taken ahead in two directions, the first would be if the system allowed both haptic and active cutting of the bone. The surgeon could start the procedure and then allow the robot to finish the procedure, with substitutions being allowed at any time. This would reduce the amount of effort required by the surgeon for the majority of the resection volume. At specific sites, such as near soft tissues like the collateral ligament and posterior capsule, resection would be required to be performed by the surgeon. An alternative idea would be the assistance of the robot to aid in force production, in the same way that power steering aids a driver. The system would apply a multiplier to the force applied to the handle of the system. This would, along with additional feedback through audio, reduce the amount of force the user is applying. This is ultimately a complex addition and would fundamentally change the system, such that it would require further FDA and CE mark approvals.

A change to the surgical tools has been shown to be an option with the introduction of the new hand piece. The Anspach burr that is currently used was designed for use in smaller bone volume resection than its current application. New tooling could allow for quicker and more efficient cutting, but increased power or speed would have to manage increased risk of thermal necrosis. Bone density measurements from a CT scan should enable a suitable burr head for the predicted bone density, but would result in an extra cost for the analysis of the CT, and the production and stock maintenance of different burrs.

Given the continued use of a surgeon to manipulate the system, consideration has to be given to the expected user kinematics, while having to generate the forces required to move the system. If fine precision movements are required for the extended cutting periods, the haptic forces need to be lower than the current system allows. This is unlikely to be the case for safety reasons, and as such the physical interface of the robotic arm needs to restrict the user's movements at the hand and wrist and utilise the stronger elbow and shoulder, but at the detriment of a loss of control. This could be achieved by increasing the turning resistance joint 5 and 6 to reduce the use of these joints. Joints 5 and 6 are largely manipulated by the wrist of the user, and in restricting these movements the user will adopt new approaches of manipulating the burr.

8.5 Future work

During the course of this project a number of new research projects, both directly related to and methodologically related to this project, are recommended as a continuation of this work.

8.5.1 Anybody modelling

Testing and review was designed to allow for the development of an anybody modelling analysis of this work. However, given the time and resource limitation, initial work on this section was not sufficient to warrant inclusion in this thesis. This work however is still valid for development. This body of work would allow for a detailed kinetic model of the force required to move the arm, but is ultimately limited in its application, as the grip force was not measured and only inferred from the EMG recordings.

Given a development of the all the forces required to manipulate a handle of an end effector, a better model of the maximal forces that a user could sustained before fatigue would be induced. A successfully developed tool, would allow a review of any handle design for a range of users without the need for extensive and expensive lab testing as used in Chapter 6. This would require development and is more extensive than was available in this project, and is the long term goals of applications such as Anybody and SIMM.

8.5.2 Grip force

One of the main issues that the observed users had, was with the longevity and grip strength required to manipulate the system. To truly understand the mechanisms, a more restrictive controlled experiment would be required to standardise posture and movements while measuring the applied grip forces from the users. Through this experiment a quantified model of the effects of gloves, vibrations and forces and torques applied through the handle can be reviewed. This gripping force is difficult to measure on a contoured shape of the handle. Approaches were reviewed, but required further specialist equipment such as force measuring gloves and force resistance sensors. An endurance model of the system could then be created to show when the user population would experience force. In addition to this a range of measures would need to be taken for the different levels of bone density to truly measure forces in the system. Given the haptic nature of the system these might be extracted from the motor work levels of the system, but could require a similar setup to the force transducer in this testing for higher accuracy.

One additional development from this testing methodology is a well-defined prehensile model of the hand for functional tasks. Inspired by (Lee and Zhang, 2005), this would expand on this setup to calculate mechanical loading on the hand to perform tasks. This was very much the aim for the anybody software development, but the complexity of the problem soon outgrew this project.

8.5.3 Optical tracking outputs

The fingers and head of the users were tracked with markers. The first marker was added to review the alignment of the thumb and finger, along with an assumed splaying angle of the finger to check for further issues with the ability of the user to grip the end effector. The head markers were added to allow the timing of gaze onto the bone or screen, given the line of sight issues, this would measure how often the users were looking at the surgical site or the screen. Expansion of the model and analysis of this already collected data would further define the posture of the hand that is resulting in the intrinsic muscles fatigue and further understanding of postures outside of the arm.

8.5.4 EMG

The difficulty comes in trying to quantify the fatigue for comparison between the two tests. While changes can be observed, it is not clear at what point some of the physiological measurements manifest themselves as discomfort, or at what point these become substantial to managing work related strain disorders. With further development of real time dynamic fatigue monitoring, the understanding of these mechanisms could be further understood. For this reason, these outcomes are not able to state a goal to reach, but instead are a means of monitoring changes in design from their impact, much like the proposed JASA methodology.

From reviewing the literature there are still no recognised means of detecting fatigue in a dynamic contraction. A Choi-Williams method has been mentioned in the literature, however due to time constraints and complexity in the techniques these were not wholly attempted. The pseudostatic methodology is a first attempt into this field and showed some sensitivity to fatigue in the muscle, but a time plot of a fatigue metric is still elusive. Further work in this field would involve applying methods of analysing the EMG along with the optical tracking and a force transducer. The aim of any of this work would be a validated means of inferring activity and fatigue relating to dynamic kinematics and kinetics. This would be a huge body of work, and numerous research groups globally are trying to achieve this. A pseudostatic type metrics, would negate the need for functional strength testing before and after, and would allow for a temporal measure of fatigue which can then be related to different tasks.

Additionally, further development and validation of the pseudostatic methodology needs to be performed. Given the lack of a gold standard, more restrained movement testing should be conducted for this calculation. Additionally, a further constraint on the changing activity levels on the points would be the true 3D JASA plots that was an original idea for this study. RMS was dropped as the activity of a fatiguing muscle, can increase without an associated increase in force. Ideally the

same force conditions could be used, but further constraint requires high sampling frequencies to ensure enough temporal information is collected.

The addition of more electrodes to the testing, or at least testing different muscles would give a better picture of all the activity, and potential physiological changes in the muscles. Tracking the activity of the flexor digitorum profundus to monitor the amount of grip being used would be of high importance given the results presented.

8.5.5 Setup

The addition of sawbones to testing would have a profound impact on a number of factors in the project. While learning curves and the additional forces have been reviewed in the main body of work, the question of the vibrations from the burr has not been reviewed. The high speed burr, especially when moving perpendicular to the long axis of the burr, vibrates and jumps. These low level vibrations are shown to increase the force produced for the same task. While gloves are shown to reduce this effect from vibration, they also cause a further increase in force production for the same task due to the lack of sensation with the object. Adding both of these to the testing protocol would be an expected to increase the force production of the grip even further, leading to further demand from the muscles and further presentation of fatigue. Additional to sawbones, biological material could also be used such as bovine bone, but this would require a CT image of the bone. Cadaveric material would be ideal, but would need to be part of another study to justify the use of this type of material.

Given the development of a EMG model using a pseudostatic type metric in the lab, the most ideal testing scenario would be applied in situ in theatres. EMG could be mounted in a sealed cover to allow for the scrubbing in process. Additionally, the mounting of the force transducer under the end effector is not considered sterile. Using this method, the sterility of the surgery would not be compromised. Given the multiple barriers and practicalities of this, it is clear why the testing was initiated in the lab.

8.5.6 Review of musculoskeletal risk factors

A number of industrial evaluation tool sets are available that review the risk factors relating to industrial working conditions. Due to their industrial application many assume that the working conditions are repeated over the work day and week. The application in a more varied surgery work flow still needs to be considered. For instance, completing the rapid upper limb assessment for the burring tasks revealed a score of 7, or a very high risk of musculoskeletal disorders, but due to the limited number of surgeries and surgical days the same conditions are not repeated enough to lead to MSD. Those at risk would be the high volume surgeons, but it is difficult to review how many

cases are required to start to lead to MSD. This would be the scope of future work of reviewing the protracted exposure of this type of surgery, known to have ergonomic limitations, with extended continual use. However, from reviewing the typical numbers of cases and typical working weeks of theatres it is unlikely that many, if any surgeons, are performing enough surgeries to sustain MSD as a result of using the robotic system. Of more interest with it current use would the effect of fatigue between cases.

8.5.7 Recovery from fatigue

Both mechanisms have described the fatigue of muscles to the point of a functional loss of strength, and indications of further coordination and control issues with the surgeon's inability to write after testing. The frequency of fatigue clinically is thought to be minimal from these results, but a further consideration to expansion of this work would be the review of recovery from this fatigue. Given the onset of fatigue understanding, the duration of effects would allow for proper planning and recovery within or even between cases if necessary. As subjective measure of fatigue are not reliable during recovery (Adamo et al., 2009) and electrophysiological testing requires activation of the recovering muscles a new series of tests and indicators of fatigue would be required.

8.6 Project conclusions

Fatigue was induced in users manipulating the robotic system within and against its haptic boundary. While extended, these burring time periods were shown to be similar to those seen in the clinical use of the robotic arm. A number of tests confirmed fatigue occur in two sites; the intrinsic and extrinsic muscles of the hand. This was a result of the sustained and mobile forces required from both the prehensile and articulating muscles of the lower arm.

Bibliography

2011 Surgical Workforce Census Report — Royal College of Surgeons [WWW Document], 2011. URL http://www.rcseng.ac.uk/surgeons/surgical-standards/docs/2011-surgical-workforce-census-report/view (accessed 8.25.16).

Abdoli-Eramaki, M., Damecour, C., Christenson, J., Stevenson, J., 2012. The effect of perspiration on the sEMG amplitude and power spectrum. J. Electromyogr. Kinesiol. 22, 908–913. https://doi.org/10.1016/j.jelekin.2012.04.009

Adamo, D.E., Khodaee, M., Barringer, S., Johnson, P.W., Martin, B.J., 2009. Low mean level sustained and intermittent grip exertions: influence of age on fatigue and recovery. Ergonomics 52, 1287–1297. https://doi.org/10.1080/00140130902984935

Al Zaman, A., Sharmin, T., Khan, M.A.A., Ferdjallah, M., 2007. Muscle fatigue analysis in young adults at different MVC levels using EMG metrics, in: IEEE SoutheastCon, 2007. Proceedings. Presented at the IEEE SoutheastCon, 2007. Proceedings, pp. 390–394. https://doi.org/10.1109/SECON.2007.342930

Alkner, B.A., Tesch, P.A., Berg, H.E., 2000. Quadriceps EMG/force relationship in knee extension and leg press: Med. Sci. Sports Exerc. 32, 459. https://doi.org/10.1097/00005768-200002000-00030

Amis, A.A., 1990. Part 2: Forearm, wrist, hand and fingers. Curr. Orthop. 4, 107–111.

Anglin, C., Wyss, U.P., 2000. Review of arm motion analyses. Proc. Inst. Mech. Eng. [H] 214, 541–555. https://doi.org/10.1243/0954411001535570

Armstrong, T.J., Radwin, R.G., Hansen, D.J., Kennedy, K.W., 1986. Repetitive Trauma Disorders: Job Evaluation and Design. Hum. Factors J. Hum. Factors Ergon. Soc. 28, 325–336. https://doi.org/10.1177/001872088602800308

Arun, K.S., Huang, T.S., Blostein, S.D., 1987. Least-squares fitting of two 3-D point sets. Pattern Anal. Mach. Intell. IEEE Trans. On 698–700.

Ayoub, M.M., Presti, P.L., 1971. The Determination of an Optimum Size Cylindrical Handle by Use of Electromyography. Ergonomics 14, 509–518. https://doi.org/10.1080/00140137108931271

Aziz, E.S., 2009. Tourniquet use in orthopaedic anaesthesia. Curr. Anaesth. Crit. Care 20, 55–59. https://doi.org/10.1016/j.cacc.2008.12.001

Baker, R., 2013. Wiley: Measuring Walking: A Handbook of Clinical Gait Analysis - Richard W. Baker [WWW Document]. URL http://eu.wiley.com/WileyCDA/WileyTitle/productCd-1908316667,subjectCd-HE90.html (accessed 8.22.16).

Ballash, M., 2012. Ergnomics of robotic orthopedic susrgery: A program to simultaneously improve operating time efficiency and quality of care. Presented at the 25th Annual Congress of ISTA, Syndney, Australia.

Bandouch, J., Engstler, F., Beetz, M., 2008. Accurate Human Motion Capture Using an Ergonomics-Based Anthropometric Human Model, in: Perales, F.J., Fisher, R.B. (Eds.), Articulated Motion and Deformable Objects, Lecture Notes in Computer Science. Springer Berlin Heidelberg, pp. 248–258.

Banger, M., Rowe, P.J., Blyth, M., 2013. TIME ANALYSIS OF MAKO RIO UKA PROCEDURES IN COMPARISON WITH THE OXFORD UKA. Bone Jt. J. Orthop. Proc. Suppl. 95-B, 89–89.

Banks, S.A., 2009. Haptic robotics enable a systems approach to design of a minimally invasive modular knee arthroplasty. Am. J. Orthop. 38, 23–27.

Banks, S.A., Fregly, B.J., Boniforti, F., Reinschmidt, C., Romagnoli, S., 2005. Comparing in vivo kinematics of unicondylar and bi-unicondylar knee replacements. Knee Surg. Sports Traumatol. Arthrosc. 13, 551–556. https://doi.org/10.1007/s00167-004-0565-x

Bargar, W.L., Bauer, A., Börner, M., 1998. Primary and Revision Total Hip Replacement Using the Robodoc (R) System. Clin. Orthop. 354, 82–91.

Basmajian, J.V., 1985. Muscles alive: their functions revealed by electromyography, 5th ed. ed. Williams & Wilkins, Baltimore.

Bäthis, H., Perlick, L., Tingart, M., Lüring, C., Zurakowski, D., Grifka, J., 2004. Alignment in total knee arthroplasty A comparison of computer-assisted surgery with the conventional technique. J. Bone Joint Surg. Br. 86, 682–687.

Bell, D.G., 1993. The influence of air temperature on the EMG/force relationship of the quadriceps. Eur. J. Appl. Physiol. 67, 256–260. https://doi.org/10.1007/BF00864225

Bell, S.W., Anthony, I., Jones, B., MacLean, A., Rowe, P., Blyth, M., 2016. Improved Accuracy of Component Positioning with Robotic-Assisted Unicompartmental Knee Arthroplasty: Data from a Prospective, Randomized Controlled Study. J. Bone Joint Surg. Am. 98, 627–635. https://doi.org/10.2106/JBJS.15.00664

Berger, R.A., 1996. The Anatomy and Basic Biomechanics of the Wrist joint. J. Hand Ther. 9, 84–93. https://doi.org/10.1016/S0894-1130(96)80066-4

Berger, W., Dietz, V., Quintern, J., 1984. Corrective reactions to stumbling in man: neuronal co-ordination of bilateral leg muscle activity during gait. J. Physiol. 357, 109–125.

Bergfeld, J.A., McAllister, D.R., Parker, R.D., Valdevit, A.D.C., Kambic, H., 2001. The Effects of Tibial Rotation on Posterior Translation in Knees in Which the Posterior Cruciate Ligament Has Been Cut. J Bone Jt. Surg Am 83, 1339–1343.

Bhardwaj, P., Nayak, S.S., Kiswar, A.M., Sabapathy, S.R., 2011. Effect of static wrist position on grip strength. Indian J. Plast. Surg. Off. Publ. Assoc. Plast. Surg. India 44, 55–58. https://doi.org/10.4103/0970-0358.81440

Bigland-Ritchie, B., Woods, J.J., 1984. Changes in muscle contractile properties and neural control during human muscular fatigue. Muscle Nerve 7, 691–699.

Biomet., 2012. Oxford partial knee-manual of the surgical technique.

Bjorgul, K., Novicoff, W.M., Saleh, K.J., 2010. Learning curves in hip fracture surgery. Int. Orthop. 35, 113–119. https://doi.org/10.1007/s00264-010-0950-7

Blackwell, J.R., Kornatz, K.W., Heath, E.M., 1999. Effect of grip span on maximal grip force and fatigue of flexor digitorum superficialis. Appl. Ergon. 30, 401–405.

Blake, O.M., Wakeling, J.M., 2014. Early deactivation of slower muscle fibres at high movement frequencies. J. Exp. Biol. 217, 3528–3534. https://doi.org/10.1242/jeb.108266

Blyth, M.J., Smith, J., Jones, B., MacLean III, A.B., Anthony, R.P., 2013. Does robotic surgical assistance improve the accuracy of implant placement in unicompartmental knee arthroplasty, in: AAOS 2013 Annual Meeting, Chicago, IL.

Böhlemann, J., Kluth, K., Kotzbauer, K., Strasser, H., 1994. Ergonomic assessment of handle design by means of electromyography and subjective rating. Appl. Ergon. 25, 346–354. https://doi.org/10.1016/0003-6870(94)90053-1

Bonato, P., Ebenbichler, G.R., Roy, S.H., Lehr, S., Posch, M., Kollmitzer, J., Della Croce, U., 2003. Muscle fatigue and fatigue-related biomechanical changes during a cyclic lifting task. Spine 28, 1810–1820. https://doi.org/10.1097/01.BRS.0000087500.70575.45

Bonato, P., Roy, S.H., Knaflitz, M., De Luca, C.J., 2001. Time-frequency parameters of the surface myoelectric signal for assessing muscle fatigue during cyclic dynamic contractions. Biomed. Eng. IEEE Trans. On 48, 745–753.

Borg, G., 1998. Borg's perceived exertion and pain scales. Human Kinetics, Champaign, IL, US.

Bovenzi, M., ZADINI, A., FRANZINELLI, A., BORGOGNI, F., 1991. Occupational musculoskeletal disorders in the neck and upper limbs of forestry workers exposed to hand-arm vibration. Ergonomics 34, 547–562.

Boyer, J., Lin, J., Chang, C., 2013. Description and analysis of hand forces in medicine cart pushing tasks. Appl. Ergon. 44, 48–57. https://doi.org/10.1016/j.apergo.2012.04.008

Branch, S.H., Goddard, M., Lang, J., Poehling, G., Conditt, M., Jinnah, R., 2012. Accuracy of Pre-Operative Planning in Robot-Assisted Unicompartmental Knee Arthroplasty. J. Bone Joint Surg. Br. 94, 18–18.

Bratt, J.H., Foreit, J., Chen, P.-L., West, C., Janowitz, B., Vargas, T.D., 1999. A comparison of four approaches for measuring clinician time use. Health Policy Plan. 14, 374–381.

Brumfield, R.H., Champoux, J.A., 1984. A biomechanical study of normal functional wrist motion. Clin. Orthop. 23–25.
Buckley, M.A., Yardley, A., Johnson, G.R., Cams, D.A., 1996. Dynamics of the Upper Limb during Performance of the Tasks of Everyday Living—A Review of the Current Knowledge Base. Proc. Inst. Mech. Eng. [H] 210, 241–247. https://doi.org/10.1243/PIME_PROC_1996_210_420_02
Buhman, D.C., Cherry, J.A., Bronkema-Orr, L., Bishu, R., 2000. Effects of glove, orientation, pressure, load, and handle on submaximal grasp force. Int. J. Ind. Ergon. 25, 247–256. https://doi.org/10.1016/S0169-8141(99)00015-3
Burger, B., Toiviainen, P., 2013. MoCap Toolbox-A Matlab toolbox for computational analysis of movement data, in: Proceedings of the Sound and Music Computing Conference 2013, SMC 2013, Logos Verlag Berlin, Stockholm, Sweden. ISBN 978-3-8325-3472-1. Logos Verlag Berlin.
Burke, T.A., McKee, J.R.P., Wilson, H.C.M., Donahue, R.M.J., Batenhorst, A.S., Pathak, D.S., 2000. A Comparison of Time-and-Motion and Self-Reporting Methods of Work Measurement. J. Nurs. Adm. March 2000 30, 118–125.
Cao, C., MacKenzie, C.L., Payandeh, S., 1996. Task and motion analyses in endoscopic surgery, in: Proceedings ASME Dynamic Systems and Control Division. pp. 583–590.
Cappozzo, A., Cappello, A., Croce, U.D., Pensalfini, F., 1997. Surface-marker cluster design criteria for 3-D bone movement reconstruction. IEEE Trans. Biomed. Eng. 44, 1165–1174. https://doi.org/10.1109/10.649988
Cardoen, B., Demeulemeester, E., Beliën, J., 2010. Operating room planning and scheduling: A literature review. Eur. J. Oper. Res. 201, 921–932.
Carse, B., Meadows, B., Bowers, R., Rowe, P., 2013. Affordable clinical gait analysis: An assessment of the marker tracking accuracy of a new low-cost optical 3D motion analysis system. Physiotherapy 99, 347–351. https://doi.org/10.1016/j.physio.2013.03.001
Cavallo, F., Sinigaglia, S., Megali, G., Pietrabissa, A., Dario, P., Mosca, F., Cuschieri, A., 2013. Biomechanics–Machine Learning System for Surgical Gesture Analysis and Development of Technologies for Minimal Access Surgery. Surg. Innov. 1553350613510612. https://doi.org/10.1177/1553350613510612
Chaffin, D.B., 1973. Localized muscle fatigue-definition and measurement. J. Occup. Environ. Med. 15, 346–354.
Chalder, T., Berelowitz, G., Pawlikowska, T., Watts, L., Wessely, S., Wright, D., Wallace, E.P., 1993. Development of a fatigue scale. J. Psychosom. Res. 37, 147–153. https://doi.org/10.1016/0022-3999(93)90081-P
Challis, J.H., 1995. A procedure for determining rigid body transformation parameters. J. Biomech. 28, 733–737.
Chandra, S., Hayashibe, M., Thondiyath, A., 2014. Dominant component in muscle fatigue induced hand tremor during laparoscopic surgical manipulation. Conf. Proc. Annu. Int. Conf. IEEE Eng. Med. Biol. Soc. IEEE Eng. Med. Biol. Soc. Annu. Conf. 2014, 6539–42. https://doi.org/10.1109/EMBC.2014.6945126
Chareancholvanich, K., Narkbunnam, R., Pornrattanamaneewong, C., 2013. A prospective randomised controlled study of patient-specific cutting guides compared with conventional instrumentation in total knee replacement. Bone Jt. J. 95, 354–359.
Chengular, Rodgers, Bernard, 1983. Wiley: Kodak's Ergonomic Design for People at Work, 2nd Edition - null The Eastman Kodak Company [WWW Document]. URL http://eu.wiley.com/WileyCDA/WileyTitle/productCd-0471418633.html (accessed 4.27.15).
Choi, J.H., Park, S.-W., Baek, S.-Y., Lee, K., 2010. Evaluation of handheld products by computing user hand fatigue. Simul. Model. Pract. Theory 18, 230–239. https://doi.org/10.1016/j.simpat.2009.10.009
Christensen, H., 1986. Muscle activity and fatigue in the shoulder muscles of assembly-plant employees. Scand. J. Work. Environ. Health 12, 582–587.

Cifrek, M., Medved, V., Tonković, S., Ostojić, S., 2009. Surface EMG based muscle fatigue evaluation in biomechanics. Clin. Biomech. 24, 327–340. https://doi.org/10.1016/j.clinbiomech.2009.01.010

Citak, Mustafa, Suero, E.M., Citak, Musa, Dunbar, N.J., Branch, S.H., Conditt, M.A., Banks, S.A., Pearle, A.D., 2012. Unicompartmental knee arthroplasty: Is robotic technology more accurate than conventional technique? The Knee.

Cj, D.L., 1983. Myoelectrical manifestations of localized muscular fatigue in humans. Crit. Rev. Biomed. Eng. 11, 251–279.

Clancy, E.A., Bertolina, M.V., Merletti, R., Farina, D., 2008. Time- and frequency-domain monitoring of the myoelectric signal during a long-duration, cyclic, force-varying, fatiguing hand-grip task. J. Electromyogr. Kinesiol. 18, 789–797. https://doi.org/10.1016/j.jelekin.2007.02.007

Clancy, E.A., Farina, D., Merletti, R., 2005. Cross-comparison of time- and frequency-domain methods for monitoring the myoelectric signal during a cyclic, force-varying, fatiguing hand-grip task. J. Electromyogr. Kinesiol. 15, 256–265. https://doi.org/10.1016/j.jelekin.2004.11.002

Clancy, E.A., Morin, E.L., Merletti, R., 2002. Sampling, noise-reduction and amplitude estimation issues in surface electromyography. J. Electromyogr. Kinesiol. 12, 1–16. https://doi.org/10.1016/S1050-6411(01)00033-5

Cleary, K., Kinsella, A., Mun, S.K., 2005. OR 2020 workshop report: Operating room of the future. Int. Congr. Ser. 1281, 832–838. https://doi.org/10.1016/j.ics.2005.03.279

Cobb, J., Henckel, J., Gomes, P., Harris, S., Jakopec, M., Rodriguez, F., Barrett, A., Davies, B., 2006. Hands-on robotic unicompartmental knee replacement A PROSPECTIVE, RANDOMISED CONTROLLED STUDY OF THE ACROBOT SYSTEM. J. Bone Joint Surg. Br. 88-B, 188–197. https://doi.org/10.1302/0301-620X.88B2.17220

Conditt, M.A., 2009. Minimally Invasive Robotic-Arm-Guided Unicompartmental Knee Arthroplasty. J. Bone Jt. Surg. Am. 91, 63. https://doi.org/10.2106/JBJS.H.01372

Conditt, M.A., Noble, P.C., Bertolusso, R., Woody, J., Parsley, B.S., 2004. The PCL significantly affects the functional outcome of total knee arthroplasty. J. Arthroplasty 19, 107–112. https://doi.org/10.1016/j.arth.2004.06.006

Confalonieri, N., Manzotti, A., Montironi, F., Pullen, C., 2008. Tissue sparing surgery in knee reconstruction: unicompartmental (UKA), patellofemoral (PFA), UKA + PFA, bi-unicompartmental (Bi-UKA) arthroplasties. J. Orthop. Traumatol. Off. J. Ital. Soc. Orthop. Traumatol. 9, 171–177. https://doi.org/10.1007/s10195-008-0015-5

Coon, T., 2008. High Efficiency Surgical Robotic Arm for UKA. Presented at the AAOS, San Francisco.

Coon, T.M., 2009. Integrating robotic technology into the operating room. Am J Orthop 38, 7–9.

Corlett, E.N., Bishop, R.P., 1976. A technique for assessing postural discomfort. Ergonomics 19, 175–182.

Crosby, C.A., Wehbé, M.A., 1994. Hand strength: Normative values. J. Hand Surg. 19, 665–670. https://doi.org/10.1016/0363-5023(94)90280-1

Dankelman, J., Grimbergen, C.A., Stassen, H.G., 2004. Engineering for Patient Safety: Issues in Minimally Invasive Procedures. CRC Press.

Davies, B., 2000. A review of robotics in surgery. Proc. Inst. Mech. Eng. [H] 214, 129–140. https://doi.org/10.1243/0954411001535309

De Magistris, G., Micaelli, A., Evrard, P., Andriot, C., Savin, J., Gaudez, C., Marsot, J., 2013. Dynamic control of DHM for ergonomic assessments. Int. J. Ind. Ergon. https://doi.org/10.1016/j.ergon.2013.01.003

De Smet, L., Tirez, B., STAPPAERTS, K., 1998. Effect of forearm rotation on grip strength. Age Years 22, 22–90.

Dedering, Å., Németh, G., Harms-Ringdahl, K., 1999. Correlation between electromyographic spectral changes and subjective assessment of lumbar muscle fatigue in subjects without

pain from the lower back. Clin. Biomech. 14, 103–111. https://doi.org/10.1016/S0268-0033(98)00053-9
Delp, S.L., Grierson, A.E., Buchanan, T.S., 1996. Maximumisometric moments generated by the wrist muscles in flexion-extension and radial-ulnar deviation. J. Biomech. 29, 1371–1375. https://doi.org/10.1016/0021-9290(96)00029-2
DiGioia, A.M., 2004. Computer and Robotic Assisted Hip and Knee Surgery. Oxford University Press.
Dingwell, J.B., Joubert, J.E., Diefenthaeler, F., Trinity, J.D., 2008. Changes in Muscle Activity and Kinematics of Highly Trained Cyclists During Fatigue. IEEE Trans. Biomed. Eng. 55, 2666–2674. https://doi.org/10.1109/TBME.2008.2001130
Dobson, P., Taylor, R., Dunkin, C., 2011. Safe splinting in hand surgery. Ann. R. Coll. Surg. Engl. 93, 94. https://doi.org/10.1308/003588411X12851639108033
Doix, A.-C.M., Gulliksen, A., Brændvik, S.M., Roeleveld, K., 2013. Fatigue and muscle activation during submaximal elbow flexion in children with cerebral palsy. J. Electromyogr. Kinesiol. 23, 721–726. https://doi.org/10.1016/j.jelekin.2012.12.005
Doorenbosch, C.A.M., Harlaar, J., 2003. A clinically applicable EMG–force model to quantify active stabilization of the knee after a lesion of the anterior cruciate ligament. Clin. Biomech. 18, 142–149. https://doi.org/10.1016/S0268-0033(02)00183-3
Dufour, J.S., Marras, W.S., Knapik, G.G., 2013. An EMG-assisted model calibration technique that does not require MVCs. J. Electromyogr. Kinesiol. 23, 608–613. https://doi.org/10.1016/j.jelekin.2013.01.013
E.E.F., K.S.G., C.A.P., J.R.J., 2005. Preface, in: Janson, E.E.F.S.G.A.P.R. (Ed.), Hand and Upper Extremity Splinting (Third Edition). Mosby, Saint Louis, pp. xiii–xvi.
Eksioglu, M., 2006. Optimal work-rest cycles for an isometric intermittent gripping task as a function of force, posture and grip span. Ergonomics 49, 180–201. https://doi.org/10.1080/00140130500465527
Eksioglu, M., 2004. Relative optimum grip span as a function of hand anthropometry. Int. J. Ind. Ergon. 34, 1–12. https://doi.org/10.1016/j.ergon.2004.01.007
El-Khoury, S., Li, M., Billard, A., 2013. On the generation of a variety of grasps. Robot. Auton. Syst. https://doi.org/10.1016/j.robot.2013.08.002
Emam, T.A., Frank, T.G., Hanna, G.B., Cuschieri, A., 2001. Influence of handle design on the surgeon's upper limb movements, muscle recruitment, and fatigue during endoscopic suturing. Surg. Endosc. 15, 667–672.
Enoka, R.M., Baudry, S., Rudroff, T., Farina, D., Klass, M., Duchateau, J., 2011. Unraveling the neurophysiology of muscle fatigue. J. Electromyogr. Kinesiol. 21, 208–219.
Erdemir, A., McLean, S., Herzog, W., van den Bogert, A.J., 2007. Model-based estimation of muscle forces exerted during movements. Clin. Biomech. 22, 131–154. https://doi.org/10.1016/j.clinbiomech.2006.09.005
Everett, T., Kell, C., 2010. Human Movement: An Introductory Text. Elsevier Health Sciences.
Fager, P.J., von Wowern, P., 2004. The use of haptics in medical applications. Int. J. Med. Robot. 1, 36–42.
Farina, D., Holobar, A., Merletti, R., Enoka, R.M., 2010. Decoding the neural drive to muscles from the surface electromyogram. Clin. Neurophysiol. Off. J. Int. Fed. Clin. Neurophysiol. 121, 1616–1623. https://doi.org/10.1016/j.clinph.2009.10.040
Farina, D., Madeleine, P., Graven-Nielsen, T., Merletti, R., Arendt-Nielsen, L., 2002. Standardising surface electromyogram recordings for assessment of activity and fatigue in the human upper trapezius muscle. Eur. J. Appl. Physiol. 86, 469–478. https://doi.org/10.1007/s00421-001-0574-0
Faust, R.A., 2007. Robotics in Surgery: History, Current And Future Applications. Nova Publishers.
Finneran, A., O'Sullivan, L., 2013. Effects of grip type and wrist posture on forearm EMG activity, endurance time and movement accuracy. Int. J. Ind. Ergon. 43, 91–99. https://doi.org/10.1016/j.ergon.2012.11.012

Freivalds, A., 2004. Biomechanics of the upper limbs: mechanics, modeling, and musculoskeletal injuries. CRC Press, Boca Raton, FL.
Fuchs, S., Frisse, D., Tibesku, C.O., Laass, H., Rosenbaum, D., 2002. Proprioceptive function, clinical results, and quality of life after unicondylar sledge prostheses. Am. J. Phys. Med. Rehabil. Assoc. Acad. Physiatr. 81, 478–482.
Fuchs, S., Tibesku, C.O., Frisse, D., Genkinger, M., Laaß, H., Rosenbaum, D., 2004. Clinical and functional comparison of uni- and bicondylar sledge prostheses. Knee Surg. Sports Traumatol. Arthrosc. 13, 197–202. https://doi.org/10.1007/s00167-004-0580-y
Functional position of the hand | definition of functional position of the hand by Medical dictionary [WWW Document], 2009. URL http://medical-dictionary.thefreedictionary.com/functional+position+of+the+hand (accessed 8.27.16).
Gamage, S.S., Lasenby, J., 2002. New least squares solutions for estimating the average centre of rotation and the axis of rotation. J. Biomech. 35, 87–93.
Gazzoni, M., 2010. Multichannel surface electromyography in ergonomics: Potentialities and limits. Hum. Factors Ergon. Manuf. Serv. Ind. 20, 255–271. https://doi.org/10.1002/hfm.20219
Gilbertson, L., Barber-Lomax, S., 1994. Power and Pinch Grip Strength Recorded Using the Hand-Held Jamar® Dynamometer and B+L Hydraulic Pinch Gauge: British Normative Data for Adults. Br. J. Occup. Ther. 57, 483–488. https://doi.org/10.1177/030802269405701209
Gnaneswaran, V., 2010. Evaluation of Periodontal Scaling Task and Development of Force-Endurance Models for Simulated Scaling Task.
Gnaneswaran, V., Jones, E., Bishu, R.R., 2013. Development of force-endurance models for simulated scaling task. Int. J. Ind. Ergon. 43, 31–39. https://doi.org/10.1016/j.ergon.2012.08.008
Gomes, P., 2012. Medical Robotics: Minimally Invasive Surgery. Elsevier.
Gomide, J.V.B., Flam, D.L., Araújo, A. de A., 2011. Recent improvements to OpenMoCap and its release to download and to development as free open source software, in: International Conference Cinema Art, Technology, Communication. pp. 1317–24.
Griffin, F.M., Insall, J.N., Scuderi, G.R., 2000. Accuracy of soft tissue balancing in total knee arthroplasty. J. Arthroplasty 15, 970–973. https://doi.org/10.1054/arth.2000.6503
Grood, E.S., Suntay, W.J., 1983. A joint coordinate system for the clinical description of three-dimensional motions: application to the knee. J. Biomech. Eng. 105, 136–144.
Groover, M.P., 2007. Work systems and the methods, measurement, and management of work. Pearson Prentice Hall, Upper Saddle River, NJ.
Guenzkofer, F., Engstler, F., Bubb, H., Bengler, K., 2011. Isometric elbow flexion and extension joint torque measurements considering biomechanical aspects, in: First International Symposium on Digital Human Modeling. Edition Hermès, pp. 14–15.
Gulati, A., Chau, R., Beard, D.J., Price, A.J., Gill, H.S., Murray, D.W., 2009. Localization of the full-thickness cartilage lesions in medial and lateral unicompartmental knee osteoarthritis. J. Orthop. Res. 27, 1339–1346. https://doi.org/10.1002/jor.20880
Gunal, I., KÖSE, N., Erdogan, O., GÖKTÜRK, E., Seber, S., 1996. Normal Range of Motion of the Joints of the Upper Extremity in Male Subjects, with Special Reference to Side*. J. Bone Jt. Surg. 78, 1401–4.
Hagag, B., Abovitz, R., Kang, H., Schmitz, B., Conditt, M., 2011. RIO: Robotic-Arm Interactive Orthopedic System MAKOplasty: User Interactive Haptic Orthopedic Robotics, in: Surgical Robotics. Springer, Boston, MA, pp. 219–246. https://doi.org/10.1007/978-1-4419-1126-1_10
Hagag, B., Abovitz, R., Kang, H., Schmitz, B., Conditt, M., 2010. RIO: Robotic-Arm Interactive Orthopedic System MAKOplasty: User Interactive Haptic Orthopedic Robotics. Surg. Robot. Syst. Appl. Vis. 219.
Hallbeck, M.S., McMullin, D.L., 1993. Maximal power grasp and three-jaw chuck pinch force as a function of wrist position, age, and glove type. Int. J. Ind. Ergon. 11, 195–206. https://doi.org/10.1016/0169-8141(93)90108-P

Halvorsen, K., 2003. Bias compensated least squares estimate of the center of rotation. J. Biomech. 36, 999–1008. https://doi.org/10.1016/S0021-9290(03)00070-8
Halvorsen, K., Lesser, M., Lundberg, A., 1999. A new method for estimating the axis of rotation and the center of rotation. J. Biomech. 32, 1221–1227.
Hansen, A., Hallbeck, S., 1996. Effects of Interdigital Spacing, Wrist Position, Forearm Position, Grip Span, and Gender on Static Grip Strength. Proc. Hum. Factors Ergon. Soc. Annu. Meet. 40, 712–716. https://doi.org/10.1177/154193129604001328
Hart, S.G., Staveland, L.E., 2005. Results of empirical and theoretical research. Ergon. Ski. Disp. Controls Ment. Workload 2, 408.
Hazelton, F.T., Smidt, G.L., Flatt, A.E., Stephens, R.I., 1975. The influence of wrist position on the force produced by the finger flexors. J. Biomech. 8, 301–306. https://doi.org/10.1016/0021-9290(75)90082-2
Heest, A.E.V., Agel, J., 2012. The Uneven Distribution of Women in Orthopaedic Surgery Resident Training Programs in the United States. J. Bone Jt. Surg. 94, e9. https://doi.org/10.2106/JBJS.J.01583
Herfarth, C., 2003. Lean surgery through changes in surgical work flow. Br. J. Surg. 90, 513–514. https://doi.org/10.1002/bjs.4165
Hill, A.V., 1938. The Heat of Shortening and the Dynamic Constants of Muscle. Proc. R. Soc. Lond. B Biol. Sci. 126, 136–195. https://doi.org/10.1098/rspb.1938.0050
Hincapié-Ramos, J.D., Guo, X., Moghadasian, P., Irani, P., 2014. Consumed endurance: a metric to quantify arm fatigue of mid-air interactions. ACM Press, pp. 1063–1072. https://doi.org/10.1145/2556288.2557130
Hingtgen, B., McGuire, J.R., Wang, M., Harris, G.F., 2006. An upper extremity kinematic model for evaluation of hemiparetic stroke. J. Biomech. 39, 681–688. https://doi.org/10.1016/j.jbiomech.2005.01.008
Hiniduma Udugama Gamage, S.S., Lasenby, J., 2001. A new least squares solution for estimation of centre and axis of rotation [WWW Document]. URL http://publications.eng.cam.ac.uk/328865/ (accessed 7.10.14).
Hodges, P.W., Bui, B.H., 1996. A comparison of computer-based methods for the determination of onset of muscle contraction using electromyography. Electroencephalogr. Clin. Neurophysiol. Mot. Control 101, 511–519. https://doi.org/10.1016/S0921-884X(96)95190-5
Hof, A.L., 1991. Errors in frequency parameters of EMG power spectra. IEEE Trans. Biomed. Eng. 38, 1077–1088. https://doi.org/10.1109/10.99071
Holewijn, M., Heus, R., 1992. Effects of temperature on electromyogram and muscle function. Eur. J. Appl. Physiol. 65, 541–545.
Hong Han, S.-, Shik Nam, K.-, -Suk Cho, Y., 2011. Normative Data on Hand Grip Strength. J. Nov. Physiother. 01. https://doi.org/10.4172/2165-7025.1000102
Honl, M., Dierk, O., Gauck, C., Carrero, V., Lampe, F., Dries, S., Quante, M., Schwieger, K., Hille, E., Morlock, M.M., 2003. Comparison of robotic-assisted and manual implantation of a primary total hip replacement. A prospective study. J. Bone Joint Surg. Am. 85-A, 1470–1478.
Hopper, A.N., Jamison, M.H., Lewis, W.G., 2007. Learning curves in surgical practice. Postgrad. Med. J. 83, 777–779. https://doi.org/10.1136/pgmj.2007.057190
Horejsi, P., 2013. USING KINECT TECHNOLOGY EQUIPMENT FOR ERGONOMICS [WWW Document]. URL http://connection.ebscohost.com/c/articles/86234514/using-kinect-technology-equipment-ergonomics (accessed 3.22.15).
Hsia, P.T., Drury, C.G., 1986. A simple method of evaluating handle design. Appl. Ergon. 17, 209–213. https://doi.org/10.1016/0003-6870(86)90008-6
Huang, N.F.R., Dowsey, M.M., Ee, E., Stoney, J.D., Babazadeh, S., Choong, P.F., 2012. Coronal Alignment Correlates With Outcome After Total Knee Arthroplasty: Five-Year Follow-Up of a Randomized Controlled Trial. J. Arthroplasty 27, 1737–1741. https://doi.org/10.1016/j.arth.2012.03.058

Hubert, N., Gilles, M., Desbrosses, K., Meyer, J., Felblinger, J., Hubert, J., 2013. Ergonomic assessment of the surgeon's physical workload during standard and robotic assisted laparoscopic procedures. Int. J. Med. Robot. 9, 142–147. https://doi.org/10.1002/rcs.1489
Imbeau, D., Farbos, B., 2006. Percentile values for determining maximum endurance times for static muscular work. Int. J. Ind. Ergon. 36, 99–108.
James, J.I., 1962. Fractures of the proximal and middle phalanges of the fingers. Acta Orthop. Scand. 32, 401–412.
Janson, R., 2007. Openability of Vacuum Lug Closures (Ph.D.). The University of Sheffield.
Jimmerson, C., Weber, D., Sobek, D.K., 2005. Reducing Waste and Errors: Piloting Lean Principles at Intermountain Healthcare. Jt. Comm. J. Qual. Patient Saf. 31, 249–257.
Jinnah, R.H., 2013. Achieving Accurate Ligament Balancing Using Robotic-Assisted Unicompartmental Knee Arthroplasty. Adv. Orthop. 2013.
Jinnah, R.H., 2009. The learning curve of robotic-assisted UKA, in: Proceedings of Knee Arthroplasty: From Early Intervention to Revision. Presented at the Institute of Mechanical Engineers, Knee Arthroplasty From Early Intervention to Revision, Royal College of Surgeons, London.
Kahol, K., Leyba, M.J., Deka, M., Deka, V., Mayes, S., Smith, M., Ferrara, J.J., Panchanathan, S., 2008. Effect of fatigue on psychomotor and cognitive skills. Am. J. Surg. 195, 195–204.
Kam, P.C.A., 2005. Uses and precautions of tourniquets. Surg. Oxf. 23, 76–77.
Kamen, G., Gabriel, D.A., 2010. Essentials of electromyography. Human Kinetics, Champaign, IL.
Kattel, B.P., Fredericks, T.K., Fernandez, J.E., Lee, D.C., 1996. The effect of upper-extremity posture on maximum grip strength. Int. J. Ind. Ergon. 18, 423–429. https://doi.org/10.1016/0169-8141(95)00105-0
Kazanzides, P., FICHTINGER, G., HAGER, G.D., OKAMURA, A.M., WHITCOMB, L.L., TAYLOR, R.H., 2008. Surgical and Interventional Robotics. IEEE Robot. Autom. Mag. IEEE Robot. Autom. Soc. 15, 122–130. https://doi.org/10.1109/MRA.2008.926390
Kim, Y.-H., Park, J.-W., Kim, J.-S., 2012. Computer-Navigated Versus Conventional Total Knee Arthroplasty. J. Bone Jt. Surg. 94, 2017–2024. https://doi.org/10.2106/JBJS.L.00142
Knudsen, M.L., Ludewig, P.M., Braman, J.P., 2014. Musculoskeletal Pain in Resident Orthopaedic Surgeons: Results of a Novel Survey. Iowa Orthop. J. 34, 190–196.
Kong, Y.-K., Lowe, B.D., 2005. Optimal cylindrical handle diameter for grip force tasks. Int. J. Ind. Ergon. 35, 495–507. https://doi.org/10.1016/j.ergon.2004.11.003
Konrad, P., 2005. The abc of emg. Pract. Introd. Kinesiol. Electromyogr. 1.
Kowalewski, T.M., 2012. Real-time Quantitative Assessment of Surgical Skill (Thesis).
Kozinn, S.C., Scott, R., 1989. Unicondylar knee arthroplasty. J. Bone Jt. Surg. 71, 145–150.
Kumar, S., 2004. Muscle Strength. CRC Press, Boca Raton.
Kumar, S., 2003. Advances In Industrial Ergonomics And Safety IV. CRC Press.
Kumar, S., Amell, T., Narayan, Y., Prasad, N., 2002. Indices of Muscle Fatigue. Proc. Hum. Factors Ergon. Soc. Annu. Meet. 46, 1095–1099. https://doi.org/10.1177/154193120204601319
Kuorinka, I., Jonsson, B., Kilbom, A., Vinterberg, H., Biering-Sørensen, F., Andersson, G., Jørgensen, K., 1987. Standardised Nordic questionnaires for the analysis of musculoskeletal symptoms. Appl. Ergon. 18, 233–237.
Kurtz, S., Ong, K., Lau, E., Mowat, F., Halpern, M., 2007. Projections of primary and revision hip and knee arthroplasty in the United States from 2005 to 2030. J. Bone Joint Surg. Am. 89, 780–785. https://doi.org/10.2106/JBJS.F.00222
La Delfa, N.J., Langstaff, N.M., Hodder, J.N., Potvin, J.R., 2015. The interacting effects of forearm rotation and exertion direction on male and female wrist strength. Int. J. Ind. Ergon. 45, 124–128. https://doi.org/10.1016/j.ergon.2014.12.012
Lamoreaux, L., Hoffer, M.M., 1995. The effect of wrist deviation on grip and pinch strength. Clin. Orthop. 152–155.

Lannin, N.A., Horsley, S.A., Herbert, R., McCluskey, A., Cusick, A., 2003. Splinting the hand in the functional position after brain impairment: A randomized, controlled trial. Arch. Phys. Med. Rehabil. 84, 297–302. https://doi.org/10.1053/apmr.2003.50031

Larsen, S.T., Ryd, L., 1989. Temperature elevation during knee arthroplasty. Acta Orthop. Scand. 60, 439–442.

LaStayo, P., Chidgey, L., Miller, G., 1995. Quantification of the relationship between dynamic grip strength and forearm rotation: a preliminary study. Ann. Plast. Surg. 35, 191–196.

Law, L.A.F., Avin, K.G., 2010. Endurance time is joint-specific: A modelling and meta-analysis investigation. Ergonomics 53, 109–129. https://doi.org/10.1080/00140130903389068

Lawson, E.H., Curet, M.J., Sanchez, B.R., Schuster, R., Berguer, R., 2007. Postural ergonomics during robotic and laparoscopic gastric bypass surgery: a pilot project. J. Robot. Surg. 1, 61–67. https://doi.org/10.1007/s11701-007-0016-z

Lee, J., Rabin, Y., Ozdoganlar, O.B., 2011. A new thermal model for bone drilling with applications to orthopaedic surgery. Med. Eng. Phys. 33, 1234–1244. https://doi.org/10.1016/j.medengphy.2011.05.014

Lee, K.-S., Jung, M.-C., 2014. Flexion and extension angles of resting fingers and wrist. Int. J. Occup. Saf. Ergon. 20, 91–101.

Lee, S.-W., Zhang, X., 2005. Development and evaluation of an optimization-based model for power-grip posture prediction. J. Biomech. 38, 1591–1597. https://doi.org/10.1016/j.jbiomech.2004.07.024

Lempereur, M., Leboeuf, F., Brochard, S., Rousset, J., Burdin, V., Rémy-Néris, O., 2010. In vivo estimation of the glenohumeral joint centre by functional methods: accuracy and repeatability assessment. J. Biomech. 43, 370–374. https://doi.org/10.1016/j.jbiomech.2009.09.029

Li, K.W., Yu, R., 2011. Assessment of grip force and subjective hand force exertion under handedness and postural conditions. Appl. Ergon. 42, 929–933. https://doi.org/10.1016/j.apergo.2011.03.001

Liang, C.A., Levine, V.J., Dusza, S.W., Hale, E.K., Nehal, K.S., 2012. Musculoskeletal disorders and ergonomics in dermatologic surgery: a survey of Mohs surgeons in 2010. Dermatol. Surg. Off. Publ. Am. Soc. Dermatol. Surg. Al 38, 240–248. https://doi.org/10.1111/j.1524-4725.2011.02237.x

Lin, M.I., Liang, H.W., Lin, K.H., Hwang, Y.H., 2004. Electromyographical assessment on muscular fatigue—an elaboration upon repetitive typing activity. J. Electromyogr. Kinesiol. 14, 661–669.

Lindstrom, L., Kadefors, R., Petersen, I., 1977. An electromyographic index for localized muscle fatigue. J. Appl. Physiol. 43, 750–754.

Lloyd, D.G., Besier, T.F., 2003. An EMG-driven musculoskeletal model to estimate muscle forces and knee joint moments in vivo. J. Biomech. 36, 765–776. https://doi.org/10.1016/S0021-9290(03)00010-1

Lobo Prat, J., 2011. A new kinematic and dynamic model for clinical evaluation of the upper extremity motion during an activity of daily living in subjects with neurological disorders.

Lonner, J.H., John, T.K., Conditt, M.A., 2009. Robotic Arm-assisted UKA Improves Tibial Component Alignment: A Pilot Study. Clin. Orthop. Relat. Res. 468, 141–146. https://doi.org/10.1007/s11999-009-0977-5

Lopetegui, M., Yen, P.-Y., Lai, A.M., Embi, P.J., Payne, P.R.O., 2012. Time Capture Tool (TimeCaT): Development of a Comprehensive Application to Support Data Capture for Time Motion Studies. AMIA. Annu. Symp. Proc. 2012, 596–605.

Luca, C.J.D., 1979. Physiology and Mathematics of Myoelectric Signals. IEEE Trans. Biomed. Eng. BME-26, 313–325. https://doi.org/10.1109/TBME.1979.326534

Lui, D.F., BAkER, J.F., Nfila, G., Perera, A., Stephens, M., 2012. Hand dominance in orthopaedic surgeons. Acta Orthop. Belg. 78, 531.

Luo, C.-F., 2004. Reference axes for reconstruction of the knee. The Knee 11, 251–257. https://doi.org/10.1016/j.knee.2004.03.003
Luttmann, A., Jäger, M., Laurig, W., 2000. Electromyographical indication of muscular fatigue in occupational field studies. Int. J. Ind. Ergon. 25, 645–660.
Luttmann, A., Jäger, M., Sökeland, J., Laurig, W., 1996a. Electromyographical study on surgeons in urology. II. Determination of muscular fatigue. Ergonomics 39, 298–313. https://doi.org/10.1080/00140139608964460
Luttmann, A., Sökeland, J., Laurig, W., 1996b. Electromyographical study on surgeons in urology. I. Influence of the operating technique on muscular strain. Ergonomics 39, 285–297. https://doi.org/10.1080/00140139608964459
MacIsaac, D., Parker, P.A., Scott, R.N., 2001. The short-time Fourier transform and muscle fatigue assessment in dynamic contractions. J. Electromyogr. Kinesiol. 11, 439–449. https://doi.org/10.1016/S1050-6411(01)00021-9
Mackey, A.H., Walt, S.E., Lobb, G.A., Stott, N.S., 2005. Reliability of upper and lower limb three-dimensional kinematics in children with hemiplegia. Gait Posture 22, 1–9. https://doi.org/10.1016/j.gaitpost.2004.06.002
MacIsaac, D.T., Parker, P.A., Scott, R.N., Englehart, K.B., Duffley, C., 2001. Influences of dynamic factors on myoelectric parameters. IEEE Eng. Med. Biol. Mag. 20, 82–89. https://doi.org/10.1109/51.982279
Magee, D.J., 2008. Orthopedic Physical Assessment. Elsevier Health Sciences.
MAKO Surgical, M., 2009. RESTORIS MCK Planning and Surgical Technique Guide.
MAKO Surgical Sues Blue Belt Technologies, 2014. . Robot. Bus. Rev.
Manal, K., Gonzalez, R.V., Lloyd, D.G., Buchanan, T.S., 2002. A real-time EMG-driven virtual arm. Comput. Biol. Med. 32, 25–36. https://doi.org/10.1016/S0010-4825(01)00024-5
Mannava, M.D., Lorentzen, C.M., Smith, B.P., 2012. Unicompartmental Knee Arthroplasty: Past, Present, Future.
Marina, M., Porta, J., Vallejo, L., Angulo, R., 2011. Monitoring hand flexor fatigue in a 24-h motorcycle endurance race. J. Electromyogr. Kinesiol. 21, 255–261. https://doi.org/10.1016/j.jelekin.2010.11.008
Markolf, K.L., Slauterbeck, J.R., Armstrong, K.L., Shapiro, M.S., Finerman, G. a. M., 1997. A Biomechanical Study of Replacement of the Posterior Cruciate Ligament with a Graft. Part I: Isometry, Pre-Tension of the Graft, and Anterior-Posterior Laxity*. J Bone Jt. Surg Am 79, 375–80.
Marshall, M.M., Mozrall, J.R., Shealy, J.E., 1999. The Effects of Complex Wrist and Forearm Posture on Wrist Range of Motion. Hum. Factors J. Hum. Factors Ergon. Soc. 41, 205–213. https://doi.org/10.1518/001872099779591178
Martini, F.H., Nath, J.L., Bartholomew, E.F., 2011. Fundamentals of Anatomy & Physiology, 9th edition. ed. Benjamin Cummings, San Francisco.
Mathiowetz, V., 2002. Comparison of Rolyan and Jamar dynamometers for measuring grip strength. Occup. Ther. Int. 9, 201–209. https://doi.org/10.1002/oti.165
Matthijsse, P., Hendrich, K., Rijnsburger, W., Woittiez, R., Huijing, P., 1987. Ankle Angle Effects on Endurance Time, Median Frequency and Mean Power. Ergonomics 30, 1149–1159. https://doi.org/10.1080/00140138708966004
McGeoch, K.L., Gilmour, W.H., 2000. Cross sectional study of a workforce exposed to hand-arm vibration: with objective tests and the Stockholm workshop scales. Occup. Environ. Med. 57, 35–42.
McGorry, R.W., Fallentin, N., Andersen, J.H., Keir, P.J., Hansen, T.B., Pransky, G., Lin, J.-H., 2014. Effect of Grip Type, Wrist Motion, and Resistance Level on Pressures within the Carpal Tunnel of Normal Wrists. J. Orthop. Res. 32, 524–530. https://doi.org/10.1002/jor.22571
Meijer, D.W., Bannenberg, J.J.G., Jakimowicz, J.J., 2000. Hand-assisted laparoscopic surgery. Surg. Endosc. 14, 891–895. https://doi.org/10.1007/s004640020019

Merletti, R., Di Torino, P., 1999. Standards for reporting EMG data. J Electromyogr Kinesiol 9, 3–4.
Merletti, R., Knaflitz, M., De Luca, C.J., 1990. Myoelectric manifestations of fatigue in voluntary and electrically elicited contractions. J. Appl. Physiol. 69, 1810–1820.
Merletti, R., Lo Conte, L.R., 1995. Advances in processing of surface myoelectric signals: Part 1. Med. Biol. Eng. Comput. 33, 362–372.
Merletti, R., Lo Conte, L.R., Orizio, C., 1991. Indices of muscle fatigue. J. Electromyogr. Kinesiol. 1, 20–33. https://doi.org/10.1016/1050-6411(91)90023-X
Merletti, R., Parker, P., 2004. Electromyography physiology, engineering, and noninvasive applications. IEEE Press ; Wiley-Interscience, Piscataway, NJ; Hoboken, N.J.
Middleton, F.R., Palmer, S.H., 2007. How accurate is Whiteside's line as a reference axis in total knee arthroplasty? The Knee 14, 204–207. https://doi.org/10.1016/j.knee.2007.02.002
Minekus, J.P.J., Rozing, P.M., Valstar, E.R., Dankelman, J., 2003. Evaluation of humeral head replacements using time-action analysis. J. Shoulder Elbow Surg. 12, 152–157. https://doi.org/10.1067/mse.2003.14
Mirka, G.A., Shivers, C., Smith, C., Taylor, J., 2002. Ergonomic interventions for the furniture manufacturing industry. Part II—Handtools. Int. J. Ind. Ergon. 29, 275–287.
Moeslund, T.B., Granum, E., 2001. A Survey of Computer Vision-Based Human Motion Capture. Comput. Vis. Image Underst. 81, 231–268. https://doi.org/10.1006/cviu.2000.0897
Mofidi, A., Lou, B., Conditt, M., Poehling, G., Jinnah, R., 2012. Assessment of Accuracy of Robotic Assisted Unicompartemental Arthroplasty (Makoplasty). J. Bone Joint Surg. Br. 94, 150–150.
Mohammad Mirbod, S., Yoshida, H., Miyamoto, K., Miyashita, K., Inaba, R., Iwata, H., 1995. Subjective complaints in orthopedists and general surgeons. Int. Arch. Occup. Environ. Health 67, 179–186.
Moritani, T., Muro, M., 1987. Motor unit activity and surface electromyogram power spectrum during increasing force of contraction. Eur. J. Appl. Physiol. 56, 260–265.
Moritani, T., Muro, M., Nagata, A., 1986. Intramuscular and surface electromyogram changes during muscle fatigue. J. Appl. Physiol. 60, 1179–1185.
Morse, J.L., Jung, M.-C., Bashford, G.R., Hallbeck, M.S., 2006. Maximal dynamic grip force and wrist torque: The effects of gender, exertion direction, angular velocity, and wrist angle. Appl. Ergon. 37, 737–742. https://doi.org/10.1016/j.apergo.2005.11.008
Motesharei, A., Rowe, P., Blyth, M., Jones, B., MacLean, A., Anthony, I., 2014. Kinematic Walking Assessment Comparing Robotic-Assisted and Conventional Unicompartmental Knee Arthroplasty. Bone Jt. J. Orthop. Proc. Suppl. 96-B, 32–32.
Motesharei, Arman, Rowe, P., Blyth, M., Jones, B., MacLean, A., Anthony, I., 2014. Kinematic walking assessment to compare robotic assisted and conventional unicompartmental knee arthroplasty. Gait Posture 39, S89.
Murgia, A., Kyberd, P.J., Chappell, P.H., Light, C.M., 2004. Marker placement to describe the wrist movements during activities of daily living in cyclical tasks. Clin. Biomech. 19, 248–254. https://doi.org/10.1016/j.clinbiomech.2003.11.012
Napier, J.R., 1956. The Prehensile Movements of the Human Hand. J. Bone Joint Surg. Br. 38-B, 902–913.
National Joint Registry for England and Wales 12th Annual Report 2015, 2015. National Joint Registry for England and Wales 12th Annual Report 2015.
Necking, L.E., Lundborg, G., Fridén, J., 2002. Hand Muscle Weakness in Long-Term Vibration Exposure. J. Hand Surg. Br. Eur. Vol. 27, 520–525. https://doi.org/10.1054/jhsb.2002.0810
Neumuth, T., Loebe, F., Jannin, P., 2012. Similarity metrics for surgical process models. Artif. Intell. Med. 54, 15–27. https://doi.org/10.1016/j.artmed.2011.10.001
Newman, J., Pydisetty, R.V., Ackroyd, C., 2009. Unicompartmental or total knee replacement THE 15-YEAR RESULTS OF A PROSPECTIVE RANDOMISED CONTROLLED TRIAL. J. Bone Joint Surg. Br. 91-B, 52–57. https://doi.org/10.1302/0301-620X.91B1.20899

Nordin, M., H. Frankel, V., 2012. Basic Biomechanics of the Musculoskeletal System, Fourth, North American Edition edition. ed. LWW, Philadelphia.
Novotny, J.E., Beynnon, B.D., Nichols III, C.E., 2001. A numerical solution to calculate internal–external rotation at the glenohumeral joint. Clin. Biomech. 16, 395–400. https://doi.org/10.1016/S0268-0033(01)00018-3
Oberg, T., Sandsjö, L., Kadefors, R., 1994. Subjective and objective evaluation of shoulder muscle fatigue. Ergonomics 37, 1323–1333. https://doi.org/10.1080/00140139408964911
O'Connor, P., Ryan, S., Keogh, I., 2012. A comparison of the teamwork attitudes and knowledge of Irish surgeons and U.S Naval aviators. The Surgeon 10, 278–282. https://doi.org/10.1016/j.surge.2011.09.001
O'Driscoll, S.W., Horii, E., Ness, R., Cahalan, T.D., Richards, R.R., An, K.N., 1992. The relationship between wrist position, grasp size, and grip strength. J. Hand Surg. 17, 169–177.
Okamura, A.M., 2009. Haptic feedback in robot-assisted minimally invasive surgery. Curr. Opin. Urol. 19, 102.
Oldenrijk, J. van, Schafroth, M.U., Bhandari, M., Runne, W.C., Poolman, R.W., 2008. Time-Action Analysis (TAA) of the Surgical Technique Implanting the Collum Femoris Preserving (CFP) Hip Arthroplasty. TAASTIC trial Identifying pitfalls during the learning curve of surgeons participating in a subsequent randomized controlled trial (An observational study). BMC Musculoskelet. Disord. 9, 93. https://doi.org/10.1186/1471-2474-9-93
Orthopaedic Surgeon Census - AAOS [WWW Document], 2004. URL http://www.aaos.org/research/orthocensus/Census.asp (accessed 11.12.14).
O'Sullivan, L.W., Gallwey, T.J., 2002. Upperlimb EMG and Discomfort for Forearm Torques Combined with Horizontal Forces, in: Proceedings of the Human Factors and Ergonomics Society Annual Meeting. SAGE Publications, pp. 1046–1050.
Padoy, N., Blum, T., Essa, I., Feussner, H., Berger, M.-O., Navab, N., 2007. A Boosted Segmentation Method for Surgical Workflow Analysis, in: Ayache, N., Ourselin, S., Maeder, A. (Eds.), Medical Image Computing and Computer-Assisted Intervention – MICCAI 2007. Springer Berlin Heidelberg, Berlin, Heidelberg, pp. 102–109.
Palmer, A.K., Werner, F.W., Murphy, D., Glisson, R., 1985. Functional wrist motion: A biomechanical study. J. Hand Surg. 10, 39–46. https://doi.org/10.1016/S0363-5023(85)80246-X
Pancherz, H., Winnberg, A., Westesson, P.-L., 1986. Masticatory muscle activity and hyoid bone behavior during cyclic jaw movements in man. Am. J. Orthod. 89, 122–131. https://doi.org/10.1016/0002-9416(86)90088-6
Parvatikar, V.B., Mukkannavar, P.B., others, 2009. Comparative study of grip strength in different positions of shoulder and elbow with wrist in neutral and extension positions.
Pearl, M.L., Sidles, J.A., Lippitt, S.B., Harryman II, D.T., Matsen III, F.A., 1992. Codman's paradox: Sixty years later. J. Shoulder Elbow Surg. 1, 219–225. https://doi.org/10.1016/1058-2746(92)90017-W
Pearle, A.D., Kendoff, D., Stueber, V., Musahl, V., Repicci, J.A., 2009. Perioperative management of unicompartmental knee arthroplasty using the MAKO robotic arm system (MAKOplasty). Am. J. Orthop. 38, 16–19.
Pearle, A.D., O'Loughlin, P.F., Kendoff, D.O., 2010. Robot-Assisted Unicompartmental Knee Arthroplasty. J. Arthroplasty 25, 230–237. https://doi.org/10.1016/j.arth.2008.09.024
Pendleton, H.M., 2012. Pedretti's Occupational Therapy, 7th Edition - 9780323059121 [WWW Document]. URL https://evolve.elsevier.com/cs/product/9780323059121?role=student (accessed 8.27.16).
Perez, G.M., Buchholz, B.O., 2000. A Study of the use of a Wrist Splint to Prevent Wmsds at a Sprout Grower, in: Proceedings of the Human Factors and Ergonomics Society Annual Meeting. SAGE Publications, pp. 225–228.
Pérez-González, A., Vergara, M., Sancho-Bru, J.L., 2013. Stiffness map of the grasping contact areas of the human hand. J. Biomech. https://doi.org/10.1016/j.jbiomech.2013.08.005

Peskun, C., Walmsley, D., Waddell, J., Schemitsch, E., 2012. Effect of surgeon fatigue on hip and knee arthroplasty. Can. J. Surg. 55, 81.

Peters, M.J.H., van Nes, S.I., Vanhoutte, E.K., Bakkers, M., van Doorn, P.A., Merkies, I.S.J., Faber, C.G., on behalf of the PeriNomS Study group, 2011. Revised normative values for grip strength with the Jamar dynamometer. J. Peripher. Nerv. Syst. 16, 47–50. https://doi.org/10.1111/j.1529-8027.2011.00318.x

Petrofsky, J.S., Lind, A.R., 1980. The influence of temperature on the amplitude and frequency components of the EMG during brief and sustained isometric contractions. Eur. J. Appl. Physiol. 44, 189–200.

Pheasant, S., 1996. Bodyspace: Anthropometry, Ergonomics and the Design of Work, 2nd Revised edition. ed. Taylor & Francis Ltd.

Phinyomark, A., Thongpanja, S., Hu, H., Phukpattaranont, P., Limsakul, C., 2012. The Usefulness of Mean and Median Frequencies in Electromyography Analysis, in: Naik, G.R. (Ed.), Computational Intelligence in Electromyography Analysis - A Perspective on Current Applications and Future Challenges. InTech.

Plate, J.F., Mofidi, A., Mannava, S., Smith, B.P., Lang, J.E., Poehling, G.G., Conditt, M.A., Jinnah, R.H., 2013. Achieving Accurate Ligament Balancing Using Robotic-Assisted Unicompartmental Knee Arthroplasty. Adv. Orthop. 2013. https://doi.org/10.1155/2013/837167

Porter, M.E., 2010. What Is Value in Health Care? N. Engl. J. Med. 363, 2477–2481. https://doi.org/10.1056/NEJMp1011024

Pryce, J.C., 1980. The wrist position between neutral and ulnar deviation that facilitates the maximum power grip strength. J. Biomech. 13, 505–511. https://doi.org/10.1016/0021-9290(80)90343-7

Punnett, L., Wegman, D.H., 2004. Work-related musculoskeletal disorders: the epidemiologic evidence and the debate. J. Electromyogr. Kinesiol. 14, 13–23. https://doi.org/10.1016/j.jelekin.2003.09.015

Qin, J., Lin, J.-H., Faber, G.S., Buchholz, B., Xu, X., 2014. Upper extremity kinematic and kinetic adaptations during a fatiguing repetitive task. J. Electromyogr. Kinesiol. https://doi.org/10.1016/j.jelekin.2014.02.001

Rab, G., Petuskey, K., Bagley, A., 2002. A method for determination of upper extremity kinematics. Gait Posture 15, 113–119. https://doi.org/10.1016/S0966-6362(01)00155-2

RADWIN, R.G., ARMSTRONG, T.J., CHAFFIN, D.B., 1987. Power hand tool vibration effects on grip exertions. Ergonomics 30, 833–855. https://doi.org/10.1080/00140138708969772

Raez, M.B.I., Hussain, M.S., Mohd-Yasin, F., 2006. Techniques of EMG signal analysis: detection, processing, classification and applications. Biol. Proced. Online 8, 11–35. https://doi.org/10.1251/bpo115

Ramsay, C.R., Grant, A.M., Wallace, S.A., Garthwaite, P.H., Monk, A.F., Russell, I.T., 2000. Assessment of the learning curve in health technologies. Int. J. Technol. Assess. Health Care 16, 1095–1108.

Rau, G., Disselhorst-Klug, C., Schmidt, R., 2000. Movement biomechanics goes upwards: from the leg to the arm. J. Biomech. 33, 1207–1216. https://doi.org/10.1016/S0021-9290(00)00062-2

Repicci, J.A., 2003. Mini-invasive knee unicompartmental arthroplasty: bone-sparing technique. Surg. Technol. Int. 11, 282–286.

Richards, J.G., 1999. The measurement of human motion: A comparison of commercially available systems. Hum. Mov. Sci. 18, 589–602.

Rietjens, G.J.W.M., Kuipers, H., Adam, J.J., Saris, W.H.M., van Breda, E., van Hamont, D., Keizer, H.A., 2005. Physiological, biochemical and psychological markers of strenuous training-induced fatigue. Int. J. Sports Med. 26, 16–26. https://doi.org/10.1055/s-2004-817914

Ritacco, L.E., Milano, F.E., Chao, E. (Eds.), 2016. Computer-Assisted Musculoskeletal Surgery. Springer International Publishing, Cham.

Roberts, S.C., Harrild, K., Mollison, J., Murphy, E., Ashcroft, G.P., 2007. Comparison of sensorineural symptoms between UK orthopaedic surgeons and gynaecologists. Occup. Med. 57, 104–111. https://doi.org/10.1093/occmed/kql141
Robertson, D.G.E., 2004. Research Methods in Biomechanics. Human Kinetics.
Rogers, D.R., MacIsaac, D.T., 2013. A comparison of EMG-based muscle fatigue assessments during dynamic contractions. J. Electromyogr. Kinesiol. 23, 1004–1011. https://doi.org/10.1016/j.jelekin.2013.05.005
Ryu, J.Y., Cooney, W.P., Askew, L.J., An, K.N., Chao, E.Y., 1991. Functional ranges of motion of the wrist joint. J. Hand Surg. 16, 409–419.
Saddik, E., 2007. The Potential of Haptics Technologies. IEEE Instrum. Meas. Mag. 10, 10–17. https://doi.org/10.1109/MIM.2007.339540
Satava, R.M., Jones, S.B., 1998. Current and future applications of virtual reality for medicine. Proc. IEEE 86, 484–489. https://doi.org/10.1109/5.662873
Scheller, W.L., 1983. The Effect of Handle Shape on Grip Fatigue in Manual Lifting. Proc. Hum. Factors Ergon. Soc. Annu. Meet. 27, 417–421. https://doi.org/10.1177/154193128302700520
Schlüssel, M.M., dos Anjos, L.A., de Vasconcellos, M.T.L., Kac, G., 2008. Reference values of handgrip dynamometry of healthy adults: A population-based study. Clin. Nutr. 27, 601–607. https://doi.org/10.1016/j.clnu.2008.04.004
Schmidt, R., Disselhorst-Klug, C., Silny, J., Rau, G., 1999. A marker-based measurement procedure for unconstrained wrist and elbow motions. J. Biomech. 32, 615–621. https://doi.org/10.1016/S0021-9290(99)00036-6
Schott, J., Puttick, M., 1995. Handedness among surgeons. BMJ 310, 739. https://doi.org/10.1136/bmj.310.6981.739b
Sexton, J.B., Thomas, E.J., Helmreich, R.L., 2000. Error, stress, and teamwork in medicine and aviation: cross sectional surveys. BMJ 320, 745.
Shao, Q., Bassett, D.N., Manal, K., Buchanan, T.S., 2009. An EMG-driven model to estimate muscle forces and joint moments in stroke patients. Comput. Biol. Med. 39, 1083–1088. https://doi.org/10.1016/j.compbiomed.2009.09.002
Shih, R.H., Vasarhelyi, E.M., Dubrowski, A., Carnahan, H., 2001. The effects of latex gloves on the kinetics of grasping. Int. J. Ind. Ergon. 28, 265–273.
Shih, Y.-C., 2007. Glove and Gender Effects on Muscular Fatigue Evaluated by Endurance and Maximal Voluntary Contraction Measures. Hum. Factors J. Hum. Factors Ergon. Soc. 49, 110–119. https://doi.org/10.1518/001872007779598091
Shin, G., D'Souza, C., 2010. EMG activity of low back extensor muscles during cyclic flexion/extension. J. Electromyogr. Kinesiol. 20, 742–749. https://doi.org/10.1016/j.jelekin.2010.03.002
Silverstein, B.A., Fine, L.J., Armstrong, T.J., 1986. Hand wrist cumulative trauma disorders in industry. Br. J. Ind. Med. 43, 779–784.
Simons, M., Riches, P., 2014. The Learning Curve of Robotically-Assisted Unicondylar Knee Arthroplasty. Bone Jt. J. Orthop. Proc. Suppl. 96, 152–152.
Slack, P., Coulson, C., Ma, X., Webster, K., Proops, D., 2008. The Effect of Operating Time on Surgeons' Muscular Fatigue. Ann. R. Coll. Surg. Engl. 90, 651–657. https://doi.org/10.1308/003588408X321710
Slavens, B.A., Harris, G.F., 2008. The biomechanics of upper extremity kinematic and kinetic modeling: applications to rehabilitation engineering. Crit. Rev. Biomed. Eng. 36, 93–125.
Soueid, A., Oudit, D., Thiagarajah, S., Laitung, G., 2010. The pain of surgery: Pain experienced by surgeons while operating. Int. J. Surg. 8, 118–120. https://doi.org/10.1016/j.ijsu.2009.11.008
Sousa, A.S., Tavares, J.M.R., 2012. Surface electromyographic amplitude normalization methods: A review. Electromyogr. New Dev. Proced. Appl.

Strohbusch, S., 2010. MAKOPlasty Robotic Knee Surgery. Presented at the ADVANCES in ROBOTIC SURGERY.
Stulen, F.B., De Luca, C.J., 1981. Frequency Parameters of the Myoelectric Signal as a Measure of Muscle Conduction Velocity. IEEE Trans. Biomed. Eng. BME-28, 515–523. https://doi.org/10.1109/TBME.1981.324738
Sturm, L., Dawson, D., Vaughan, R., Hewett, P., Hill, A.G., Graham, J.C., Maddern, G.J., 2011. Effects of fatigue on surgeon performance and surgical outcomes: a systematic review. ANZ J. Surg. 81, 502–509.
Subramanian, P., Kantharuban, S., Subramanian, V., Willis-Owen, S.A.G., Willis-Owen, C.A., 2011. Orthopaedic surgeons: as strong as an ox and almost twice as clever? Multicentre prospective comparative study. BMJ 343, d7506–d7506. https://doi.org/10.1136/bmj.d7506
Sugama, R., Kadoya, Y., Kobayashi, A., Takaoka, K., 2005. Preparation of the Flexion Gap Affects the Extension Gap in Total Knee Arthroplasty. J. Arthroplasty 20, 602–607. https://doi.org/10.1016/j.arth.2003.12.085
Susta, D., O'Connell, D., 2009. WRIST POSITION AFFECTS HAND-GRIP STRENGTH IN TENNIS PLAYERS. ISBS - Conf. Proc. Arch. 1.
Szeto, G.P.Y., Ho, P., Ting, A.C.W., Poon, J.T.C., Cheng, S.W.K., Tsang, R.C.C., 2009. Work-related Musculoskeletal Symptoms in Surgeons. J. Occup. Rehabil. 19, 175–184. https://doi.org/10.1007/s10926-009-9176-1
Taelman, J., Adriaensen, T., Spaepen, A., Langereis, G.R., Gourmelon, L., Van Huffel, S., 2006. Contactless emg sensors for continuous monitoring of muscle activity to prevent musculoskeletal disorders, in: Proceedings of the First Annual Symposium of the IEEE-EMBS Benelux Chapter. pp. 223–226.
Task analysis, 1971. , Training information paper. H.M.S.O, London.
Taylor, F.W., 1911. The principles of scientific management. Harper & Brothers, New York, London.
Terrell, R., Purswell, J.L., 1976. The influence of forearm and wrist orientation on static grip strength as a design criterion for hand tools, in: Proceedings of the Human Factors and Ergonomics Society Annual Meeting. pp. 28–32.
Thewlis, D., Bishop, C., Daniell, N., Paul, G., 2013. Next generation low-cost motion capture systems can provide comparable spatial accuracy to high-end systems. J. Appl. Biomech. 29, 112–117.
Thewlis, D., Bishop, C., Daniell, N., Paul, G., 2011. A comparison of two commercially available motion capture systems for gait analysis: high end vs low-cost.
Tian, R., Duffy, V.G., McGinley, J., 2007. Effecting Validity of Ergonomics Analysis During Virtual Interactive Design, in: Duffy, V.G. (Ed.), Digital Human Modeling, Lecture Notes in Computer Science. Springer Berlin Heidelberg, pp. 988–997.
van der Helm, F.C., 1997. A standardized protocol for motion recordings of the shoulder, in: First Conference of the International Shoulder Group. pp. 7–12.
van der List, J.P., Chawla, H., Pearle, A.D., 2016. Robotic-assisted knee arthroplasty: an overview. Am J Orthop 45, 202.
VICON, 2017. Nexus Motion Capture Software [WWW Document]. VICON. URL http://www.vicon.com/products/software/nexus (accessed 8.1.17).
Viitasalo, J.H., Komi, P.V., 1977. Signal characteristics of EMG during fatigue. Eur. J. Appl. Physiol. 37, 111–121.
Vøllestad, N.K., 1997. Measurement of human muscle fatigue. J. Neurosci. Methods 74, 219–227.
Walker, P.S., Yildirim, G., Arno, S., Heller, Y., 2010. Future directions in knee replacement. Proc. Inst. Mech. Eng. [H] 224, 393–414. https://doi.org/10.1243/09544119JEIM655
Weinbroum, A.A., Ekstein, P., Ezri, T., 2003. Efficiency of the operating room suite. Am. J. Surg. 185, 244–250. https://doi.org/10.1016/S0002-9610(02)01362-4
Weinstock, D., 2008. Lean healthcare. J Med Pr. Manage 23, 339–41.

Whiteside, L.A., 2005. Making Your Next Unicompartmental Knee Arthroplasty Last: Three Keys to Success. J. Arthroplasty 20, 2–3. https://doi.org/10.1016/j.arth.2005.03.029
Williams, S., Schmidt, R., Disselhorst-Klug, C., Rau, G., 2006. An upper body model for the kinematical analysis of the joint chain of the human arm. J. Biomech. 39, 2419–2429. https://doi.org/10.1016/j.jbiomech.2005.07.023
Willms, K., Wells, R., Carnahan, H., 2009. Glove attributes and their contribution to force decrement and increased effort in power grip. Hum. Factors J. Hum. Factors Ergon. Soc. 51, 797–812.
Wolf, A., Jaramaz, B., Lisien, B., DiGioia, A.M., 2005. MBARS: mini bone-attached robotic system for joint arthroplasty. Int. J. Med. Robot. Comput. Assist. Surg. MRCAS 1, 101–121. https://doi.org/10.1002/rcs.20
Woltring, H.J., 1991. Representation and calculation of 3-D joint movement. Hum. Mov. Sci. 10, 603–616. https://doi.org/10.1016/0167-9457(91)90048-3
Wu, G., van der Helm, F.C.T., (DirkJan) Veeger, H.E.J., Makhsous, M., Van Roy, P., Anglin, C., Nagels, J., Karduna, A.R., McQuade, K., Wang, X., Werner, F.W., Buchholz, B., 2005. ISB recommendation on definitions of joint coordinate systems of various joints for the reporting of human joint motion—Part II: shoulder, elbow, wrist and hand. J. Biomech. 38, 981–992. https://doi.org/10.1016/j.jbiomech.2004.05.042
Wu, T., Tian, R., Duffy, V.G., 2012. Performing ergonomics analyses through virtual interactive design: Validity and reliability assessment. Hum. Factors Ergon. Manuf. Serv. Ind. 22, 256–268. https://doi.org/10.1002/hfm.20267
Yim, J.-H., Song, E.-K., Khan, M.S., Sun, Z.H., Seon, J.-K., 2013. A comparison of classical and anatomical total knee alignment methods in robotic total knee arthroplasty: classical and anatomical knee alignment methods in TKA. J. Arthroplasty 28, 932–937. https://doi.org/10.1016/j.arth.2013.01.013
Youm, Y., McMurthy, R.Y., Flatt, A.E., Gillespie, T.E., 1978. Kinematics of the wrist. I. An experimental study of radial-ulnar deviation and flexion-extension. J. Bone Joint Surg. Am. 60, 423–431.
Youn, W., Kim, J., 2009. Development of a compact-size and wireless surface EMG measurement system, in: ICCAS-SICE, 2009. Presented at the ICCAS-SICE, 2009, pp. 1625–1628.
Zatsiorsky, V.M., 1998a. Kinematics of Human Motion. Human Kinetics.
Zatsiorsky, V.M., 1998b. Kinematics of Human Motion. Human Kinetics.
Zhou, H., Hu, H., 2008. Human motion tracking for rehabilitation—A survey. Biomed. Signal Process. Control 3, 1–18. https://doi.org/10.1016/j.bspc.2007.09.001

Appendix Contents

Appendix 1 Time Analysis actions tables

The following table is a detail of the action number, description and start stop definitions used in the time analysis of the MAKOplasty surgery.

Order position	Section	Action	Description of Stage Start	Description of stage stop
	1	Set up		
	2	Patient in		
1	3	Marker for marking the position of the patella	Manipulation of the patella	Final pen stroke
2		Incision of the main wound and bone prep	Metal on skin	Give tools away
3		Grading of the joint	First talking to the MPS	
4	4	Tibial incision	Metal on skin	
5		Tibial Bone pin 1 drilled	Pin in hole	Drill detached
6		Tibial Bone pin 2 drilled	Pin in hole	Drill detached
7		Tibial Array Clamp		
8		Tibial Array	Insertion into clamp	Finish tightening of all the bolts
9		Femoral incision	Metal on Skin	
10		Femur bone pin 1	Pin in hole	Drill detached
11		Femur bone pin 2	Pin in hole	Drill detached
12		Femoral Array Clamp		
13		Femoral array	Insertion into clamp	Finish tightening of all the bolts
14		Pre-registration Manual Cleaning	Tool in hand	
15		Bone reference markers	Pin in wound	Release of the last pin from tool
16		Hip joint centre capture (start/stop)	Starts recording	Confirmation of the RIO
17		Rough Joint positioning 1-5	Start of the first position	Confirmation of the last position
18		Bone marker tib fem times 2	Tool in hand	final Confirmation of the system

19		1. Surface registration with sharp probe Femur	Tool in hand	Confirmation for final completion of registration
20		1. Position 1. 3 times	First point	Confirmation for final completion of registration
21		2. Position 2. 3 times	First point	Confirmation for final completion of registration
22		3. Position 3. 1 time	First point	Confirmation for final completion of registration
23		2. Surface registration with sharpe probe	Tool in hand	
24		4. Position 1. 3 times	First point	Confirmation for final completion of registration
25		5. Position 2. 3 times	First point	Confirmation for final completion of registration
26		6. Position 3. 3 times	First point	Confirmation for final completion of registration
27		7. Position 4. 3 times	First point	Confirmation for final completion of registration
28		8. Position 5. 3 times	First point	Confirmation for final completion of registration
29		3. Surface registration with sharp probe	Tool in hand	
30		9. Position 1. 1 time	First point	Confirmation for final completion of registration
31		10. Position 2. 1 time	First point	Confirmation for final completion of registration
32		11. Position 3. 1 time	First point	Confirmation for final completion of registration
33		12. Position 4. 1 time	First point	Confirmation for final completion of registration
34		13. Position 5. 3 time	First point	Confirmation for final completion of registration

35		14. Position 6. 3 time	First point	Confirmation for final completion of registration
36		Processing time		
37		1. Additional registration points sharpe probe	Tool in hand	
38		15. Position 1. 3 times	First point	Confirmation for final completion of registration
39		16. Position 2. 3 times	First point	Confirmation for final completion of registration
40		Finding the points on the screen	Tool in hand	
41		17. Position 1.	First point	Confirmation for final completion of registration
42		18. Position 2.	First point	Confirmation for final completion of registration
43		19. Position 3.	First point	Confirmation for final completion of registration
44		20. Position 4.	First point	Confirmation for final completion of registration
45		21. Position 5.	First point	Confirmation for final completion of registration
46		22. Position 6	First point	Confirmation for final completion of registration
47		Tibial Surface registration with sharp probe	Tool in hand	
48		23. Position 1. 1 time	First point	Confirmation for final completion of registration
49		24. Position 2. 1 time	First point	Confirmation for final completion of registration
50		25. Position 3. 1 time	First point	Confirmation for final completion of registration

51		26. Position 4. 1 time	First point	Confirmation for final completion of registration
52		27. Position 5. 1 time	First point	Confirmation for final completion of registration
53		4. Surface registration with sharpe probe	Tool in hand	
54		28. Position 1. 3 times	First point	Confirmation for final completion of registration
55		29. Position 2. 3 times	First point	Confirmation for final completion of registration
56		30. Position 3. 3 times	First point	Confirmation for final completion of registration
57		31. Position 4. 3 times	First point	Confirmation for final completion of registration
58		32. Position 5. 3 times (Sharpe Probe)	First point	Confirmation for final completion of registration
59		33. Position 6. 3 times (Sharpe Probe)	First point	Confirmation for final completion of registration
60		34. Position 7. 3 times (Sharpe Probe)	First point	Confirmation for final completion of registration
61		35. Position 8. 6 times (Sharpe Probe)	First point	Confirmation for final completion of registration
62		Processing		
63		2. Additional registration points sharpe probe	Tool in hand	
64		36. Position 1. 3 times	First point	Confirmation for final completion of registration
65		37. Position 2. 3 times	First point	Confirmation for final completion of registration
66		Finding the points on the screen Sharpe probe	Tool in hand	

67		38. Position 1.	First point	Confirmation for final completion of registration
68		39. Position 2.	First point	Confirmation for final completion of registration
69		40. Position 3.	First point	Confirmation for final completion of registration
70		41. Position 4.	First point	Confirmation for final completion of registration
71		42. Position 5.	First point	Confirmation for final completion of registration
72		43. Position 6.	First point	Confirmation for final completion of registration
73		Soft tissue manual checking	(Vague section as it can happen at a number of time points) Leg in hand	Placement of the leg in the leg holder
74		Capturing points through range of motion:	First Capture point	Confirmation of last capture point
75		Recaptured with valgus stress	First Capture point	Confirmation of last capture point
76		Checking graph and Intra-operative adjustments	From assumed appearance of graph	Acceptance of the graph
77	5	Bringing robot in	Asked to bring in the robot	dropping of the robot in final place
78		Robot registration (Cube centre)	In the haptic of the cube	Confirmation from RIO of the test
79		Rotating end effector	Assumed screen indicating test	Confirmation from RIO of the test
80	6	Robot registration with markers (NEW SYSTEM)	Tool in hand	Confirmation from RIO of the test
81		Tibial milling	Confirmation in the Haptic	Stop milling
82		Tibial Depth Check	Tool in hand	Completion of measurement
83		Continued milling	End effector in hand	
84		Tibial post 1	Confirmation in the Haptic	Stop milling
85		Tibial post 2	Confirmation in the Haptic	Stop milling

86		Tibial Manual Cleaning	Tool in hand	
87	7	Robot and Femoral bone marker registration	Tools in hand	Confirmation by the robot
88		Femoral resection	Confirmation in the Haptic	Stop milling
89		Femoral Depth Check	Tools in hand	Completion of measurement
90		Continue resection	Confirmation in the Haptic	Stop milling
91		Femoral post 1	Confirmation in the Haptic	Stop milling
92		Femoral post 2	Confirmation in the Haptic	Stop milling
93		Femoral Keel	Confirmation in the Haptic	Stop milling
94		Femoral Manual Cleaning	Tools in Hand	Tools down
95		Levage		
96	8	Tibial Trial	Trial in Hand	Tools down
97		Femoral trial	Trial in hand	Tools down
98		Implant Depth Check	Confirmation in the Haptic	Stop milling
99		Polytrial	Trial in hand	Tools down or placement complete without tools
100		Manual joint Balancing	First manipulation of the joint	Final manipulation
101		Capture movement with trials	First Capture	Final Capture
102		Graph interpretation		
103		Trial Removal	Tools in hand	Last tool down
104		Poly Trial Removal	Tools in hand	Last tool down
105	9	Final Manual Cleaning		
106		Wash (levage)	Tools in hand	Last tool down
107		Injections		
108		Cloth insertion		
109		Change of gloves	First action of changing glove e.g. packet, taking off	Both gloves on.
110		Further Injections		
111	10	Tibial Cementing	Tools in hand	Tools down

112		Tibial placement	Implant in hand	Tools down
113		Femoral Cementing	Tools in hand	Tools down
114		Femoral placement	Femoral Component in hand	Tools down
115		Cement Cleaning		
116		Poly trial insertion	Poly in hand	Tools down
117		Cement setting	Leg in hand	Leg Down
118		Bone marker removal		
119		Trial Poly removed		
120		True Poly inserted	Poly in hand	Tools down
121		Capture movement with poly trial and actual implants	First Capture	
122	11	Array and pin removal		
123		Suturing		
124		Dressing		
		Leg holder fixing		
	12	Patient off bed		

Appendix 2 Pseudo-static EMG review

Surface EMG is a highly variable signal when measured from the surface for dynamic movements. Dynamics movement of the underlying muscles leads to a number of complication with assumption about the signal. Early work on this analysis was limited to isometric contractions, however this does not portray a continual review of the fatigue of a muscles and only confirms the change between a pre and post testing state. A system for this projects testing was developed to attempt to assess the EMG signal over a dynamic range. This methodology and review of the results is presented in the following appendix.

2.1 Bicep Curl:

The bicep curl is a high degree of rotation, force varying movement relative to joint angle is shown in (Hartmann et al., 2001). As the elbow reached 90 degrees the movement arm of the weight (or band in this case) is maximal and the muscle must work at its hardest to overcome this point. However, given a fast contraction, the inertial effects at this stage can assist moving beyond this point and minimise peak force required.

Additionally, there are different muscle controls required for concentric (flexion) and eccentric (extension) as more energy is required in raising the weight. The muscles force is also length dependent, so an extended arm is at the weaker point in the force length relationship, with peaks on this graph occurring roughly around 90 degrees where is it need to maintain larger forces for smoother and controlled movements of the arm.

The bicep curl was chosen here as it is simple setup with a weight against gravity and uses large superficial muscles in the two heads of the bicep brachii.

2.2 Methodologies:

A single user was used in this development of the methodology. The user started with the arm hanging as the side without the weight. A weight was positioned to allow this to be picked up without significant movement. The user then performed elbow flexor to at least 90 degrees until exhaustion.

Two electrode monitored the activity of the two heads of the bicep brachii at 1000Hz, along with a goniometer, at 200Hz, to track the movement of the user during unrestrained bicep curls with a 10kg until fatigue. Prior to electrode attachment, relevant areas of skin were prepared by light abrasion and alcohol swabs, to decrease electrical resistance, allowing optimal electromyography signal detection. A further reference electrode was placed on the wrist and recommended by the EMG suppliers (Biometrics).

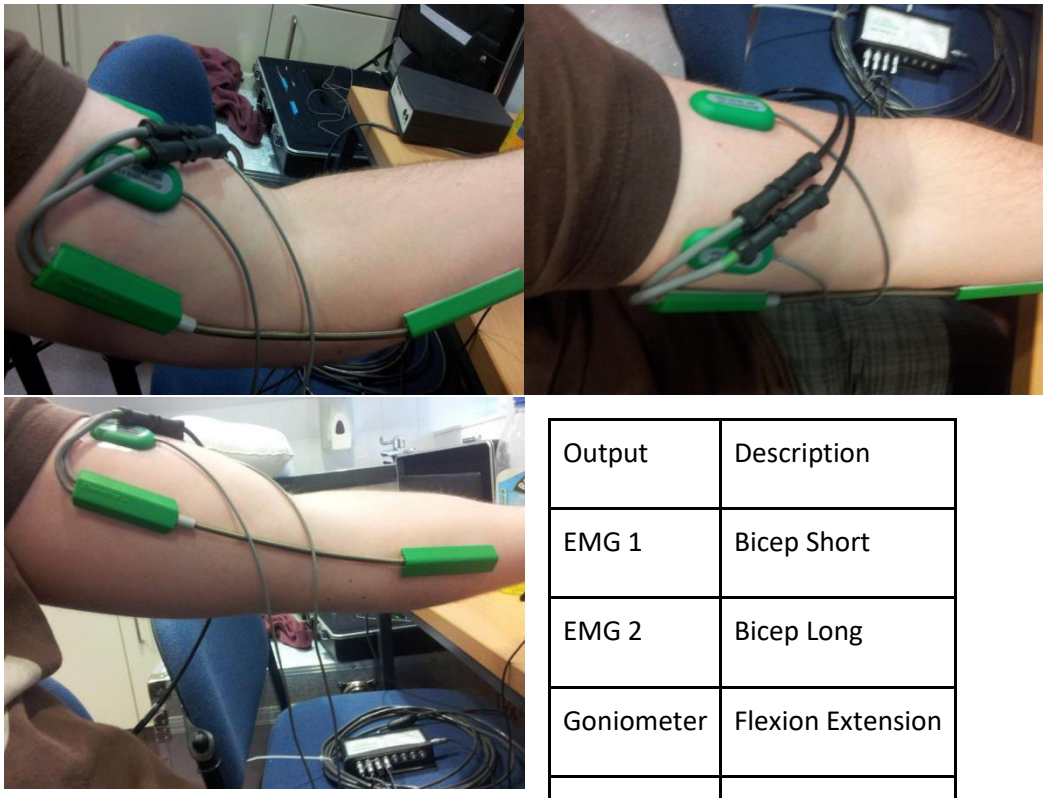

Figure 2.2-1 Pictures of the attachment site of the EMG and goniometer. Top left, medial elbow picture. Top right, above picture of the left arm. Bottom right, additional medial elbow picture with arm in extension.

Output	Description
EMG 1	Bicep Short
EMG 2	Bicep Long
Goniometer	Flexion Extension
Goniometer	Supination

Figure 2.2-2 List of the inputs to the Biometrics system for both the EMG and goniometer

The data was captured with a Biometrics datalink system into the Biometric proprietary software as a means of collecting the raw signal. This data was then reviewed for frequency changes in an attempt to review the temporal state of fatigue in the muscle. Fatigue was confirmed when the participant could no longer complete any further repetitions. This cycle was completed 5 times with an extended rest period between cycles on testing, no limit was placed on the number of movement repetitions.

The EMG signal was analyses for instantaneous median frequency change over the tests. Details of these calculations can be found in Section 6.4. Along with the EMG frequency change the angle data was also used to sample the frequency in a Pseudostatic approach.

The EMG signal is known to change as the muscle dynamical shifting relative to the electrode. For this reason, an additional test was developed to represent the change in median frequency at the same joint angle, referred to here in this project as Pseudo-static. Given the repetitive movement of the test, the joint should pass through the same joint angle numerous times (Figure 2.3-2). The joints angle defined bins (10 degrees) over the time course of the movements, the EMG median frequency (Figure 2.3-3) was sampled for these bins. For a single bin a number of median frequencies were therefore measured over the time course. A linear regression was applied to these values to give a single gradient value. As some angles are used more than others, the total length of time that the bins are used are different. To reduce the impact of short period, high gradient changes the length of time the gradient was calculated was multiplied by that gradient to give the change in median frequency (y=mx). A typical result of all these mean gradients is shown below (Figure 2.3-4). Finally, all these changes in frequencies were averaged to give a single change in frequency for the whole

test. A positive result would indicate no fatigue, while a negative result would indicate fatigue in the targeted muscle.

2.3 Results:

Table 2.3-1 shows the frequency of repetition and the total number of repetitions that were completed before exhaustion. The initial test (Test 1) was the slowest with the most repetitions. The subsequent tests were quicker, but with decreasing speed of the final repetitions and the number of repetitions with time. For each of the trial the first repetition is quicker than the last repetitions.

	Test 1	Test 2	Test 3	Test 4	Test 5
Mean frequency of all repetitions (Hz)	0.39	0.49	0.47	0.45	0.47
First repetition frequency (Hz)	0.42	0.50	0.49	0.44	0.52
Last repetitions frequency (Hz)	0.33	0.45	0.45	0.45	0.37
Number of repetitions	16	15	10	10	11

Figure 2.3-1 Table of the frequency of repetition and the number of repetitions

Below (Figure 2.3-2) is a typical example of the output from the joint angle measurement from the goniometer. Here 17 repetitions were completed before fatigue stopped the testing. Given the lack of restraint the movements are reasonably consistent range of motion.

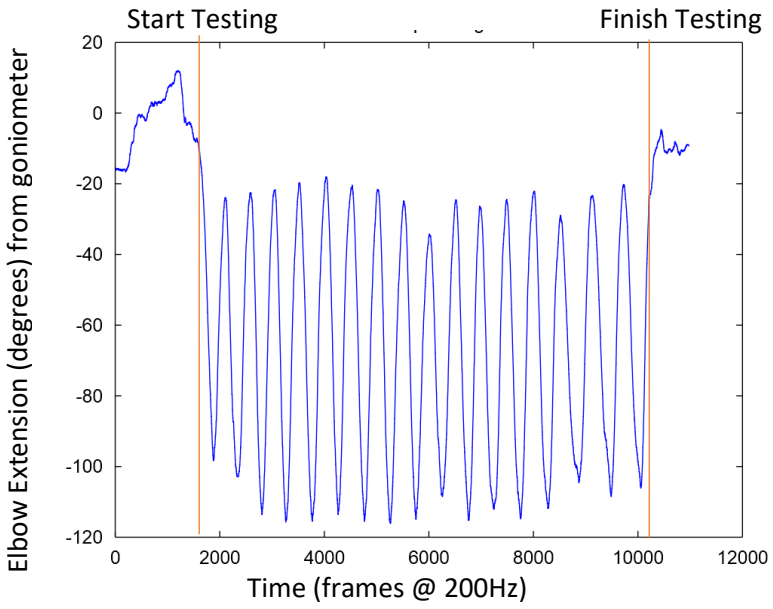

Figure 2.3-2 Elbow Flexion measure during the bicep testing to exhaustion. Red line indicated the start and finish (at exhaustion) of testing

During this same period the median frequency could be monitored below (Figure 2.3-3). A quadratic regression line has been added to clarify the movement of median frequency. Here y is the median frequency and x is time in seconds.

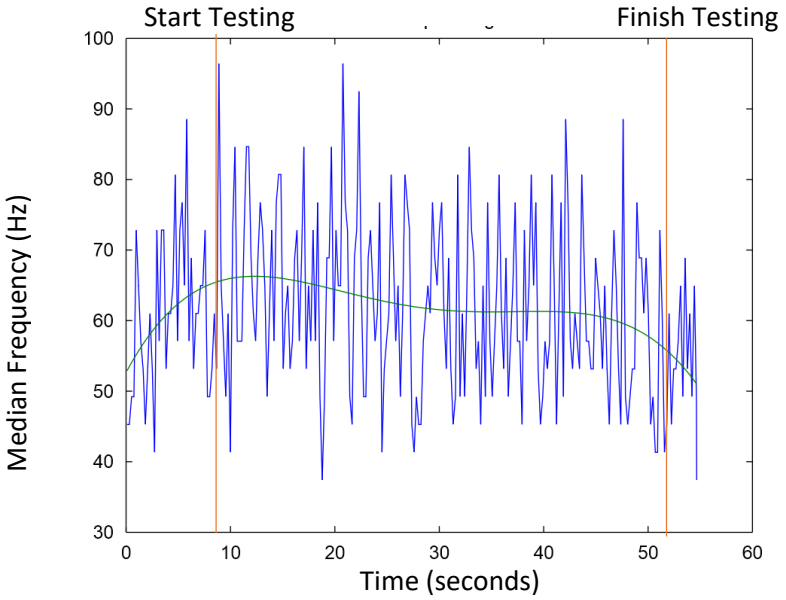

Figure 2.3-3 Instantaneous median frequency change during a test cycle. Regression model added in green to show the overall trend of the analysis. This line shows an increase in activity for the first 10 seconds and then a gradual decline after this point. Red lines indicate the beginning and end of movements

The median frequency can be seen to initially increase and then the regression model is then shown to decrease over time. The initial 10 seconds increase in median frequency can be associated with the passive hanging of the arm and then positioning of the arm with the start of the testing, not requiring the use of the bicep while hanging at the side of the participant with the weight in hand. With the start of movement, the median frequency starts from a high at roughly 65Hz this then slowly decreases. Similarly, at the end of testing the muscle sits at a resting, but still active, frequency of 53 Hz when not required for the movements. Arguably this could be a representation of fatigue over the time course of the testing. The muscle is known to be fatigued and is representing the shift in median frequency reported in the literature.

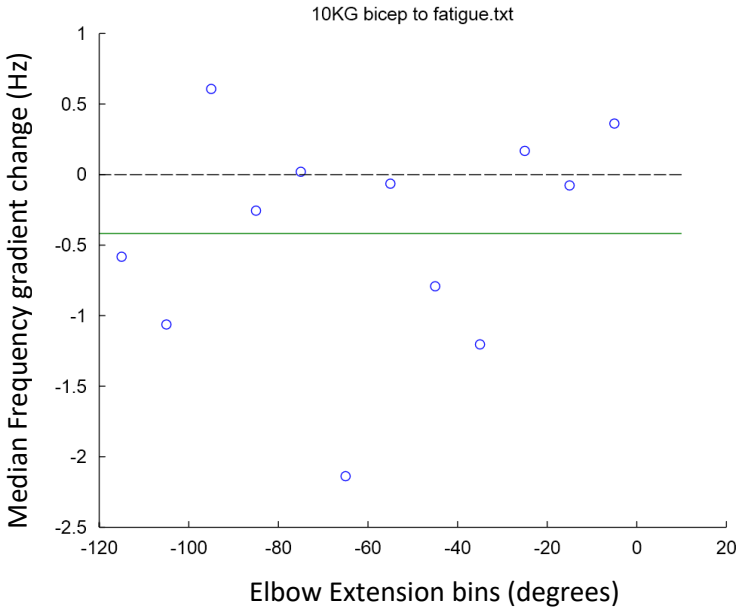

Figure 2.3-4 Pseudo-static graphical presentation of data. The points represent the bin angles and the gradient change in the frequency for those bins over the time course of the testing. The green line is the mean gradient for all of the bins

Here, in Figure 2.3-4, the x axis are the bins of the joint angles, with the y corresponding to the linearly regressed gradient that can be multiplied by the time between results, giving a change in frequency (y=mx), and then further weighted for the number of times the bin is filled. Given the windowing of the median frequency the signal was reduced to fewer points, here from 54870 samples to 252. This required the angle data to also be decimated to match these sample points. This reduction limits this processing to slower movements to allow for reduced sampling rate to describe the movement. Given the speed of the movement being roughly 90 degrees per second a relatively large bin had to be defined due to angular resolution at 10 degrees.

On the whole most of the data represents a decrease in frequency for the angle bin, however this is by no means consistent for all the bins. The active range of motion was between 20 and 110 consistently, so outside of this these values can be ignored.

The green line in the graph represents the average of all the bins, effectively the Average gradient change for each tests. These are all presented below in Table 2.3-1.

Table 2.3-1 Table of the mean gradients for the short and long head of the bicep for the repeated tests.

	Test 1	**Test 2**	**Test 3**	**Test 4**	**Test 5**
Short Head	-0.4183	-0.7133	-0.4575	-0.7906	-1.1140
Long Head	-0.7633	-0.7740	-0.7859	-0.8688	-1.1700

Firstly, all the overall mean frequency changes are shown to be negative. This agrees with the known fact that the muscle was exercised to exhaustion and hence agrees with the known state of the muscle. Of further interest here is the gradual decrease in the frequency changes with the repeated tests. This is further presented in Figure 2.3-5.

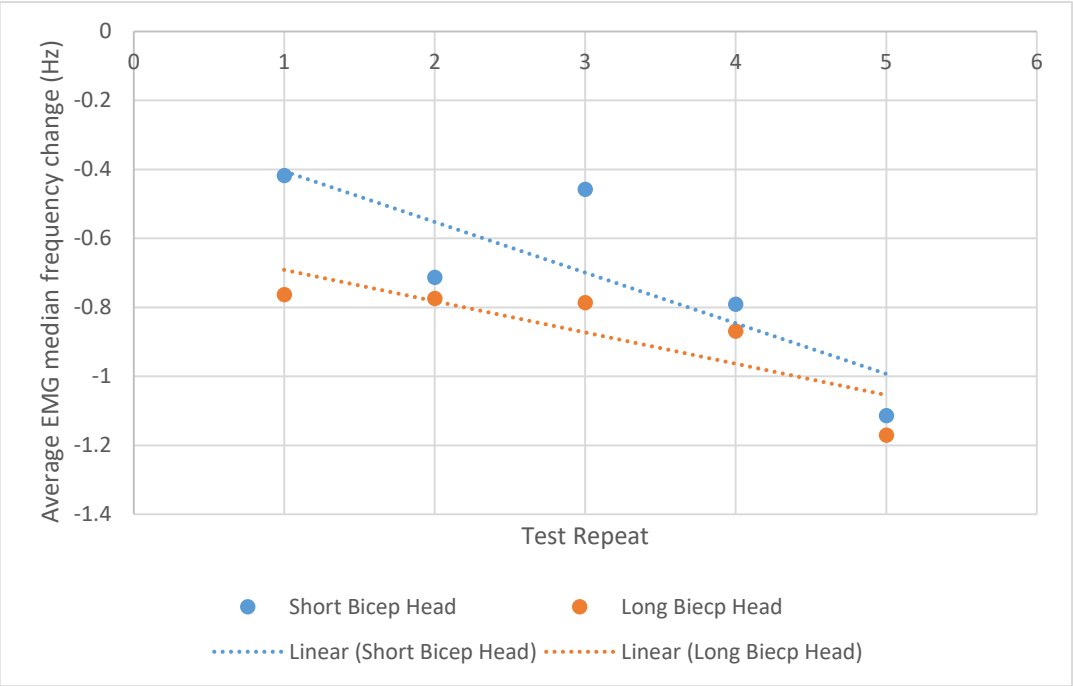

Figure 2.3-5 Graph of the mean frequency changes for the repeated tests. General trend is an increasing negative frequency change for repeating tests

The magnitude of the change in frequency is matched in both muscle heads. The overall trend indicates an increasing negative change in the median frequency with repetition of exhaustion.

2.4 Review

Pseudo-static evaluation is by no means validated as part of this review, but does seem to show some sensitivity to fatigue as a potential metric. The key results of this testing is the apparent increasing of the negative change of the median frequency. The theory behind the change in the median frequency is the de-recruitment of exhausted fibres to prevent injury. The higher frequency fibres are designed for high force anaerobic functions and will fatigue first in tasks. This trend will continue through to lower frequency fibres until the muscle can no longer produce the force required to perform the task or other preservative functions (motivation) prevent continuation of the action. These result in the decrease of the median frequency of the muscles. This is seen clearly in Figure 2.3-3 for a single task. On the repeating of the task muscles must be recruited in a different pattern to lead to this greater decrease in frequency Figure 2.3-5. Time in-between testing allow for some recovery of all muscle fibre types. However, the decreased is speculated to be the initial engagement of the same muscle fibres but followed by more catastrophic de-recruitment of high and lower frequency muscle fibres. The fatiguing of mid-range frequency fibres leads to a steeper gradient and a higher overall median frequency change in the muscle.

Another demonstration to the change in frequency could be seen in the speed of the movements. The speed of the repetition were slower by the end of exercise (Figure 2.3-2), with a slight decrease in average frequency of the repetition from tests 2 to 5. Between tests 2 to 5 the de-recruitment of the higher frequency fibres that are required for faster, higher force, movements are speculated to have occurred. This is an observable indicator of fatigue and is shown in the difference between the first and final repetitions frequency, with the first frequency being faster than the last, as would be expected, for all tests.

This experimentation was not an extensive review of this method as a fatigue metric, but suitable data was recorded to allow this analysis will be applied and reviewed in the main project work to show similar sensitivity to the dynamic effects with users manipulating the MAKO RIO system. Future work would aim to develop this theory and methodology further.

Appendix 3 MatLab Code development

This chapter reviews the methodology used to capture motion and posture from the biomechanical testing instrumentation (Optitrack) and the resulting calculations. Additionally, the flow of the information in the MatLab code from function to function is presented in the last section.

The kinematic calculations can be developed and special functions added to the process with the power of MatLab. While VICON systems have similar functionality in bodybuilder, and now interface with MatLab, this was not available at the time of testing. Additionally, Motive had no script based language and required the purchasing of secondary calculation packages such as Visual3D (C-Motion, Germantown, MD, USA). VICON's proprietary models, while validated, are not open to review. Instead of this purchase, a set of MatLab functions were developed to enable further understanding and control deploying the principals defined in the literature review (Winter, 2009; Zatsiorsky, 1998).

3.1 Optitrack

3.1.1 Biomechanics CROSS workflow

This section will review the workflow and calculation of the optical tracking process. Given the lack of biomechanical calculation support within the capture software a separate MatLab based approach was developed.

3.1.2 Expansion to the surgeon model

The surgeon model defined functional joint centres and axes of the upper limb from marker movements relative to local coordinate frames. While marker clusters would have been ideal for this situation, the lack on free space on the arm with access for EMG electrode and slow movements meant that a simple marker system was taken inspired by (Rettig et al., 2009). The main difference being the markers were not rigidly fixed to one another and instead positioned over anatomical prominences described below.

Marker placements

Marker placements were chosen for ease of identification, reproducibility and minimal subcutaneous thickness to boney landmarks.

Shoulder markers and Thorax

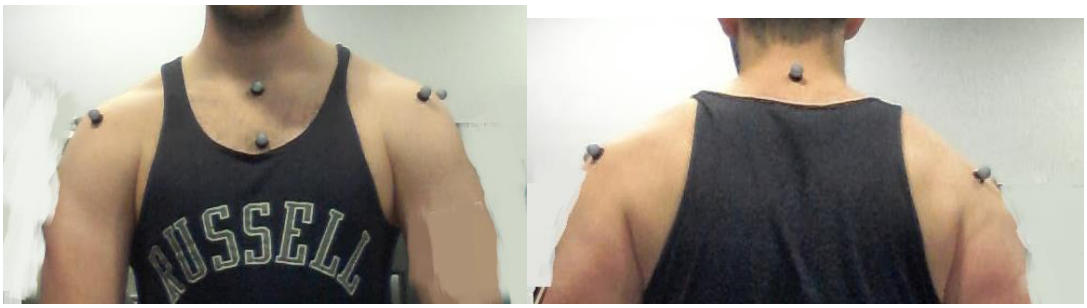

Figure 3.1-1 Marker Placement on shoulder and Thorax

To find the anterior shoulder marker the clavicle was located and tracked along to the acromion, until the most anterior and lateral bony prominence was found. The posterior shoulder marker was positioned by following the scapular spine to find the most posterior and lateral bony prominence of the acromion angle. Jugular notch marker was positioned on the most superior and anterior part of

the sternum to ensure attachment over bone and not the skin recess of the notch. The most distal part of the sternum as possible to allow fixation. If clothing was restrictive of access, the marker was place above the clothing as far from the sternum as possible.

Spine

C7 spinous process was positioned on the first prominent spiny process at the top of the back. Due to the loose clothing T10 was define from where the spin met the beltline.

Hip

Equidistance both sides lateral of T10 marker. The specific pelvic tilt was not of interest and so these markers along with T10 define a non-anatomic pelvic plane for describing thoracic movements.

Elbow markers

With a 90 degree flexed elbow, the medial and lateral epicondyle of the Humerus were found.

Wrist Markers and Hand

The styloid process of both the Ulna and radius describe the position and approximate axis of the wrist. The 2nd and 5th Metacarpal heads, along with the Mid Proximal metacarpal base 3 and 4 define the orientation of the hand relative to the wrist. These three markers are considered a semi-rigid body and calculated as a cluster.

Finally the Mid interphalangeal joints 1 and 2. These were included for expansion and future work.

Figure 3.1-2 Marker Position on Hands and Wrist

3.1.3 Surgeon Model calculations

Taking the joint coordinate system approach as describe in (Grood and Suntay, 1983), local reference systems were defined for the segments of the arm along anatomical reference lines. Functionally calculated rotation axes could then be defined from these local segment reference frames to better describe the movements of the joint. For all of the reference frames, the preceding joint describes the orientation of zero degrees. At this point no corrections were made for anatomical alignment, for instance the carry angle of the elbow and forearm was not corrected for and would be shown as a constant angle, however this angle was not reviewed in the kinematics as this is not considered a degree of free in the movement.

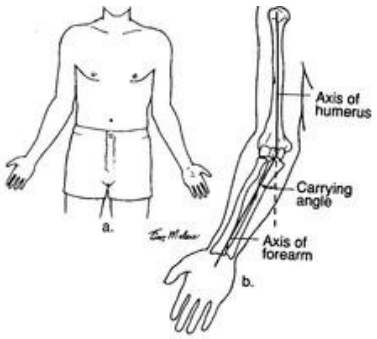

[1]

Figure 3.1-3 Diagram of carry angle

[1] http://www.ssbcrack.com/2013/09/excessive-carrying-angle-of-elbow-ssb.html

The following reference frames are defined in order of calculation. The Thoracic frame was define first given the subsequence frame of the arm requiring the Thorax as a based. This is exactly the same as the RIO with the large base of the robotic arm forming the origin and 0 angle orientations.

3.1.3.1 Thoracic Reference Frame

Yt is define from the Midpoint of C7 and Jugular Notch to Midpoint of T10 Sternum. This is effectively the direction of the spine. Zt is perpendicular to the plane of C7, Jugular Notch, T10, Sternum. Xt is defined as the CROSS product of Yt and Zt. Resulting in the reference frame below.

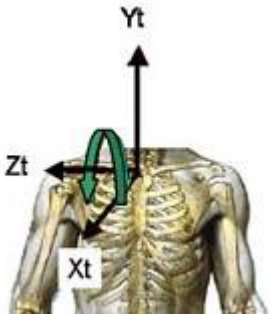

Figure 3.1-4 Thoracic reference frame (Wu et al., 2005)

3.1.3.2 Clavicle reference frame:

The clavicle of the dominant side was taken as a reference frame to isolate any movements of the torso relative to the arm. Additionally, the centre of rotation of the humeral head was considered to be stationary in this frame given its articulation with the glenoid cavity. Here Zs is the Jugular notch to Mid shoulder front and Back, with Xs being defined as the cross product of Y_{Thorax} and $Z_{Clavicle}$. Finally, Ys was defined as the cross product of Zs and Xs.

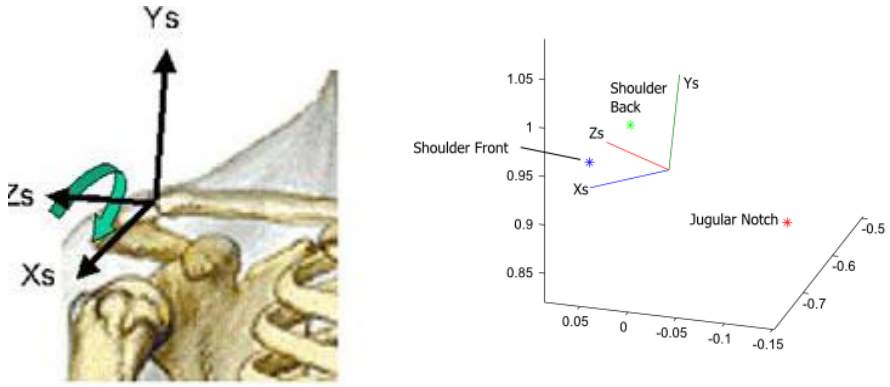

Figure 3.1-5 Clavical reference frame (Left) (Wu et al., 2005) with MatLab calculation output (Right)

3.1.3.3 Upper Arm reference frame:

The upper arm used the medial and lateral Condyles of the Humerus to describe the functional centre when moved in the calibration process. The rotation centre of the shoulder would become a virtual marker and be defined in time from the clavicle reference frame. This would then define a new marker frame for the upper arm. This was a temporary reference frame before the functional anatomical reference frame of the elbow could be defined and similarly allow for the isolation of the wrist markers to define the forearm reference system. The testing reference frame is made up of Yh Elbow to shoulder Centre, Zh Functional Axis of Elbow movement, with Xh being produced from the Cross product of Yh and Zh.

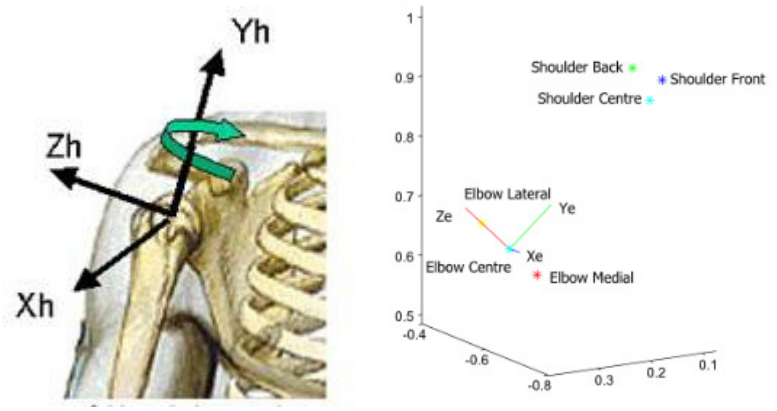

Figure 3.1-6 Humerus Reference frame (Left) (Wu et al., 2005) with MatLab calculation output (Right)

Due to difficulty getting the subjects to isolate the movement of the wrist, only a rotational centre of the wrist was defined. This was used to define an axial axis to be defined and the wrist marker axis was used to describe the flexion extension angle. Yf is defined from Mid wrist to mid elbow, with Zf being defined from the Ulna Styloid to radial Styloid (Medial to lateral).

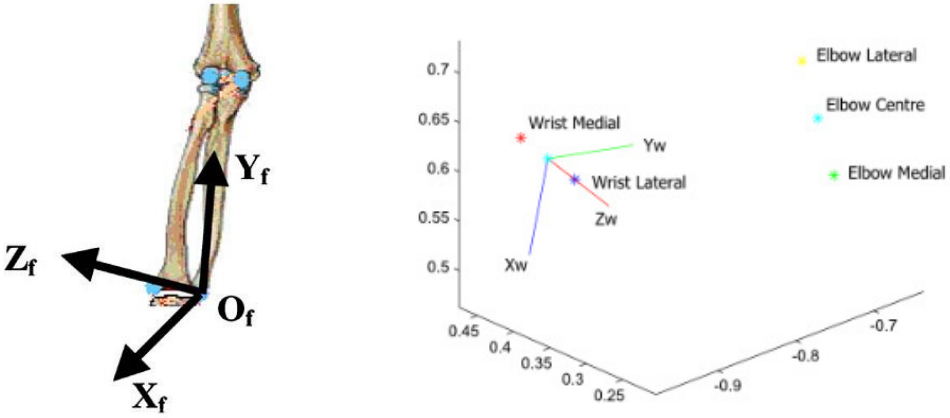

Figure 3.1-7 Forearm Reference frame (Left) (Wu et al., 2005) with MatLab calculation output (Right)

3.1.3.4 Hand reference frame:

The hand reference system could be defined from 3 markers placed on the back of the hand allowing an assumed rigid cluster to be defined. Yhand is defined from the Mid Metacarpal head finger 2 and 5 to capitate, with Zhand from Finger 5 to finger 2 metacarpal head. Xhand is formed from the Cross production of Yhand and Zhand.

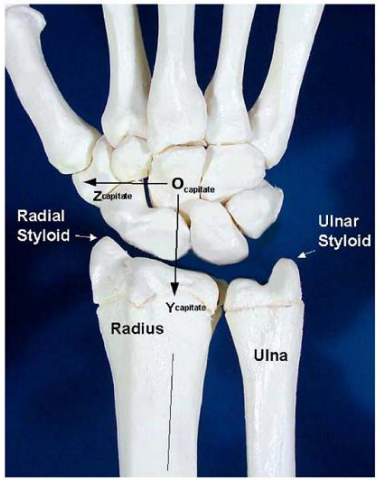

Figure 3.1-8 Reference frame of the hand

3.1.3.5 Angle calculations

Given the definition of the local reference frames of the body segments, relative rotation matrices with time could be constructed and define three dimensional rotation angles around the anatomical reference frames. This Cardanic/Euler angle decomposition of a rotation matrix results in the three orthogonal axes rotations. While the anatomical reference frame is not orthogonal, this can be corrected to orthogonal axes as a good assumption of the joint angles. For this example the rotation order is [3, 2, 1].

$$R = R_z(\varphi)R_y(\theta)R_x(\gamma) = \begin{bmatrix} R_{11} & R_{12} & R_{13} \\ R_{21} & R_{22} & R_{23} \\ R_{31} & R_{32} & R_{33} \end{bmatrix}$$

$$= \begin{bmatrix} \boldsymbol{\cos\theta\cos\gamma} & \boldsymbol{\sin\varphi\sin\theta\cos\gamma + \cos\varphi\sin\gamma} & \boldsymbol{-\cos\varphi\sin\theta\cos\gamma + \sin\varphi\sin\gamma} \\ \boldsymbol{-\cos\theta\sin\gamma} & \boldsymbol{-\sin\varphi\sin\theta\sin\gamma + \cos\varphi\cos\gamma} & \boldsymbol{\cos\varphi\sin\theta\sin\gamma + \sin\varphi\cos\gamma} \\ \boldsymbol{\sin\theta} & \boldsymbol{-\sin\varphi\cos\theta} & \boldsymbol{\cos\varphi\cos\theta} \end{bmatrix}$$

Equation 3.1-1 Three dimensional rotation Matrix

$$R_{31} = \sin\theta$$

$$\theta = \text{asin}(R_{31})$$

Equation 3.1-2 Rotation matrix term in isolation

Similarly taking advantage of the smaller functions:

$$\frac{-R_{32}}{R_{33}} = \tan(\varphi)$$

$$\varphi = atan2(R_{32}, R_{33})$$

Equation 3.1-3 atan2

Here the function atan2 is used to work out the quadrant the angle will fall [-π, π] from the sign of the two terms from the rotation matrix.

Similarly

$$\frac{R_{21}}{R_{11}} = \tan\gamma$$

These can be show in the code below. The cyclic or anticyclic permutations of the order of the rotations define where the functions are in the matrix and also the sign, for this reason the following corrections have to be added. This already assumes a Cardanic system is being applied. Given that there are two solutions to the inverse, two outputs are also produced. The second output, is only used when the solutions approach π or –π, but this is not usually the case in this testing, so the first output a(i) is used.

```
if (rem(j-i+3,3)==1)     sig=1;    % cyclic
    else             sig=-1;   % anti cyclic
end

    a(1)= atan2(-sig*R(j,k),R(k,k));
    a(2)= asin(sig*R(i,k));
    a(3)= atan2(-sig*R(i,j),R(i,i));

    b(1)= atan2(sig*R(j,k),-R(k,k));
    b(2)= rem( pi-asin(sig*R(i,k)) + pi , 2*pi )-pi;
    b(3)= atan2(sig*R(i,j),-R(i,i));
```

3.1.3.6 Axes definition:

The definitions of the axes are denoted at the joint and in this thesis and project is labelled as such as this is used in the MatLab code, but also included here is the definitions names of the segments that are also described with these axes. Truly, these are the segment axes. For these reference axes the rotation orders that are recommended for use in the upper arm were taken from (Wu et al., 2005). The output is order sensitive in that changing the order can affect the accuracy of the angle output as some anatomical rotations can be defined in multiple axes.

3.2 MatLab workflow

The main MatLab file is initiated by running `BiomechanicsCROSS`. This runs and controls the order of processing in the protocol for each test, with the ability to add additional testing. The main workflow of this file is shown diagrammatically below in Figure 3.2-2. The main inputs (Optitrack, EMG and Force Transducer) to the workflow are shown in Orange in the diagram. Given the multiple different systems for capturing the data this follows three main tracks that converge at the files sorting stage and joint analysis of data.

BiomechanicsCROSS requires the Graphical user interface to be pointed to the right user's files and starts all the calculations for that user and test sequence. The first check is for the existence of the processed C3D files with `filecheck`. Once the files are confirmed as existing or not, this is passed onto either the model output program or the assessment algorithms. The main output from these files is the MarkerData database with all the processed and imported marker data. This data is still in a raw format at this point.

The MarkerData is then passed through a `filter` and `filling` protocol. The raw data was manually labelled and filled to an extent, but with the limited tools sets available in Optitrack's Motive, further protocols were needed to ensure the data was complete and cleaned. The RIO movements were produced at a separate development stage and so was developed in a separate program format. This was largely due to the markers being arranged into clusters and no compensations for soft tissue movements required. The initial calculations are from the calibrations movements performed at the beginning of the testing. This worked by defining the functional joint centres of the robot in relation

to the marker clusters. From these a Denavit-Hartenberg inspired model of the robot was created. For all the testing protocols the RIO angles could be extracted from the marker data. The user's movements were calculated in the BiomechanicsCalculations protocol. Similar to the RIO calculations the calculation were based on functional joint axis and centre calculations based on markers placed on bony anatomy describing segment movements.

The signal processing algorithms of the EMG processing were then performed. This protocol associated the EMG signal with the appropriate movement file and naming structure based on recording length and sequence. Additional naming's for the pre-burring testing are also assessed. From this naming protocol the synchronised files could be called for joint analysis.

Finally the ForceTransducer calculations from the force transducer voltage recordings were recorded. Calibration files for the transducers were obtained to convert the six channel voltage recording to the force and moment measurements experienced by the system. The reference frame of the transducer was converted to the Optitrack tracking systems, for more intuitive analysis. Additional corrections for the orientation of the End effector were taken into account to minimise the action of the weight of the handle on the force transducer.

From this point the movement angle for the RIO and user, EMG and force at the end effector have been calculated. This allowed a combined analysis of all of the various model outputs for the assessment of user fatigue. Visualisation GUIs were also developed to present the data for understanding. Below are examples of the EMG GUI showing the raw, spectral, median frequency and RMS plots; along with the C3D 3D plot of the marker information with joint angle graph call up and scroll bar for playback.

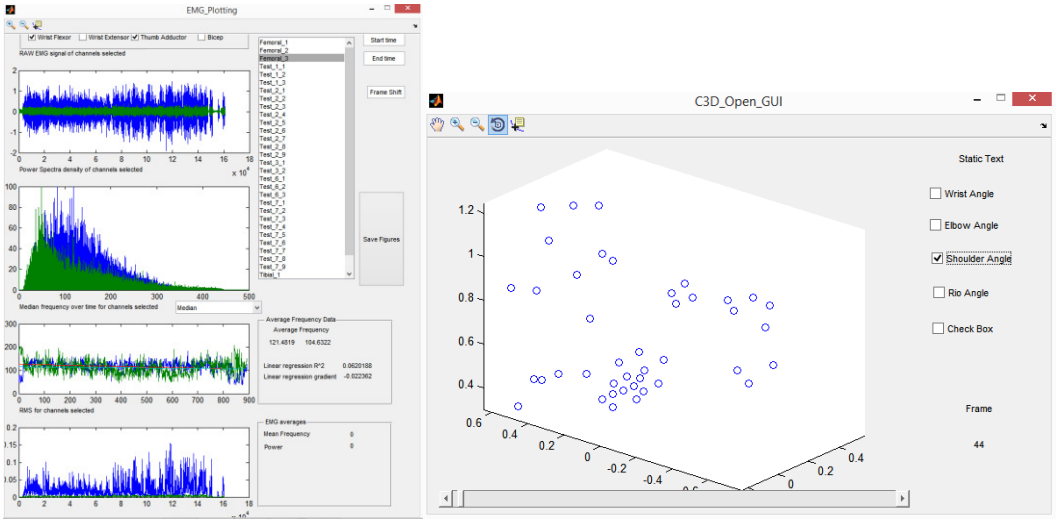

Figure 3.2-1 EMG GUI example (Left) C3D Open GUI (Right)

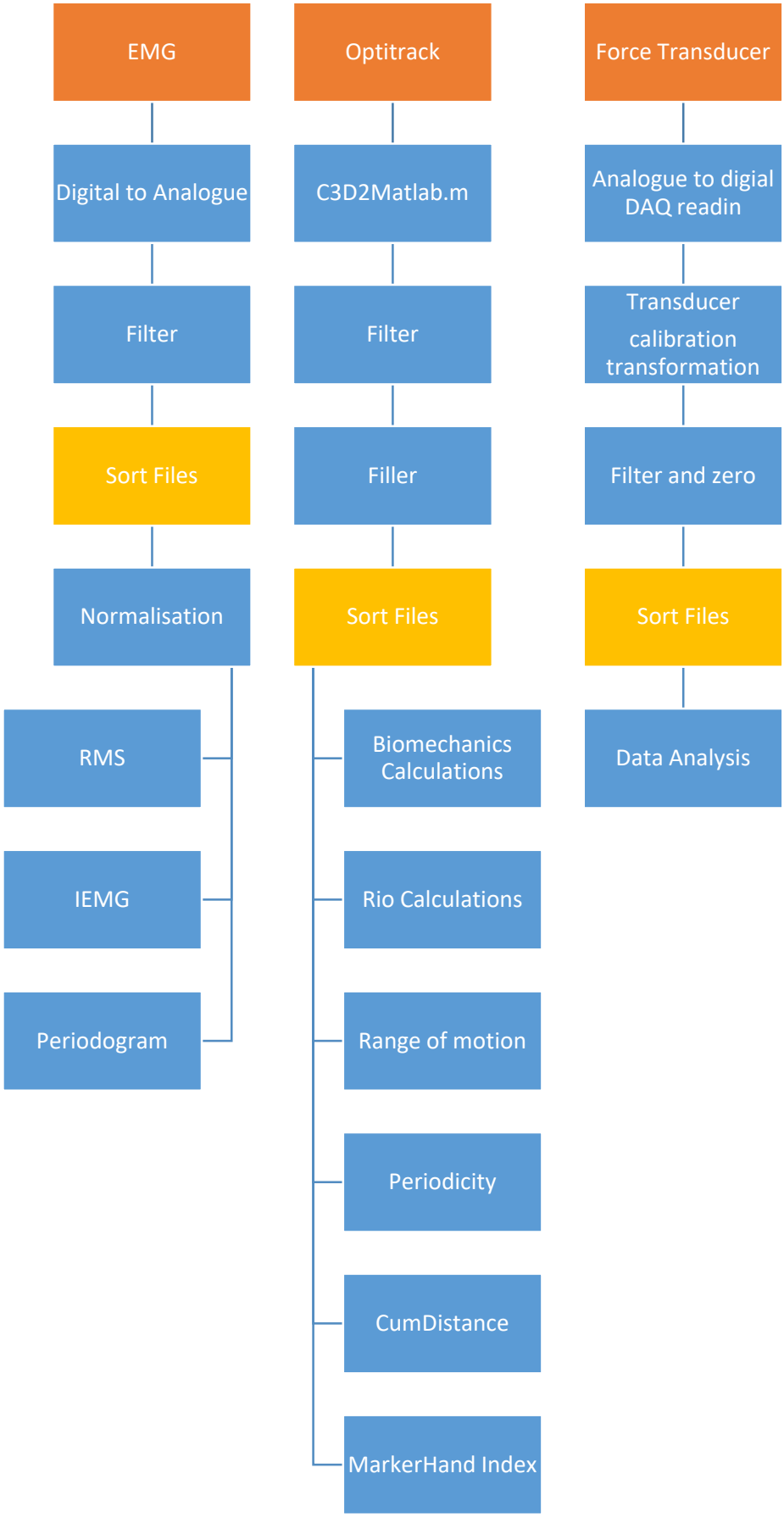

Figure 3.2-2 Flow Diagram of MatLAB code in three strands

3.3 Conclusion:

This chapter was a review of the MatLab coding and technical handling of the data from the three components used in the following testing chapter.

Appendix 4 Questionnaire for RIO Testee Users

This is the proposed VOC of consumer testing for subjects for testing the causes of localised fatigue with MAKO RIO use.

Please review the following questions:

4.1 Surgeon specific details

1. Age:
2. Height:
    a. Meters or Feet and inches
3. Weight
    a. Kg:
4. Dominant hand:
    a. Left
    b. Right
    c. Ambidextrous
5. Number of surgeries in total:
6. How long have you been using the RIO. Approx.
    a. Months: Years:
7. How many would you do in a maximum day:
    a. Number:

4.2 Fatigue

Use of any mechanical system may cause user fatigue. Have you experienced any fatigue associated with the RIOs use? If so, what is/are the sources and duration of the fatigue?

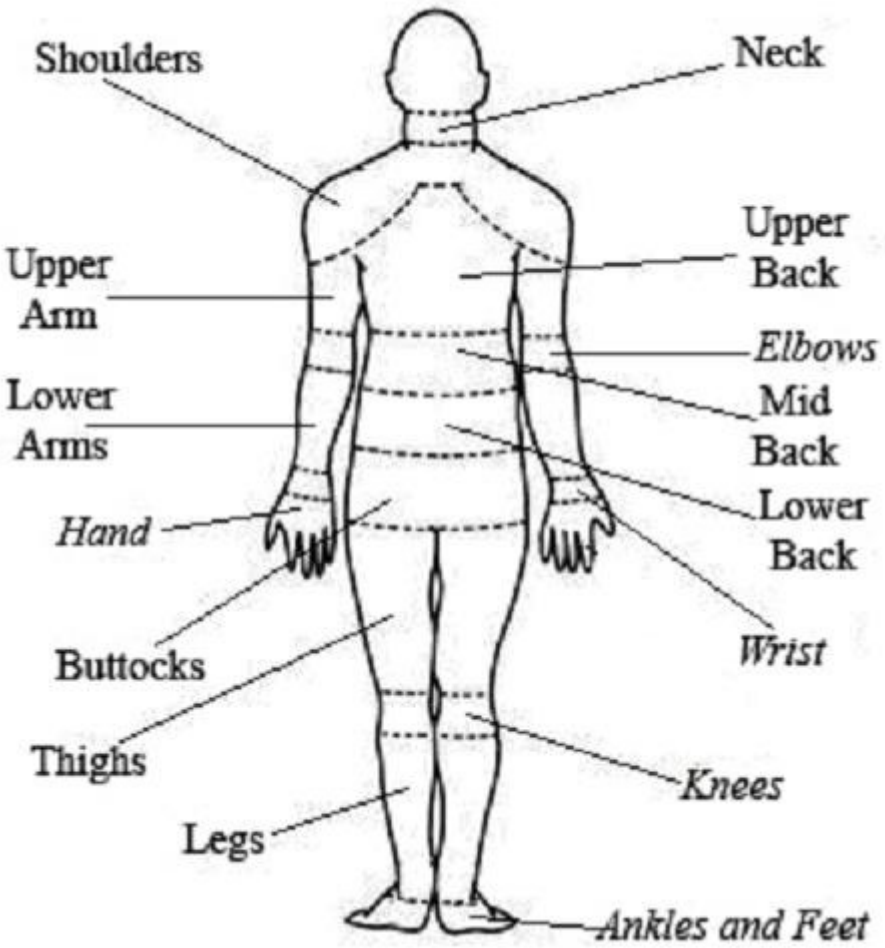

Area (to be filled out)	No discomfort		Mild discomfort			Distracting discomfort		Duration (approx. In minutes) [2]
	1	2	3	4	5	6	7	
	1	2	3	4	5	6	7	
	1	2	3	4	5	6	7	
	1	2	3	4	5	6	7	
	1	2	3	4	5	6	7	

[2] Duration was verbally explained as the starting point of the fatigue and , if it faded, the points at which is stopped. This was recorded qualitatively and interpreted in section numerically as described in 5.6.4 of main thesis.

Bibliography

Grood, E.S., Suntay, W.J., 1983. A joint coordinate system for the clinical description of three-dimensional motions: application to the knee. J. Biomech. Eng. 105, 136–144.

Hartmann, J., Tünnemann, H., Klavora, P., Gaskovski, P., 2001. Fitness and strength training for all sports: theory, methods, programs. Sport Books Publisher, Toronto.

Rettig, O., Fradet, L., Kasten, P., Raiss, P., Wolf, S.I., 2009. A new kinematic model of the upper extremity based on functional joint parameter determination for shoulder and elbow. Gait Posture 30, 469–476. https://doi.org/10.1016/j.gaitpost.2009.07.111

Winter, D.A., 2009. Biomechanics and motor control of human movement, 4th ed. ed. Wiley, Hoboken, N.J.

Wu, G., van der Helm, F.C.T., (DirkJan) Veeger, H.E.J., Makhsous, M., Van Roy, P., Anglin, C., Nagels, J., Karduna, A.R., McQuade, K., Wang, X., Werner, F.W., Buchholz, B., 2005. ISB recommendation on definitions of joint coordinate systems of various joints for the reporting of human joint motion—Part II: shoulder, elbow, wrist and hand. J. Biomech. 38, 981–992. https://doi.org/10.1016/j.jbiomech.2004.05.042

Zatsiorsky, V.M., 1998. Kinematics of Human Motion. Human Kinetics.